Regulation of gene silencing: From microRNA biogenesis to post-translational modifications of TNRC6 complexes

DISSERTATION

zur Erlangung des
DOKTORGRADES DER NATURWISSENSCHAFTEN (Dr. rer. nat.)
der Fakultät Biologie und Vorklinische Medizin
der Universität Regensburg

vorgelegt von
Johannes Danner

aus Eggenfelden

im Jahr 2017

Das Promotionsgesuch wurde eingereicht am: 12.09.2017

Die Arbeit wurde angeleitet von:

Prof. Dr. Gunter Meister

_____

Johannes Danner

Summary

'From microRNA biogenesis to post-translational modifications of TNRC6 complexes' summarizes the two main projects, beginning with the influence of specific RNA binding proteins on miRNA biogenesis processes. The fate of the mature miRNA is determined by the incorporation into Argonaute proteins followed by a complex formation with TNRC6 proteins as core molecules of gene silencing complexes.

miRNAs are transcribed as stem-loop structured primary transcripts (pri-miRNA) by Pol II. The further nuclear processing is carried out by the microprocessor complex containing the RNase III enzyme Drosha, which cleaves the pri-miRNA to precursor-miRNA (pre-miRNA). After Exportin-5 mediated transport of the pre-miRNA to the cytoplasm, the RNase III enzyme Dicer cleaves off the terminal loop resulting in a 21-24 nt long double-stranded RNA. One of the strands is incorporated in the RNA-induced silencing complex (RISC), where it directly interacts with a member of the Argonaute protein family. The miRNA guides the mature RISC complex to partially complementary target sites on mRNAs leading to gene silencing. During this process TNRC6 proteins interact with Argonaute and recruit additional factors to mediate translational repression and target mRNA destabilization through deadenylation and decapping leading to mRNA decay.

Viral miRNA Biogenesis. Surprisingly, miRNAs were identified in human herpes, papilloma and polyoma viruses. These miRNAs regulate viral and host gene expression and influence infection efficiency. The miRNA biogenesis is strictly regulated and by northern blotting different expression profiles of infected cell lines were detected.

To identify RNA-binding-proteins involved in post-transcriptional regulation of miRNA biogenesis, a mass spectrometric pull down assay with *in-vitro* transcribed pre-miRNA was established. The obtained data generated together with bioinformatical analyses a valuable set of potential regulatory candidates. The interaction of a subset of potential regulators was verified by repeating the pull-down with overexpressed Flag-/Ha-tagged proteins. For further functional characterization, the influence of RBPs on pre-miRNA processing was analyzed in knockout cell lines in which candidate RBPs have been depleted. Overexpression of the potential candidates further confirms a strong impact on the miRNA biogenesis.

Taken together, mass spectrometric approaches identified RNA-binding-Proteins involved in viral miRNA biogenesis.

Post-translational modifications of TNRC6 proteins. TNRC6 and Ago proteins play a central role in the gene silencing mechanism. The Interaction of both proteins is based on two Tryptophan's

binding into two specific pockets in the PIWI domain of Ago proteins. TNRC6 proteins (also referred to as GW proteins) contain Gly/Trp-repeats and serve as binding platform for many components of the gene silencing machinery.

To assess whether gene silencing is regulated by post-translational modifications, TNRC6 proteins were analyzed by mass spectrometry. To analyze endogenous proteins, we established monoclonal antibodies against TNRC6A-C for immunopurificaiton of TNRC6 proteins from cell lysates. The validity and specificity of the antibodies was further verified by mass spectrometric selected reaction monitoring analyses. Followed by a detailed mass spectrometric analysis, multiple endogenous phosphorylation sites on TNRC6 proteins were detected. The obtained data identified conserved phosphorylation sites both among the TNRC6 paralogs and within different species. Functional analyses of phospho-mimicking and non-phospho mutants showed low effects on the downstream gene silencing processes. Localization studies and Ago-binding assays also indicate no effects of the phospho-sites on TNRC6 function.

Taken together, post-translational modifications on TNRC6 proteins with potential, but so far unknown function in gene silencing were identified.

Zusammmenfassung

"From microRNA biogenesis to post-translational modifications of TNRC6 complexes" fasst die beiden Hauptprojekte dieser Doktorarbeit zusammen.
miRNAs werden als primäre transkripte (pri-miRNA) von der RNA Polymerase II transkribiert. Die weitere Verarbeitung erfolgt durch den Mikroprozessor-Komplex, der das katalytisch aktive Enzym Drosha enthält, welches die pri-miRNA zu Vorläufer-miRNAs (pre-miRNA) spaltet. Nach dem Exportin-5-vermittelten Transport der pre-miRNA in das Zytoplasma, spaltet das RNase III-Enzym Dicer die terminale Schleife der pre-miRNA ab, was zu einer 21-24 nt langen doppelsträngigen RNA führt. Einer der beiden Stränge wird in den RNA-induzierten Silencing-Komplex (RISC) eingebaut, wo er direkt mit einem Mitglied der Argonaute-Proteinfamilie wechselwirkt. Der reife RISC-Komplex bildet durch komplementäre Basenpaarung der miRNA zur mRNA den Gene-silencing Komplexe. Während dieses Prozesses interagiert ein TNRC6-Protein mit Argonaut und durch Rekrutierung von zusätzlichen Faktoren wird die Translation reprimiert und die Ziel-mRNA destabilisiert und abgebaut.

Virale miRNA Biogenese. Überraschenderweise wurden miRNAs bei humanen Herpes-, Papillom- und Polyomaviren identifiziert. Diese miRNAs regulieren die Virus- und Wirtsgenexpression und beeinflussen den viralen Lebenszyklus.
Die miRNA-Biogenese ist streng reguliert und durch Nothern Blotting wurden verschiedene miRNA Expressionsprofile von infizierten Zelllinien nachgewiesen. Zur Identifizierung von RNA-bindenden Proteinen, die an der post-transkriptionelen Regulation der miRNA-Biogenese beteiligt sind, wurde eine massen-spektrometrische Pull-Down-Anwendung mit *in vitro* transkribierter Pre-miRNA etabliert. Die gewonnenen Daten, die zusammen mit bioinformatischen Analysen erzeugt wurden, sind ein wertvoller Datensatz von potenziellen regulatorischen Proteinen. Die Wechselwirkung einer Teilmenge von potentiellen Regulatoren wurde durch Wiederholen des Pull-downs mit überexprimierten Flag-/ Ha-markierten Proteinen verifiziert. Für eine weitere funktionelle Charakterisierung wurde der Einfluss von RNA-bindenden Proteinen (RBP) auf die pre-miRNA-Verarbeitung in Knockout-Zelllinien analysiert.
Zusammenfasst, wurden in massenspektrometrischen Analysen RNA-bindende Proteine identifiziert, die an der viralen miRNA-Biogenese beteiligt waren.

Posttranslationale Modifikationen von TNRC6-Proteinen. TNRC6- und Ago-Proteine spielen eine zentrale Rolle im Gen-Silencing-Mechanismus. Die Interaktion beider Proteine basiert auf zwei

Tryptophan Bindungen, die in zwei spezifische Taschen in der PIWI-Domäne von Ago-Proteinen binden. TNRC6-Proteine (auch GW-Proteine genannt) enthalten repetitive Glycin/ Tryptophan-Aminosäureabschnitte und dienen als Bindeplattform für viele Komponenten der Gen-Silencing-Maschinerie.

Um zu beurteilen, ob Gen-Silencing durch posttranslationale Modifikationen reguliert wird, wurden TNRC6-Proteine durch Massenspektrometrie analysiert. Um endogene Proteine zu analysieren, wurden monoklonale Antikörper gegen TNRC6A-C für Immuno-Aufreinigungen von TNRC6-Proteinen aus Zelllysaten etabliert. Die Gültigkeit und Spezifität der Antikörper wurde durch massenspektrometrische ausgewählte Analysen weiter verifiziert. Nach einer detaillierten Analyse wurden mehrere endogene Phosphorylierungsstellen in TNRC6-Proteinen nachgewiesen. Die erhaltenen Daten identifizierten konservierte Phosphorylierungsstellen sowohl unter den humanen TNRC6-Paralogen als auch innerhalb verschiedener TNRC6 proteine anderer Tiere. Funktionsanalysen von Phospho-Mimik- und Nicht-Phosphorylierbaren-Mutanten zeigten geringe Auswirkungen auf die nachgeschalteten Gen-Silencing-Prozesse. Lokalisierungsstudien und Ago-Bindungsversuche zeigen auch keine Wirkungen der phosphorylierten Aminosäuren auf die TNRC6-Funktion an.

Zusammengefasst wurden posttranslationale Modifikationen an TNRC6-Proteinen identifiziert und charakterisiert.

Publications

Schraivogel D., Schindler S.G., Danner J., Kremmer E., Pfaff J., Hannus S., Depping R. & Meister G. **Importin-β facilitates nuclear import of human GW proteins and balances cytoplasmic gene silencing protein levels**. Nucleic Acids Res. 2015

Johannes Danner, Balagopal Pai, Ludwig Wankerl and Gunter Meister. **Peptide-Based Inhibition of miRNA-Guided Gene Silencing.** Methods Mol. Biol. 2017

Miguel Quévillon Huberdeau, Daniela M. Zeitler, Judith Hauptmann, Astrid Bruckmann, Lucile Fressigné, Johannes Danner, Sandra Piquet, Nicholas Strieder, Julia C. Engelmann, Guillaume Jannot, Rainer Deutzmann, Martin J. Simard and Gunter Meister. **Phosphorylation of Argonaute proteins affects mRNA binding and is essential for microRNA-guided gene silencing *in vivo.*** EMBO Journal 2017

Johannes Danner, Thomas Treiber, Nora Treiber, Emma Kraus, Eduard Hochmuth, Astrid Bruckmann, Christina Paulus, Michael Nevels, Hans-Helmut Niller, Adam Grundhoff and Gunter Meister.
Seduction of viral miRNA biogenesis during viral life cycle
Manuscript in preparation

Mariangela Morlando, Sama Shamloo, Johannes Danner, Astrid Bruckmann, Gunter Meister and Irene Bozzoni.
The Interplay between lnc31, pre-lnc31 and YBox1 in differentiating muscle cells (working title)
Manuscript in preparation

Presentations and Posters

Parts of this thesis were presented at the following meetings/ conferences

Symposium - From functional Genomics to Systems Biology 2014 in Munich with Poster presentation

> Exploiting peptide and antibody purification strategies to analyze post-translational modification of endogenous Argonaute and GW182

Biosysnet Group member meeting 2014 in Munich with Talk

> Regulation of microRNA biogenesis on human latent EBV and lytic CMV

Biosysnet Retreat 2015 in Wildbad Kreuth with Poster presentation

> Dissection of herpesviral microRNA biogenesis

Microymposium 2015 in Vienna with Poster presentation

> Exploiting peptide and antibody purification strategies to analyze post-translational modification of endogenous Argonaute and TNRC6 proteins

Microymposium 2016 in Vienna with Poster presentation

> Post-translational modifications of endogenous Argonaute and TNRC6 proteins

RNA Society meeting 2017 in Prague with Poster presentation

> Hyper-phosphorylation of an unstructured loop of Argonaute proteins triggers dissociation from mRNAs

Summary
Zusammmenfassung
Publications
Presentations
Contents

1 INTRODUCTION

1.1 Mammalian microRNA biogenesis

miRNAs are the core molecule for selective regulation of gene expression by initiating translational repression and mRNA decay.

miRNAs can be multiply located within the genome and they are organized as individual single unit or as cluster (V. N. Kim, Han, and Siomi 2009; Chaulk et al. 2011; Libri et al. 2013; Y.-K. Kim, Kim, and Kim 2016). Most of the miRNA genes are organized within different genomic organization patterns, mainly in intronic regions of mRNAs (Monteys et al. 2010), non-coding RNAs (nc-RNAs) (Libri et al. 2013) or independent intergenic transcription units (P. Ramalingam et al. 2014). miRNAs can be derived from other non-coding RNAs like snoRNAs, lncRNAs (Röther and Meister 2011) or tRNAs (Hasler et al. 2016), from splicing (mirtron pathway) or out of short hairpins (Y.-K. Kim, Kim, and Kim 2016).

Transcriptional regulation of pri-miRNA. The initial biogenesis and simultaneously a highly regulated step is the transcription of primary miRNA (pri-miRNA) transcripts. pri-miRNA transcripts are mainly RNA Polymerase II generated and hence contain 5' caps with 7-methyl guanosine and a 3' poly (A) tail (Cai, Hagedorn, and Cullen 2004; Y Lee et al. 2004; He et al. 2007; Raver-Shapira et al. 2007; Tarasov et al. 2007). At a co-transcriptional level, transcription factors like p53, MYC, ZEB1/2 or MYOD are known to promote or block transcription by Pol II (Pol III). For instance, p53, MYC and MYOD1 promote transcription of the miR-234-cluster, miR-17-cluster and miR-1cluster. In contrary MYC and ZEB1/ 2 inhibit transcription of mir-15a-cluster and mir-200-cluster (Rnas et al. 2008; V. N. Kim, Han, and Siomi 2009; Krol, Loedige, and Filipowicz 2010; Ha and Kim 2014; Louloupi et al. 2017).

1.1.1 Processing of primary miRNAs by the microprocessor complex

Primary miRNA processing is the first catalytic cleavage step of the canonical biogenesis pathway. The pri-miRNA transcript is incorporated into the microprocessor complex. This complex consists of the minimal components RNAse III enzyme Drosha and a dimer of DGCR8 (Figure 1) (Gregory et al. 2004; Denli et al. 2004; Han et al. 2004; Landthaler, Abdullah Yalcin and Tuschl 2004; Kwon et al. 2016). The pri-miRNA transcript forms a double-stranded RNA (dsRNA) stem-loop-structured hairpin with a stem length of usually 35 base pairs (bp) and ssRNA bulges. A single-stranded (ss) loop raises as apical structure and an adjacent ssRNA basal junction marks the end of the stem (Han et al. 2006; Nguyen et al. 2015). DGCR8 contains two double-stranded RNA-binding domains (dsRBDs) (Roth, Ishimaru, and Hennig 2013; Quick-cleveland et al. 2015; Nguyen et al. 2015; Kwon

et al. 2016). Drosha is structurally very similar to Dicer (low sequence conservation), but exhibits unique compartments like a zinc-finger motif (Figure 1) (Nguyen et al. 2015).

Drosha and DGCR8 function together as distance measuring system for specific hairpin structured RNAs (Kwon et al. 2016). Therefore, the DGCR8 dimer positions at the upper part of the stem and Drosha at the lower part of the stem. Catalytic Drosha cleavage occurs after positioning of the microprocessor at the height of 11 bp of the stem (Han et al. 2006; Nguyen et al. 2015). This aims in a typical stem-loop-structured 60-70 bp long hairpin known as precursor miRNA (pre-miRNA) with a 2 nucleotide 3' overhang (Morlando et al. 2008). Drosha deletions result in the loss of canonical processed miRNAs (Y.-K. Kim, Kim, and Kim 2016). Because of the main intronic origin of the pri-miRNA transcripts, splicing and microprocessor cleavage are interconnected and influence each other's efficiency (Y.-K. Kim and Kim 2007; Kataoka, Fujita, and Ohno 2009).

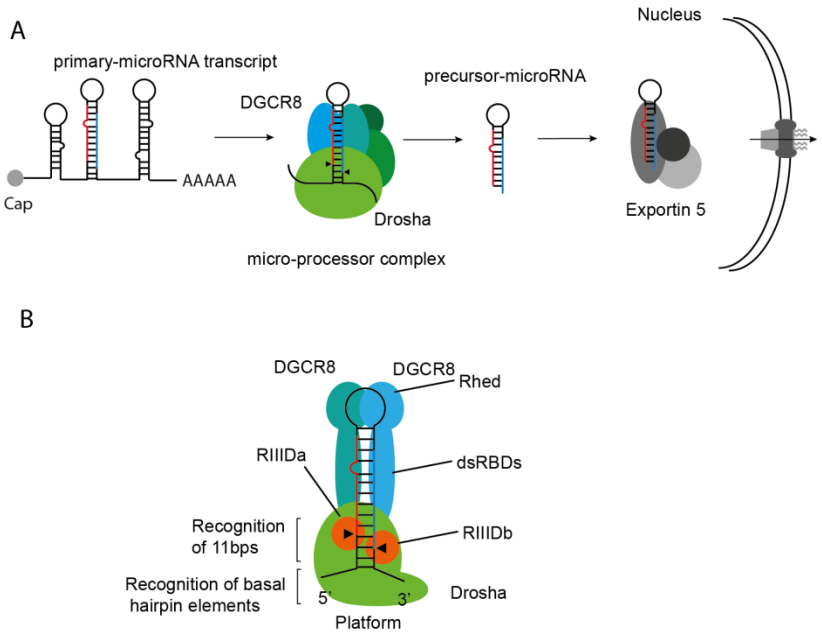

Figure 1 Cleavage of pri-miRNA transcript by Drosha and export by Exportin 5.
A stem loop structured primary-miRNA transcript with a 5‘ cap and a 3‘ poly-A-tail is transcribed by Pol II and recognized by the microprocessor complex consisting of Drosha and two DGCR8 proteins. Drosha cleaves the transcript resulting in a 70-100 bp long hairpin, called pre-miRNA. This small RNA is recognized by the nuclear export receptor Exp5 and transported into the cytoplasm and further processed by Dicer. (B) Indication of structural composition of DGCR8/ Drosha.

The pre-miRNA hairpin-structure is then exported to the cytoplasm with a canonical RNA export mechanism with Exportin-5 (Exp5) in a Ran-GTP depended manner (Yi et al. 2003; Bohnsack, Czaplinski, and Gorlich 2004; Y.-K. Kim, Kim, and Kim 2016). The loading of the pre-miRNA into Exp5-RanGTP remains unclear, but additional factors of the microprocessor complex like ILF-3 could have a major role (Libri et al. 2013).The structural mannerism of the pre-miRNA results in a specific recognition of Exp5-RanGTP (Okada et al. 2009). After nuclear exporting, the complex decomposes and the released pre-miRNA is bound by a multi-protein complex containing Dicer (K. Miyoshi et al. 2009). Interestingly, after knockout of Exp5 cytoplasmic transport still occurs suggesting redundant or alternative mechanisms (Y.-K. Kim, Kim, and Kim 2016).

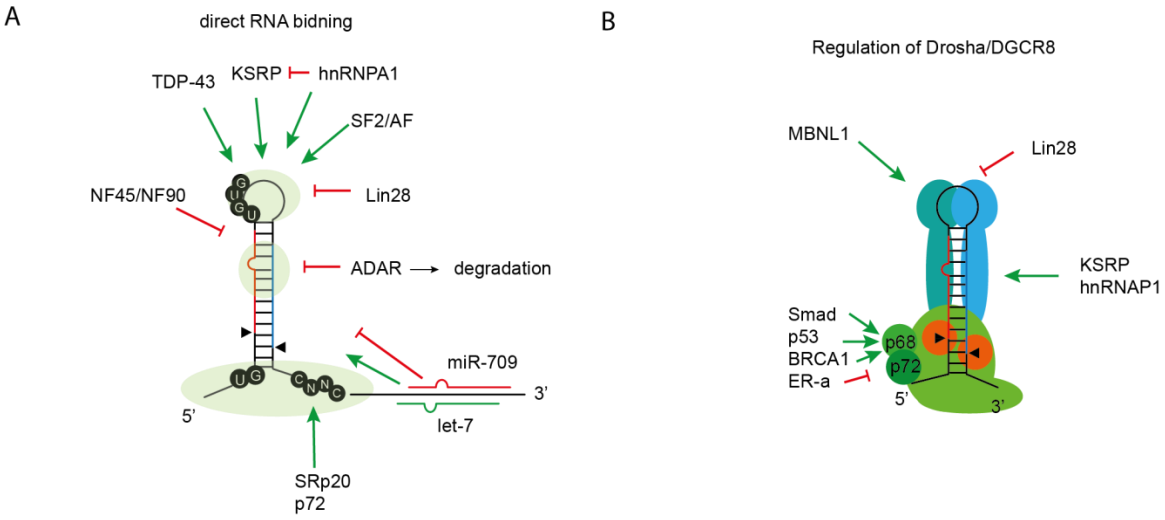

Figure 2 Examples of regulatory RBPs/RNAs.
(A) Schematic overview of a representative pri-miRNA structure containing a mature miRNA indicated in red. Interaction sites for potential regulators as well as conserved sequence motifs are highlighted. Regulatory RBPs/ miRNAs influencing the miRNA biogenesis by direct binding to the hairpin structured pri-miRNA are indicated in red by inhibiting or in green by promoting the process. (B) Regulatory RBPs/ miRNAs influencing the miRNA biogenesis are indicated in red by inhibiting or in green by promoting the process.

Regulatory mechanisms. As already suggested, the miRNA biogenesis is not only tightly regulated at a transcriptional level, but even more at the following biogenesis steps (Libri et al. 2013; Ha and Kim 2014; S. Li, Wang, Fu, and Dorf 2014). The efficiency of pri-miRNA and pre-miRNA processing underlies the sequence and/ or resulting structural characteristics of the hairpin (Auyeung et al. 2013). These specific RNA compositions are recognized by hairpin-interacting RNA-binding proteins (RBPs) which promote or block the processing steps (Han Wu et al. 2010; Trabucchi et al. 2009; Gu et al. 2011; X. Zhang et al. 2011; Connerty, Ahadi, and Hutvagner 2015; Du et al. 2015). Recently a large proteomics-based hairpin-pull-down screen identified several hundred potential interactors which regulate Drosha processing (Treiber et al. 2017). In the following part few regulatory RBPs which influence processing are briefly described.

Regulation of processing by proteins that interact with the pri-miRNA. The pri-miRNA transcript contains several conserved sequence elements that are important for processing. The loop contains a UGUG motif and at the basal flanking sites an UG and a CNNC motif (Ha and Kim 2014; Roden et al. 2017). The splicing factor Srp20 (Ajiro et al. 2015) and the DEAD-box RNA helicase p72 (DDX17) interact with the CNNC motif and promote Drosha processing (Figure 2 A) (Sabin et al. 2009; Guil and Cáceres 2007).

The RBP TAR DNA-binding protein 43 (TDP43) positively interferes with Drosha processing by binding to the terminal loop sequence of pre-miR-143 and pre-miR-547 (Kawahara and Mieda-Sato 2012; Ha and Kim 2014). Interestingly the serine/ arginine-rich SR protein (SF2/ASF) promotes processing by altering the structure of pri-miR-7. The mature miR-7 regulates the mRNA transcript

of SF2 down by gene silencing, suggesting an negative feedback loop for steady-state production of miR-7 (Han Wu et al. 2010). The RBP Rbfox3 regulates both inhibition and improvement of processing depending on the pri-miRNAs. It was suggested that many pri-miRNAs are regulated and particularly shown that interaction of Rbfox3 with the loop region of pri-miR-15a resulted in processing. In contrary binding to the stem of pri-miR-485 resulted in an inhibition of the microprocessor recruitment (K. K. Kim et al. 2014). The RBPs hnRNPA1 and KSRP (KH-type splicing regulatory protein) interact with the terminal loop of several pri-miRNAs e.g. pri-miR18a, pri-miR-16, pri-miR-21 and promote their processing (Figure 2 A) (Michlewski et al. 2008; Michlewski and Cáceres 2010; Guil and Cáceres 2007; X. Zhang et al. 2011; Briata et al. 2012) In contrary hnRNPA1 negatively regulates pri-let-7a processing while competing with KSRP for the stem binding site. The nuclear factors 45 and 90 inhibit processing by interaction to pri-let-7a or pri-miR-21 (Sakamoto et al. 2009). The RNA editing enzymes ADAR1 and ADAR2 are known to transform an adenosine to an inosine within specific pri-miRNAs, which inhibits Microporocessor hairpin interaction (Figure 2 A)(Cho, Myung, and Chang 2017).

Regulation of pri-miRNA processing by proteins that interact with the microprocessor complex. The RBP p68 (DDX5) together with p72 (DDX17) are recruited to Drosha by interaction to the hairpin and promote pri-miRNA processing (Figure 2 B). It is known that several additional factors interact with p68/p72 and further block or promote the processing. For Instance, promoting interactors are BRCA1 (breast cancer susceptibility gene 1), SNIP1 (SMAD nuclear interacting protein), ARS2 (arsenite resistance protein 2) or the TGF-β induced transcription factors SMAD1-3 and 5 (Figure 2 B). In contrary, the estrogen receptor alpha inhibits processing by an interfering interaction to p68/p72 (Davis et al. 2008; Sabin et al. 2009; Kawai and Amano 2012; Vos et al. 2015; Thillainadesan et al. 2012; Suzuki et al. 2009; Fukuda et al. 2007). Interestingly, the helicases p68/p72 are involved in the processing of nearly one-third of the known pri-miRNAs, according to studies within knock-out mice (Fukuda et al. 2007)

Regulation of pri-miRNA processing by miRNAs. Several examples where miRNAs are transported back to the nucleus for the regulation of pri-miRNA processing are known. The interaction to the pri-miRNA is formed by complementary base pairing within the flanking regions of the primary transcript. For example, in *C. elegans* the processing of pri-let-7 is promoted by an auto-regulatory mechanism of let-7 which interacts with the pri-let-7 3’ flanking region. The mechanism of how the miRNA-Alg-1 complex promotes processing is not fully understood (Figure 2 A) (R. Tang et al. 2012; Zisoulis et al. 2012).

Drosha/ DGCR8 regulatory modifications. The functionality of the microprocessor complex is additional regulated by PTMs. Drosha localization in the nucleus is regulated by phosphorylation

of S300 and S302 by GSK3. DGCR8 exhibits higher stability when phosphorylated by ERK. Sumoylation at K707 by SUMO1 stabilizes DGCR8 by inhibiting ubiquitination (C. Zhu et al. 2015; Fletcher et al. 2017). Further Drosha is stabilized by acetylation which inhibits ubiquitination. In contrary the affinity to pri-miRNAs and hence processing is increased by deacetylation of DGCR8 by HDAC1 (histone deacetylated by histone deacetylase1) (X. Tang et al. 2010; X. Tang et al. 2011; X. Tang et al. 2013; Casseb et al. 2016).

1.1.2 Dicer cleavage of pre-miRNAs and RISC loading

In the cytoplasm the pre-miRNA is released from the Exp5-RanGTP complex and immediately incorporated into Dicer. Dicer is structurally similar to Drosha a RNase III enzyme. It contains also two RNase III catalytic cleavage sites. For proper positioning and function, additional co-factors are needed. The cofactor TAR RNA binding protein 2 (TRBP) and the protein activator of PKR (PACT) contain both double-stranded-RBDs and additionally promote the substrate interaction (Gregory et al. 2005; Chendrimada et al. 2010; Yoontae Lee et al. 2006; H. Y. Lee et al. 2013). TRBP functions as a pre-miRNA length determining compartment through a defined positioning of the hairpin by interaction with the helicase domain of Dicer (Fukunaga 2005). The function of PACT remains elusive and is still unclear (Figure 3) (H. Y. Lee et al. 2013; Y. Kim et al. 2014; Ha and Kim 2014). TRBP mainly interacts with the apical loop and the upper part of the stem. After the pre-miRNA is positioned, Dicer interacts with the precursor and cleaves off the terminal loop. This occurs within the catalytically active centre of the RIIId domains. The cleavage product is a 21-24 nt long double-stranded RNA with 2 nucleotides 3’-overhangs, a 5’-phosphate and a 3’-hydroxyl group (H. Zhang et al. 2004; MacRae et al. 2006; Taylor et al. 2013; Wilson et al. 2015; Fareh et a l. 2016; Song and Rossi 2017). The ssRNA terminal loop as additional cleavage product is degraded. After cleavage occurred, the RISC loading complex is assembled. Therefore, Dicer interacts with Ago via the Piwi and the RNase III domain. Additionally Ago recruits co-chaparones with the components heat shock protein 90/70 (Hsp90) and FK506-binding immunophilins Fkbp4/5. The HSP70/HSP90 complex loads the RNA duplex into Ago in an ATP dependent manner (Iwasaki et al. 2010). During the loading process one strand of the miRNA heteroduplex is selected and imparted to Ago while the chaperones stabilize the opening and incorporation process into Ago (Figure 3).

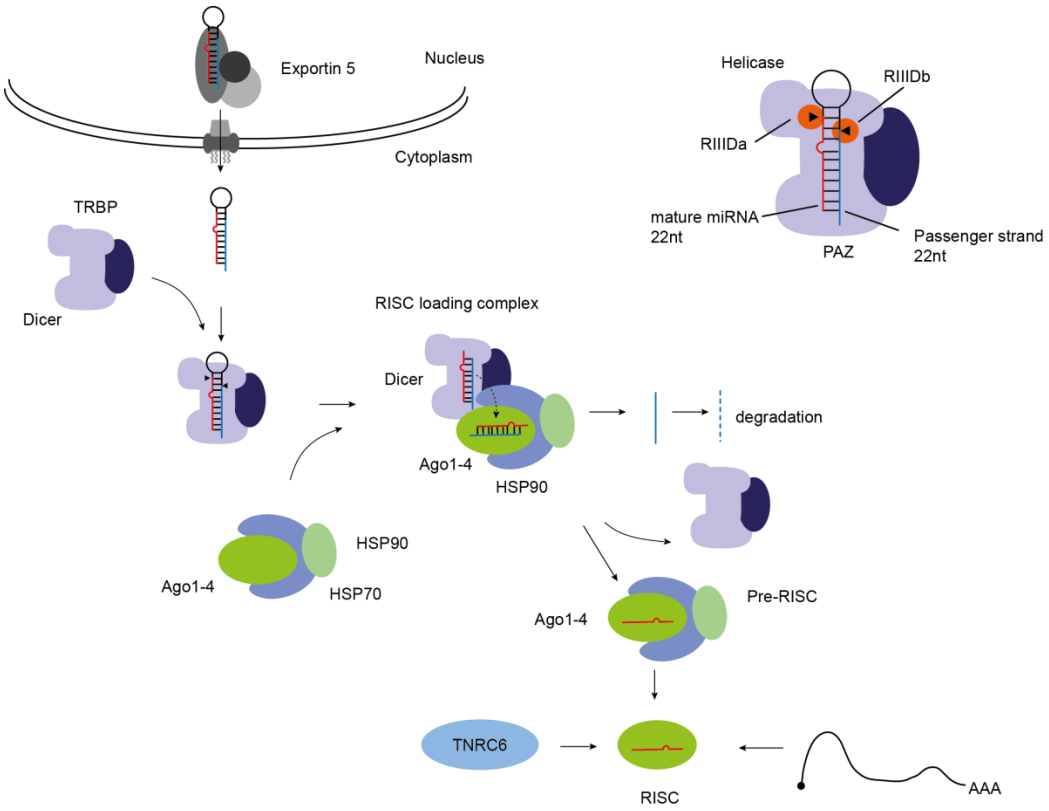

Figure 3 Dicer cleavage of the pre-miRNA and RISC complex loading.
This small RNA is recognized by the nuclear export receptor Exp5 and transported to the cytoplasm and further processed within the catalytic domains of the Dicer/TRBP complex. Dicer/TRBP form a multi-subunit complex where TRBP is responsible for positioning of the pre-miRNA. This results in a double-stranded RNA with 22 nt length. The mature strand is incorporated into Ago during RISC loading and leads to the mature RISC complex assembly.

An unwinding of the dsRNA strand is mediated by the N domain of Ago and the selection of one strand which is maybe supported by TRBP has to be performed (Kwak and Tomari 2012). However, statistical and thermodynamically rules suggest that the strand with a stable 5' end is preferentially loaded (Dueck and Meister 2014; T. Miyoshi et al. 2010; Natalia J Martinez et al. 2013; Iwasaki et al. 2010; Nakanishi et al. 2016). After loading Dicer and the co-chaperones dissociate which leads to the mature RISC complex (Kawamata and Tomari 2010; Dueck and Meister 2014; K. Miyoshi et al. 2009).

Regulation of processing by proteins that interact with the pre-miRNA. Rbfox2 another RBP is suggested to be important for cancer and neurodegeneration induced by the mis-regulation of miR-107 and miR-20b. This miRNAs are suppressed by the interaction with Rbfox2 under certain conditions. This leads to a inhibition of Dicer cleavage and hence processing (Yu Chen et al. 2016). At the Dicer cleavage stage, several RBPs seem to compete for the binding to the terminal loop of the pre-miRNAs. For instance MBNL1 competes with Lin28 and hence U tailing and degradation is blocked (Androsavich and Chau 2014; Rau et al. 2011).

Surprisingly also base modifications of pre-miRNAs regulate Dicer interaction. For Instance Dicer recognition of the 5' monophosphate is blocked by methylation of the 5’ end of the pre-miR-145 by the human RNA-methyltransferase BCDIN3D (Xhemalce, Robson, and Kouzarides 2012; Park et al. 2011).

Regulatory mechanisms during Dicer cleavage. As already suggested the miRNA biogenesis is not only tightly regulated at transcriptional level, but even more at the pre-miRNA biogenesis step by many RBPs which interact with the pre-miRNA and the Dicer/TRBP complex (Figure 4) (Libri et al. 2013; Ha and Kim 2014; S. Li, Wang, Fu, and Dorf 2014). Here, few examples which influence Dicer cleavage are presented. The most prominent example of negative influence on pre-miRNA processing is the stem cell factor lin28 that interacts with the members of the let-7 family (also observed for miR-107, miR143, etc.). The RBP lin28 consisting of a Cold shock and a CCHC-type Zincfinger domain interacts with the GGAG motif of the terminal loop of the pre-let-7 members except let-7a-3/c-2. Through the interaction the enzymes terminal uridyltransferases TUT4 (ZCCHC11) or TUT7 which uridylates the pre-miRNAs are recruited (Figure 4) (L. Wang et al. 2017; Triboulet, Pirouz, and Gregory 2015). This short poly (U) tail at the 3’ end of the pre-miRNAs interferes negatively with Dicer cleavage and leads to 3’ to 5’ degradation of the pre-miRNA by DIS3L2. The inhibition of pre-let-7 biogenesis blocks important developmental processes, causing the cells to stay at a stem cell level (Newman, Thomson, and Hammond 2008; Rybak et al. 2008; Heo et al. 2008; Heo et al. 2009; Viswanathan, Daley, and Gregory 2008; Thornton et al. 2014; Shyh-Chang and Daley 2013; Triboulet, Pirouz, and Gregory 2015; Hao-ming Chang et al. 2013). Interestingly, lin28 is a phospho-protein which is modified by ERK/MAPK at several residues and hence stabilized in pluripotent stem cells (Tsanov et al. 2017; Xiangyuan Liu et al. 2017). In contrary of inhibition, TUT4, TUT2 and TUT 7 are reported to monouridylate a specific set of pre-miRNAs including pre-let-7 at the 3’. This additional uridylation promotes Dicer cleavage in non-stem cells which lack Lin28 (Heo et al. 2012).

Regulation of pre-miRNA processing by other RNAs. Other RNAs can block dicer pre-miRNA interaction and recognition. For instance the adenoviral RNA VA1 competes with the pre-miRNAs for Dicer interaction and hence inhibits the processing (Libri et al. 2013).

A recent study reports a dysregulation of miR-7 and miR-671 induced by a downregulation of circRNA Cdr1as that interacts with the named miRNAs. Interestingly, the data illustrates the downregulation of the miR-7 by the loss of the circRNA, hence an influence on pre-miRNA processing is suggested (Figure 4) (Piwecka et al. 2017).

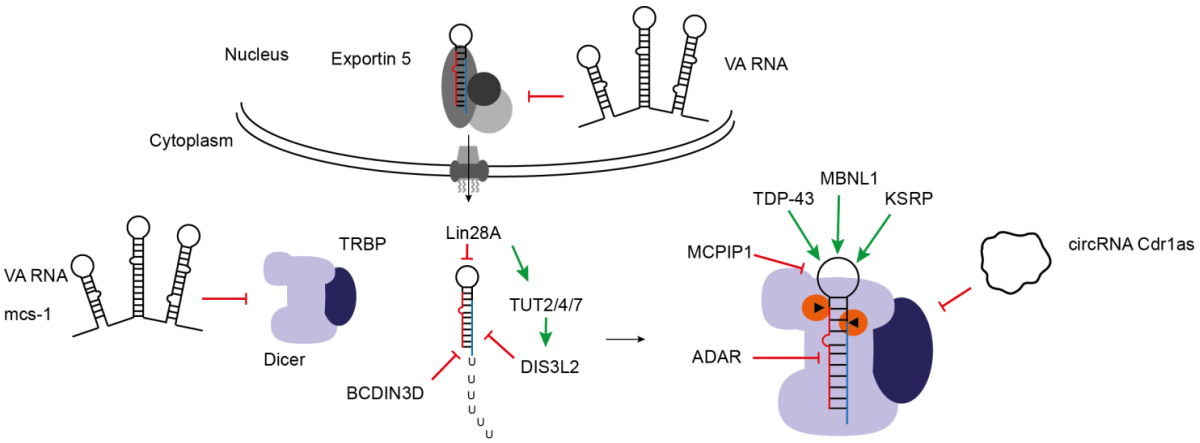

Figure 4 Regulation of Dicer cleavage.
This small RNA is recognized by the nuclear export receptor Exp5 and transported to the cytoplasm and further processed by Dicer. This results in a double-stranded RNA with 22 nt length. The mature strand is incorporated into Ago during RISC loading and leads to the mature RISC complex. During this stepwise process many RBPs positively (green arrows) or negatively (red arrows) influence this process. Regulatory RNAs influencing the miRNA biogenesis are indicated in red by inhibiting the process.

Regulation of pre-miRNA export. The export mechanism is known to be blocked by few RNAs that bind to Exportin-5. For instance the adenoviral non-coding RNA VA1 inhibits miRNA export to the cytoplasm by competing with the endogenous pre-miRNAs for binding to Exportin- 5. Hence less pre-miRNAs are transported to the cytoplasm (Figure 4) (Y.-K. Kim, Kim, and Kim 2016; Libri et al. 2013; Lu and Cullen 2004; Grimm et al. 2006).

Dicer/ TRBP modifications and further functions. The Dicer/ TRBP complex is stabilized by TRBP phosphorylation by the MKK1/Erk pathway which causes selectively enhanced miRNA processing for growth-promoting miRNAs (Paroo et al. 2009). An additional phosphorylation occurs at S283/286 by S6 kinase which leads also to enhanced miRNA processing and links the miRNA biogenesis machinery to the mTOR pathway (C. Xu et al. 2016). A recent study reports the phosphorylation of TRBP by MAPK, which stabilizes the complex to Lin28a. This interaction leads to reduced let-7 levels and hence to an induced neuronal dendritic spine growth (Amen et al. 2017).

Further sumoylation of TRBP at K52 inhibits ubiquitination at K48, stabilizes the complex and promotes RISC loading (C. Chen et al. 2015). In *C. elegans* oocytes it was observed that Dicer is phosphorylated by ERK which causes inhibition of Dicer activity. This inhibition is reactivated before fertilization starts in the oocytes (Drake et al. 2014). Of note, Dicer seems to have a certain nuclear role in double-stranded DNA repair when phosphorylation is induced by DNA damage at S1016, S1728 and S1852 (Burger et al. 2017).

1.2 Gene silencing and translational repression

The mature RISC complex contains a miRNA incorporated in Ago. It finds its mRNA target during a less understood scanning mechanism through complementary base pairing of the seed sequence with the 3' untranslated region (3'UTR) of the targets. The state of Ago during scanning in terms of protein interactors and regulatory modifications remains speculative. The minimal RISC is supposed to interact with mRNA and/or the TNRC6 proteins. However, it is still unclear whether interactions are at the same time, sequential or simultaneous. Further, it is assumed that the target scanning process and also translational repression and /or storage takes place or is next to structured protein networks of various size called p-bodies (Patel, Barbee, and Blankenship 2016; Zipprich et al. 2009; J. Liu et al. 2005; Wilczynska and Bushell 2015; S. Lee and Vasudevan 2013; Kamenska et al. 2016). As a consequence of Ago-miRNA-mRNA-TNRC6 complex assembly, translational repression and mRNA decay are initiated. These processes are mainly induced by proteins and enzymes that are recruited sequentially or in parallel by TNRC6. Ago functions conclusively as initial target finding enzyme and mediates through binding to TNRC6 gene silencing (Jonas and Izaurralde 2015; Dueck and Meister 2014).

1.2.1 Interplay of TNRC6 and Ago

1.2.1.1 TNRC6 functions as core binding platform of the gene silencing process

TNRC6 proteins belong to the family of GW proteins. The best known member is GW182 found in *D. melanogaster* (human homolog TNRC6A). Mammals express two additional paralogs TNRC6B, C and many uncharacterized isoforms. In general, TNRC6 proteins are structurally and functionally conserved from an evolutionary point of view. They may have evolved by the development of multicellularity and whole genome duplication to three paralogs within the vertebrates (Zielezinski and Karlowski 2015; Mauri et al. 2017). TNRC6 proteins consists of two main regions, the N-terminal Ago binding domain (ABD) and the C-terminal silencing domain (SD). Glycine-Tryptophan (GW, W, GWG, WG) repeats are randomly distributed over the whole proteins, especially in the ABD and the SD. Ago proteins interact through specific binding of two binding pockets located in the PIWI domain with two Ws located in the TNRC6 ABD (see Figure 6 and Table 1) (Braun et al. 2011; Jonas and Izaurralde 2015; Huntzinger and Izaurralde 2011; Pfaff et al. 2013). This specific interaction is conserved within the mammalian Ago 1-4 proteins. Interestingly, there are very limited regions within this various GW repeats in the ABD where Ago proteins interact.

However, the specificity or selectivity of this process is not understood. It is suggested that a specific distance of 10 amino acids combined with a specific amino acid pattern determines the binding process (Pfaff et al. 2013; Hauptmann et al. 2015). Altogether, three binding hot spots on TNRC6A are known. These hotspots may interact also with Agos at the same time (Elkayam et al. 2017). It is further known that the TNRC6 paralogs may contain a different number of Ago interaction sites. They are partly conserved, e.g. TNRC6B possesses two and TNRC6A has three interaction sites (Takimoto, Wakiyama, and Yokoyama 2009; Nishi et al. 2013; Pfaff et al. 2013; Hauptmann et al. 2015a; Baillat and Shiekhattar 2009). TNRC6 proteins are suggested to function redundantly and to interact with all Ago1-4 proteins without preferential combinations.

Table 1 Domain organization of mammalian TNRC6 paralogs (adapted from Uniprot database).

Paralog	Domain	Position [aa]	Length	Function
TNRC6A	ABD	1-932	932	Interaction with Argonaute family proteins
	RRM	1781-1853	73	Function unknown
	PAM2	1604-1622	19	PABPC1-interacting motif-2
	Gln-rich	93-127	35	Function unknown, p-body localization?
	Ser-rich	192-365	174	Function unknown
TNRC6B	ABD	1-994	994	Interaction with Argonaute family proteins
	RRM	1648-1720	73	Function unknown
	PAM2	1472-1490	19	PABPC1-interacting motif-2
	SD	1218-1723	506	Interaction with CNOT1 and PAN3
	Pro-rich	825-880	56	Function unknown
	Gln-rich	1150-1220	71	Function unknown, p-body localization?
TNRC6C	ABD	1-926	926	Interaction with Argonaute family proteins
	RRM	1565-1632	68	Function unknown
	PAM2	1381-1399	19	PABPC1-interacting motif-2
	SD	1260-1690	431	Interaction with CNOT1 and PAN3
	n.n.	1596-1690	95	Interaction with the CCR4-NOT
	n.n.	1371-1690	320	Sufficient for translational repression when tethered to target
	UBA	933-978	46	Ubi interaction site
	Gly-rich	204-430	227	Function unknown
	Thr-rich	756-777	22	Function unknown
	Pro-rich	1215-1248	34	Function unknown, p-body localization?

The central part of TNRC6 contains a number of gene silencing independent domains. A typical ubiquitin-associated (UBA)-like domain which is involved in the proteasomal degradation (Figure 6). The UBA-like domain folds into a trimeric helix bundle with hydrophobic regions for ubiquitination probably by the E3 ubiquitin ligase TRIM65 (S. Li, Wang, Fu, Berman, et al. 2014; Buchberger 2002; V. S. and A. F. Lau 2009).

Next to the UBA a nuclear localization signal (NLS) and a nuclear export signal (NES) are located within the middle region in TNRC6A (Figure 6). Recently the structural composition of the TNRC6A NLS interacting with importin α was solved (Chaston et al. 2017). TNRC6B and C contain just a NES at a similar position; the location of the NLS is unknown. The NLS and NES recruit additional proteins like importin β which leads to nuclear shuttling (Nishi et al. 2013; Schraivogel et al. 2015).

All TNRC6 proteins contain several domains where specific residues are enriched e.g. a glutamine- and proline-rich region in TNRC6B. The location of these domains is partly conserved. However, their function is unknown, but mechanisms in p-body assembly/location are suggested for the Q-rich region within TNRC6B (Lazzaretti, Tournier, and Izaurralde 2009).

The C-terminal SD contains a PAM2 motif, a RRM and many Ws important for the interaction with the CCR4-Caf1-NOT and the trimeric Pan2-Pan3 complex (Figure 6. A interaction of TNRC6 with the decapping complex is not known. Interestingly, the SD mediates translational repression and mRNA decay when proximal mRNA is present (Zipprich et al. 2009; Lazzaretti, Tournier and Izaurralde 2009; Eulalio, Tritschler, et al. 2009). While Ago has the target recognition and gene silencing initiation function, TNRC6 serves as a binding platform and as mediator for all downstream processes (see Figure 6 and Table 1).

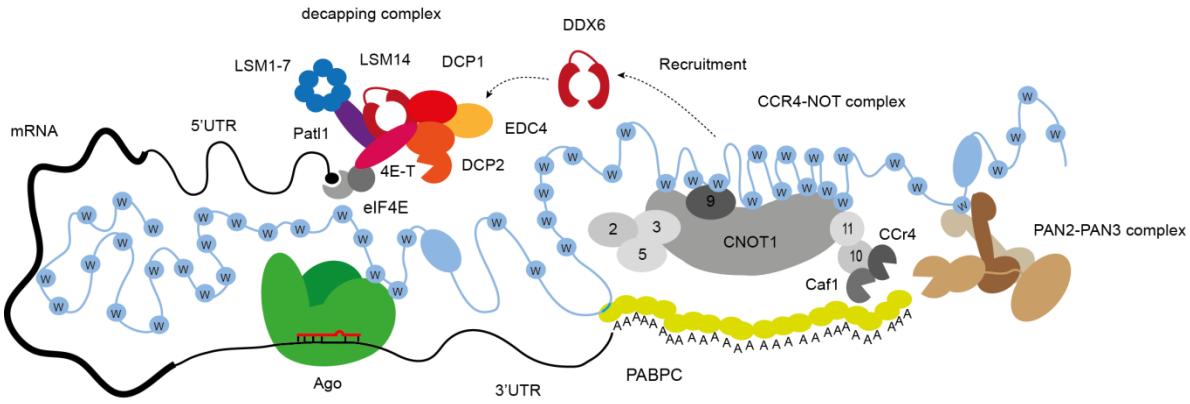

Figure 5 Schematic model based on functional and structural aspects of the miRNA-mediated gene silencing process. A functional miRNA-mediated gene silencing complex requires at least one Argonaute protein, one TNRC6 protein, several Poly-A-binding proteins (PABPC1), and the PAN2–PAN3 and CCR4–caf1-NOT deadenylase complexes. The decapping complex is recruited by DDX6 and consists of the core subunits EDC4, DCP1-2 and others. Translational repression and destabilization of the target mRNA leads to 5'-to-3' decay through exonucleases like XRN1 which is in direct neighbourhood within the p-bodies.

The RRM of *D. melanogaster* GW182 (human homolog TNRC6A) lacks the ability to bind RNA. Nevertheless, it is required for the full function of gene silencing and is therefore suggested to may bind additional unknown protein interactors. The atypical RRM and UBA are the only defined structured parts of TNRC6 proteins.

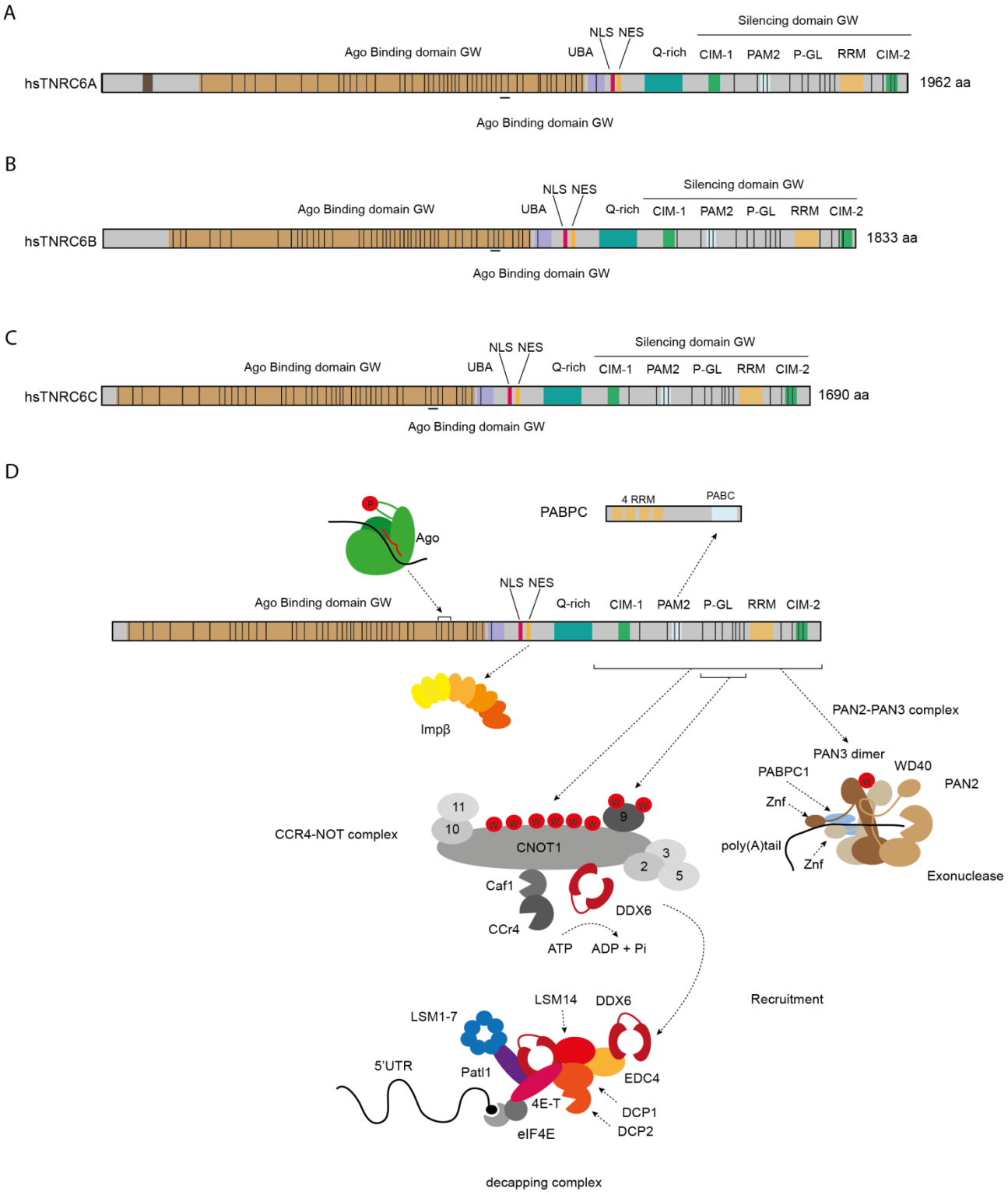

Figure 6 Schematic model of TNRC6 domain organization based on functional and structural aspects of the miRNA-mediated gene silencing process.
(A), (B), (C), (D) domain organization of TNRC6A-C. Vertical black bars represent the relative positions of tryptophan's. Different domains and regions are marked in different colour, abbreviations can be found within the text. (D) Ago proteins bind to two Ws in the ABD. Importin beta may bind to the NLS/NES region to transport TNRC6 into the nucleus. CRM1 (not shown) interacts in the same region as imp beta.Pan2-Pan3 trimer interacts through Pan3 dimer with a W from TNRC6. CCR4-Caf1-NOT complex interacts with TNRC6 with several Ws interactions of cNOT1 and cNOT9. Decapping complex is not interacting with TNRC6.

The PAM2 motif interacts with the first PABPC1 linked to the poly (A) tail and thus leads to an indirect mRNA positioning (Jonas and Izaurralde 2015) (Figure 6). The interaction with the CCR4-Caf1-NOT deadenylation complexes is thought to be similar to the Ago-TNRC6 interaction, meaning that the interaction relies on tryptophan insertion into binding pockets to the respective protein partner. After recruiting the complex by Ago-TNRC6, deadenylation will be completed and the mRNA will be finally degraded. In case of miRNA independency, translational control through deadenylation also occurs (Collart, Panasenko, and Nikolaev 2013; Gupta et al. 2016).

Binding occurs with the main subunit cNOT1 that possesses a similar function as TNRC6. cNOT1 is also considered as a scaffold binding platform for the catalytic deadenylases Caf1 and CCR4a and other subunits(Figure 6).

The interaction of cNOT1 with TNRC6 relies on several Ws together with the regions CCR4-interacting-motif1/ 2 (CIM-1/ CIM-2). Furthermore, NOT9 contacts two Ws of TNRC6 with unknown position and interacts with cNOT1. Both interactions are limited to the silencing domain which causes the downstream silencing effects (see Figure 6 and Table 1) (Braun et al. 2011; Chekulaeva, Filipowicz and Parker 2009; Chekulaeva et al. 2011a; Fabian et al. 2013a; Ying Chen et al. 2014).

The trimeric Pan2-Pan3 deadenylation complex consists of the catalytic deadenylase Pan2 and two Pan3 proteins. This complex mediates mRNA association both through PABPC1 interaction and by direct binding to the poly(A) tail through a zinc finger domain (see Figure 6 and Figure 6) (Wolf et al. 2014; Jonas et al. 2014). It is thought that the Pan3 dimer assembly leads to a formation of a W binding pocket which further stabilizes and strengthens the interaction to TNRC6 (see Figure 6)(Braun et al. 2011; Christie et al. 2013; Jonas et al. 2014; Wolf et al. 2014).

All three TNRC6 paralogs function redundantly and promote post-translational gene silencing (PTGS). Individual K.O.s indicated no reduction in tethering assays. Inhibition of all three paralogs leads to a strong de-repression comparable to de-repression assays conducted with the T6B peptide (Hauptmann et al. 2015a; Danner et al. 2017). As binding platforms, TNRC6 proteins are required to be unstructured to allow a flexible and dynamic change of interaction partners as well as to assemble within bigger structured gene silencing compartments (see Figure 6) (Jonas and Izaurralde 2015).

There are many reports in literature that report on additional binding partners of TNRC6 proteins. These are not yet fully related to a functional subunit or understood. For instance, recent reports suggest additional interactions with LIM1, which binds to the ABD, and is suggested to have a regulatory role within the gene silencing mechanism (S. Li, Wang, Fu, Berman, et al. 2014; E. Wu et al. 2016; Bridge et al. 2017).

1.2.1.2 Subcellular localization of TNRC6-Ago complexes

The mammalian miRNA mediated gene silencing is suggested to occur in the cytoplasm. Therefore, the associated functional proteins are also mainly located in the cytoplasm. The function determines localization, hence depending on main or auxiliary function, the subcellular position of the proteins to other cellular compartments can switch. For instance it is reported that gene silencing occurs at terminal axons or that TNRC6 proteins have putative functions in the nucleus (Figure 7) (Kalantari, Chiang, and Corey 2016; N. R. Sharma et al. 2016; Schratt et al. 2006). Hence many different cell lines and tissues exhibit a particular localization and expression pattern of TNRC6 and Ago Proteins (Schraivogel et al., n.d.; Rüdel et al. 2008; Keith T. Gagnon, Liande Li, Bethany A. Janowski 2012; Hauptmann et al. 2015b).

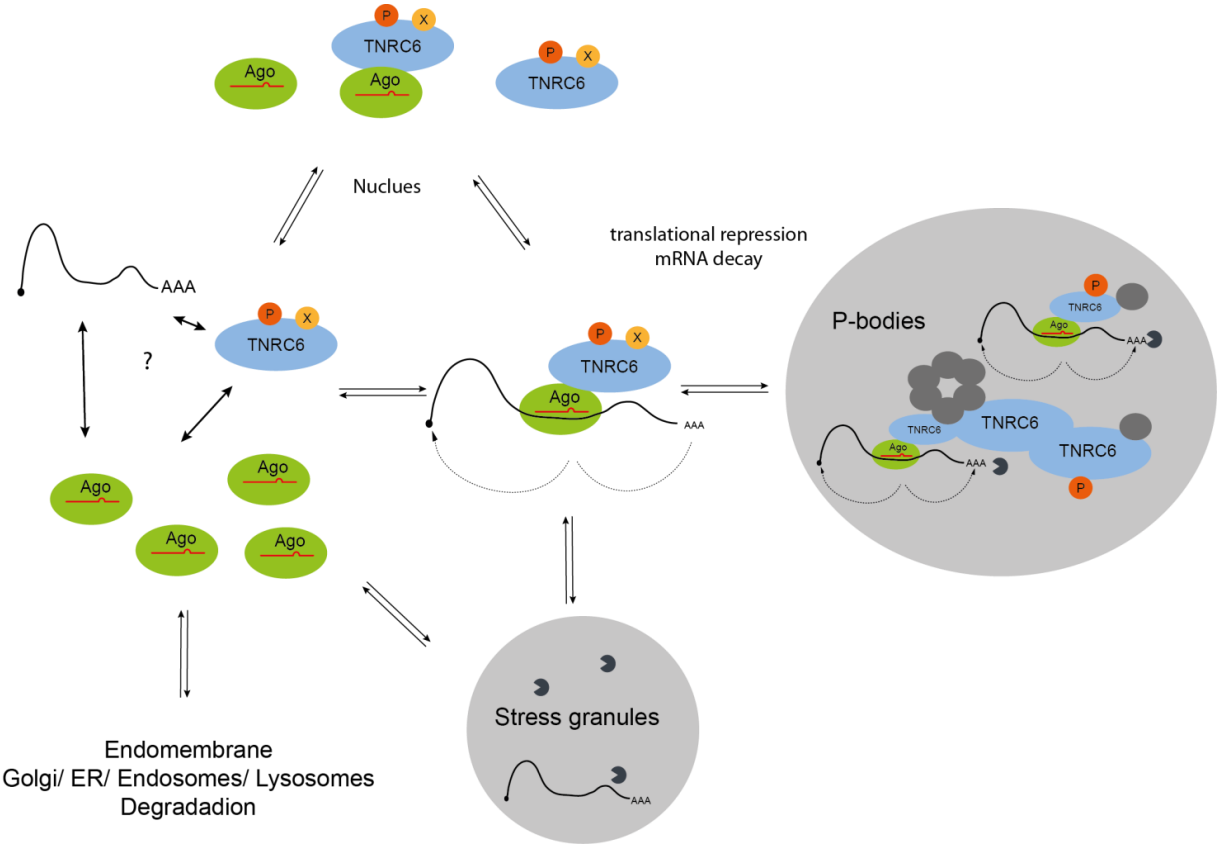

Figure 7 Subcellular localization of the gene silencing process.
A dynamic fast switching system triggered by regulatory stimuli determines the intracellular localization of Ago-TNRC6 complexes from single molecules to highly structured networks.

TNRC6 and Ago proteins seem to shuttle into the nucleus as single molecules or as complex. Ago is imported through canonical redundant mechanisms and has potential chromatin associated functions (Ameyar-Zazoua et al. 2012). TNRC6 is mainly imported into the nucleus by importin alpha/beta and exported by CRM1 dependent mechanisms (Schraivogel et al.,2015). It is

suggested that TNRC6 may act as binding platform for different nuclear processes such as splicing and transcription. However, this assumption is speculative and relies on proteomic screens which were performed lacking conclusive functional assays and necessary controls (Kalantari et al. 2016). According to IF stainings, TNRC6 proteins localize within the cytoplasm in small complexes and large structured processing-bodies (p-bodies) when bound to Ago. The functional subunit, called p-bodies was, extensively studied in the last decades and many mRNA related functions were found such as mRNA decay (deadenylation, decapping complexes, exonucleases), translational repression (TNRC6-Ago), PTGS (TNRC6-Ago, deadenylase and decapping complexes) and nonsense mediated decay (UPF1/2/3 etc.) (Kulkarni, Ozgur, and Stoecklin 2010; S. Lee and Vasudevan 2013). The architecture of p-bodies exhibits a structural binding network and fast, dynamic and flexible changing mRNA-complexes (Figure 7). Purification of p-bodies is difficult, therefore, most studies use IFs to detect p-bodies in overexpressed conditions (Rüdel et al. 2008). Optical detection of small endogenous p-bodies yield unreliable data and estimation of size is difficult. It is suggested that the real processing bodies are smaller, dynamic and fast changing/adapting network systems which can also store mRNA-RBP complexes. However, this remains speculative (Meister et al. 2005; Pillai et al. 2005; Leung, Calabrese, and Sharp 2006; Eulalio et al. 2007; Eulalio, Behm-Ansmant, and Izaurralde 2007; Rajgor et al. 2014; S. Lee and Vasudevan 2013; Pitchiaya et al. 2017).

Overexpressed TNRC6 itself co-localizes mainly with p-body markers like Lsm4. Interestingly Ago proteins show weaker co-localization with p-bodies (Schraivogel et al. 2015; Nishi et al. 2013). Above all in an endogenous manner, it was even shown that p-body location is not required for TNRC6-Ago interaction (Lazzaretti, Tournier, and Izaurralde 2009). This findings suggests, that Ago proteins and PTGS are located around the p-bodies (N. R. Sharma et al. 2016; Pitchiaya et al. 2017). Ago can also be found in other compartments, e.g. in extracellular signalling vesicles (exosomes) (McKenzie et al. 2016) and under certain stress conditions in stress granules (Figure 7) (Anderson and Kedersha 2008; Detzer et al. 2011; Rieckher and Tavernarakis 2017; Buchan and Parker 2009). In general, gene-silencing complexes such as the RISC loading complex are associated with the endomembrane system consisting of the ER, Golgi complexes, endosomes and lysosomes (Figure 7) (Y. J. Kim, Maizel, and Chen 2014; D Gibbings et al. 2012; Derrick Gibbings et al. 2013; N J Martinez and Gregory 2013; Barman and Bhattacharyya 2015).

1.2.2 Canonical post-transcriptional gene silencing

The initiation of translational repression and mRNA degradation is induced by binding of the miRNA seed sequence to the target. Binding occurs through complementarity of the bases 2 - 8 of the miRNA with the 3' UTR of the mRNA or in rare cases in other regions like the 5' UTR (Hafner et al. 2010; Hausser et al. 2013; G. Li et al. 2016; Ørom, Nielsen, and Lund 2008). Thereby, repression is triggered while the translational initiation closed loop structure is assembled (Figure 8). This structure is formed by the poly (A) tail bound to the cytoplasmic poly (A)-binding Protein (PABPC1) which interacts with eIF4G within the 5'cap structure (Jackson, Hellen, and Pestova 2010).

The target finding process is suggested as highly regulated through internal or external signals (Giraldez et al. 2005; van Rooij et al. 2007; Avraham and Yarden 2012). Furthermore, the question of target capability of many miRNAs remains unsolved, because a single miRNA can bind many mRNAs and the other way round, a mRNA can interact with many miRNAs. The occurrence of proper target finding is not well understood, as it also strongly depends on the mRNA/transcript expression profile (and turnover) of specific cell and tissue types (Rüegger and Großhans 2012; Dueck et al. 2012; Jacobsen et al. 2013; S. Wu et al. 2010).

To induce mRNA degradation, GW182 (or human paralogs TNRC6A-C) interacts through the minimal miRISC with the mRNA. Additionally, PABPC1 binds the PAM2 motif within TNRC6 to form a stable structured complex (Figure 8) (in *D. melanogaster* with additional W interactions) (Chekulaeva 2011). The detailed mechanism of the interaction of PABPC1 to TNRC6 is controversial discussed. It is assumed that translational repression is independent of this interaction because deadenylation through CCR4-Caf1-NOT and Pan2-Pan3 still occurs which leads to mRNA decay (Fabian et al. 2009; Braun et al. 2011; Jinek, Coyle, and Doudna 2011; Zekri, Kuzuoğlu-Öztürk, and Izaurralde 2013; Fabian et al. 2013b). Nevertheless, the interaction of TNRC6 with PABPC1 may decompose the closed loop structure through eIF4G dissociation (Figure 7) (Zekri et al. 2009; Fabian et al. 2009).

Nevertheless, within the canonical pathway the translational repression complex is formed, the closed loop structure is opened and subsequently the deadenylase complexes consisting of the CCR4-Caf1-NOT and Pan2-Pan3 are recruited. Both units interact with several Ws of the C-terminal silencing domain of TNRC6 (Makino et al. 2015; Zipprich et al. 2009; Chekulaeva et al. 2011b; Lazzaretti, Tournier, and Izaurralde 2009; Eulalio, Huntzinger, et al. 2009; Eulalio, Tritschler, and Izaurralde 2009).

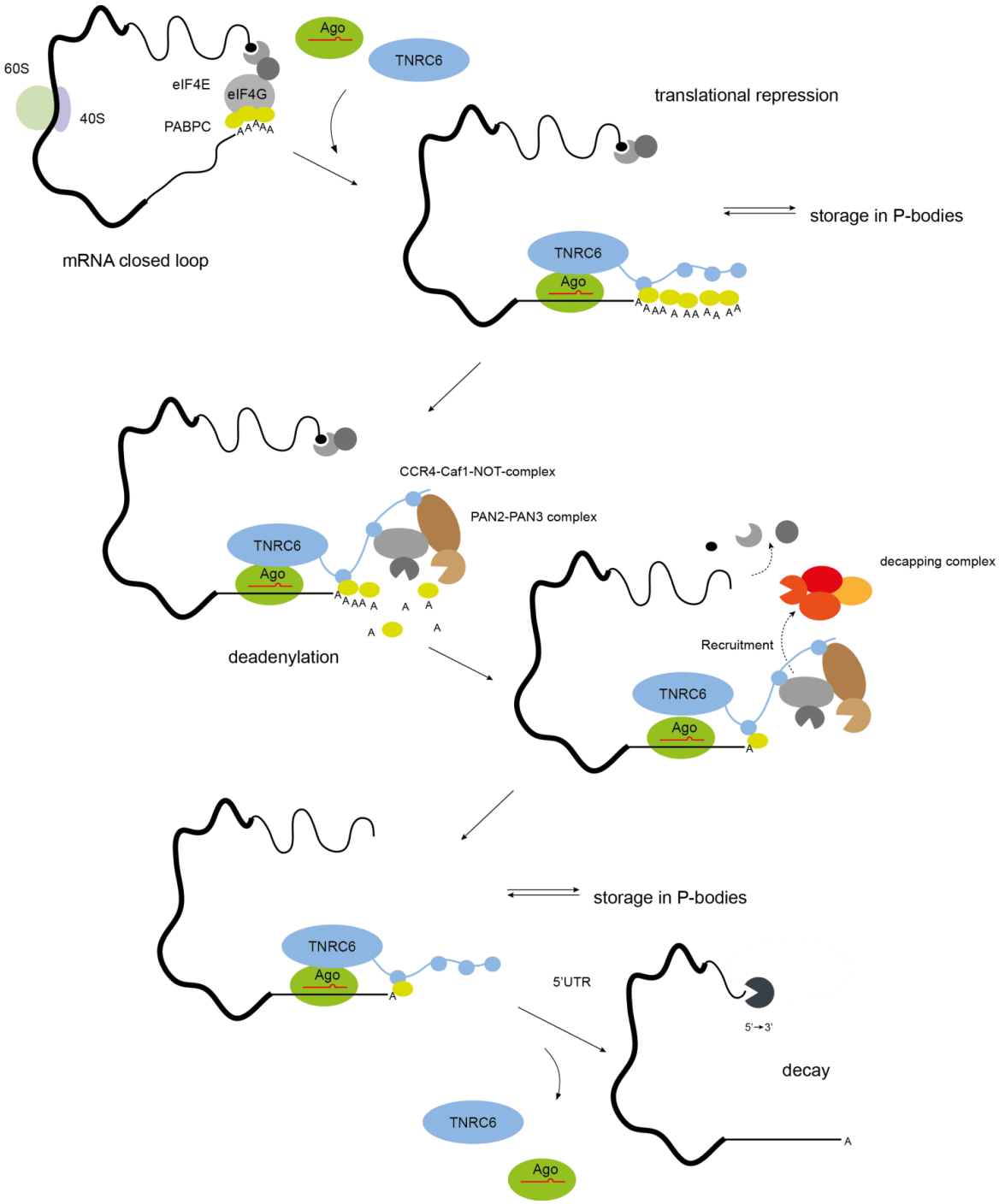

Figure 8 Small RNA mediated gene silencing by the mature RISC complex.
Different steps of the miRNA mediated gene silencing process are combined in a schematic chronological multistep illustration based on structural and functional information. Briefly, the minimal miRISC mediates gene silencing through complementary mRNA target binding together with TNRC6. Binding of RISC to a partially complementary mRNA at the seed sequence region results in repression of translation. This subsequently leads to deadenylation through the deadenylase complexes CCR4-Caf1-Not and Pan2 –Pan3 that are recruited by their mediator TNRC6. The mRNA is further destabilized through 5'decapping initiated by a DDX6 mediated recruitment of the decapping complex consisting of EDC1/2. After completing the mRNA destabilization, translational repression complex detaches which leads to 5' to 3' decay through p-body located exonucleases like XRN1.

Deadenylation and parallel dissociation of PABPC1 is then thought to be initiated by Pan2-Pan3 as first step. Followed by further diminishing of the poly (A) tail by the CCR4-Caf1-NOT complex until completing of deadenylation leads to a parallel DDX6 mediated recruitment of the decapping complex (Fabian and Sonenberg 2012; Subtelny et al. 2014; Wahle and Winkler 2013; Yamashita et al. 2005). Interestingly, only the CCR4-Caf1-NOT complex leads to complete deadenylation and subsequent decay (Huntzinger et al. 2013; Piao et al. 2010; Behm-Ansmant et al. 2006; Eulalio, Tritschler, and Izaurralde 2009; Yamashita et al. 2005). The Dead-box helicase DDX6 interacts with the MIF4G domain of cNOT1 (Ying Chen et al. 2014). Upon interaction it is activated and is suggested to recruit the decapping complex through interaction with EDC3 and DCP1-DCP2 after its dissociation (Figure 8) (Makino et al. 2015; Tritschler et al. 2009; Mathys et al. 2014; Jonas and Izaurralde 2015). Additionally DDX6 mediates, together with the eIF4E transporter protein 4E-T, pat1 and the associating Lsm1-7 proteins, the mRNA decay machinery to the 5‘ cap via direct interaction to eIF4E (Nishimura et al. 2015; Sharif and Conti 2013; Ozgur et al. 2015; Peter et al. 2015).

The decapping complex which is located within the p-bodies consists of DCP1, EDC4, DDX6 and its catalytical core subunit DCP2 (Figure 7) (Huntzinger and Izaurralde 2011; Jonas and Izaurralde 2015). After decapping and deadenylation the stability of the mRNA falls below a critical limit. This induces a rapid degradation of the mRNAs by decapping complex associated 5’ to 3’ exonulceases such as XRN1. Interestingly, XRN1 depletion results in the accumulation of deadenylated mRNAs bound by the RISC and decapping machinery (Nishimura et al. 2015; Sun et al. 2013; Behm-Ansmant et al. 2006; Nishihara et al. 2013).

The other components dissociate after decapping and deadenylation and the (minimal) RISC may be recycled, degraded or re-initiated in a new gene-silencing round (Quevillon Huberdeau et al. 2017; Golden et al. 2017).

1.2.3 Translational repression and other ways of mRNA decay

Next to direct mRNA decay, translational mRNA repression complexes are stored within p-bodies, stress granules or other compartments. The regulation, the possible re-activation, and the reason of storage is not well understood (Kulkarni, Ozgur, and Stoecklin 2010; Ayache et al. 2015; Dudek et al. 2010; E. Wu et al. 2016). It is suggested that translational repression occurs before mRNA destabilization. Hence, a block of decapping and deadenylation is necessary to stabilize translational repression complexes.

The length of the poly (A) tail may play a role in terms of a sequential degradation process, where decapping is initiated after a certain length of the tail is reached (Djuranovic, Nahvi, and Green 2012; Béthune, Artus-Revel, and Filipowicz 2012; Subtelny et al. 2014). This idea is supported by *in vitro* methods such as constitution assays and Tail-seq. There it was shown that the deadenylation rate is influenced by additional RBPs, the sequence/structure of the mRNA itself, and the length of the poly (A) tail (Stowell et al. 2016; Hyeshik Chang et al. 2014).
It is suggested, that the 3' UTR may modulate the fate of its mRNA, through length, additional secondary structures and RNA modifications that allow binding of regulatory RBPs which further modify, inhibit or promote translational repression (Mishima and Tomari 2016).

1.2.4 Regulation of miRNA mediated gene silencing by post-translational modifications and interacting modifying enzymes

The regulation of miRNA expression and activity can occur at every level at the biogenesis and the gene silencing pathway, including transcription, miRNA processing, target site binding and the formation of the gene silencing complex (Dueck and Meister 2014; Huntzinger and Izaurralde 2011; Jonas and Izaurralde 2015). In the following part the regulatory post-translational modifications of different steps of the gene silencing pathway, especially TNRC6 and Ago will be introduced.
TNRC6 proteins were identified as autoimmune phospho-proteins. Unfortunately their role as phospho-protein is still unclear (Eystathioy T, Chan EK, Tenenbaum SA, Keene JD, Griffith K 2002). As large protein(s), they contain numerous serines, threonines and tyrosines, interestingly often directly next to the GW repeats. According to the database phosphosite.org, many residues seem to be phosphorylated (30-50). Few of them are reported with high numbers of records. Many of these records are whole phospho-proteome studies, but they point out few sites to appear more often.
It was further shown that multi dephosphorylated phospho-sites surrounding the PAM2 motif which interacts with the MLLE domain of the PABPC1 strengthens the interaction. Thus, it is suggested that the multi-phosphorylation of this sites regulate/inhibits the interaction to PABPC1. This would be then important in the first steps of Ago-TNRC6-miRNA-mRNA complex assembly and maybe for the release of the mRNA (Figure 9) (Huang et al. 2013). PABPC1 exhibits several

residues which may also be modified and thus be of importance for typical interaction to PAM2 motifs (Brook et al. 2012; Brook and Gray 2012).

The function of all this phospho-sites remains unknown maybe they have importance for nuclear shuttling, recycling, complex stabilization and assembly, degradation or even p-body formation. However, it was shown that highly phosphorylated Ago proteins interact with TNRC6 proteins in the "normal" way (Golden et al. 2017; Quevillon Huberdeau et al. 2017), leaving the question if also TNRC6 is highly phosphorylated or in addition to PABPC1 interaction non-phosphorylated.

The degradation of TNRC6 proteins by ubiquitin dependent pathways and instant influence on miRNA mediated PTGS seems to be regulated by tripartite motif 65 (TRIM65) which is a E3 ubiquitin ligase (S. Li, Wang, Fu, Berman, et al. 2014; S. Li, Wang, Fu, and Dorf 2014).

TNRC6 expression is regulated at a transcriptional stage through PI3-Akt-mTOR and JAK-stat-Pim that act at a cap-dependent way on the transcripts levels and influence the ribosomal output. Consequently, the miRNA pathway is influenced. This regulation of the transcript levels occurs during the transition from a stimulated/active to an non-stimulated/quiescent state. This leads Ago into an inactive state and TNRC6 seems to be degraded over time (Olejniczak et al. 2013; Olejniczak et al. 2016; La Rocca et al. 2015).

Argonaute proteins are shown to be differentially modified with modifications such as phosphorylation, sumoylation, ADP-ribosylation and hydroxylation. In Table 2 the best known modifications from the last years of intensive research are listed. Many of the modifications are exclusively detected in particular conditions like hypoxia or increased stress while others like the pS387 may be stable in different cellular states and standard growth conditions.

The conserved S824-834 phosphorylation cluster is up to five times phosphorylated. It seems to have reduced binding ability to target mRNAs through this heavy negatively charged flexible loop. An interference with the negatively charged mRNA through proximity to the binding cleft is suggested. This modification may be regulated through the kinases CK1/GSK3 and the phosphatase 6 complex (Golden et al. 2017; Quevillon Huberdeau et al. 2017).

Another report suggests LIMD1 and WTIP as modification dependent RISC complex interactors. Thereby the AB motif of LIMD1 directly binds to the linker 2 between PAZ and MID domain of AGO2 when the Akt3 dependent S387 is phosphorylated (Bridge et al. 2017; James et al. 2010). Other groups suggest a role of KRAS to be important for the localization of Ago2 in multi-vesicular endosomes which is prevented by the stable pS387 (McKenzie et al., 2016).

Table 2 Overview of reported Ago2 modifications (adapted from Wilczynska and Bushell 2015).

Modification [aa]	Function	pred. Mod. Enzyme	Reference
Phosphorylation S[387]	p-body localization of Ago2; enhancement of miRNA -mediated repression	MAPKAPK2 kinase Akt3	(Zeng et al. 2008) (Horman et al. 2013) (Rüdel et al. 2011)
Y[393]	Induced in hypoxia; decreased interaction to Dicer inhibition of miRNA maturation	EGFR	(Shen et al. 2013)
Y[529]	Reduced p-body localization; impaired miRNA binding transient loss of miRNA binding by Ago2; reduced interaction to TNRC6 proteins	?	(Rüdel et al. 2011)
S [824-834]	Cluster-phos.; reduced target binding	GSK3?, CK1?	Huberdeau et al. 2017
		Phosphatase 6	(Golden et al. 2017)
Sumoylation K[402]	Increase in protein stability	Sumo1/2/3	Sahin et al. 2014; Josa-Prado, Henley, and Wilkinson 2015 Sahin et al.2014
Hydroxylation P[700]	Stabilization of Ago2 and enhancement of miRISC function in hypoxia; Increase in miRNA abundance	[C-P4H(I)]	(H. H. Qi et al. 2008)
ADP-ribosylation	Enhancement of stress granule formation; relief of miRNA repression	poly(ADP-ribose)	(Leung et al. 2011)
Ubiquitination	Specific degradation of Ago2 , degradation during T-cell activation	Trim71	(Rybak et al. 2009) (J. Chen, Lai, and Niswander 2012; Loedige et al.2013

Recycling mechanisms. The sequential pathway of gene silencing is upon regulation quiet well understood. However, it is completely unknown if there are recycling mechanisms after mRNA destabilization which return Ago-miRNA and TNRC6 back to certain pools for a new cycle after complex decomposition (Figure 9). It is unclear if Ago-miRNA is degraded, stored or unloaded/re-loaded with a new miRNA. The same is true for TNRC6, which interacts with Ago, the deadenylation, decapping complexes and other proteins. For TNRC6 as binding platform there would be even the possibility that a core complex of TNRC6 and deadenylation complex stays for direct and fast action when an Ago protein together with an mRNA target arrives. Further different complex states depending on the fate of TNRC6 including all steps of gene silencing are thinkable. Certain hypothesis is addressed for Ago proteins and suggests an recycling of the minimal miRISC depending on the state of phosphorylation (Figure 9) (Quevillon Huberdeau et al. 2017; Golden et al. 2017; La Rocca et al. 2015). Another report suggest that phospho-regulation of Ago2 through

Akt3 seems to be important for interaction to GW182 and p-body localization (Horman et al. 2013).

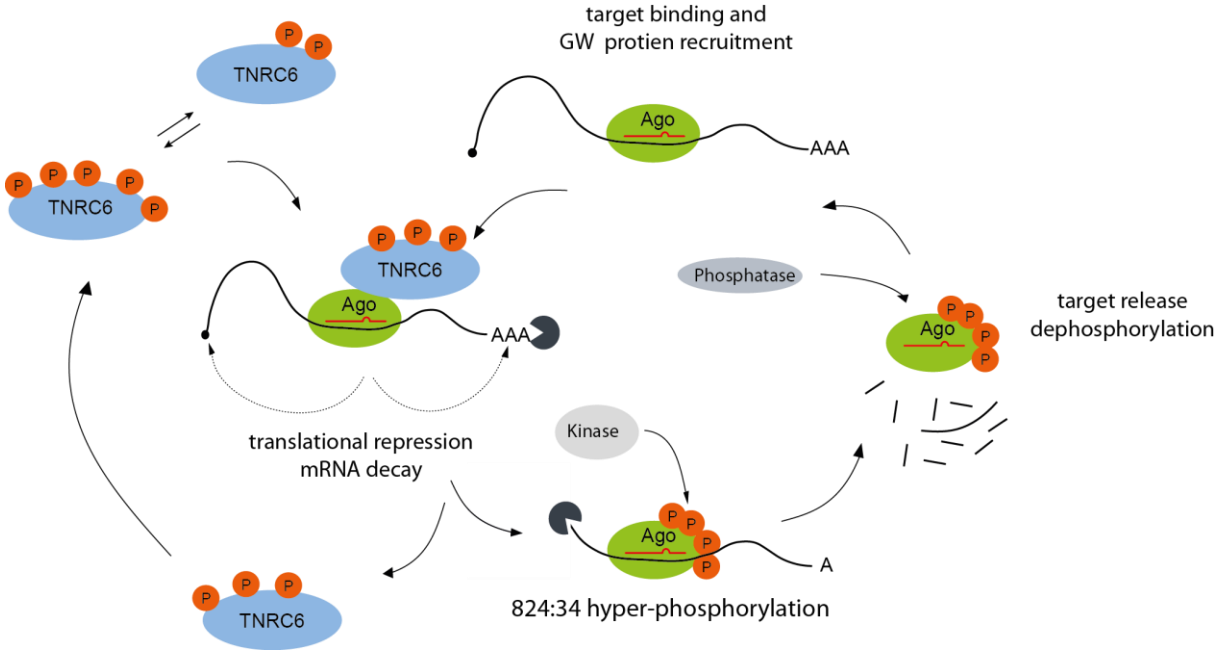

Figure 9 Recycling mechanism of gene silencing and translational repression.
After Ago-miRNA-TNRC6-Ago complex is formed, mRNA is destabilized and released from a hyper-phosphorylated Ago for decay. The phosphorylation pattern of TNRC6 proteins may change during gene silencing according to the sequential function.

1.3 RNA binding proteins

All classes of RNAs are associated with RNA-binding proteins. Together they form Ribonucleoprotein complexes (RNPs) with diverse functions. These complexes contain at least one RBP that interacts with RNA. All different RBPs share the common feature of binding specifically RNAs through RNA-binding-domains (RBDs) (Lunde, Moore, and Varani 2007; Gerstberger, Hafner, and Tuschl 2014). A RBP can include one class of the same or a combination of different classes of RBDs. Typical structural conserved RBDs are the RRM domain (RNA recognition motif), KH domain (K homology), DEAD and DEAH box helicase, or dsRBDs (double-stranded RBD) (Lunde, Moore, and Varani 2007). In the following part KH domains and RRMs are introduced in detail.

KH domain. The protein human heterogeneous nuclear ribonucleoprotein K (hnRNP K) was the first example of a KH domain containing protein. Within hnRNP K the domain was characterized as ssRNA binding domain. In hnRNP K three copies of the KH domain are forming together the interacting RBD (Musco et al. 1996; Grishin 2001). KH domains can be modular assembled within the proteins as di-, tetra- or multimers. Two different classes of KH domains (I and II) are existent. KH domain I is typically found in eukaryotes and KH II in prokaryotes. The two classes are not sequence conserved and the typical KH minimal domain consisting of two beta-strands and two alpha-helices (β1-α1-α2 β2) are also not structurally conserved (Ostareck-Lederer, Ostareck, and Hentze 1998; Valverde, Edwards, and Regan 2008). The KH domain I contains altogether three beta strands which are antiparallel arranged as beta-sheet. The three alpha-helices are adjacent to the beta sheet. A RNA interaction cleft is assembled by the α1-helix, a GXXG-connection loop, α2-helix and the β2-strand. Four nucleic acids can associate with the hydrophobic binding pockets and residues within the cleft. Additional structural elements form an expanded KH domain and allow the interaction with more than four nucleic acids (Baber et al. 1999; Garc??a-Mayoral et al. 2007; Nicastro, Taylor, and Ramos 2015).

KH domains are found in many RBDs with various different functions (e.g. hnRNP proteins, KSRP or FMR1). The interaction and hence the function depends on the modular and functional architecture of the KH domains. They can act cooperatively together at one interaction site on the RNA or as completely independent domains which interact with different parts of the RNA (Nicastro, Taylor, and Ramos 2015; Lunde, Moore, and Varani 2007).

RNA Recognition Motif. The RRM is the most prominent RBD within the RBPs and they are often organized in multiple copies within the RBPs. This class of RBDs was first identified in hnRNP A1,

spliceosomal protein U1A, PABP, sex-lethal and La (Adam et al. 1986; Swanson et al. 1987; Handa et al. 1999; Deo et al. 1999; Ding et al. 1999; Avis et al. 1996; Pérez Cañadillas and Varani 2003). This domain is structurally conserved within the species and usually composed of 80-90 amino acids. It contains several α-helix and β-sheet sandwich units which form a α1β1β2β3α2β4 topology. Within different RBPs the structural composition varies according to the function of the protein and the interacting nucleic acids. For binding of ssRNA several conserved interactions on the surface of the β-sheet are necessary (Avis et al. 1996; Deo et al. 1999; Handa et al. 1999). A salt bridge is formed between specific residues (usually Arg/Lys) and the sugar-phosphate backbone. Another important hydrophobic interaction is accomplished by aromatic residues and the nucleobases. This interactions result in a stable complex formation (Maris, Dominguez, and Allain 2005; Lunde, Moore, and Varani 2007).

There are also reports that the RRM domain interacts specifically with proteins. For instance the α1-helix of U2AF is three times longer as usual and then the interaction to a nearby β-sheet is solvent which leads to protein interaction with SF1 (Kielkopf et al. 2001; Kadlec, Izaurralde, and Cusack 2004; R.-M. Xu et al. 1997).

The class of RBPs contain a huge bandwidth of different identified protein types and many unknown candidates, binding domains and dynamic networks which all determine the fate of RNA from transcription until decay (Gerstberger, Hafner, and Tuschl 2014). The classes of RNA binding domains are growing and many unusual domains are discovered to associate with different classes of RNA (Rammelt et al. 2011; Glisovic et al. 2008; McKee et al. 2005; Anantharaman 2002; Baltz et al. 2012; Castello et al. 2012). For instance the NHL domain of *D. melanogaster* protein brain tumor (BRAT) was identified as new RBD. BRAT forms together with Pumillio and Nanos a complex which interacts with the hunchback mRNA and hence its translation is repressed. The NHL domain assembles as a six-bladed beta propeller recognizing ssRNA at its positively charged top surface (Loedige et al. 2014; Loedige et al. 2015).

1.4 miRNA containing viruses

1.4.1 Viral life cycle

Viruses are non-reproductive genetic systems. In general, all viruses have a similar architecture. They consist of a coat and viral genes encoded with nucleic acids. Hence, the virus needs a system for reproduction. Due to this reason, viruses have to invade other living cells and use the cells replication systems for reproduction. Therefore, the viruses undergo the lytic life cycle, in which the host cell is often destroyed by virus production and excretion. There are several stages of the lytic cycle that are classified by the genes that are expressed. For instance, in CMV three phases during the lytic infection can be distinguished: Immediate-earl, very early and late phase.

In general, the virus life cycle is similar within all classes of viruses. This means the virus forces the host to produce viral proteins and the viral the genome. Afterwards the virus is assembled and leaves the cell to invade new hosts. In the following chapter, the lytic life cycle of CMV and the latent phase of EBV is briefly described as an example.

Lytic life cycle. The virus attaches to the cell, enters into the cell and enters through specific mechanisms involving target molecules and receptors. Once inside the cell, the genomic DNA is transported immediately into the nucleus, where the viral genomic program is initiated by strong promotors (Beltran and Cristea 2015; Herbert and Nag 2016). Subsequently the virus takes over the entire genetic program of the host, the viral genome is replicated, and viral coat proteins for particle assembly are produced in large amounts by the host. The genome is packed into the assembled coat and the viruses destroys the host when leaving the cell (Beltran and Cristea 2015).

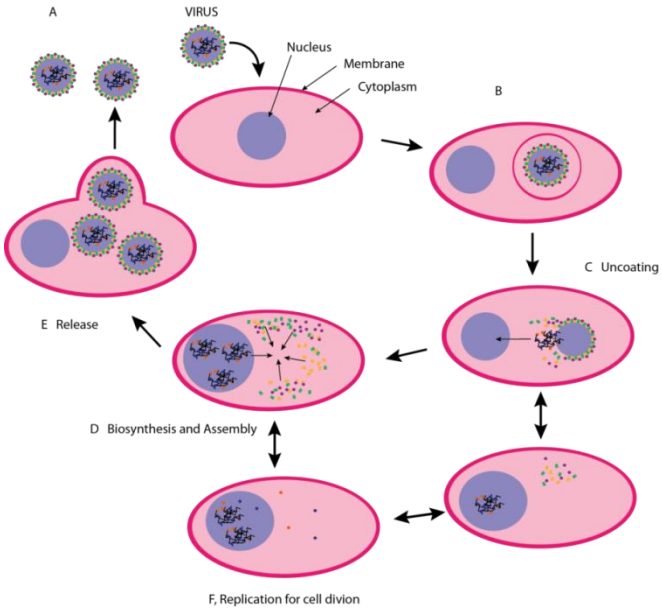

Figure 10 Schematic representation of the latent and lytic virus life cycle (CMV served as example). (A) Virus particles attach specifically to cell surface receptors and enters into the cell cytoplasm through endocytosis. (B), (C), After uncoating, capsid-DNA complex is delivered into the nucleus (D). In the nucleus the immediate-early genes are transcribed, followed by the early genes and subsequently the late genes. Viral genome is replicated and capsid proteins were expressed. Late phase initiates the nuclear capsid assembly, export and cytoplasmic tegument formation in the assembly complex. (E) Virus is released into the intracellular space. (F) Shuttling to latent viral phase without active virus production. Persistent virus can be reactivated and switch again to the lytic phase (modified after Handke et al. 2012; Beltran & Cristea 2015).

Latent life cycle. Under distinct conditions, viruses can switch into a latent cycle for a persistent remaining in the nucleus of the host cell (Speck and Ganem 2010; Cobbs et al. 2002; Sissons et al. 2002; J. H. Sinclair and Reeves 2013; J. Sinclair and Reeves 2014; Arcangeletti et al. 2016). In this process the virus is replicated when the cellular genomic DNA replicates. During cell division, the viral genome copies are attached to the chromosomes by specific proteins. This insures that a genome copy is taken into the new cells during segregation. Typically, the virus suppresses its own gene expression to a certain limit and mimics additionally specific signalling pathways. Hence, the host cell is not detecting the virus and an immune response can be avoided. For instance in EBV the Epstein-Barr nuclear antigen 1 (EBNA1) is the only protein expressed in latency. Among many functions the tethering of the viral genome to the chromosomes is executed by EBNA1 (Hong Wu, Kapoor, and Frappier 2002; Yates, Warren, and Sugden 1985; Frappier 2012). The EBV proteins LMP1 and LMP2A mimic CD40 and a B-cell receptor (Uchida 1999; Miller et al. 1994). This leads to reduced signalling of certain immune response pathways. EBV is reactivated when stimuli like normoxia, hypoxia or DNA damage occur. Also some cellular signalling pathways that are required for differentiation as well as extracellular mediated signals like TGF-β1 cause reactivation and subsequent a switch to the lytic life cycle. The stimuli lead to an activation of the transcription factors Zp and Rp. These factors promote the switch to the lytic cycle by massive activation of the lytic genetic program (Luftig 2016; Kenney and Mertz 2014).

1.4.2 Function of miRNAs in human herpes viruses

In mammals and higher eukaryotes, thousands of different miRNAs have been identified, characterized and extensively studied. However, miRNAs are also present in some specific DNA viruses (Pfeffer et al. 2005; Sewer et al. 2007; Sullivan et al. 2005). Here, several of the herpes, papilloma and polyoma viruses containing miRNAs are introduced (Table 1). Also viral miRNAs are intensively studied and it was observed that most of them are transcribed by RNA Pol III (Diebel, Smith, and van Dyk 2010). Drosha and Dicer process the viral miRNAs in a similar way as the host miRNAs. Finally, they are incorporated in Ago proteins and gene silencing occurs.

It is further suggested that the viral miRNAs target host as well as viral genes and the other way round host miRNAs regulate host and viral genes (

Figure 11)(Carl, Trgovcich, and Hannenhalli 2013). Viral microRNAs are suggested to function redundantly together with the host miRNAs, meaning that they act within regulatory networks and share the same targets, especially genetic defence systems are potential targets (D. Ramalingam and Ziegelbauer 2017; Dölken, Malterer, et al. 2010). Further host defensive miRNAs

are downregulated and conducive ones are upregulated, this suggests drastic changes within the miRNA pattern of the host (Motsch et al. 2012). Especially during a fast dynamic lytic cycle viral miRNAs in contrary to the host, miRNAs may have a minor role, but they could be more important by inducing and maintenance of the persistent latent virus life.

Table 3 Classification of virus families and their viral microRNAs (adapted from Grundhoff and Sullivan 2012).

name	virus strain, family	pri/ pre -miRNAs	mature miRNAs
Epstein-Bar-virus	Gamma-Herpesviridae	25	44
Cytomegalo-virus	Beta-Herpesviridae	15	26
Herpes-Simplex-Virus 1	Alpha-Herpesviridae	18	27
BK polyomavirus	Polyomaviridae	1	2
Merkel-Cell-polyomavirus	Polyomaviridae	1	2
Human Papilloma V. 41	Papillomaviridae	1	?

For instance the expression of viral miRNAs in EBV during the latent persistent phase is very high and it seems that they target antiviral genes (Kang, Skalsky, and Cullen 2015; Hooykaas et al. 2016). The viral expression levels in the latent and lytic phase were intensively studied and reports suggest that many miRNAs are highly expressed and processed in both lytic and latent phase. Some are blocked at a particular processing step in either the latent or lytic phase and some seem to be not present at all (Stern-Ginossar et al. 2009; Forte and Luftig 2011; Jurak et al. 2010; Murphy et al. 2008; Flores et al. 2013).

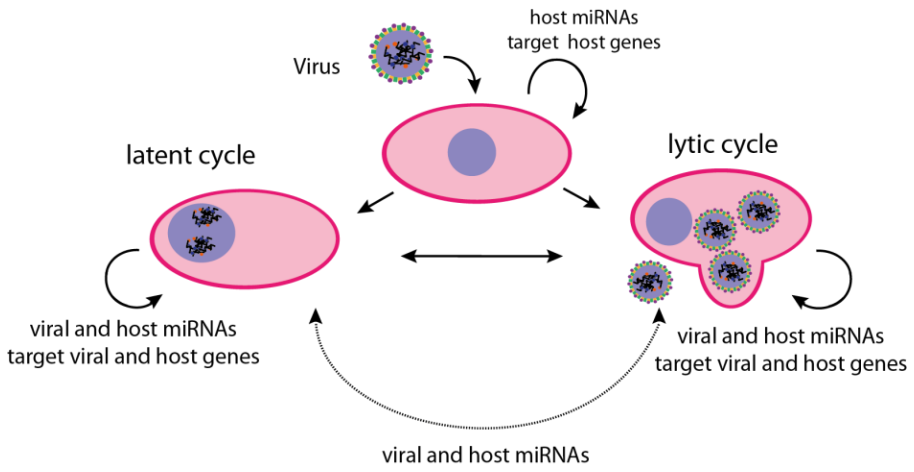

Figure 11 The influence of viral and host miRNAs on viral and host targets for controlling viral latent and lytic life cycles.

This differential expression occurs because also the viral miRNAs are organized in either clusters (EBV) or individual at intronic regions of pre-mRNAs. Interestingly, also within viruses clustered

miRNAs, although transcribed together as one primary transcript, are frequently differentially expressed and processed which suggests regulatory networks like for mammalian miRNAs that function also in viral miRNA biogenesis. In the following part, an overview of CMV, HSV1 and EBV microRNAs and their summarized functions is listed in appendix Table 16).

CMV. The miRNAs of CMV are mainly individual organized in intronic regions of immediate-early or early genes and highly expressed during infection of primary cells suggesting a role in the lytic life cycle (Pfeffer et al. 2005; Grey and Nelson 2008; Dhuruvasan, Sivasubramanian, and Pellett 2011; Fruci, Rota, and Gallo 2017).

HSV1. miRNAs are partly conserved to HSV2 and they are organized in small clusters or individual. They locate within overall within the whole genome; just few are in the latency associated transcripts (LAT) region. In the latency phase, only LAT miRNAs are expressed. This means that only 9 of the 17 HSV1 miRNAs are expressed, processed and loaded into RISC (B. R. Cullen 2004; Flores et al. 2013; Jurak et al. 2010; R. L. S. and B. R. Cullen 2013; Kramer et al. 2011; Jennifer Lin Umbach et al. 2009; Jennifer L Umbach et al. 2010). During lytic infection just few of the miRNAs are expressed, most of them seem to be blocked during miRNA biogenesis (Kramer et al. 2011).

EBV. 25 EBV pre-miRNAs and 44 mature miRNAs were identified in EBV positive B cells (Jijoye, C666-1,SNU-719, etc). The BHRF1 miRNAs are generated by splicing of the bhrf1 gene and only expressed in latency phase III. The BART miRNAs are organized in 2 large clusters and mainly expressed in latency I/II. Interestingly, a depletion of all EBV miRNAs in the EBV-B95-8 strain, still immortalized B cells in cell culture, suggesting a minor role of EBV miRNAs during latency in B cells (Cai, Hagedorn, and Cullen 2004; Grundhoff, Sullivan, and Ganem 2006; Xing and Kieff 2007; J. Y. Zhu et al. 2009; Hooykaas et al. 2016; Haar et al. 2015). The targets of the viral miRNAs are genes involved in apoptotic and immune defense mechanisms (listed in appendix table 16).

1.4.3 Polyoma and Papilloma viruses

Papilloma and polyoma viruses belong to the class of human oncogenic viruses like many of the prior described herpes viruses, they have also cancerous potential and cause e.g. Merkel cell carcinoma tumours (Toker C., 1972; Stamatiou et al. 2016).

Briefly, Polyoma viruses belong to the family of the polyomaviridae and are classified as ortho-polyomaviruses with typical members such as MCV, SV40, JC and BK human polyomavirus. The genome size of this dsDNA virus clade usually is around 5 kb and contains a small amount of genes like the early genes large T antigen (LT), alternative T antigen open reading frame (ALTO),

microRNA (miRNA) or the late capsid and coating protein genes (VP1-3) (Stakaityte et al. 2014; Richards et al. 2015).

Interestingly, within MCV (similar in SV40, BKV and others) the viral miRNA that is located antisense to the LT coding region regulates early viral genes. This results in a decrease of early genes, especially the LT antigen (base complementarity induces cleavage of the transcript) and may support the switch to the late phase of the viral life cycle (Sullivan et al. 2005; Gil Ju Seo, Chen, and Sullivan 2009; Xi Liu et al. 2011; G J Seo et al. 2008; Richards et al. 2015; Stakaityte et al. 2014; C. J. Chen et al. 2016).

Table 4 Viral miRNAs of BKV, MCV, HPV41.

mature miRNAs	target/ function	publication
BKV-mir-B1, SV-miR1 MCV-mir-M1, JCV-miR-1 Richards et al. 2015	binds to Lt-Ag complementary and cleaves target, reduced cytotoxic T cell– mediated lysis of infected cells	Sullivan et al. 2005; Seo et al. 2009; Liu et al. 2011; Seo et al. 2008;
HPV41-miR-H1	miRNA was identified by the lab of Prof. Dr. Adam Grundhoff and was not yet published	

2 RESULTS

2.1 Part I: Identification of RBPs that regulate the viral miRNA biogenesis

2.1.1 Aims of part I

The general biogenesis from primary transcripts to mature microRNAs that is a two-step process is well understood in many species. It involves either the differential expression of precursors and mature miRNAs, or the differential expression of miRNAs originating from primary transcripts. This regulation is thought to be especially important under conditions where transcriptional and translational profile changes occur that are for example triggered by viruses. It is likely that RBPs can contribute to such a regulation process on posttranscriptional levels. In this project, we studied the influence of RBPs on the viral miRNA biogenesis of herpes, papilloma and polyoma viruses.

To identify proteins involved in post-transcriptional regulation of miRNA biogenesis, a large mass spectrometric screen with pri/pre-miRNA pull-down assays was set up in a viral background. In the following studies, the interaction of the potential regulators was validated, verified and further characterized.

Brief overview of planned workflow:

1. Viral pre-miRNA binding proteins were identified
2. Results were analyzed *in silico*
3. Binding proteins were validated by *in vitro* assays
4. Characterization of specific RNA binding proteins

2.1.2 Viral miRNA expression profile of EBV, CMV and HSV1

As initial starting point, the miRNA expression profiles of the different viruses were observed to determine differences that may be caused by regulatory processes.

The amount of mature and pre/pri-miRNAs was analyzed by northern blotting in the EBV positive cell lines Raji and Jijoye. Deep sequencing experiments conducted by a former lab member (Michaela Beitzinger) showed high variety in the expression levels of miRNAs. For northern blotting 20 µg of total RNA from EBV positive cell lines Raji and Jijoye was separated by RNA-UREA-PAGE, blotted onto nitrocellulose membranes and viral miRNAs were detected with radioactive labelled DNA oligos complementary to the 3p or 5p mature miRNAs. The selected northern blots in Figure 12 A-C suggest positive or negative influence during the crucial steps of processing.

Blocking or promoting of miRNA biogenesis leads to different levels and hence, stronger or weaker signals of pre-miRNA and mature miRNA. The ebv-miR-BHRF1-1 is located within a miRNA cluster next to the gene BHRF1 (Cai, Hagedorn, and Cullen 2004; Grundhoff, Sullivan, and Ganem 2006; Xing and Kieff 2007; J. Y. Zhu et al. 2009; Hooykaas et al. 2016; Haar et al. 2015) and the levels of the processed miRNAs and pre-miRNAs differ from ebv-miR-BHRF1-2 or BHRF1-3 (Figure 12 A). This suggests that the co-transcribed cluster is regulated during miRNA processing and thus, the levels of pre-miRNAs and miRNAs differ from each other.

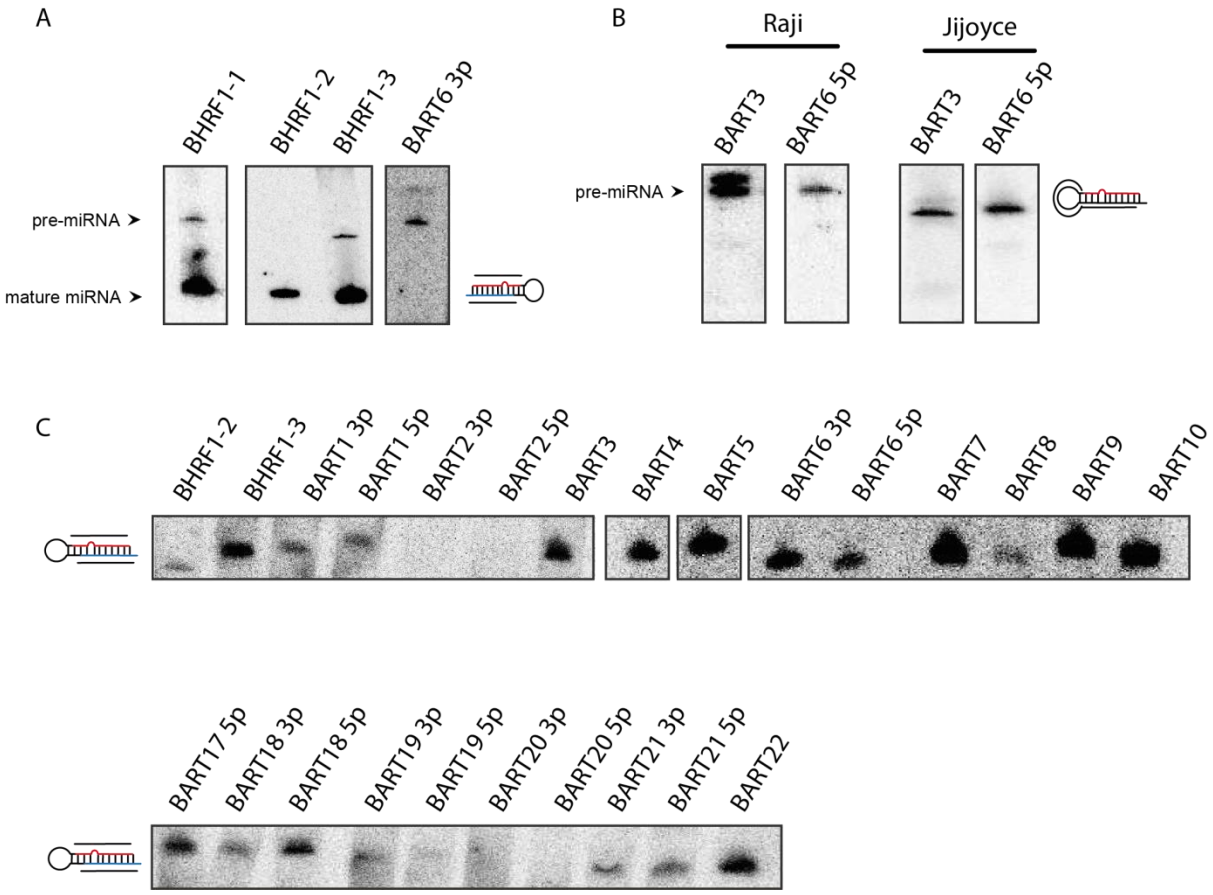

Figure 12 Detection of viral miRNAs by northern blot.
(A) Detection of EBV-miRNAs and pre-miRNAs by northern blots crosslinked with 20 µg of total RNA extracted from the EBV positive cell line Raji. Binding of DNA probe is depicted next to the blots. (B) Comparison of pre-miRNA expression in Raji and Jijoye cells with *in vitro* transcribed RNA probes for pre-miR detection only. Binding of the RNA probes is depicted next to the blots. (C) Expression profile of miRNAs detected by northern blot from EBV positive Jijoye cells.

For the ebv-miR-BART6-3p processing stops at the pre-miRNA level, no mature miRNA could be observed. For detection of pre-miRNAs, *in vitro* transcribed RNA probes were used with a hybridization temperature of 65 °C. Probes were designed to interact with both, the mature and the pre-miRNA, or to interact only with the pre-miRNA (Figure 12 B). In Figure 12 C a subset of EBV miRNAs was detected by northern blotting to observe the expression levels. The illustrated

signals within the northern blots suggest a differential expression of the detected mature EBV miRNAs in Jijoye cells.

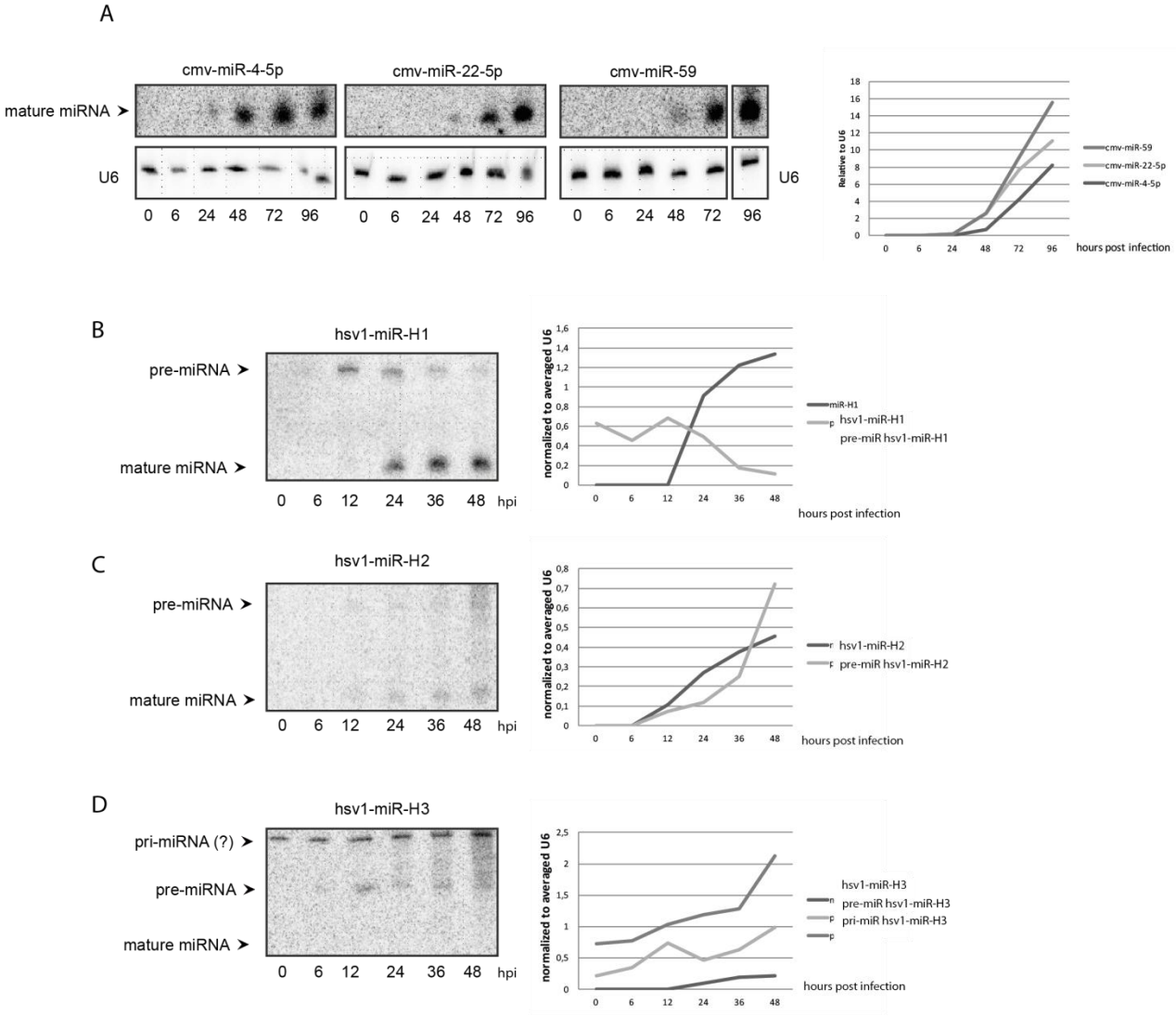

Figure 13 miRNA expression levels during viral infection.
(A) Detection of viral miRNAs after infection of primary MRC5 cells with CMV strain AD169 with MOI = 5. RNA was extracted after different time points and standard northern blots were performed. The miRNA expression levels were quantified according to U6 loading control. (B), (C), (D) Detection of viral miRNAs after infection of primary MRC5 cells with HSV1 strain KOS with moi = 5. RNA was extracted after different time points and standard northern blots were performed. The miRNA/ pre-miRNA/ pri-miRNA expression levels were quantified according to U6 loading control.

Furthermore, expression levels of some viral miRNAs during infection with human CMV and HSV1 was assessed at different time points after infection. An equal amount of RNA was extracted of every time point and was loaded onto a 12 % PA-gel and miRNAs were detected by northern blotting with using DNA oligos (Figure 13 A-D). Selected CMV-miRNA expression increases from 0 to 96 hours post infection (hpi) (levels were quantified by normalization to U6 loading control; Figure 13 A). Clear detection of miRNAs and a lack of signals for pre-miRNAs (not shown) suggest a strong transcription and an efficient processing of mature miRNAs after 24 to 48 hpi. Surprisingly, infection with HSV1 leads to more divergent viral miRNA profiles compared to CMV

(Figure 13 B - D). The expression of the pre-miRNA of hsv1-miR-H1 can be detected already after 12 hpi, whereas the mature miRNA is not yet processed. The expression of pre-miRNA decreases at later time points, while the levels of mature miRNA increase with a distant time shift (Figure 13 B). hsv1-miR-H2 is similar to the CMV miRNA analyzed. Levels of both pre-miRNA and mature miRNA increase during progression of viral infection (see Figure 13). In contrast, hsv1-miR-H3 biogenesis might be blocked at the pri/pre-miRNA processing step and no mature form can be detected (Figure 13 D). Taken together, these different miRNA biogenesis profiles suggest not only a transcriptional regulation but also a regulation at the different viral miRNA processing steps.

2.1.3 Identification of pre-miRNA binding proteins by mass spectrometric approaches

RNA binding proteins that block or promote the different processing steps cause the differential miRNA biogenesis. For identification of specific hairpin binding proteins that are potential regulators of the miRNA biogenesis, a mass spectrometric screening approach with pre-miRNA pull-downs for the investigation of protein-interactors was first established for ebv-miR-BHRF1-1, ebv-miR-BART10 and ebv-miR-BART18 (data not shown). For the pull-down, *in vitro* transcribed pri/pre-miRNAs with a 5’ T7 promotor extension complementary bound to a 2’O-methyl-RNA linker (Figure 14) was incubated with cell lysates. That lysates were either actively infected or the virus was persistent within the used cell lines.

After pull-down, magnetic beads were washed and associated proteins were loaded onto a 4 - 12 % gradient SDS-gel, separated and analyzed by mass spectrometry (Figure 14). pri/pre-miRNA pull-downs were generated in biological replicates and preclearing pull-downs which were generated during the preclearing of the lysates by magnetic beads coupled without pre-miRNA. The preclearing samples served as background binding control because of a lack of standardized pre-miRNA that is not interacting with RBPs as negative control. The mass spectrometric obtained data is presented as heatmap with clear delineation of potential protein-RNA binding proteins. The heatmap included many different data-sets of every different excised gel part which was analyzed. After combination of the single data-sets, a raw heatmap containing all information was created. For further protein selection, specific hits had to appear as duplicate with high probability scores. Afterwards specific hits were compared to the background and the preclearing and were rearranged as heatmap for specific binders. For normalization, probability scores were summarized as "lane counts" for one protein lane and all hits were normalized to the lane counts. The pull-downs with the different viruses result in four different tables that are presented in the following chapters.

A first data analysis allows the grouping of interactors into the following categories. First, specific binding actions in which one RBP interacts with one pre-miRNA. Second, one hairpin may interact with different proteins. Third, one protein interacts with different pri- and pre-miRNAs. Fourth, a few hairpins interact with a few proteins and fifth, one part of a whole protein complex interacts with one or more pre-miRNAs.

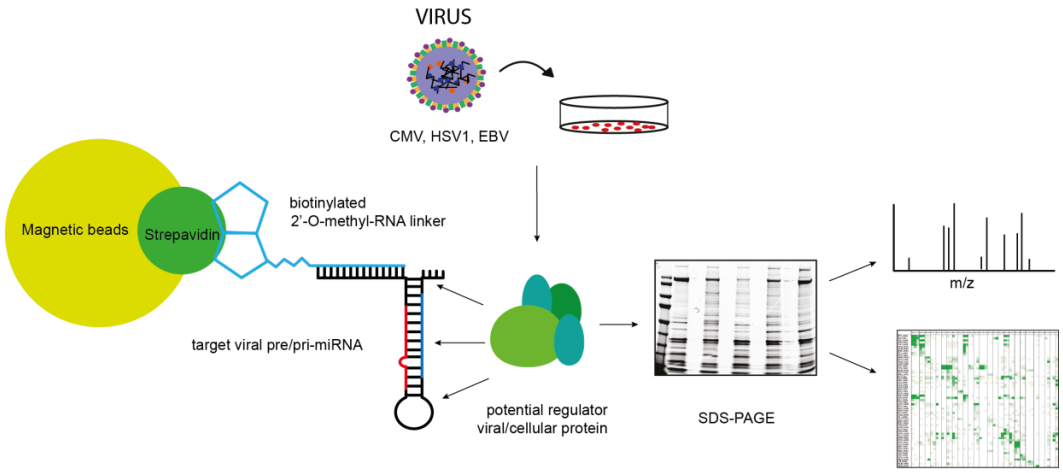

Figure 14 Schematic representation of the pri/pre-miRNA pull-down.
Experimental set-up of the pre/pri-miNRA pull-down with magnetic streptavidin beads coupled to *in vitro* transcribed pre/pri-miRNAs through a 2'O-methyl RNA biotin linker. Prepared beads were incubated with cell lysates of EBV positive or CMV/ HSV1 infected cells. Proteins were separated by a 4-12 % gradient SDS-gel, coomassie stained and tryptic digested for mass spectrometric analysis. Obtained data was analyzed with MS excel.

2.1.3.1 RBPs associated with CMV pre-miRNAs

CMV encodes 15 different pre-miRNAs. To identify functional relevant regulators, RNP candidates were further grouped and analyzed. The heatmap shows that the mass spectrometric identified proteins of the hairpin pull-down are assigned to specific pre-miRNAs. Proteins with high background binding or weak binding were rejected. The pull-downs were performed in biological duplicates and only duplicate hits were counted. After all criteria were considered, the heatmap summarized around 100 specific proteins, clustered on the y-axis according to their interacting pre-miRNAs that are listed at the x-axis. There are potential regulators with one specific hit like SART3 or Rbfox2, without any or weak background. Other factors seem to bind two hairpins like CPSF5 or Zincfinger 346. Weak binding actions or even no obvious or distinct binding by potential candidates can be explained by low or no protein expression in the used cell lines. To get a first functional glimpse and to support specific binding, GO term analysis associates the potential RBPs to different cellular pathways such as RNA processing or mRNA processing with high p-values (Figure 16 A). 13 candidates can be linked to viral processes or viral life cycle which are listed on the right side of the table in Figure 16 A (original data obtained with go.princeton.edu).

Continued on next page

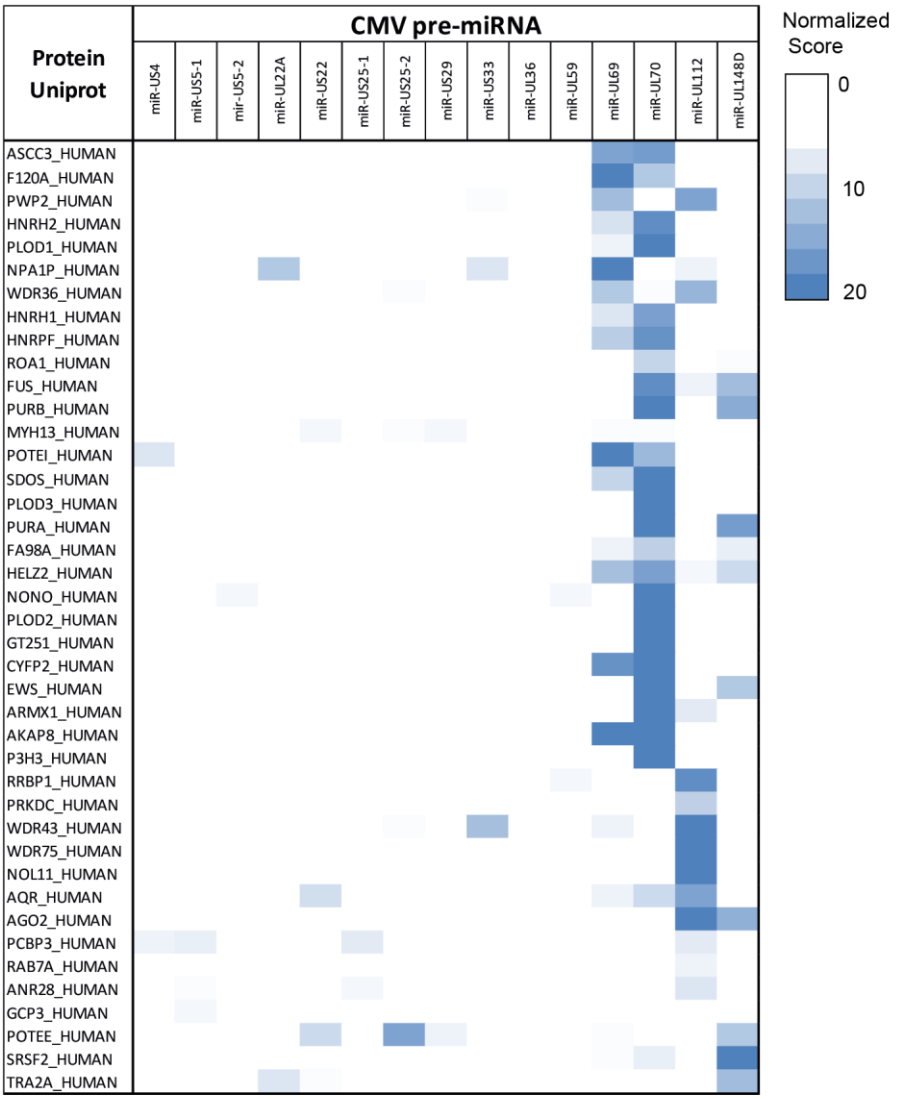

Figure 15 Heatmap of specific CMV hairpin RBPs.

Heatmap of proteins identified by mass spectrometry. Uniprot gene symbols are listed on the y-axis and pre-miRNAs are listed on the x-axis. Annotated protein hits were defined by score (obtained with Mascot and proteinscape) and normalized to the summarized counts of one protein. Pull-downs were performed in replicates and were averaged afterwards. The probability of specific binding is indicated in blue shades (from white = 0 to blue = 20).

Subcellular localization annotations illustrate that many candidates are located within the nucleus suggesting interactions on the pri-miRNA level. Others are exclusively cytoplasmic or within distinct cellular locations, which implements a role within pre-miRNA processing (Figure 16 B). Many candidates contain one or more known RNA binding domains. The dominant RBD class with a frequency of about 40 % is the RRM (Figure 16 C). Around 25 % of the listed candidates are not known to be associated with RNA or related mechanisms like RNA processing.

Furthermore, a subset of potential CMV proteins binding to hairpin-structured RNAs was identified which are early expressed during viral infection and have potential or known functions in the viral life cycle (shown in appendix Figure 39). The identified factors have not yet been associated with RNA binding and related processes. These factors probably resemble unspecific

binders due to high background levels and many unspecific binding actions. Therefore, the focus was shifted to the associated human candidates. Taken together, the statistical analysis suggests the specific identified RBPs as RNA associated proteins of the cmv-pre-miRNAs.

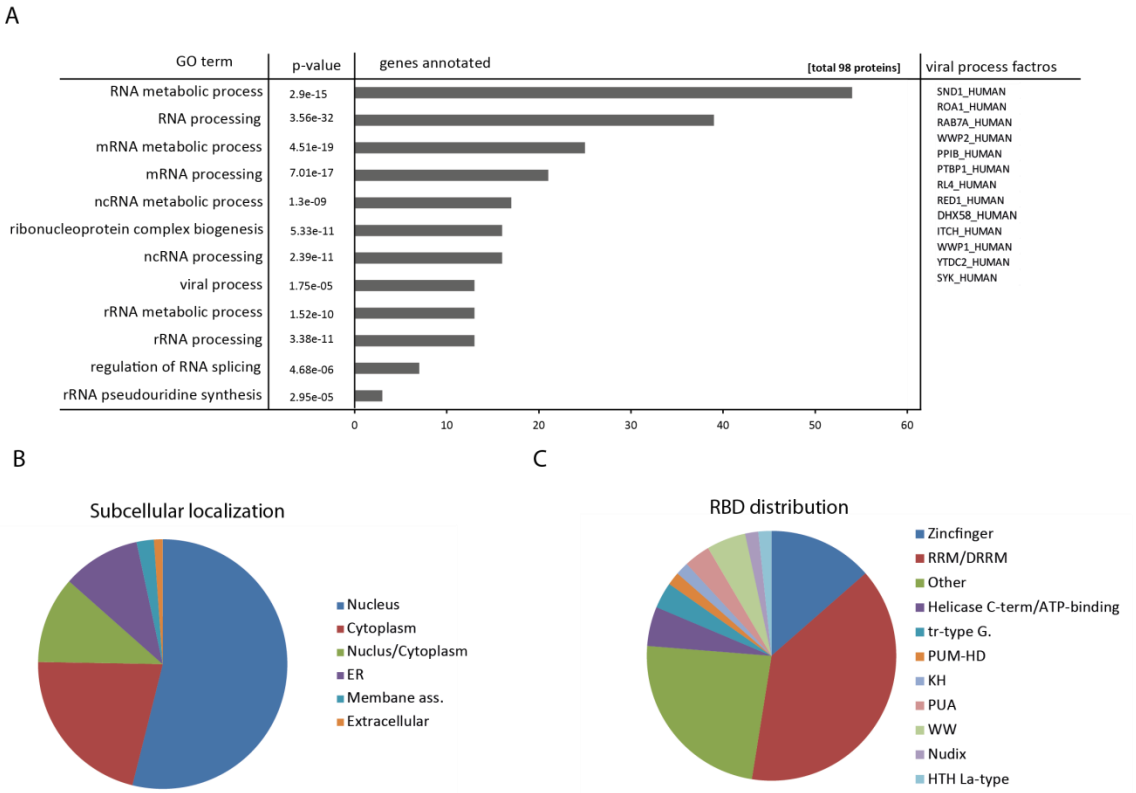

Figure 16 Functional analysis of identified RBPs.

(A) GO term analysis classifications with high p-values and cluster frequency. (B) Subcellular localization of identified proteins (classified with Uniprot database). (C) Distribution of RNA binding domains within the identified proteins.

2.1.3.2 RBPs associated with EBV and HSV1 pre-miRNAs

EBV encodes 22 different pre-miRNAs. To identify functional relevant regulators, a pre-miRNA hairpin pull-down was performed. RNP candidates that specifically bound to the exposed ebv-pre-miRNA were further grouped and analyzed. The heatmap is illustrated in appendix Figure 40.

HSV1 encodes 18 pre-miRNAs. A mass spectrometric screen of hsv1-pre-miRNA pull-downs identified potential regulators of miRNA biogenesis. The potential hairpin interactors are illustrated in appendix

Figure 41. The hsv1-miR-11 was excluded from the experiments as sequence and structure specific characteristics of the hairpin resulted in methodical problems.

2.1.3.3 RBPs associated with BKV, MCV, HPV41 pre-miRNAs

The Merkel-cell-polyoma, the BK polyoma and the human papilloma virus 41 each express one specific miRNA, which is not conserved in other viruses. To identify how these miRNAs are processed, a pri/pre-miRNA pull-down was performed using their pre-miRNAs as described above. However, in contrary to the experiments performed in chapter 2.1.3.1, MRC5 cells could not be actively infected with the viruses because of methodical and technical issues.

A

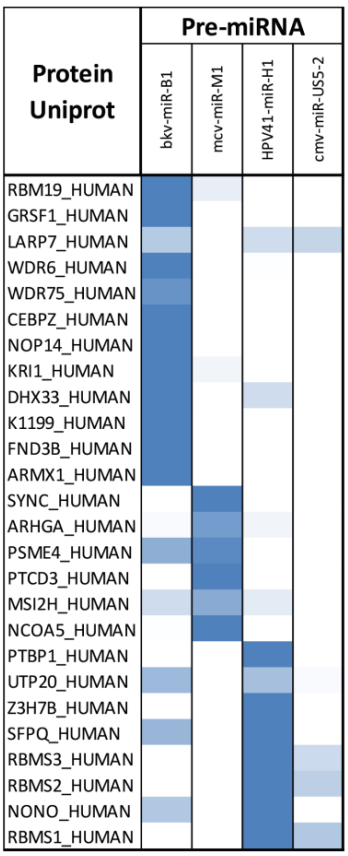

r = 0,84

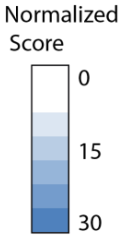

B

Gene Ontology term	Cluster frequency	Corrected P-value	Genes annotated to the term
RNA processing	42.3%	8.28e-09	NONO_HUMAN, RBMS2_HUMAN, RBMS1_HUMAN, NOP14_HUMAN, PTBP1_HUMAN, WDR75_HUMAN, LARP7_HUMAN, GRSF1_HUMAN, DHX33_HUMAN, SFPQ_HUMAN, UTP20_HUMAN
gene expression	65.4%	9.39e-05	RBMS2_HUMAN, PTCD3_HUMAN, RBMS3_HUMAN, RBMS1_HUMAN, NOP14_HUMAN, WDR75_HUMAN, PSME4_HUMAN, CEBPZ_HUMAN, DHX33_HUMAN, SFPQ_HUMAN, UTP20_HUMAN, NONO_HUMAN, SYNC_HUMAN, GRSF1_HUMAN, LARP7_HUMAN, PTBP1_HUMAN, NCOA5_HUMAN
ncRNA 5'-end processing	7,70%	0.00022	UTP20_HUMAN, NOP14_HUMAN

C

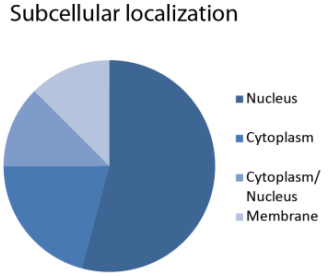

D

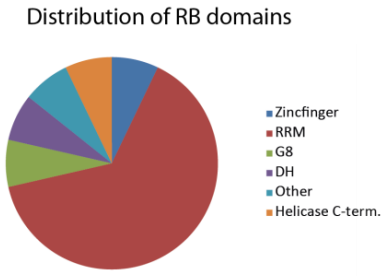

Figure 17 Heatmap of specific BKV/MCV/HPV41 hairpin RBPs and *in silico* analysis.
(A) Heatmap of proteins identified by mass spectrometry. Uniprot gene symbols are listed on the y-axis and pre-miRNAs are listed on the x-axis. Annotated protein hits were defined by score (obtained with Mascot and proteinscape) and normalized to the summarized counts of one protein. Pull-downs were performed in replicates and averaged afterwards. The probability of specific binding is indicated in blue shades (from white = 0 to blue = 30). Correlation of CMV pull-down results with r = 0.84 to the repeated results of cmv-miR-US5-2 indicates high reproducibility of the pull-down approach. (B) GO term analysis classifications with high p-values and cluster frequency. (C) Subcellular localization of identified proteins (classified with Uniprot database). (D) Distribution of RNA binding domains within the identified proteins.

Preclearing samples as well as an additional pull-down with cmv-miR-5-2 served as controls. The cmv-miR-5-2 pull-down was used as positive control. The additional pull-down with a pre-miRNA of CMV was necessary to compare and correlate the small data set of the papilloma and polyoma virus pull-down with the CMV data set because a negative control of the pri/pre-miRNA is not

defined and hence was missing. Thus an additional pull-down with the cmv-miR-5-2 was performed together with the BKV, MCV and HPV41 pull-downs to compare the data sets and to obtain a marker for the reproducibility of the pull-down experiments. The correlation between the different cmv-miR-5-2 pull-downs of r = 0.84 suggests a significant overlap of both data sets (Figure 17 A).The heatmap depicts specific single hits for most of the annotated proteins like GRSF1, NOP14, Sync or PTBP1.

GO term analysis links the found proteins to different RNA based regulatory functions (Figure 17 B, also included in appendix Figure 42) and Uniprot analyses reveal that most of the proteins contain RNA binding domains and that they are located mainly within the nucleus (Figure 17 C).

Taken together, the statistical analysis suggests the specifically identified RBPs as RNA associated proteins.

2.1.4 pri-miRNAs sequence alignments with RBP consensus motifs

RBPs interact with RNAs via RBDs that recognize and bind RNA sequence motifs. To identify such sequences, bioinformatical sequence alignments were performed using sequences of the different RBP interacting pri/pre-miRNAs. In Table 5 examples of sequence motifs are summarized.

The proteins GRSF1 (G-rich sequence factors 1) and Pum2 (Pumilio homolog 2) contain RNA binding domains with a well-known consensus sequence. GRSF1 interacts with viral, cytoplasmic and mitochondrial ssRNAs within G-rich elements of the 5'UTR with a consensus motif of AGGGA/U/G (Antonicka et al. 2013; Jourdain et al. 2013; Noh et al. 2016; Ufer et al. 2008). MSAs were performed and analyzed according to the location of the consensus sequences. Within the pri-miRNAs (bkv-miR-B1, hsv-miR-H3, hsv1-miR-H6 and hsv1-miR7) bound to GRSF1 the MSA depicts several motifs highlighted in yellow within the sequence which may be conserved through pri/pre-miRNAs (Figure 18 A). The predicted binding sites are located in the double stranded stem and the single stranded loop of the hairpin structure (Figure 18 B, highlighted in yellow).This suggests that the known binding motif which is located within the ssRNA terminal loop is specifically recognized by RBDs within GRSF1. However, the sequence motif is also found in the stem of the hairpin and thus, specific binding has to be biochemically confirmed.

Pum2 binds to a consensus motif with the sequence UGUA(N)AUA (Loedige et al. 2013). The MSA shows a perfectly conserved sequence within ebv-miR-3/4/10 (Figure 18 C, highlighted in yellow) and the location within the hairpins is exclusively in the loop region (Figure 18 D). This suggests that Pum2 interacts with the ssRNA region within the terminal loop that exhibits the binding motif.

For additional multiple sequence alignments and hairpin alignments of PURA, NOL11, PTBP1 and PLOD3 see appendix Figure 44.

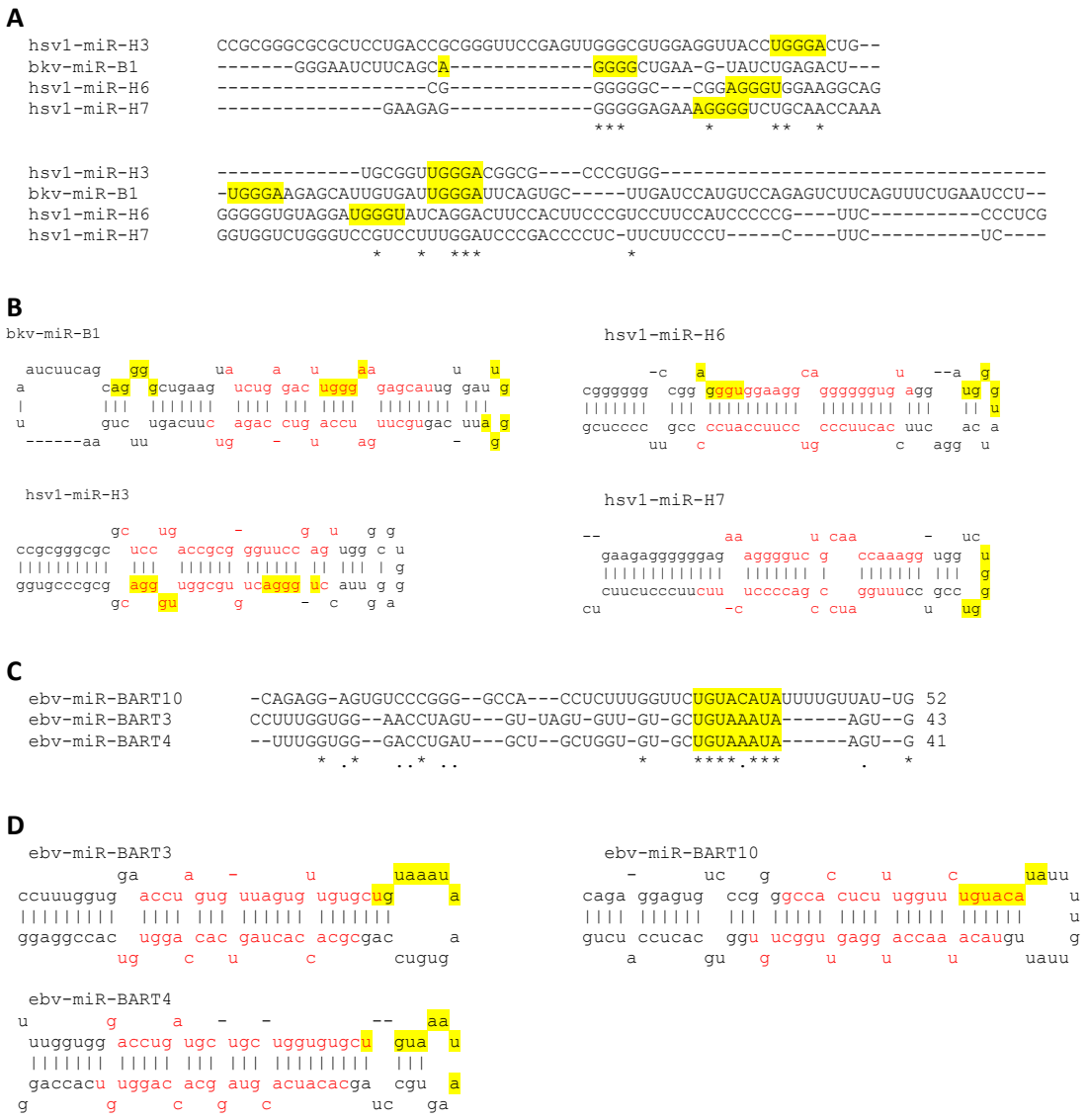

Figure 18 Multiple sequence alignments (MSA) from pri-miRNAs interacting with one particular candidate.
(A) MSA of pri-miRNA sequence of hsv1-miR-H3/-H4/-H7 and bkv-miR-B1 performed with Clustal Omega from EMBL-ebi-tools. (B). Location of the consensus sequence within the pri-miRNA hairpins marked in yellow, sequence of mature miRNAs are highlighted in red. Complementary base pairing is illustrated with lines between the corresponding bases. Hairpin structures were taken from the miRBase database (C) MSA of the pri-miRNA sequence of ebv-miR-3/4/10 performed with Clustal Omega from EMBL-ebi-tools. (D) Location of consensus sequence within the pri-miRNA hairpins marked with yellow, sequence of mature miRNAs are shown in red. Complementary base pairing is illustrated with lines between the corresponding bases. Hairpin structures were taken from the miRBase database.

Table 5 ***In silico*** **characterization of pri/pre-miRNA binding candidates (with Uniprot, Genecard, NCBI CDD, EMBL InterPro/SMART and other references).**

protein	bound miRNAs	consensus seq.	RNA bin. domain
GRSF1	hsv1-miR-H3/-H4/-H7 bkv-miR-B1	AGGGA/U/G	RRM
PUM2	ebv-miR-3/4/10	UGUA(N)AUA	Pumilio rpts./PUM-HD
PURA	hsv1-miR-H3 cmv-miR-70/148	GGN	PUR
NOL11	cmv-miR-112 bkv-miR-B1	not known	WD-40
PTBP1	hsv1-mir-H8 cmv-miR-59 hpv41-miR-1	not known	RRM
PLOD3	hsv1-miR-H3/H6 cmv-miR-70	not known	not known

2.1.5 Validation of specific pre-miRNA-RBP interactions

The identified potential hairpin interacting proteins have to be validated, because methodical and technical performance may promote unspecific binding of false positives. As a first validation step, the DNA-sequence of a subset of candidates was amplified and cloned into human expression vectors with an N-terminal Flag/HA-tag. Proteins were transiently overexpressed in HEK 293T cells and the pri/pre-miRNA pull-down approach (as described in 2.1.3) was repeated and confirmed by western blotting using antibodies against the HA-Tag (Figure 19 A). Several candidates were tested for EBV, CMV and BKV/ HPV41 (Figure 19 B-D). For EBV, the candidates show a specific interaction to NOL8, TRIM25, PUM2 and c9orf114. In contrast, SK2L2 also bind to the control pull-down with an unrelated pri/pre-miRNA. In case of CPSF5 and CPSF7, which exist as complex only CPSF5 shows weak bidning to the hairpin.

The interaction validation for the papilloma and polyoma virus hairpins shows a specific and clear binding pattern for the selected candidates GRSF1, ARMX1, PTBP1 and Zincfinger 7b compared to the control pull-down (this experiments were partly done by my bachelor student Barbara Ritter; Figure 19 C).

For cytomegalovirus, human as well as viral potential interactors were tested. The data depicted in Figure 19 D confirms specific binding of Rbfox2, UNG, SDOS and PTBP1. The viral Factors UNG, UL97, UL77 and PP65 show weak or unspecific binding in this experimental set-up (data not shown expect for UNG). Taken together many of the identified potential hairpin interacting candidates

seem to bind specifically to the exposed viral pri/pre-miRNAs. Others could not be validated as specific binders in this experimental set-up.

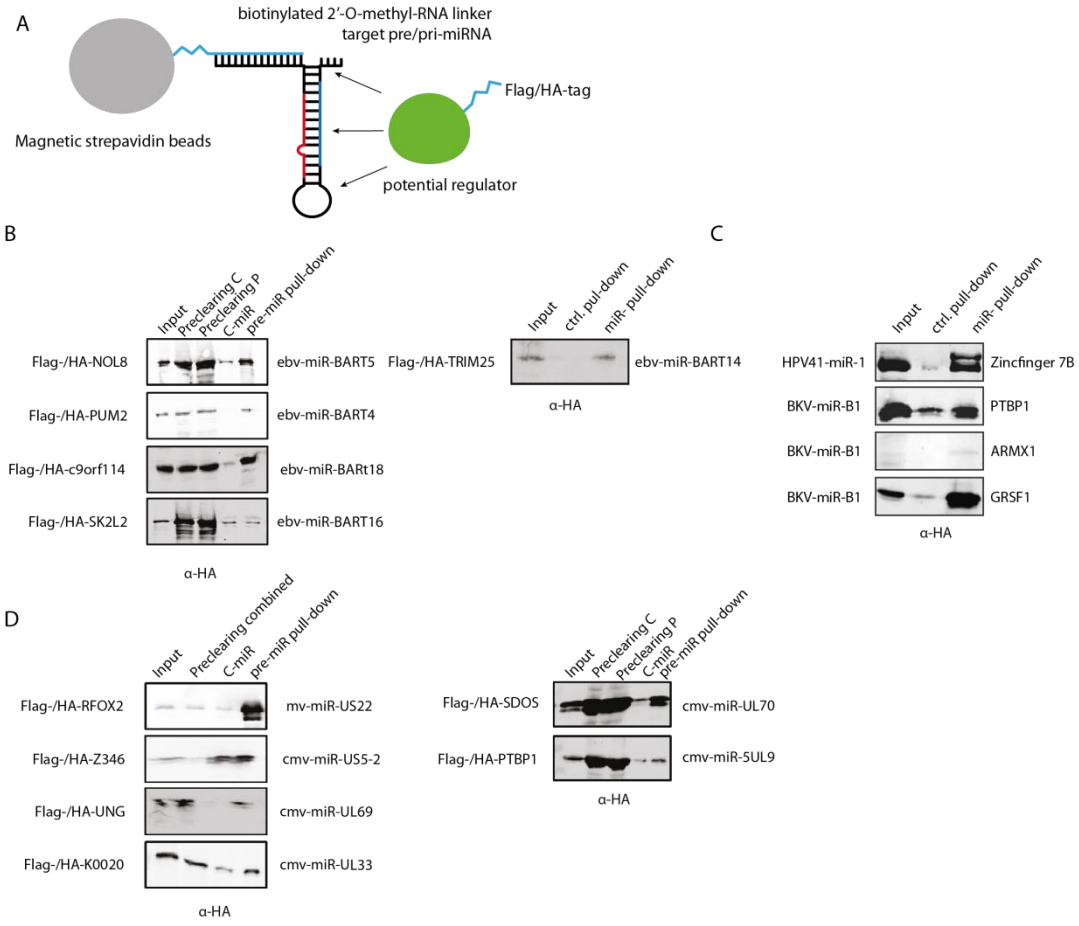

Figure 19 Validation of the specific pri/pre-miRNA protein interactions.
(A) Validation of the identified protein pri-miRNA interactions by repeating the pri-miRNA pull-down workflow with Flag/HA-tagged overexpressed constructs and detection by western blots. After preclearing of the lysate, pull-downs were performed with specific pri-miRNAs and on unrelated control. For overexpression, 5 to 15 µg of VP5-constructs were used per 15 cm^2 dish. (B), (C), (D) Pull-down of Flag/HA-tagged potential interactors using different miRNA hairpins. 5 % of the lysates were loaded as input.

2.1.6 Influence of RBP candidates on viral miRNA processing

To examine potential effects of the identified RBP candidates on processing of pri/pre-miRNAs, Flag/HA-candidate RBPs were overexpressed in HEK293T cells at different time points. As viral miRNAs are not present in HEK 293T cells, effects of overexpressed regulators may change the levels of the different miRNA processing species (Figure 20 A - D).

These effects can be caused by inhibition or activation of Drosha or Dicer cleavage by a specific interaction of the RBP with the hairpin that could block or stabilize the recruitment of the processing complexes. Western blotting using specific antibodies against the HA-tag controlled overexpression of proteins. Cells were harvested 15 or 30 hours after transfection and changes of

mature and pre-miRNA levels were detected using northern blotting probes against the mature miRNAs. Signals were quantified using a Phosphoimager (PMI) and normalized to the U6 loading control. The candidate Nol8 was validated as specific interactor of ebv-pri/pre-miR-BART5 (Figure 19 B). In Figure 20 A and B the signal intensities of the ebv-pre-miRNA-BART5 are decreased compared to the samples without Nol8 overexpression at both time points. Although the overexpression of Nol8 slightly decreases the level of pre-miRNAs, the mature miRNA levels of the ebv-miR-BART5 seem to be unaffected at both time points represented by an equal signal intensity (Figure 20 A and B). This suggests that Nol8 may block processing of ebv-miR-BART5.

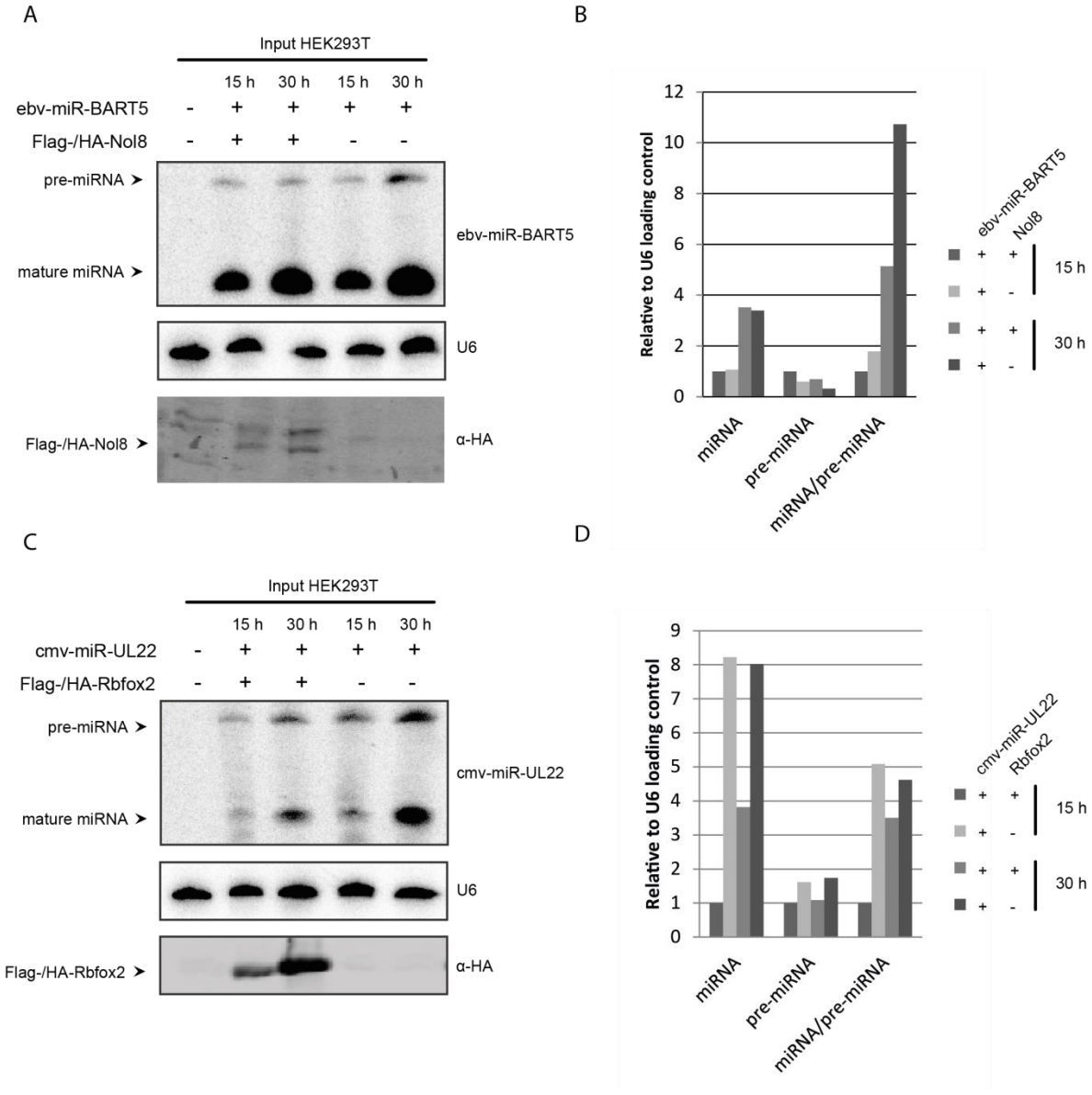

Figure 20 Influence of potential regulators on miRNA levels.
(A) Schematic overviews of myc-Drosha-IP. (B) Overexpression was performed with standard CaPi-transfection using 5 µg of plasmid for proteins and 10 µg of plasmid for miRNA in HEK293T cells. 5 % of lysate was taken as input control. IP was performed with 50 µl Protein Sepharose G beads coupled with 3 µg of myc antibody. The whole IP was loaded onto a 10 % SDS-PA-gel. (C), (D) For overexpression of proteins and miRNAs, HEK 293T cells were transfected using CaPi method. Protein overexpression was controlled by western blot using HA-antibody. 20 µg of total RNA was loaded for standard northern blotting. Signal quantification was performed using PMI software and normalized to U6 loading control levels.

The RBP Rbfox2 inhibits microprocessor processing by interacting with the terminal loop of different pri-miRNAs and reduces Dicer levels by downregulation of miR-20b and miR-107 (Yu Chen et al. 2016). The suggested consensus sequence GCAUG is also present in the terminal loop of cmv-miR-US22 (data not shown). Rbfox2 specifically interacts with the cmv-miR-US22 (Figure 19 C) and may also influence viral miRNA processing steps. The signal intensities of both, the overexpressed mature miRNA and overexpressed pre-miRNA of cmv-miR-US22 are clearly reduced compared to the control with normal expression of Rbfox2 (Figure 20 C and D).

This suggests that Rbfox2 inhibits miRNA processing by blocking of microprocessor processing of cmv-miR-US22.

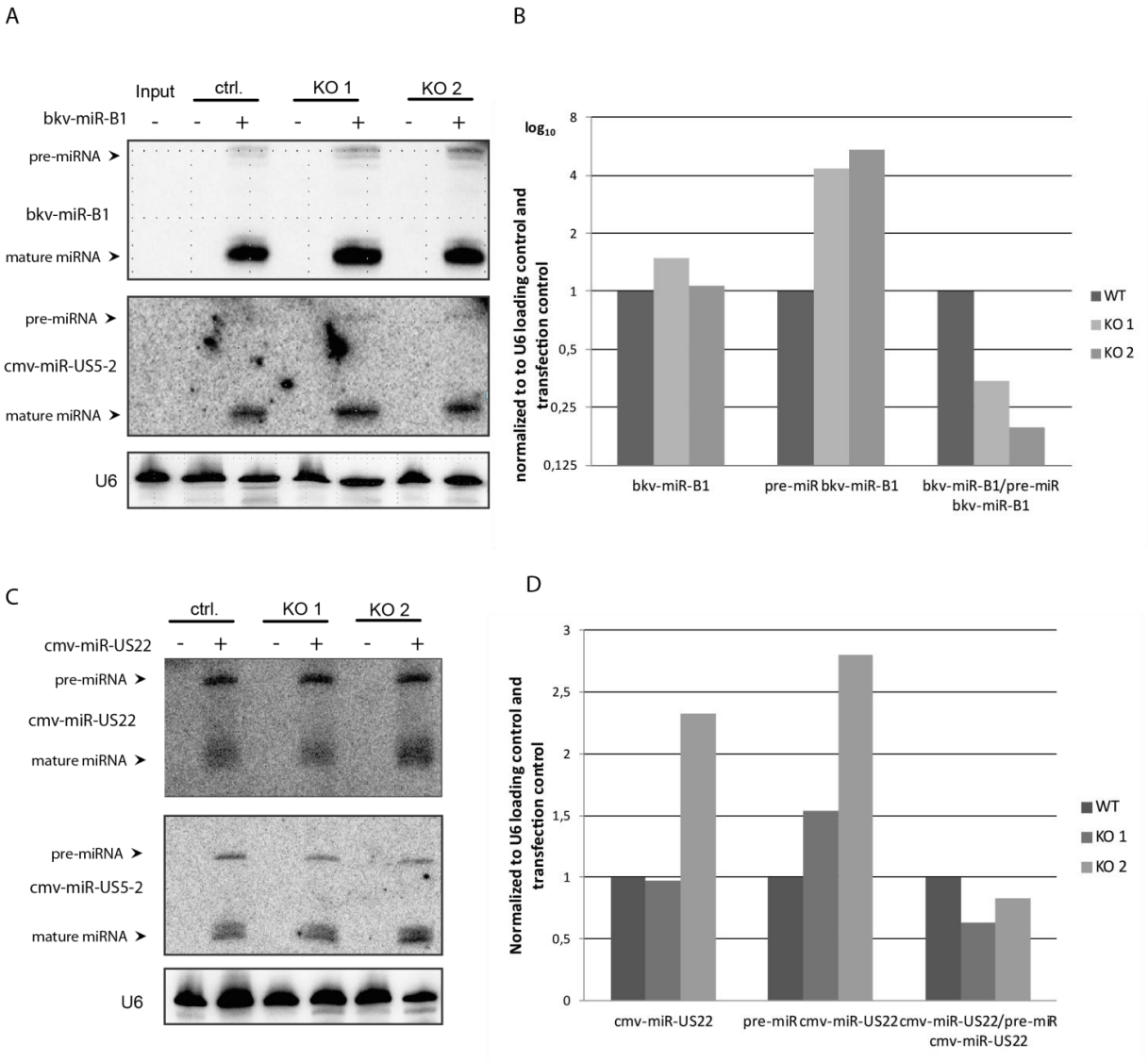

Figure 21 Influence of potential regulators on miRNA levels.
(A), (C) HEK293T K.O. cell lines were produced using the CRISPR/Cas9 method. Cells were cultured in 6-wells and transfected with 0.5 µg of each miRNA expression and control plasmid with unrelated miRNA cmv-miR-US5-2. For northern blotting, 20 µg of total RNA was loaded and separated on a 12 % PA-gel. For detection of miRNAs and pre-miRNAs, complementary DNA probes were used. (B), (D) Signals were quantified using PMI software and normalized to both U6 loading control and the unrelated transfection control.

In addition, GRSF1 and Rbfox2 HEK293T K.O. cell lines (produced by Dr. Thomas Treiber and Dr. Nora Treiber, partly published in Treiber et al. 2017) were transfected with miRNA expression vectors to further analyze the effects on miRNA biogenesis. Unrelated miRNAs were co-expressed as transfection control (Figure 21 A - D). For quantification, data was normalized to the U6 loading control and to the transfection control. Northern blots in Figure 25 A and B depict higher signal intensities for mature miRNAs in the K.O. cells and further much stronger levels of pre-miRNAs. The ratios of miRNAs to pre-miRNAs in Figure 25 B suggest that the efficiency of processing is low. Thus, the cytoplasmic GRSF1 isoform may bind to the hairpin loop and influence pre-miRNA cleavage. This suggests that GRSF1 is promoting the miRNA processing of the bkv-miR-B1.

Rbfox2 K.O. clearly leads to higher pre-miRNAs levels and to a very slight increase of the mature miRNA when compared to WT control (Figure 25 C and D). This result suggests that Rbfox is a negative regulator of miRNA biogenesis of the cmv-miR-US22.

Taken together, a few examples were presented in this chapter where RBPs influence viral miRNA processing.

2.2 Part II: Post-translational modifications of TNRC6 proteins

2.2.1 Aims of part II

As described in the introduction the importance and the functional principles behind gene silencing are reasonable well understood and our knowledge about miRNA-guided gene regulation during embryonic development, homeostasis and disease is increasing every day. However, less is known about post-translational modifications of the RISC complexes and dynamic signalling pathways.

The aim of this part of the thesis was to establish a strategy to analyze protein modifications of TNRC6 proteins and to functionally characterize these potential modifications.

Brief overview of planned workflow:

1. Specific antibodies against TNRC6 proteins will be established and functionally characterized
2. Purification strategies for TNRC6 and Ago will be optimized
3. Mass spectrometric analysis of modifications of TNRC6 and Ago complexes
4. Functional validation and characterization of TNRC6 phosphorylation sites

2.2.2 Purification and characterization of TNRC6 containing complexes

2.2.2.1 Characterization of monoclonal antibodies against TNRC6 proteins

For the production of monoclonal antibodies against TNRC6 proteins, several different overexpressed fragments of TNRC6A-C, such as the RRMs or the C-terminal parts of the three paralogs were used to immunize rats and mice (listed in material and methods, Table 14). Immunization was performed by the group of Dr. med. Elisabeth Kremmer and Dr. Regina Feederle in the monoclonal antibody core facility (MAB) at the Helmholtz center in Munich. Monoclonal antibody hybridoma supernatants were received from our collaborators and tested in western blotting, immunopurification and partly in immunofluorescence experiments. Antibody screening was performed with input samples of HEK 293T cell lysates and overexpressed Flag/HA-TNRC6A-C proteins that served as positive control. Gel-separated proteins were blotted on nitrocellulose

membranes and incubated with the appropriate TNRC6A-C antibodies. Detected signals were confirmed as TNRC6 proteins with HA-antibody against the tag. Positive candidates were further analyzed regarding their subtype specificity (IgG1, IgG2a, IgG2b, IgG2c with secondary antibodies linked to HRP; data not shown) and were afterwards purified in a large scale set-up from Robert Hett (colleague in the lab).

Enrichment of TNRC6 proteins was further tested by using lysates from different human cell lines (data shown for HEK293T and Hela cells only) for immunoprecipitation with the antibodies 6G3, 7A9 and 11C12. Therefore, monoclonal antibodies were coupled to Protein Sepharose G beads, incubated with HEK 293T/ HeLa cell lysates, washed and loaded onto a 6 % SDS-PA-gel and detected per western blotting with the same antibodies used for IP (Figure 22 A). Monoclonal antibodies were further characterized for their specificity in knockdown experiments (performed by Daniel Schraivogel and partly published in Schraivogel et al., 2015).

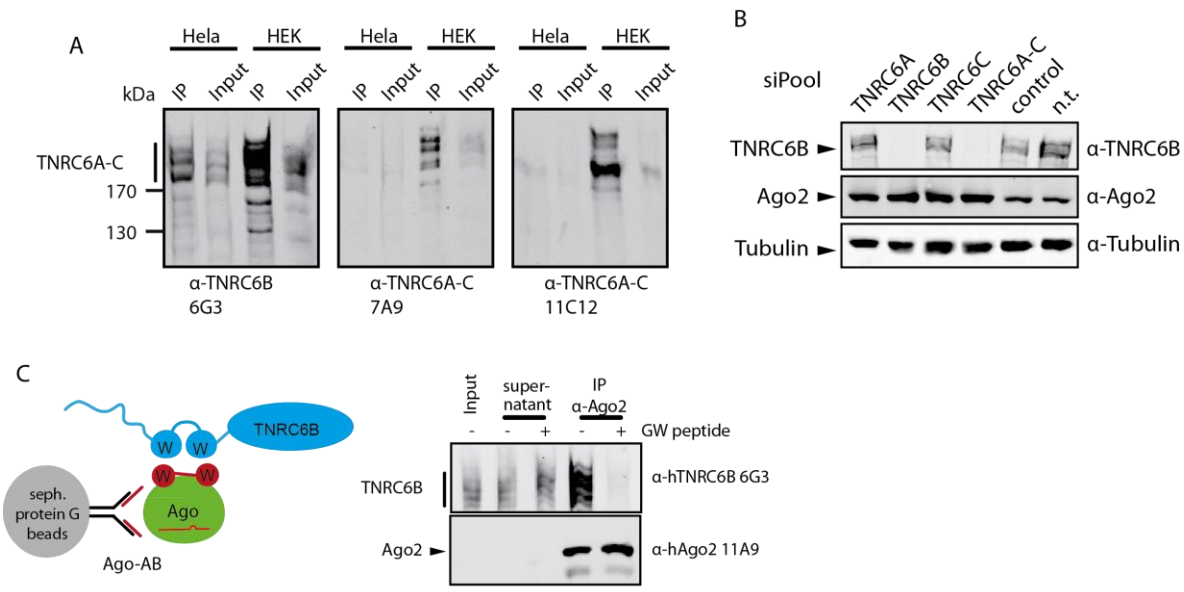

Figure 22 Characterization of monoclonal antibodies against TNRC6 proteins.
(A) Monoclonal antibodies were coupled to Protein Sepharose G beads and incubated with HEK293T and HeLa cell lysates. The proteins were detected with the same antibody that was used for immunoprecipitation. (B) For further characterization of the antibodies, knockdown assays with siPools against endogenous TNRC6A-C showed particular specificity for the proteins compared to control and non-transfected (n.t.) samples. (C) The association of Ago and endogenous GW proteins is disrupted by the GW peptide. Co-immunoprecipitations of Ago2 and TNRC6B were conducted either in presence or absence of an excess amount of the GW peptide, showing high specificity of the TNRC6B antibody.

To confirm antibody specificity, differential knockdowns of TNRC6 proteins using siPools were performed and detected by western blotting. The reductions of endogenous protein levels illustrate specific antibody detection because in knockdown samples signals should be decreased and unspecific detection would remain. Figure 22 B shows that the monoclonal antibody 6G3 is

specific for TNRC6B. In case of the 6G3 antibody, co-immunoprecipitations of Ago2 and TNRC6B were conducted either in the presence or absence of a recombinantly produced TNRC6 peptide that competes for Ago1-4 binding (Figure 22 C, performed and published in Hauptmann et al. 2015). Both experiments also show that TNRC6 proteins are stable in input samples but seem to get degraded quickly in immunoprecipitation experiments which might be generally problematic for biochemical investigations. Antibody tests and selectivity are summarized in Table 6. To optimize the purification process of TNRC6-Ago complexes, the antibodies were purified (performed by Robert Hett, see in 4.2.4.2).

Table 6 **Antibody specificity** (confirmed by MS analysis).

antibody	specificity	method
C RRM 4D7	TNRC6 A,B,C	WB, IP
B RRM 6G3	TNRC6 B	WB, IP, IF
C RRM 7A9	TNRC6 A,B,C	WB, IP, IF
RRM 7C5	TNRC6 A,B,C	WB, IP
B RRM 10B1	TNRC6 B	WB, IP
TC6 C 11C12	TNRC6 A,B, C (mainly C)	WB, IP

Figure 23 A illustrates that TNRC6 co-IPs performed with purified antibodies show reduced background levels, higher sample purity as well as distinct and clear bands for TNRC6 as well as Ago1-4 proteins compared to co-IPs with non-purified hybridoma supernatants. The immunoprecipitated TNRC6 and Ago1-4 proteins were analyzed by mass spectrometry. The obtained MS data analysis assigns the indicated coomassie bands to the respectiveTNRC6 proteins and emphasizes the selectivity of the used antibody 7A9 for all three TNRC6 proteins with high probability scores and sequence coverages especially when the purified antibodies were used (Figure 23 A and B). Besides immunoprecipitation of endogenous TNRC6A-C, the newly established antibodies are capable of co-immunoprecipitating endogenous human Ago1-4 at high purity. This allows continuative experiments such as MS-based phospho-analysis.

Following large-scale purifications from HEK 293T cell lysates with around 100 mg of total protein were performed to enrich enough endogenous TNRC6 proteins for a detailed phospho-proteomic analysis. Therefore immunopurifications with the ABs 6G3, 7A9 and 11C12 were conducted and coomassie-stained SDS-PA-gels confirm a high antibody selectivity for TNRC6 proteins and large amounts of purified endogenous proteins (Figure 23 C in the upper part of the gel). Additionally to Ago proteins, Pabpc1 which is interacting with TNRC6 and is associated with the target mRNA was enriched and identified by mass spectrometry (listed in appendix 5.1.4 Table 18).

A

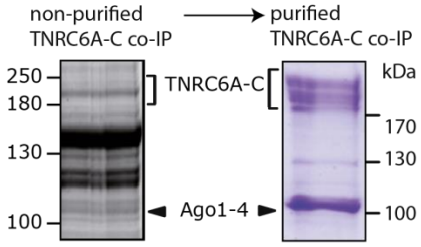

B

Protein	Mass [kDa]	Sequence coverage	
TNRC6B	193.8	0.42	0.66
TNRC6A	210.2	0.09	0.60
TNRC6C	175.9	0.11	0.69
AGO2	97.1	0.42	0.75
AGO1	97.2	0.25	0.79
AGO3	97.3	0.26	0.64
AGO4	97.1	0.08	0.57
		non-purified →	purified

C

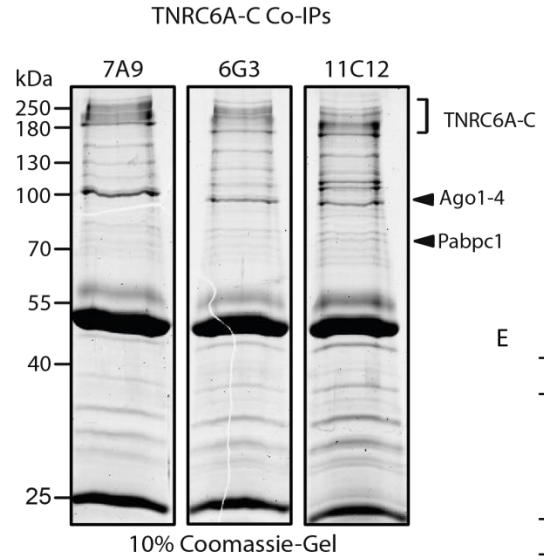

D

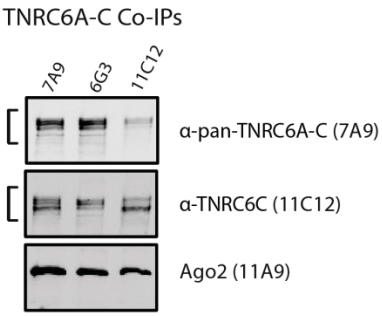

E

Protein	Mass [kDa]	Sequence coverage		Identified peptides	
TNRC6B	193.8	77.6	70.2	251	229
TNRC6A	210.2	71.0	60.4	168	158
TNRC6C	175.9	51.8	64.4	65	102
		upper part	lower part	upper part	lower part

F

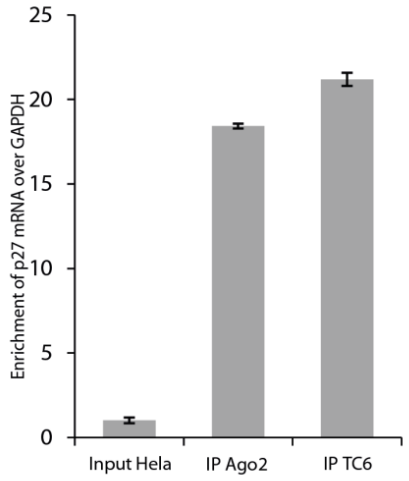

Figure 23 Further functional characterization of the TNRC6 antibodies.
(A) Different monoclonal antibodies against TNRC6 proteins were coupled to Protein G Sepharose beads and incubated with HEK293T cell lysates. To increase sample purity, the antibodies were purified by affinity and size exclusion chromatography. The immunoprecipitated TNRC6 and Ago1-4 proteins were identified and analyzed by mass spectrometry. For further characterization of the tested antibodies TNRC6A-C and Ago1-4 were identified by mass spectrometry. The (co)-immunoprecipitated proteins were cut from a coomassie-stained gel and subjected to in-gel tryptic digest. (B) The MS data analysis shows a selectivity of the used antibody to all TNRC6 paralogs with high scores and sequence coverages. The possibility to co-precipitate all human Ago proteins will facilitate the analysis of post-translational modifications of TNRC6-interacting Ago proteins. (C) Comparison of co-IPs with (D) antibody specificity analyzed by western blot detection of TNRC6A-C co-IPs illustrates higher selectivity of the 11C12 AB against TNRC6C. (E) The MS data analysis of a TNRC6A-C 7A9 co-IP indicates selectivity of the used antibody for all three TNRC6 proteins with high scores and sequence coverages. The data was obtained after division of the SDS-gel in an upper and lower part. (F) Confirmation of complex integrity by qRT-PCR. The target p27 was tested upon binding to Ago2 enriched in RNA-IP experiments with 7A9 vs. 11A9 antibody from HEK 293T cells. RNA from each IP was extracted, cDNA was synthesized and mRNA enrichment was measured by qRT-PCR. Relative enrichment of the target mRNA p27 was normalized to GAPDH. Experiment was performed in three technical replicates.

Enrichment of TNRC6 and Ago proteins was confirmed by specific signals in western blots using 10 % of the second elution of the IPs (Figure 23 D). Due to methodical limitations the part of the SDS-PA-gels which contain TNRC6 proteins were excised as a lower and upper part. Interestingly, this approach leads to the qualitative separation of the TNRC6 paralogs. According to sequence coverage and specifically identified peptides, TNRC6A and B are enriched in the upper part while TNRC6C is more located in the lower part (Figure 23 E). This qualitative observation is supported by protein size as well as by small differences that can be observed within the western blots and the coomassie-stained gels. Figure 23 D shows the western blot signal for TNRC6 in the lane of the 11C12 co-IP that appears after incubation with 11C12 antibody. This suggests a certain selectivity of 11C12 for TNRC6C. However, this assumption remains speculative and has to be additionally validated by other experiments. TNRC6/Ago complexes associate with target mRNAs. To test whether the established antibodies immunoprecipitate such complexes or interrupt mRNA interactions, qRT-PCRs were performed on a target. Therefore, RNA-IPs with Ago2 11A9 antibody and TNRC6 7A9 antibody were performed and mRNA enrichment of the p27 mRNA target was confirmed by qRT-PCR (Figure 23 F).

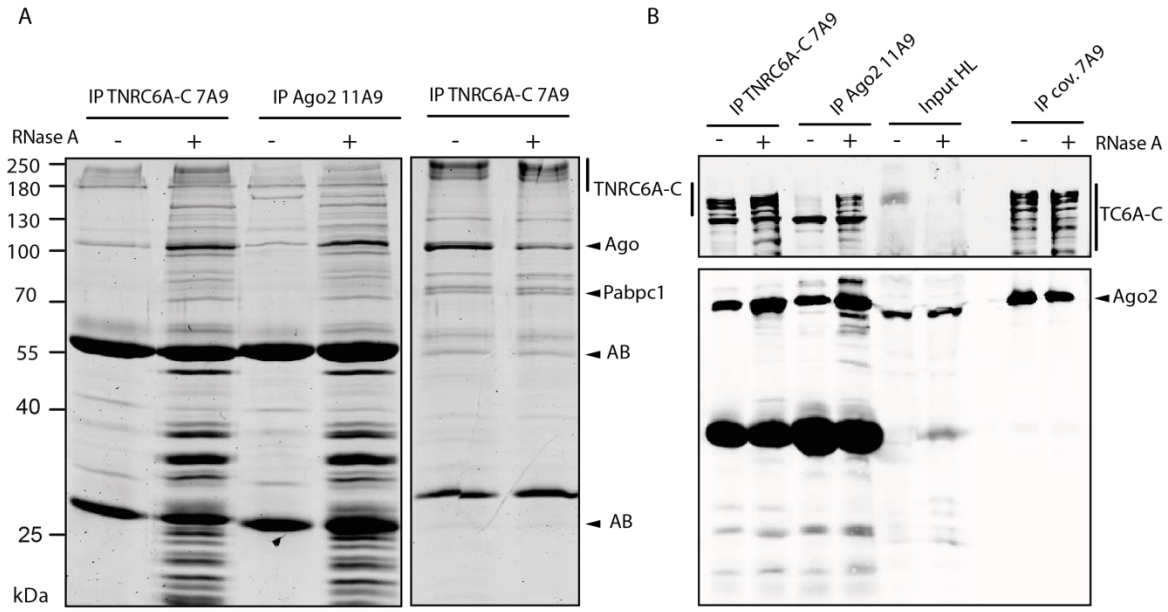

Figure 24 Further analysis and optimization of immunopurifications.
(A) Comparison of co-IP efficencies of 7A9, 11A9 and cov. coupled 7A9 with/without RNase A treatment of HEK-lysates in a coomassie-scaled manner. (B) Western blot was performed with 5 % of the first elution of the IPs as control.

To achieve higher sample purity and larger amounts of enriched TNRC6-Ago complexes for phospho-proteomic analysis, IP conditions were optimized by testing different lysis and elution conditions (Figure 23 A, B). In the left part of Figure 23 A RNase A was added during cell lysis and afterwards TNRC6 and Ago IPs were performed. The treatment resulted an enrichment of TNRC6A-C and Ago1-4 in both IPs. This result was additionally confirmed by western blotting

(Figure 23 B). This suggests that RNA degradation by RNase A results in a better accessibility to TNRC6-Ago complexes.

Furthermore, antibodies were covalently coupled to the beads and cell lysates were applied. To reduce unspecific background within the SDS-gels, a selective elution of the antibody bound proteins was performed with glycine adjusted to pH=2.5 (right part in Figure 23 A). The lanes with reduced background were excised and analyzed with mass-spectrometry. The analysis identified many known interactors of the whole gene silencing pathway (protein list in appendix Table 18).

Taken together, TNRC6 specific antibodies were established and the characterization underlined the power of our antibodies as useful tool for further phospho-proteomic analysis

2.2.2.2 Immunopurification of TNRC6-Ago complexes from mouse tissues

The TNRC6 antibodies are a useful tool to enrich TNRC6-Ago complexes in human cell lines. To widen their usage applicability the antibodies were tested for cross reactivity with TNRC6 proteins in other species.

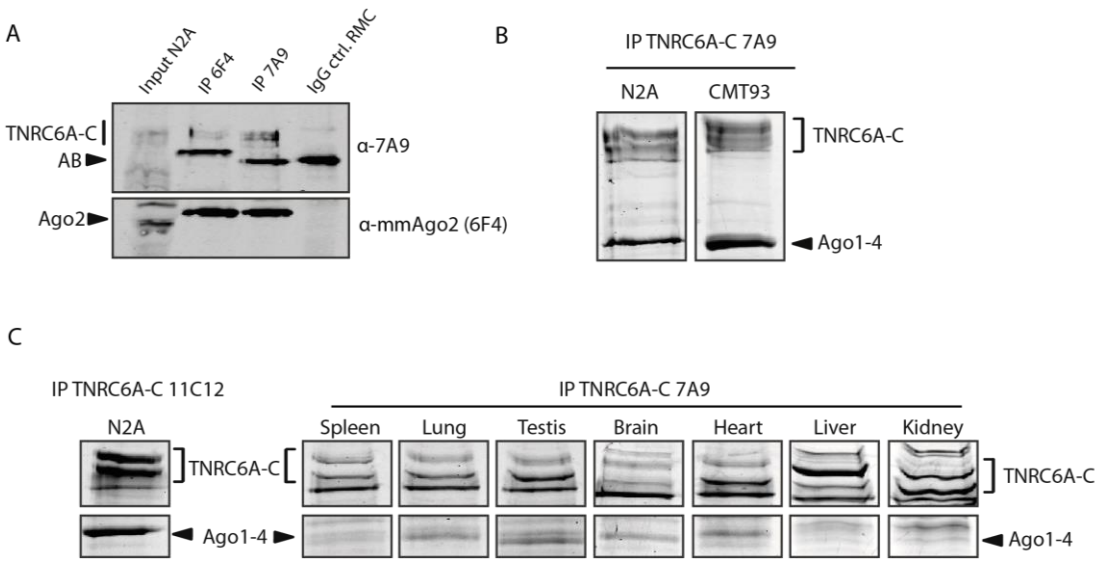

Figure 25 Purification of murine TNRC6-Ago complexes.
(A) Western blot detection of mmAgo2 and TNRC6A-C IPs performed with mmAgo2 6F4 and TNRC6A-C 7A9 antibodies. 5% of input was loaded and RMC-IP served as IgG control. (B) Coomassie-stained 10% SDS-gels loaded with immunoprecipitated 7A9-IPs from N2A mouse brain cells and CMT93 spleen cells. (C) Immunopurified murine TNRC6 and Ago1-4 from different mouse tissues. IP from N2A lysates served as positive control.

TNRC6 proteins were first aligned in multiple sequence alignments (MSA). The results show a relatively weak conservation among the human paralogs (around 0,4-0,45; listed in the appendix Figure 44), but a very strong conservation between species (mmTNRC6A : hsTNRC6A =0.9473; mmTNRC6B : hsTNRC6B =0.9644; mmTNRC6C : hsTNRC6A =0.9138; listed in the appendix Figure 44).

To test specificity of TNRC6 antibodies for the mouse homologs, IPs were performed with cell lysates from N2A nervous mouse cells where Ago1-4 and TNRC6 proteins are highly expressed and detected by western blotting. For comparison, an IP with the mmAgo2 specific antibody 6F4 (Frohn et al. 2012) and an IgG control with the unrelated RMC antibody were performed. This illustrated that the 7A9 antibody can enrich Ago as well as the 6F4 with an even better enrichment rate of TNRC6 proteins (Figure 25 A). Continuous coomassie-scaled purifications with 7A9-IPs from N2A and CMT93 cells were conducted (Figure 25 B). Furthermore, endogenous TNRC6 and Ago1-4 was purified from different mouse tissues (Figure 25 C). Both coomassie-scaled purifications indicate that mouse TNRC6 proteins are immunoprecipitated with high quantity and selectivity by the monoclonal TNRC6 antibodies.

The purification was then used for quantification studies of endogenous TNRC6 expression levels (see chapter 2.2.3.2) and phospho-proteomic analysis (see chapter2.2.3.2).

2.2.2.3 Quantification of TNRC6 expression levels in cells and mouse tissues

The TNRC6 antibodies can enrich human and mouse TNRC6-Ago complexes. To further characterize the antibody specificity, a detailed analysis for the preference of different TNRC6 paralogs for Ago interaction was performed. Most of the studies analyzing TNRC6 proteins are based on qualitative mass-spectrometry or qRT-PCR data sets. Thus the protein expression levels and paralog distribution remains speculative. For a complete understanding of the functionality of the produced and purified monoclonal antibodies, selected-reaction-monitoring (SRM) measurements were executed from different IPs as well as from input samples to examine endogenous paralog distribution. The SRM method is used for peptide quantification, therefore defined amounts of a stable isotope-labeled peptide is spiked into the sample before tryptic digestion. The synthetic and the peptide of interest will be detected at the same time and can still be distinguished by their isotopic mass difference. Unique peptides were selected for every human and mouse TNRC6 paralog and used for SRM analysis (location within the proteins depicted in Figure 26 A).

To assess the specificity of the antibodies, first the general distribution of TNRC6 paralogs was measured in HEK 293T cell lysates. Figure 26 B depicts the averaged distribution of the paralogs. Here, TNRC6A is the highest expressed with about 45 %, followed by TNRC6B with 30 % and TNRC6C with 25 %. For determination of the AB specificity, IPs with monoclonal TNRC6 and Ago antibodies were performed and analyzed with SRM. In Figure 26 C the quantification indicates

that the antibody 6G3 exclusively enriches TNRC6B. The monoclonal antibody 7A9 enriched TNRC6 B with 50 %, TNRC6A with 35 % and TNRC6C with 15 %. This suggests that the 7A9 enriches all three paralogs with a weak preference for TNRC6B compared to the inputs. The antibody 11C12 enriched in IPs with N2A cell lysates all TNRC6 paralogs with a preference for TNRC6C with 50 % (Figure 26 left side). This results suggests the antibodies to enrich TNRC6 proteins with certain preferences for different paralogs.

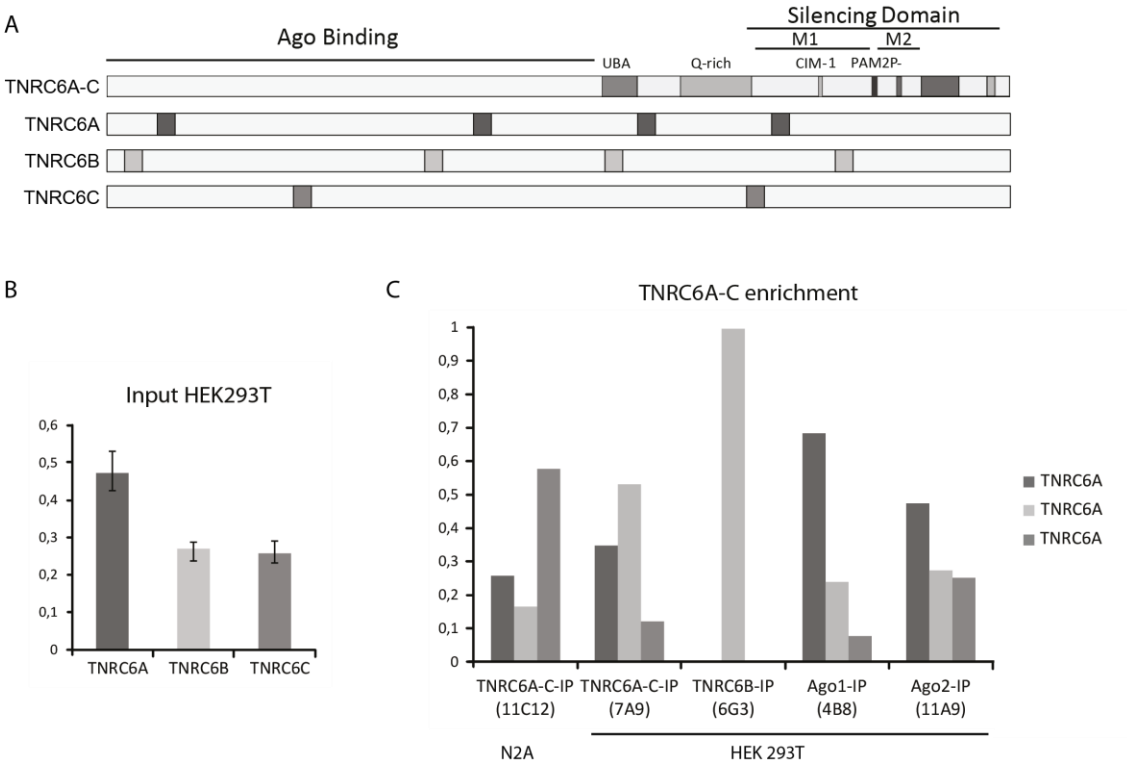

Figure 26 Quantification of TNRC6A-C and Ago1–4 levels.

(A) Schematic representation of unique SRM peptide localization within TNRC6 proteins. (B) Quantitative analysis by SRM measurements with stable isotope-labeled peptides of endogenous TNRC6A-C proteins from 50 and 100 µg HEK293T cell lysate. The relative amount of one TNRC6 paralogue related to the total TNRC6 pool is shown. Error bars represent the standard deviation of identical samples that were quantified with at least two different paralogue-specific peptides. (C) Enrichment and distribution of TNRC6 proteins by immunoprecipitation with different TNRC6- and Ago-specific antibodies.

The expression profile for TNRC6 proteins in different cell lines and mousse tissues is completely unknown.

To get a first insight, transcript levels of TNRC6 were assessed by qRT-PCRs. To analyze the different human TNRC6 paralogs, cDNA from different cell lines was used. In general, qRT-PCR results indicate that the amount of TNRC6B and TNRC6A transcripts is relative high and distributed similar between 40-50 %, with a 5-15 % higher expression of TNRC6A compared toTNRC6B, while TNRC6C possesses the lowest expression of about 5-10 % (Figure 27 A). In HEK 293T cells the expression of TNRC6B is up to 60 % and thus higher than TNRC6A and C. However, the analysis of

transcript levels just allows assumptions on the endogenous expressed proteins, because differential regulation on TNRC6 mRNAs levels can occur (Olejniczak et al. 2016).

Due to the small differences between the paralog transcript distributions detected by qRT-PCR, the TNRC6 expression profiles of different mouse tissues were analyzed with SRM measurements of 7A9-co-IPs.

Figure 27 Transcript levels of TNRC6A-C measured by qRT-PCR in different cell lines.

RNA from each cell line was extracted, cDNA was synthesized and mRNA enrichment was measured by qRT-PCR. Relative enrichment of the different TNRC6 proteins was normalized to GAPDH. The experiment was performed in three technical replicates.

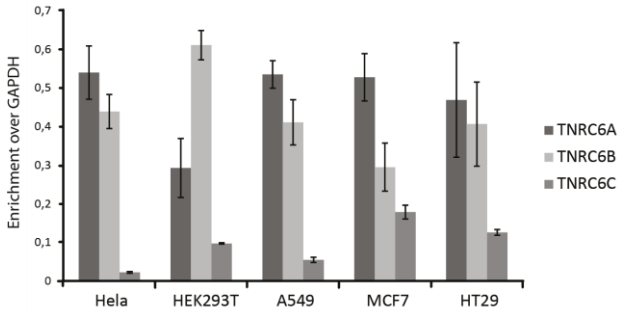

Purified TNRC6-Ago complexes from mouse tissues with 7A9-IPs (Figure 28) show a strong enrichment of TNRC6B in brain, heart, liver, kidney (comparable to HEK293T) and lung. Unfortunately inputs could not be measured because SRM measurements are technically limited and need certain protein amounts for significant measurements. In spleen and testis the TNRC6C signal is about 50 % higher compared to the other paralogs. Surprisingly, TNRC6A is expressed to a level up to 15 % in all mouse tissue samples compared to the other paralogs and the data obtained from HEK 293T lysates (Figure 26 B). This suggests that TNRC6 protein expression probably is tissue specific and might be regulated at the transcript level.

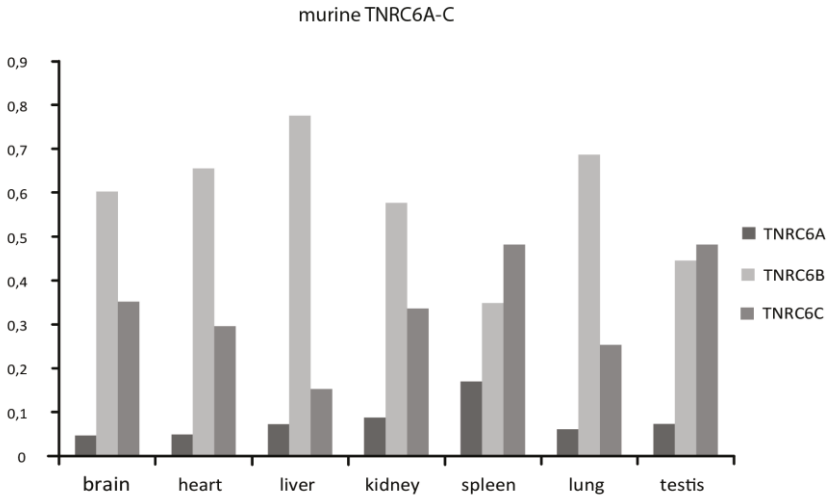

Figure 28 Quantification of TNRC6A-C levels in murine tissues.

Endogenous TNRC6 proteins were purified from different murine tissues using a 7A9-TNRC6-IPs and quantified via SRM approach.

TNRC6 proteins seem to have particular distributions in different cell lines and tissues. As these proteins function redundantly and Ago proteins also have distinct expression distributions, interaction preferences of Ago and TNRC6 proteins may be possible. To study the distribution of

Ago bound to TNRC6 proteins, 6G3- and 7A9-co-IPs were performed and analyzed by SRM. In Figure 29 both immunoprecipitations seem to enrich a similar distribution profile of Ago1-4. Compared to Ago-APP and inputs (Hauptmann et al., 2015) the distribution of Ago proteins in the two TNRC6-IPs is not significantly different (Ago2 0.6 - 0.7 > Ago1 0.2 - 0.3 >= Ago3 0.2 > Ago4 0.01). Ago1- and Ago2-co-IPs were performed to examine the distribution of interacting TNRC6 (Figure 26 C, left part of the graph). Both IPs show a similar distribution of co-immunprecipitated TNRC6 paralogs. This suggests that the usage of the ABs produces no preferences during complex purification.

Taken together, the quantification of the input and the IPs suggests that the monoclonal antibodies enrich TNRC6 with weak preferences. The 7A9 antibody enriches all three paralogs with a light preference for TNRC6B. The 6G3 antibody exclusively recognizes TNRC6B and the 11C12 antibody has a higher preference for TNRC6C. TNRC6 distribution profiling in mouse tissues resulted in tissue specific expression profiles of the different paralogs. The TNRC6 and also Ago proteins seem to interact with each other without preferences. Thus, it is suggested that the interaction profile depends on the differential cell line and tissue specific expression of the TNRC6 and Ago proteins.

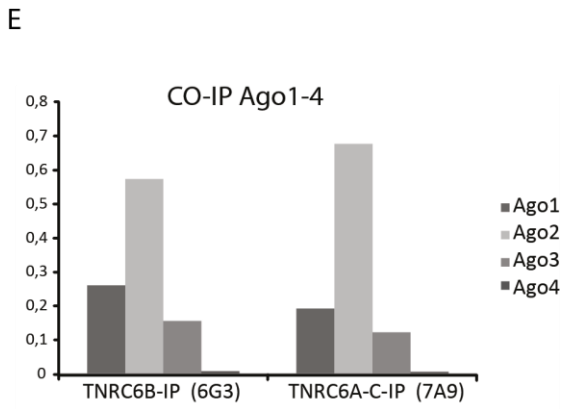

Figure 29 Quantification of co-immunoprecipitated Ago proteins
Ago1-4 protein levels were quantified from a 6G3-TNRC6B-and a 7A9-TNRC6A-C co-IP and analyzed by SRM.

2.2.3 Phosphorylation of mammalian TNRC6 proteins

2.2.3.1 Detection of endogenous phosphorylation sites of human TNRC6

Proteins are often regulated by post-translational modifications such as phosphorylation. To assess whether TNRC6 proteins are phosphorylated, endogenous TNRC6-Ago complexes were enriched using specific antibodies, separated on a SDS-PA-gel. The excised protein bands were digested and the peptides were eluted for mass spectrometric detection. Additionally, TNRC6-phospho-peptides were enriched with the TiO_2 FASP method where the TiO_2 column matrix selectively interacts with phospho-peptides. After washing, the bound phospho-peptides are eluted and analyzed by MS (performed by Dr. Astrid Bruckmann) (workflow schematically depicted in Figure 30 A). For statistical significance, data was obtained from technical as well as biological replicates. Only stable detected and overlapping phospho-sites within the technical (Figure 30 B) and the biological (Figure 30 C) replicates were considered in the analysis.

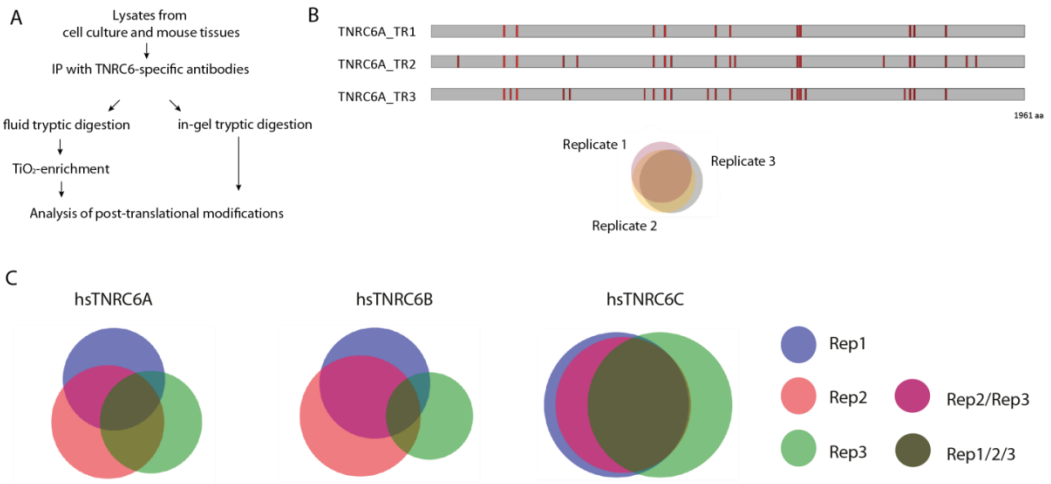

D

hsTNRC6A	hsTNRC6B	hsTNRC6C
S[739]	S[385]	S[465]
S[771]	T[480]	S[568]
S[943]	S[879]	S[714]
S[991]	S[1336]	T[777]
S[1217]	S[1432]	S[1011]
S[1585]	S[1461]	S[1016]
S[1599]	S[1512]	S[1674]
S[1704]	T[1517]	
	S[1816]	
	S[1832]	

Figure 30 Mass spectrometric detection of potential phosphorylation sites in endogenous TNRC6A-C proteins. (A) Schematic overview of the mass spectrometric workflow. (B) Grey bars represent the different TNRC6 paralogs, phosphorylation sites of technical replicates are indicated in red. Venn diagrams depict overlapping phosphorylation sites of technical replicates. (C) Venn diagrams depict overlapping phosphorylation sites of biological human replicates. Diagrams were conducted with the browser based software Biovenn. (D) Summarized phospho-sites of biological replicates. Selected phospho-sites are found in at least two replicates. Red: conserved among all paralogs; Green: conserved among two paralogs.

In Figure 30 B the technical replicates (TNRC6_TR1-3) for MS measurements of TNRC6A represented as grey bar and detected phospho-sites as red bars are shown at the relative position within TNRC6A. The overlapping phospho-sites of all three technical replicates (TNRC6_TR1-3) were combined as one biological replicate as illustrated in the Venn diagram (Figure 30 B).

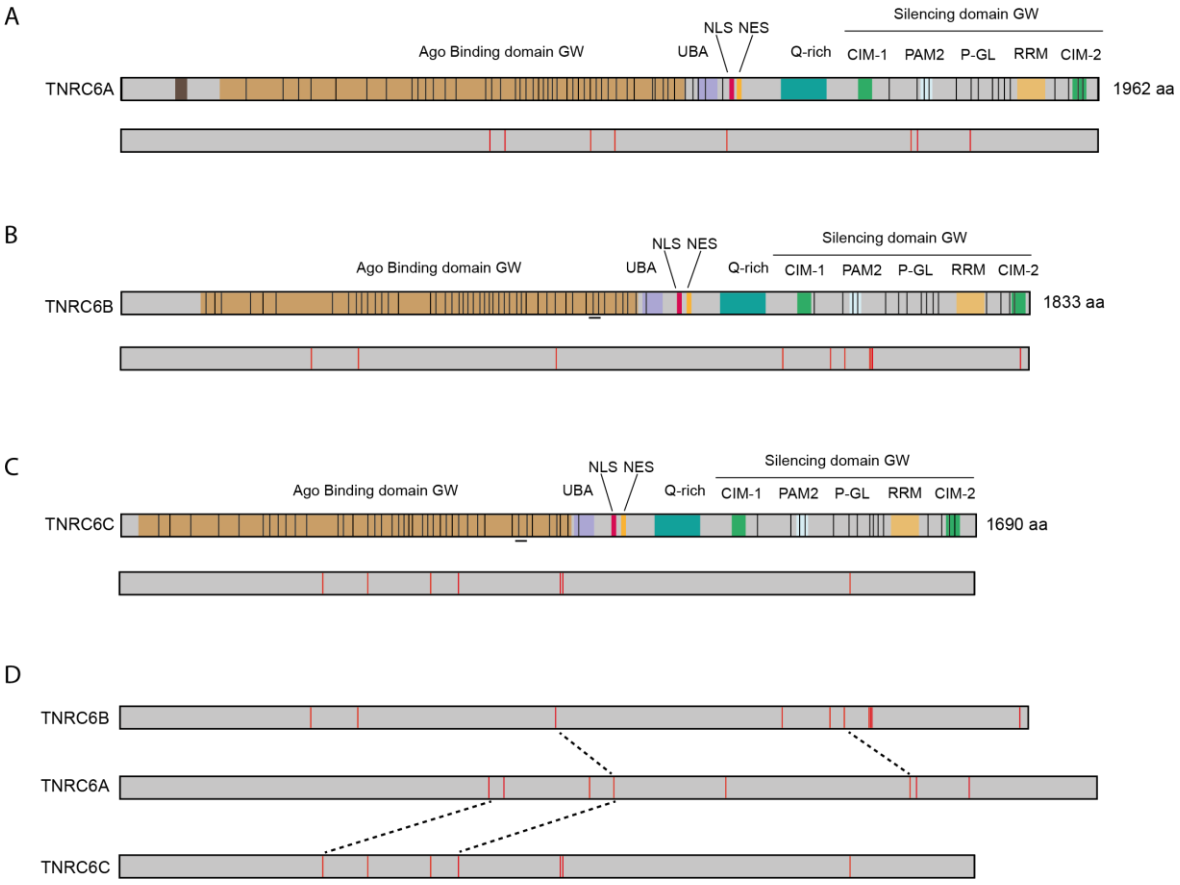

Figure 31 Mass spectrometric detection of potential phosphorylation sites in endogenous TNRC6A-C proteins.
(A), (B), (C) Overview of potential phosphorylation sites according to their individual localization within the TNRC6 paralogs. Grey bars represent TNRC6 proteins, red bars represent potential phosphorylation sites and black lines between the phospho-sites indicate conservation. Hs: Homo sapiens. Schematic TNRC6 illustrations are described in the chapter 1.2.1.1. (D) Schematic illustration of the location of phospho-sites conserved between the different paralogs.

Different biological replicates of one TNRC6 paralog were combined and were assumed as existing sites when two out of three replicates were overlapping (depicted in Venn diagrams for all paralogs, Figure 30 C). The phospho-sites are summarized in the table shown in Figure 30 D. The sites marked in red are present in the three paralogs; the green sites are found only in two paralogs. Phospho-sites, which fulfill parts of the criteria are listed in the appendix Table 17. Finally, the phospho-sites are schematically illustrated at the position within the protein domain structure in Figure 31 D. The sites are in a first view randomly distributed within the different paralogs. It is likely that this is just an excerpt of the whole phospho-pattern and further analysis may increase the number of stable measured sites within the TNRC6 proteins.

Some of the identified sites are located in the Ago binding domain but not at an obviously important position. Only in case of TNRC6A the S739 is located next to the decisive tryptophans for Ago interaction. This site is also conserved in TNRC6C but was not identified in our analysis (marked lines between the paralogs illustrate conserved sites; Figure 31 D). The TNRC6A S1217 (and a weak S1212) is directly located at the well-characterized nuclear export signal (NES). The sites located in the silencing domain are conserved in TNRC6B but far away from any particular domain (Figure 30 D). Since the current model suggests that TNRC6A-C may execute the same function, it may be expected that they exhibit a similar phosphorylation pattern.
Surprisingly, only one site is conserved among all three paralogs (marked in red in Figure 30 D) which is located at a functional undefined part of the proteins next to a proline-rich region. For TNRC6B and TNRC6C phospho-site position can be classified analogous to TNRC6A.

2.2.3.2 Detection of endogenous phosphorylation sites of TNRC6 in mice

To study whether the phosphorylation sites identified in human cells are conserved in mouse, the TNRC6 enrichment was also performed from mouse cell lysates and mouse tissues (as described in Figure 25). The obtained mass spectrometric data from 7A9-IPs of murine CMT93, N2A and partly from the mouse tissues were taken together and analyzed in the same way as described above using similar replicative and statistical criterias. This resulted in a high confidence set of mouse TNRC6 phospho-sites that were identified and selected (analogous to Figure 31 A-D, depicted in appendix Figure 46 A-E). The overlapping sites of both data-sets are summarized in Table 7 and Figure 32.

Table 7 Comparison of human and murine phospho-sites (red: conserved among all paralogs, green conserved among two paralogs, grey conserved amino acid not measured).

hsTNRC6A vs. mmTNRC6A		hsTNRC6B vs. mmTNRC6B		hsTNRC6C vs. mmTNRC6C	
S[739]	S[724]	S[385]	S[421]	S[465]	S[465]
S[771]		T[480]	S[912]	S[568]	S[568]
S[943]		S[879]	S[1044]	S[714]	S[714]
S[991]	S[976]	S[1336]	S[1312]	T[777]	T[776]
S[1217]	S[1202]	S[1432]	S[1408]	S[1011]	S[1006]
S[1585]	S[1520]	S[1461]	S[1437]	T[1016]	
S[1599]	S[1534]	S[1512]	S[1314]	T[1674]	T[1674], T[1678]
S[1704]	S[1639]	T[1517]	S[1488]		S[1358]
S[1582]	S[1520]	S[1816]	S[1792]		
	S[1540]	S[1832]	S[1808]		
			S[1191]		
			S[90]		
			S[95]		

In general, the conservation of phospho-sites between mouse and human is very high since residues are conserved. Although many conserved Ss, Ts, Ys may not be measured due to technical issues. The phospho-pattern between the two species is very similar and there are also similarities between the paralogs. These conserved patterns indicate a conserved role or function of the phosphorylated sites in mouse and human.

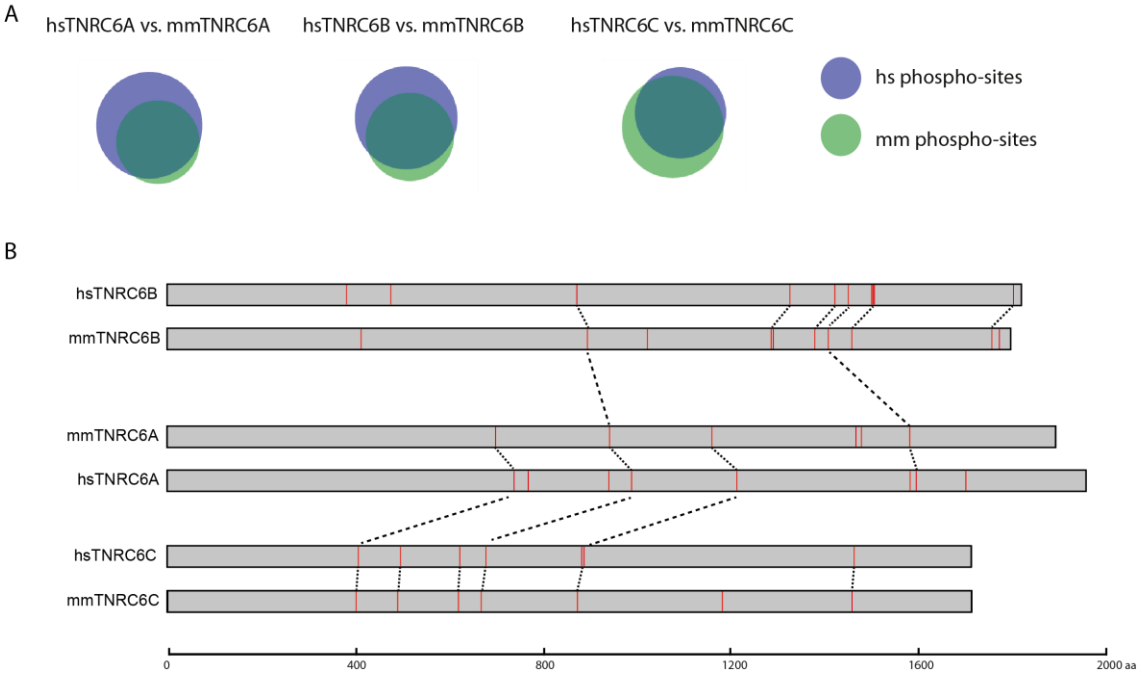

Figure 32 Mass spectrometric detection of potential phosphorylation sites in endogenous TNRC6A-C proteins. (A) Venn diagrams depict overlapping phosphorylation sites of biological human replicates. Diagrams were conducted with the browser based software Biovenn. (B) Overview of potential overlapping phosphorylation sites of immunoprecipitated TNRC6 proteins. Human and murine TNRC6A-C is pairwise indicated in grey bars. Unique and conserved phosphorylation sites are indicated in red. Black lines indicate conserved phospho-sites among the three human and three murine TNRC6 paralogs. All measurements were conducted in replicates on a MAXIS 4G mass spectrometer.

2.2.3.3 Detection of endogenous phosphorylation sites of nuclear TNRC6

In prior phosphorylation MS measurements, whole cell lysates were used for immunoprecipitation of TNRC6 proteins (Figure 24 and Figure 25). Unfortunately, differences between the cytoplasmic TNRC6 and Ago proteins and the postulated nuclear versions could not be distinguished in these measurements. To address potential differences, TNRC6A alanine mutants (received from Daniel Schraivogel) within the nuclear localization signal (ΔNLS) and the nuclear export signal (ΔNES) were used for further analysis of nuclear TNRC6 proteins (Figure 33 A). These mutants have been

shown to localize exclusively in the nucleus or the cytoplasm according to their respective mutation.

The NLS/NES of TNRC6B and TNRC6C are less well defined and therefore, only TNRC6A was in the focus of interest. First, nuclear/cytoplasmic fractionations were performed from stable and inducible HEK 293T Flp/in Trex TNRC6A ΔNLS, ΔNES and HEK 293T cells. Input samples were analyzed by western blotting. The western blot signals depict relatively pure biochemical fractionations, as evident from the analysis of the nuclear marker Lamin A/C and the cytoplasmic marker α-Tubulin (protocol adapted from Gagnon et al. 2014; detailed description in 4.2.4.1.2, Figure 33 B). Theoretically, the ΔNES-mutant should enrich in the nucleus after induction and the ΔNLS mutant should be restricted to the cytoplasm (Schraivogel et al. 2015). Both assumptions could not be clearly confirmed in this analysis, although the controls suggest only limited cross contamination of the extracts. In the following parts, the ΔNLS mutant was not further analyzed because the cytoplasmic TNRC6 was already analyzed without overexpression (Figure 33 B).

The Quantification of the IPs from the fractionated lysates yield similar results compared to the cytoplasmic distribution (as already described in Figure 26 E; Figure 33 C). Coomassie - scaled purifications after fractionation lead to a decrease in protein enrichment with 7A9 and myc-IPs, because protein amount was sufficient for quantification, but insufficient for phospho-analyses. This was caused by a nearly complete loss of nuclear proteins during washing steps (Figure 33 D). To solve this problem, a fast fractionation with a higher amount of cytoplasmic cross-contamination was established and afterwards myc-IPs from this lysates massively enriched the overexpressed TNRC6A-ΔNES mutant and WT (Figure 33 E). Then gel bands were excised and prepared for MS phospho-analysis. The table in Figure 33 F shows high confidence phospho-sites exclusively found within the ΔNES mutants. Within these phospho-sites, the S1212 and the S1217 (also weakly observed in other measurements) were directly located next to the NES amino acid signal (Figure 33 G).

This suggests a potential function in the regulation of nuclear/cytoplasmic transport. Furthermore, T644 was the dominant phospho-site, altough its position is located in the Ago binding domain at a position with no particular/ unknown function. Additionally, the promising phospho-site positions are conserved among mouse and rat and the phospho-sites S1212 and S1217 were also detected weakly in measurements with mouse cells (Figure 33 H).

The analysis of nuclear TNRC6 reveals phosphorylation sites that seem to be specific for nuclear enriched TNRC6.

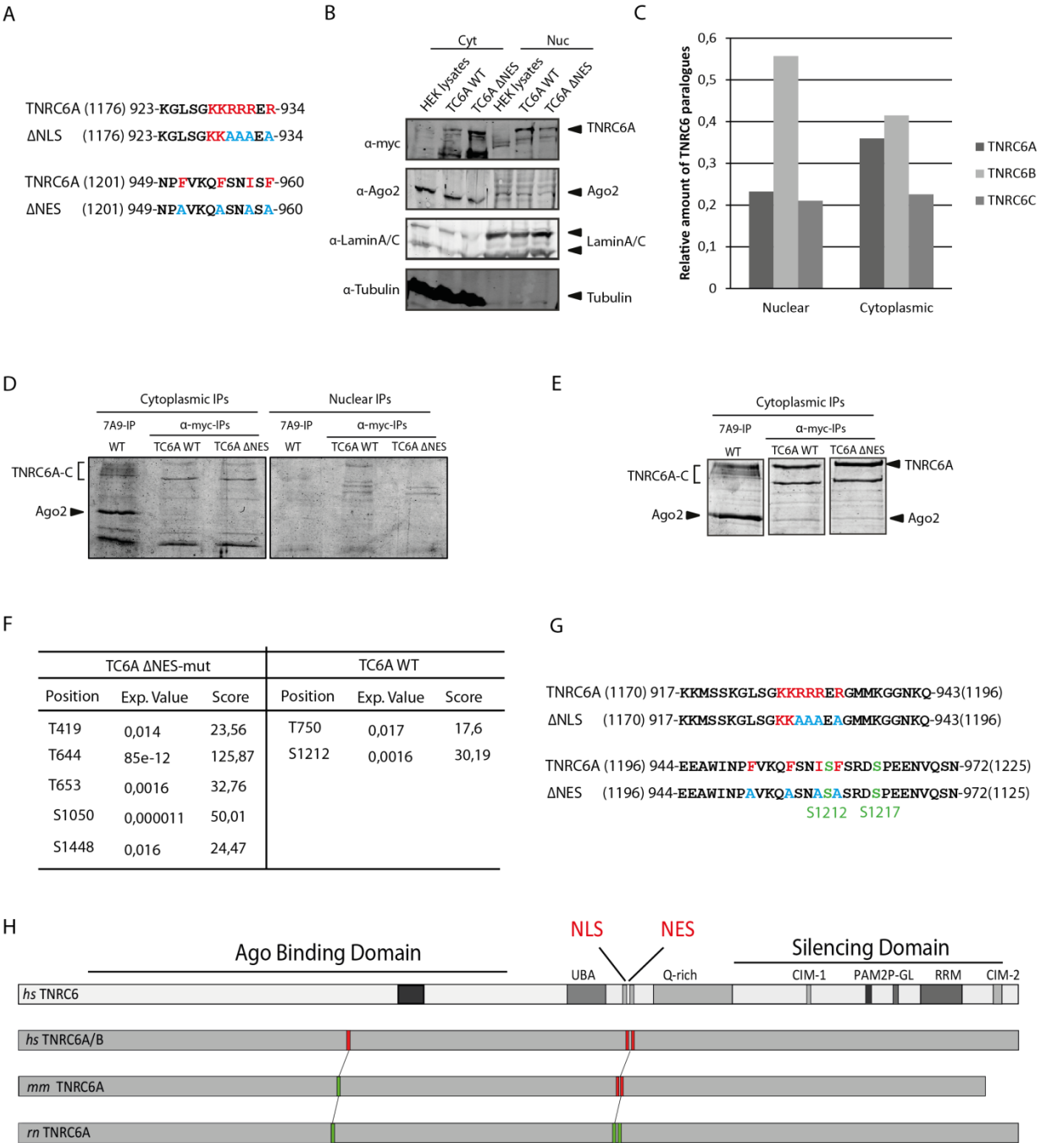

TC6A ΔNES-mut			TC6A WT		
Position	Exp. Value	Score	Position	Exp. Value	Score
T419	0,014	23,56	T750	0,017	17,6
T644	85e-12	125,87	S1212	0,0016	30,19
T653	0,0016	32,76			
S1050	0,000011	50,01			
S1448	0,016	24,47			

Figure 33 Detection of phosphorylation sites of nuclear TNRC6 WT, ΔNLS- and ΔNES-mutants.
(A) Amino acid sequence of TNRC6A WT, NLS-, NES-mutant and the alanine deletion mutants (as described in Schraivogel et al. 2015 and Nishi et al. 2013). (B) Fractionation of HEK293T, TREX-FLP/IN HEK TNRC6A WT and TREX-FLP/IN HEK TNRC6A ΔNES cells. Similar amounts of nuclear and cytoplasmic extracts were loaded and detected by western blotting. Fractionations were performed in an adapted version of Gagnon et al. 2014. Tubulin and Lamin A/C served as marker for lysate purity. (C) Quantification of immunopurified TNRC6 levels from nuclear and cytoplasmic lysates. (D) Immunopurification of overexpressed and endogenous TNRC6 and Ago proteins after nuclear/cytoplasmic fractionation. Proteins were separated on a 10 % SDS-PA-gel and coomassie-stained. (E) Enrichment of overexpressed and endogenous TNRC6 from HEK 293T cell lysates and preparation for mass spectrometric phospho-analysis. (F) Table showing unique phospho-sites of overexpressed TNRC6A WT and mutant. (G) Aa sequence of the phosphorylation sites directly located at the NES of TNRC6A. (H) Schematic overview of the location of measured phospho-sites within TNRC6A colored in red and conservation within other species (not measured; Hs: Homo sapiens, Mm: mus musculus, Rn: rattus norvegicus.).

2.2.3.4 Detailed computational and experimental analysis of the TNRC6 phosphorylation sites regarding localization, conservation and accessibility

For the obtained conserved phosphorylation sites, kinase prediction tools were used to search for potential kinases. Therefore, the browser based program NET phos 3.1 (Blom et al. 2004) was used to generate a probability list for different kinases (data shown in the appendix Table 19). The conserved sites share the same predicted kinases. However many prediction probability values are low and often the amino acid sequence information maps to none of the kinases. The kinases NEK9, BAZ1B and SHIP2 can be found in our MS analysis of a 7A9-IP suggesting a possible role in RISC phosphorylation. However, the co-IP data and the predictions yield no overlapping candidates. This data suggests that many kinases could have potential roles in the phosphorylation of TNRC6 proteins and that further analysis needs to be performed.

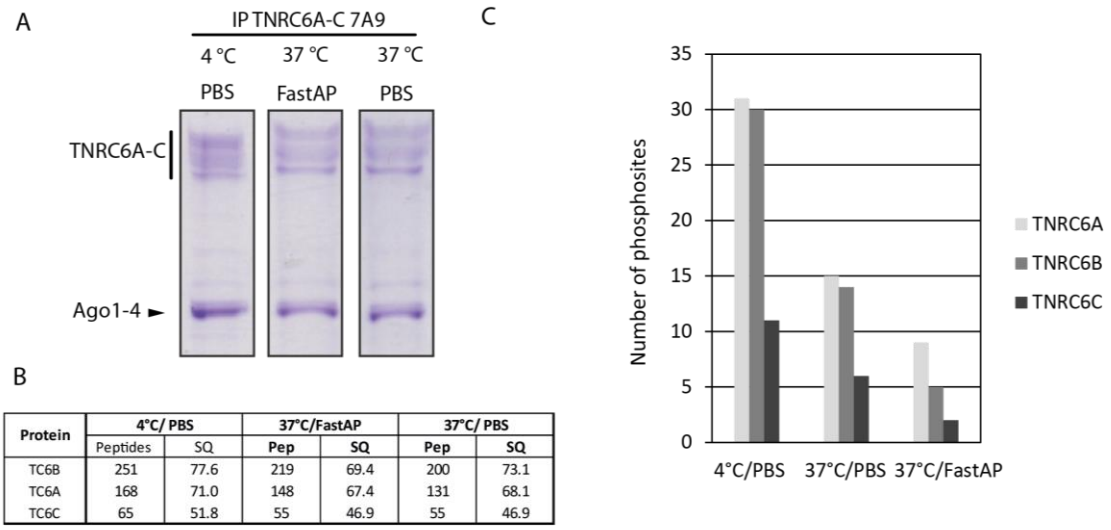

B

Protein	4°C/ PBS		37°C/FastAP		37°C/ PBS	
	Peptides	SQ	Pep	SQ	Pep	SQ
TC6B	251	77.6	219	69.4	200	73.1
TC6A	168	71.0	148	67.4	131	68.1
TC6C	65	51.8	55	46.9	55	46.9

Figure 34 De-phosphorylation assay of enriched TNRC6-Ago-complexes.
(A) Large-scale 7A9-IPs were performed with HEK293T cell lysates. After washing, enriched proteins were incubated for 30 min either at 4°C/PBS or 37°C/ PBS or 37°C/FastAP (Alkaline phosphatase) and MS measurements were performed (B) Summary of different treatment conditions of the measured peptides and resulting sequence coverages (SQ). (C) Graph shows decreasing amounts of measured phosphorylation sites.

A de-phosphorylation assay was established to study the accessibility and stability of the phosphorylated sites on TNRC6 proteins and to hypothesise structural, conformational and stability changes within the gene silencing complexes after de-phosphorylation. In Figure 34 A coomassie-stains of the 7A9-IPs illustrate that de-phosphorylation has minor effects on TNRC6-Ago complex stability under this experimental conditions. In the MS measurements high sequence coverages and peptide amounts postulate again a high stability of the complex within all three

TNRC6 paralogs under different reaction conditions (Figure 34 B). The de-phosphorylation assay itself drastically decreases the amount of phosphorylated-sites and just a few sites remain phosphorylated due to reaction conditions (Figure 34 C). In appendix Table 20 the decrease of the particular residues which are de-phosphorylated are listed together with the corresponding p-values which depict the statistical significance. For TNRC6C the 4 °C and 37 °C controls contain similar phospho-sites and p-values < 0.05 (Figure 34 C and appendix Table 20). The sample treated with FastAP includes just one remaining site, although TNRC6C peptides were comparable detected according to SQ and amount of peptides (Figure 34 B). The same is true for TNRC6A and B. Some sites seem to be more stable than others. For example, the S739 in TNRC6A that is located directly next to the Ago binding site is detectable in all different approaches. The same is true for some other residues like the conserved TNRC6A S991 and TNRC6B S879 (appendix Table 20).
However, the assay has to be repeated due to statistical and technical issues for further conclusions regarding the stability and the accessibility of certain phosphorylation sites.

2.2.4 Characterization of TNRC6 phospho-mutants

As a first functional analysis, tethering assays were performed to investigate the downstream effects of potential phospho-sites on gene silencing after the TNRC6-Ago-miRNA-mRNA complexes were formed. Tethering assays mimic effects on translation independent from Ago-miRNA complexes. To show effects on translation the protein of interest is tethered by the interaction of the λ-N-peptide to a 5box-B *Renilla* fusion mRNA which leads to the recruitment of mRNA destabilization factors and hence, to the decay and the loss of the *Renilla* signal. Therefore, cells were transfected with NHA and λNHA WT-, alanine- and glutamate-phospho-mutants of TNRC6 with appropriate controls. The signals of the ratio of affected Renilla and unaffected Firefly was calculated from different replicates and normalized to the NHA transfection control. In general, all phospho-mutants (with weak variations) are fully functional and the signal of the *Renilla*-target RNA is as strong as the WT TNRC6 control (Figure 35 A). To screen upstream effects on the interaction of TNRC6 with Ago, co-IPs with Flag-tagged TNRC6A phospho-mutants were performed. Figure 35 B indicates no effect of the phospho-site mutation on the TNRC6-Ago interaction. IF co-localization studies were performed to detect changes of the subcellular localization of TNRC6 phospho-mutants. IFs showed a perfect match of the Lsm-4 p-body-marker and the HA-tagged TNRC6 phospho-mutants (Figure 36). Compared to the overexpressed TNRC6A WT also no differences could be observed in localization or number of p-bodies. This first phospho-

site characterization experiments suggest minor effects of single phosphorylation sites on the functionality of TNRC6 to recruit Ago and the downstream decapping and deadenylation complexes.

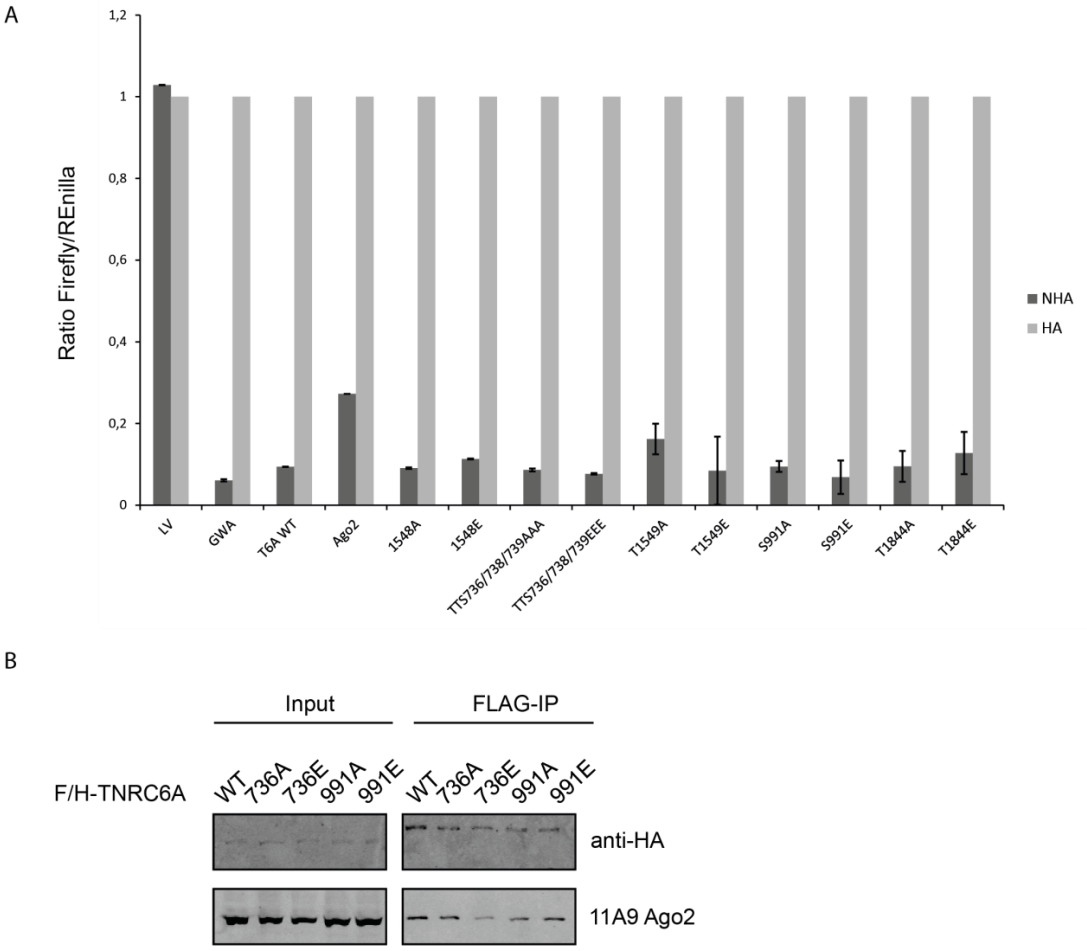

Figure 35 Characterization of TNRC6 phosphorylation sites.
(A) Tethering assays with Flag-/HA-tagged WT TNRC6 and several phospho-mimicking and non-phosphorylatable-mutants. *Renilla* luciferase (RNL) activity was detected in extracts of HeLa cells co-transfected with constructs expressing the RNL-5BoxB reporter, Firefly luciferase (FF) and λNTNRC6, phospho-mutants and WT Ago2.WT λNTNRC6 and Ago2 served as positive control. The expression levels of *Renilla* luciferase were normalized to co-transfected Firefly luciferase signals. (B) Co-immunoprecipitation of Ago1-4 with TNRC6 mutants. Flag-/HA-TNRC6 WT and phospho-mutants were overexpressed in HEK 293T cells, immunopurified by anti- FLAG-IP, separated on a SDS-PAGE, and analyzed by Western Blotting. Co-immunoprecipitated TNRC6 proteins were detected by using anti-HA antibody, Ago2 was detected by 11A9 antibody.

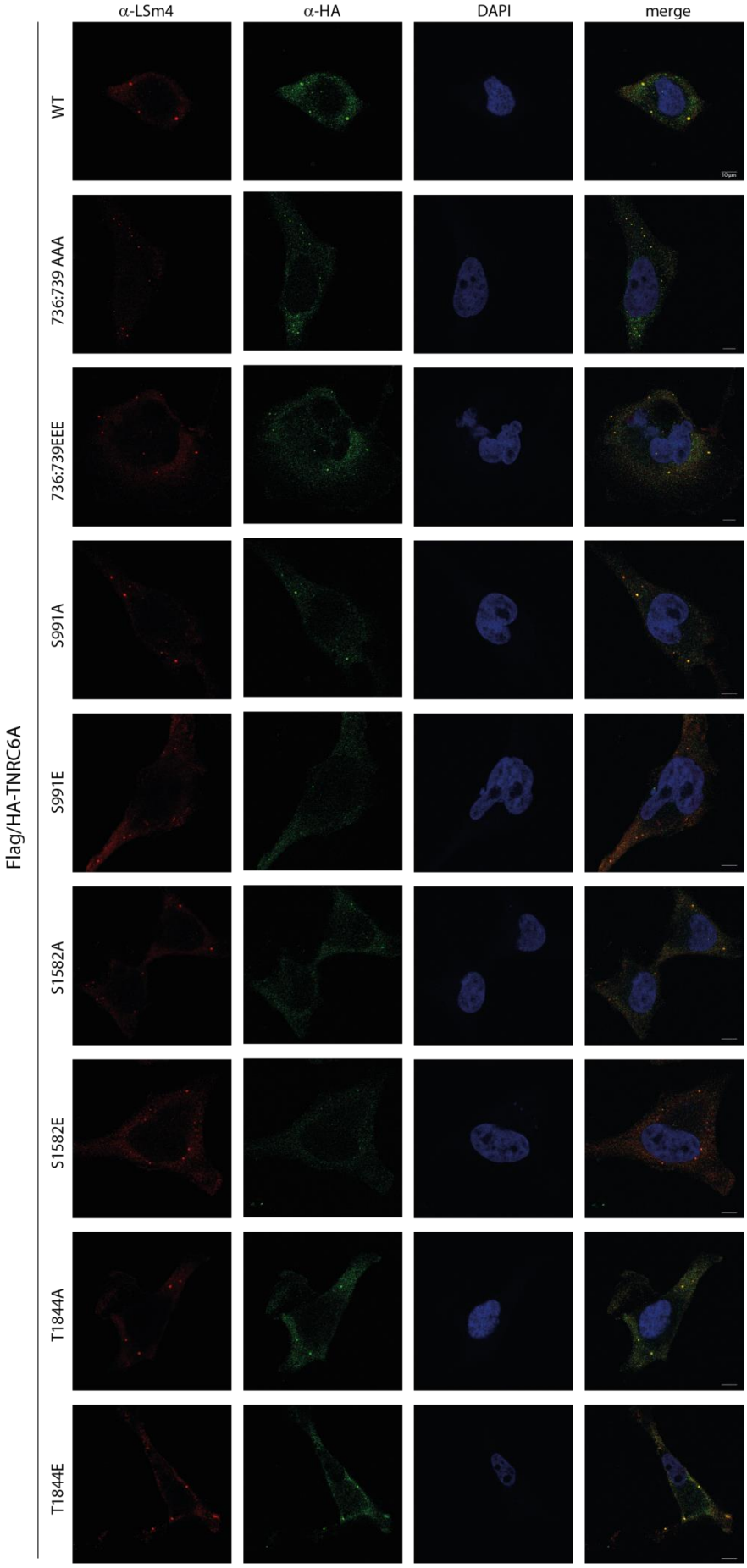

Figure 36 Characterization of TNRC6 phosphorylation sites with IFs.
Immunofluorescence of over-expressed TNRC6 mutants. TNRC6 WT and mutants were detected in immunofluorescence with anti-HA antibody staining (shown in green). For co-localization studies, Lsm4, a p-body marker, was stained with a specific antibody (shown in red). DAPI staining (blue) indicates the nucleus.

3 DISCUSSION

3.1 Part I: Dissection of viral miRNA biogenesis

This part of the discussion chapter dedicates the identified interactors of hairpin structured pri-/pre-miRNAs of the different herpes papilloma and polyoma viruses. The validation and possible regulatory effects on the miRNA biogenesis are discussed. Additionally an outlook based on results of this project will be given.

3.1.1 Viral miRNA expression profile of EBV, CMV and HSV1

To assess an overview of the expressed miRNAs in the different model systems used for the pull-downs, northern blots were performed with different DNA and RNA probes. The detection of nearly all mature viral miRNAs was possible within the EBV positive suspension cell line Jijoye. Within the Raji cell line just few could be detected. Therefore, all follow-up experiments were achieved with Jijoye cells.

The other herpes virus miRNAs were detected at different time points while an active and massive infection with a moi = 5 to reach an infection efficiency of up to 100 %. For CMV exclusively mature miRNAs were detected after 24 to 48 hours during the transition from the early to the late phase of the virus life cycle. This suggests an important role of the CMV miRNAs during infection. Indeed it is known that highly expressed CMV miRNAs have certain regulatory functions in immune evasion and viral replication (compare appendix Table 16).

In contrast, HSV1 exhibits a differential pattern of the chosen miRNAs and pre-miRNAs, suggesting particular specific regulatory mechanisms to block or inhibit the processing of the mature miRNA during the infection (B. R. Cullen 2004; Flores et al. 2013; Jurak et al. 2010; R. L. S. and B. R. Cullen 2013; Kramer et al. 2011; Jennifer Lin Umbach et al. 2009; Jennifer L Umbach et al. 2010).

The miRNAs of BKV, MCV and HPV41 could not be detected by northern blotting because a good model system where sufficient amounts of total RNA could be extracted was not available.

3.1.2 Identification of miRNA hairpin binding

Technical and methodical challenges. The hairpin pull-down work-flow contains critical parts at distinct steps. For instance the pull-down was performed overnight and RNA or proteins as well as complexes could have been lost because of degradation. In contrary non-physiological interactions and hence new structures and complexes may have been assembled due to the used incubation conditions. Additionally unspecific binding events may be caused by mild washing conditions and thus background binding increases and may covers weak specific binders. To be further critical, the *in vitro* RNA-pull-down approach with high concentrations of the bait system, favouring buffer conditions, lacking subcellular compartments and lacking cellular regulation may produce also non-physiological, unspecific binding actions with many false positive candidates.
Concerning other methodical issues the virus (CMV and HSV1) infected cell lysates of different time points had to be mixed. This had the consequence that the highly expressed viral coat and particle proteins were massively and unspecific bound by the experimental pull-down set up and the possibility that weak binders were covered by these strong binders is high. In addition, the pull-downs with the BKV, MVC and HPV41 miRNAs were performed in MRC5 cells, but without an active infection. Thereby factors that are specifically expressed during a viral invading or the cellular immune response are lacking.
To minimize side effects, biological replicates were performed and unspecific binding actions were analyzed with the "bead-proteome" of the magnetic beads of the preclearing controls.

MS challenges. Further technical challenges concerning the MS sample preparation, measurements and data analysis will be just briefly reviewed. For standardized and equal conditions, precast gels were used and samples were prepared with the same work-flow. The obtained data and further processing is based on the probability score as qualitative value. To present semi quantitative results, emPAI-values (Ishihama et al. 2005) were generated and are used for future directions and illustrations, unfortunately no emPAI values were considered for this thesis. However, the main output generated by scores and emPAI values constantly stays comparable.

Potential binders. The protein-hairpin interaction pull-down identified proteins with different types of binding patterns, first one RBP interacts specific to one hairpin, second, one hairpin interacts with different proteins. Third, one protein interacts with different pri/pre-miRNAs. Fourth few hairpins interact with few proteins and fifth one part of a whole protein complex

interacts with one or more pre-miRNAs. In all of these different binding classes many unusual binders were identified. These ones often lack known RBDs or are known to function in completely unrelated metabolic processes.
In addition, the whole obtained data reflects a difference between very specific interactions based on structure, consensus sequences and binders which can be classified as sequence unspecific RNA interactors. Many of these belong to different classes of interactors like spliceosomal or metabolic proteins (Lunde, Moore, and Varani 2007; Gerstberger, Hafner, and Tuschl 2014).
However, compared to other large protein-RNA interaction studies, the data-set contains many known factors and RBPs which specifically interact with RNA (Castello et al. 2012; Treiber et al. 2017).

Bioinformatical analysis reveals a first conclusion without any validation experiments. First, the link to RNA can be made with GO term analysis, as expected many RNA associated functional mechanisms and pathways with typical housekeeping functions are present. The potential of the proteins to interact with RNA (compulsive required) was analyzed and many contain RBDs, but also many are not classified or the data bases are incomplete or obsolescent.
The hints of the subcellular localization have minor relevance, because many data bases of the subcellular localization of many proteins are again incomplete, obsolescent, unknown or critically discussed in the scientific field. For a more distinct analysis, subcellular co-localization with Drosha and Dicer should have been checked.

MSA. The analysis based on consensus sequences with MSAs gained insights in potential conserved binding sites, but also revealed that lacking data on different candidate consensus sequences makes the analysis nearly impossible. For many cases the MSAs showed no overlapping sequences, but a single analysis of the structural hairpin elements would be necessary. But a sequence based analysis without considering structural information (or just predicted ones) shows the weakness of this analysis and simultaneously strengthens the aspect that also secondary structure is important for selectivity.

To summarize this part, it is not possible to avoid unspecific binding and false positives. Therefore the screening data was validated and further characterized by biochemical assays.

3.1.3 Validation and influence of specific pre-miRNA protein interactions

The first validation step was mo the repetition of the hairpin pull-down with overexpressed Flag-/HA-interactor proteins in an unrelated cellular system without a viral infection. Basically, just the binding reaction was repeated. The different proteins varied in their expression level and few candidates did not express at all. Unfortunately the strong expressed proteins lead to strong unspecific binding to the beads and to the unrelated hairpin control. When possible, the approach was adjusted to more optimal conditions, but in many cases the overshooting expression resulted in unspecific bindings. However, many candidates could be shown to be specific interactors of the according pri/pre-miRNA, although background binding occurred. To proof the interaction from both sides, a RNA-IP with the hairpin-interacting protein should be performed and detected by northern blotting and highly sensitive qRT-PCRs.

In a next step viral miRNAs were overexpressed together with the potential regulator in a viral free background to force the processing pathway through high accessibility of RNA and potential regulator. The effects on the processing efficiency are rather mild, but give hints for the potential regulatory function. The mild results are caused from the endogenous background and the lack of controls.

A better assay in terms of sensitivity and without background was established in a cellular hairpin interactor knockout background. The idea was, to force the effect of blocking or promoting the processing without endogenous proteins. The cells were produced within the publication of Treiber et al. 2017. The unaffected hairpin can of course be influenced by present endogenous factors, but this would be equal in all used cell lines, thus this side effect on the control was neglected. The results that were detected reveal an effect on the processing activity of the regulators on the miRNA biogenesis. Unfortunately, effects are again mild. This can be caused by massive overshooting overexpression of the hairpins and thus clear effects remain weak. Also just one candidate RBP was depleted and still others could influence the miRNA processing and then no effects would be visible. Such effects are conceivable when RBPs compete for the same binding site and one competitor is missing.

Also a viral background which may have supported the effects is missing and thus regulatory pathways which may activate additional functions of RBPs are not present.

From a methodical sight, endpoint assays by northern blotting were performed and maybe cover weak effects. For a better visualization, different time points after infections or transfections should have been studied. Additionally the effects should be confirmed by other methods such as

qRT-PCRs or small RNA deep sequencing. The variances in this assay and clear results could be optimized by further biological and technical replicates.

For the RBP Rbfox2 as the best example, the results in Figure 20 and Figure 21 strongly together with the reports from the literature (Yu Chen et al. 2016) support that it is a negative regulator for cmv-miR-US22 biogenesis. This nice example clearly shows further extensive research will reveal the effects of the identified RBPs on miRNA biogenesis.

3.1.4 Future perspectives and a model for the viral miRNA biogenesis

The identified candidates together with the known fates of the miRNAs provide insights in the biogenesis of viral miRNAs and lead to the following working model Figure 37. This model illustrates that the viruses through a distinct regulation of the miRNA biogenesis influence many cellular processes. By blocking or promoting miRNA biogenesis a particular miRNA profile is generated which helps the virus to establish the lytic or the latent life cycle.

For further RBP characterization, consensus sequences within the pre-miRNAs will be studied with bind and seq. assays and hairpin binding mutants. Afterwards, RNA-binding domains will be analyzed with truncated protein versions in EMSAs and co-IPs. This will be studied in detail by Dr. Nora Treiber and Dr. Thomas Treiber. The MS data based on scores will be re-analyzed by considering the semi quantitative emPAI values.

To maintain a full picture viral infection assays will be investigate and elucidate whether our RBP candidates are important for individual steps of viral infection (lytic cycle) or long term viral persistence (latent cycle). This will be performed together with Prof. Michael Nevels and Dr. Christina Paulus for CMV. Knock out cell lines will be infected and virus production and maturation will be analyzed at different steps of the viral life cycle (very early, immediate early, early and late phase). Furthermore, infection rescue assays with mutated consensus sequences within the pre-miRNAs will confirm the crucial role of the RBPs on the virus.

For papilloma and polyoma viruses, where miRNAs play a pivotal role in switching from early to late infection stages, the identified RBPs which associate with the BKV, MCV and HPV41 pri/pre-miRNAs will also be tested in a similar infection system as for CMV. Strikingly, first hints for drastic effects during *in vivo* infection studies with BKV in GRSF1 HEK 293T knock out cells were detected for the virus replication and particle formation (data not shown). The viral work has been and will be further performed in close collaboration with Prof. Adam Grundhoff (Heinrich-Pette Institut Hamburg).

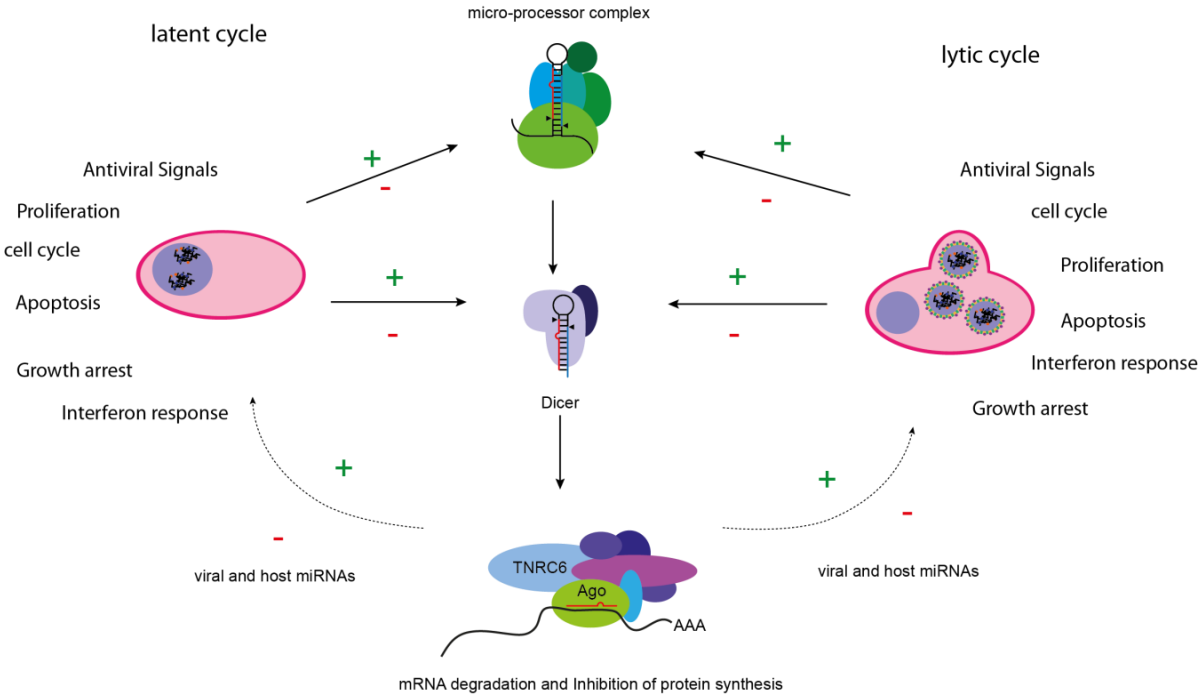

Figure 37 Schematic model of the effect of viral miRNAs on the host and the virus.
Inhibition or promotion of certain miRNAs by regulatory RBPs during biogenesis may influence the latent or lytic cycle of the virus. Thereby several important functions such as cell cycle control, apoptosis and cellular immune response are affected. The virus influences with its own and host miRNAs the expression of regulatory RBPs to influence miRNAs. Hence the virus produces optimal homeostatic conditions to survive.

Future perspectives will elucidate the effect of miRNAs and their regulation on the viral life cycle. Within the virus field a strong role of the viral (and host) miRNAs in the initiation of the latent viral stage is suggested. Furthermore, a distinct and highly regulated equal level of miRNAs is needed which controls a light promoting system of many different pathways and cellular growth regulation for the viral persistence (like suggested in the introduction 1.4.2). This can be kept with a regulation network of a redundant human and viral gene regulation system influencing the cellular processes to maintain long-term (life-long) persistence within the host.

3.2 Part II: Post-translational modifications of TNRC6 proteins

The second part of the discussion dedicates the established antibodies, their characterization and the usage for immunopurification of TNRC6-complexes from different species. Furthermore, newly identified TNRC6 phospho-sites are summarized, obtained functional data is discussed and reviewed with regard to the current literature. Additionally, an outlook based on future directions will be illustrated.

3.2.1 Immunopurification and enrichment of TNRC6-Ago-complexes from different species with monoclonal TNRC6 antibodies

Antibodies. The novel established and characterized monoclonal TNRC6 antibodies demonstrate a valuable tool for the characterization of the human TNRC6-Ago-miRNA-mRNA complexes. The advantages of these antibodies compared to other approaches are a high selectivity and the ability to purify stoichiometric amounts of Ago and TNRC6 proteins. The presented data, in particular selectivity tests, competing assays (see in 2.2.2.1) and MS interaction studies as well as IFs presented in Schraivogel et al. 2015 lead to the development of new enrichment strategies for TNRC6 proteins. The purification of the antibodies clearly increased the quality of the immunopurifications and made the TNRC6 proteins visible as stable proteins when bound to Ago. Even the target RNAs were successfully enriched with high yield and comparable to Ago IPs. Compared to literature (Meister et al. 2005; Hock et al. 2007) also many known interactors and maybe also unknown ones were co-immunoprecipitated A potential disadvantage is the recognition of the monoclonal antibodies of the RRM domain. This interaction could lead to a loss of interaction partners within the RRM domain or even within the whole SD domain.

For large scale purifications, the lysates were treated before clearing with RNase A (Kalantari, Chiang, and Corey 2016; Kalantari et al. 2016). This leads to a higher accessibility of the TNRC6-Ago complexes, but maybe the functional integrity of the gene silencing network is lost. Degrading the mRNA could have favoured the decomposition of the silencing complexes resulting in a breakdown of larger p-body structures. Thus, the proteins are in a free state and the lysate conditions lead them again together to reunification. As PAPBC1 is still detectable with high yield,

a break down to smaller structures could be also assumed. However, this remains speculative and cannot be proofed easily.

The universal applicability of the TNRC6 antibodies compared to Ago-APP is limited through the conservation of the RRM domain between the species. Additionally the very well conserved TNRC6 proteins can also be purified from mouse and rat tissues with high specificity. The purity and quantity was depending on the lysates, total protein amount. In general, the purification and detection was efficient when the proteins were highly expressed. However, in full-differentiated cell lines where gene silencing action is weak also the purified amounts of TNRC6 proteins were low.

3.2.2 Quantification of TNRC6 levels by SRM

The antibodies were subsequently used together with SRM analyses to measure protein expression levels of the TNRC6 and partly also from Ago proteins.

All monoclonal antibodies of which the immunoprecipitated TNRC6 proteins were analyzed showed their own specificities. Due to this fact the antibodies can be now used even better, depending on the question.

In general, the binding actions between TNRC6A-C and Ago1-4 indicate an equal distribution relative to their expression level as already partly observed in Hauptmann et al. 2015.

All together the results depict that the antibodies work and that they reflect the cellular spectrum of TNRC6 and Ago proteins. Furthermore, different cell lines and tissues may have a specific transcription and expression pattern, but this remains speculative and additional experiments have to be performed.

Technical challenges. The SRM measurements are sensitive enough to analyze complex input samples. However the data obtained from these measurements are at the lower limit of detection and thus the inaccuracy of the analysis had to be considered.

Additionally high varieties in the properties and the resolution of the different used peptides were detected. Because the peptides itself have certain characteristics which may influence the sample preparation and the measurement. For instance, TNRC6A was quantified using 4 peptides. All of them were single reviewed and would lead to a comparable, but different expression profile. Therefore, the measurements were averaged with different calculation methods and compared to each other.

For a full picture many more SRM measurements with more peptides from different cell lines and tissues (and replicates) are compulsory necessary.

3.2.3 Detection of endogenous phosphorylation sites of mammalian TNRC6 proteins

The enrichment of TNRC6 and also Ago proteins was the main focus of the antibody production (Hauptmann et al. 2015; Quevillon Huberdeau et al. 2017). The obtained data from many different measurements taken from different species and approaches can be summarized in several modification sites. Many of these sites were already detected in phospho-proteomic approaches (K. Sharma et al. 2014; Mertins et al. 2016; Robles, Humphrey, and Mann 2017) and listed in different publications or databases (www.phophosite.org). Previous detection approaches mainly focused on other questions or hypothesis than specific phosphorylation sites of few proteins. Therefore, many sites could not be observed or reproduced which are publicly listed. A closer look on these datasets reveals that nearly all serines, threonines and tyrosines in TNRC6 are phosphorylated.

The mass spectrometric phospho-site detection of the Ago-TNRC6 complexes (focus on TNRC6) in technical and biological replicates resulted in several unique and conserved phospho-sites. These residues are stably measured and therefore maybe the sites needed for a functional complex.

Interestingly, the residues which were inconsistent or weak phosphorylated could get more in the focus of interest, after more replicates are performed, because weak sites could be regulatory sites which lead the complex through the pathway. Besides, the measurements are restricted and first we are forced to keep certain standards. However, also “weak” measured sites will stay in the focus of interest, not only the stable measured ones.

The non-conserved phospho-sites itself seem to be randomly located all over the protein paralogs. Many phospho-sites were found to locate in random areas with no distinct or known functions, suggesting that these proteins need at particular positions a negative charge to function in the usual way.

It remains unclear how flexible this phospho-patterns may change and through the variety of isolated complexes it will first stay unclear. TNRC6 is seen as binding platform and could need just the negative charge at distinct regions/positions for a micro structural change and a proper functionality like suggested for the regulation of PABPC1 binding (Huang et al. 2013).

Interestingly, many phospho-sites are conserved between the species, which support the idea of a conserved function of the detected sites. Also for many sites measured in other species, at least the amino acid is conserved, supporting the assumption that this peptide was just not measured

with modification, but still could be modified. This conclusion may increase the number of predicted phospho-sites.

The location of the phospho-sites seems first randomly, but different functional interaction parts of TNRC6 seem to be non-phosphorylated. For instance, the whole silencing domain seems to be nearly non-phosphorylated.

Interestingly, the three different proteins with the same function have many unique sites that are just conserved among the species and not the paralogs. Due to many different and fast changes within the complex it could be that there is a stable pattern to keep the system functional. This pattern could be specific for every TNRC6 paralog.

Technical issues. Briefly the technical challenges in measuring a flexible system with inflexible approaches had to be overcome but first detection itself in a stable way had to be optimized. The first challenging part was to get enough endogenous protein material. After overcoming this, the analysis itself had to be optimized, to get a good ionization efficiency and fragmentation patterns. But also minor important points like semi tryptic digestions or not digested peptides or too big peptides had to be optimized. After obtaining the raw data, the analysis pipeline and its restrictions were optimized. Further, the position of a phospho-site within a peptide containing many phosphorylate-able residues needed confirmation through additional raw data analysis (also for multiple phosphorylated-peptides) (Boersema, Mohammed, and Heck 2009; Palumbo and Reid 2008; Steen et al. 2006).

The question for kinases is unanswered. Unfortunately, the detection of phospho-sites is just the starting point for more differential analysis. The first upcoming question about the modifying enzymes remains up to this point unsolved. There are different possibilities that would be probable in terms of cellular mechanisms. The prediction of kinases with tools are limited to the properties of the known kinases and also phosphatases. The tool suggests common and broadly involved kinases based on the sequence characteristics, thus K.O.s of these would result in cell death. For Ago proteins some kinases are suggested to specifically phosphorylate particular residues (Quevillon Huberdeau et al. 2017; Zeng et al. 2008). Hence, it is possible that the functional unit of Ago-TNRC6 complexes is modified together.

This suggests that the close neighbouring systems of gene silencing, translational repression, p-body formation and translational activity could have the same regulatory machinery, meaning that the kinases and phosphatases are always present at the centres of action. Following this conclusion the co-immunoprecipitated potential interactors may contain already all modifying enzymes to keep this mechanisms running. Many possibilities are imaginable in a fast changing

system with limited access. Summarized, predictions give just hints to the known fact that the protein needs the phospho-sites to function, but how and why cannot be answered.

Detection of nuclear phosphorylation sites of TNRC6 proteins. The nuclear/cytoplasmic fractionation approach is a qualitative biochemical assay with a high potential for cross-contaminations. Hence, all unique sites could be contamination side effects. Therefore, follow-up experiments with LMB treatment which blocks the nuclear export could help to further confirm unique sites of nuclear TNRC6.

Data of nuclear TNRC6 phospho-sites was mainly obtained from overexpression and without replicates. Many sites were overlapping with the endogenous data-set and therefore the measurements seemed trustfully and valuable. Few appearing phospho-sites that are measured with high yield are not or just weak appearing in the data-set of the mainly cytoplasmic TNRC6. A function of the phospho-sites has to be carefully validated, because the function of nuclear TNRC6 in contrast to the cytoplasmic ones is still unclear and highly debated in the field (Nishi et al. 2013; Schraivogel et al., n.d.; Gagnon et al. 2014; Kalantari et al. 2016).

It can be postulated that phosphorylation sites could have a potential regulatory function for the transport into the nucleus. Interestingly S1212 (or/and S1217) are located at the NES and the negative charge may influence the binding to the importins or CRM1.

3.2.4 Characterization of selected TNRC6 phospho-mutants

The second upcoming question aims the function of the phosphorylated sites. As basic functional assays, tethering, Ago interaction and localization studies per IFs were performed to analyze effects on gene silencing (similar to Huberdeau et al. 2017). The tethering assays concentrate the functional analysis on all aspects independent from Ago containing miRNAs. Therefore, all downstream effects are monitored. Taken together, no downstream effects are influenced by the exchange of one particular residue neither by phospho-mimicking glutamate mutants nor by non-phosphorylateable alanine mutants. Since IFs illustrate a perfect overlap with various visible differential structured p-bodies, again no effects on the functionality, can be observed (just a subset of IFs is shown. The influence of phospho-sites on the Ago TNRC6 interaction seems also not be different. However, these assays rely on overexpression of TNRC6 proteins. Thus effects on gene silencing and Ago interaction could be just not detected, because overexpression was insufficient. The localization within p-bodies is again just observed during overexpression and could conclusively lead to hidden effects that are not detectable with IFs.

As one phospho-site seems to have minor effects on the functionality of TNRC6 it is suggested that many phospho-sites are required for a proper function. This suggests on the one hand that TNRC6 is heavily phosphorylated and that one phospho-site is maybe not crucial for the function. On the other hand it can be concluded that TNRC6 needs phosphorylation for proper function. This leads to the hypothesis that a pattern of negative charges overall the whole protein is needed for proper function and the loss of one phospho-site is not decisive. A monitoring of different stages of the gene silencing pathway with TNRC6 truncations combined with phospho-mutants could proof certain functions.

De-phosphorylation assay. The de-phosphorylation depending on the stability and abundance of the peptides suggests a high variance within the phosphorylation pattern, because it seems that only the relative position is important and the negative charge, but not typical conformational changes like for many other phospho-proteins. Additionally, it proofs the accessibility of the phospho-sites, thus the residues are not protected or hidden by the complex assembly.
Due to the reason that the different detected phospho-peptides vary in their characteristics and hence technical detection as well as statistical analysis differs among the peptides. This leads to the effect that some peptides are strongly detected and others not. For further conclusions, the de-phosphorylation assay has to be repeated.

3.2.5 Model and Outlook for the PTM project

The universal applicability of the established antibodies opens various possible approaches. The detection of phospho-sites was in the main focus. Taken together, there are no clear signs for distinct functions of TNRC6 phospho-sites. Maybe, just complex integrity is influenced. At least we know that the Ago-TNRC6 protein complex is heavily phosphorylated while acting in the gene silencing pathway.
Apart from all advantages, the limit of the antibodies was in the differential analysis of all the different steps of the gene silencing pathway.
To solve the question of associated kinases or phosphatases a large scale knockdown screen with fluorescent Ago and TNRC6 will be performed. Additionally, the mass spectrometric detection of associated proteins will be investigated with new approaches. Furthermore, a new purification strategy with functional protein truncations and the possibility to distinguish between different complexes will be established. The prior mentioned new approaches will be then combined with different *in vitro* phosphorylation assays and structural analysis experiments.

Taken together the following model illustrates that in general the gene silencing process from a sequential point of view is quiet well understood. But many questions within the field are unsolved like the regulatory mechanisms which control the system, if there are recycling systems for both Ago and TNRC6 proteins or how all these modifications make the difference in terms of function

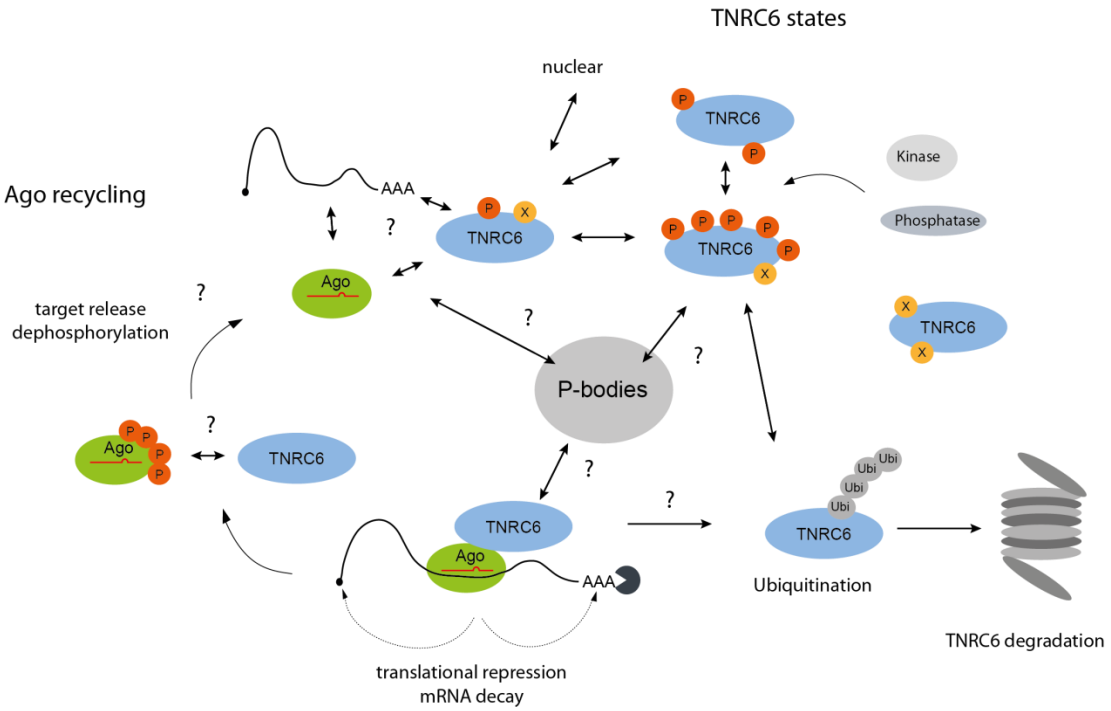

Figure 38 Schematic model of gene silencing networks with a focus on TNRC6.
Within the gene sileincing pathway many different stages are postulated, however none of these steps is understood in the way of regulatory mechanisms. It is known that Ago-TNRC6 complexes perform together with many other large complexes gene silencing. The state of regulatory modifications as well as involved signaling pathways for TNRC6 is completely unknown. Hence many questions have to be solved in the future to understand gene silencing, complex/p-body formation and translational repression in a distinct way.

4 MATERIALS AND METHODS

4.1 Materials

4.1.1 Consumables and chemicals

All Chemicals for buffers and solutions were obtained from Sigma-Aldrich (St. Louis, USA), Merck (Whitehouse Station, USA), Roth (Karlsruhe, Germany), AppliChem GmbH (Darmstadt, Germany) and Thermo Fisher Scientifc (Waltham, USA).

Radiolisotope-labeled chemicals were purchased from Hartmann Analytic GmbH (Braunschweig, Germany).

Heavy-isotope-labeled peptides for SRM measurements were purchased from JPT Peptide Technologies GmbH (Berlin, Germany).

Oligonucleotides were synthesized by Metabion GmbH (Planegg, Germany).

Cell culture reagents were purchased from Sigma-Aldrich (St. Louis, USA).

All Enzymes, oligonucleotides, and molecular weight markers for molecular biological methods were obtained from Thermo Fisher Scientifc (Waltham, USA) or New England Biolabs (Ipswich, USA).

The composition of individual buffers is specified with the respective method they were used for.

4.1.2 Instruments and technical equipment

Table 8 Instruments and technical equipment

device	supplier company (location)
SDS-Page, Western blot, Northern blot	
Screen Eraser-K	Bio-Rad (Hercules, USA)
Trans-Blot SD	Bio-Rad (Hercules, USA)
Wet-blot	Bio-Rad (Hercules, USA)
Odyssey Infrared Imaging System	LI-COR Biosciences (Lincoln, USA)
Power Supply EV233	Consort (Turnhout , Belgium)
Personal Molecular Imager TM (Phosphoimager)	Bio-Rad Laboratories, Inc. (Hercules, USA)
Film Processor CP 1000	AGFA (Mortsel, Belgium)
Geiger Counter LB123 EG&G	Berthold (Bad Wildbad, Germany)
Hybridization oven T 5042	Heraeus (Hanau, Germany)
PowerPac HC Power Supply	Bio-Rad (Hercules, USA)
Centrifuges	
Centrifuge 5415D	Eppendorf (Hamburg, Germany)
RT-fuge	Eppendorf (Hamburg, Germany)
Megafuge 40R	Thermo Scientific (Rockford, USA)
Cell culture equipment	

HeraCell 240i CO2 Incubator	Thermo Scientific (Rockford, USA)
Mass spectrometers	
maXis plus UHR-QTOF CaptiveSpray nanoBooster Source	Bruker (Billerica, USA)
QTRAP®4500 AB SCIEX NanoSprayIII Ion source AB SCIEX	AB SCIEX(Framingham, USA)
Chromatography system for both mass spectrometers: UltiMate 3000 RSLCnano System Thermo Fisher Scientifc with Acclaim® PepMap100 C18 Nano-Trap column and Acclaim® PepMap C18 column	(Waltham, USA)
Other equipment	
FastPrep®24 (with Lysing Matrix D)	
Thermomixer compact Eppendorf	(Hamburg, Germany)
Incubator Model B6200 Heraeus	(Hanau, Germany)
Biofuge pico Thermo Scientific	(Rockford, USA)
HeraSafe KS Thermo Scientific	(Rockford, USA)
Branson Sonifier 450 Heinemann	(Schwäbisch Gmünd, Germany)
Milli-Q PLUS and Reference A+	Millipore (Billerica, USA)
Ultraspec 3300 pro Amersham Biosciences	(Little Chalfont, UK)
Avanti J-20 XP Centrifuge Beckman Coulter	(Krefeld, Germany)
Quantum ST4 PeqLab	(Erlangen, Germany)

4.1.3 Bacterial strains, cell lines and viruses

Table 9 Bacterial strains

strain	genotype specifications
XL1-blue	F– recA1 endA1 gyrA96 thi-1 hsdR17 supE44 relA1 lac F'[proABlacI qZ_M15 Tn10 (TetR)
BL 21	B F- dcm+ Hte ompT hsdS(rB- mB-) gal endA Hte

Table 10 Viruses

strain	family	genotype specifications
EBV (within +B cells	human herpes virus	DNA virus
CMV (AD169)	human herpes virus	DNA virus
HSV1 (KOS)	human herpes virus	DNA virus
MCV	human polyoma virus	DNA virus
BKV	human polyoma virus	DNA virus
HPV41	human papiloma virus	DNA virus

Table 11 **Mammalian cells**

strain	genotype specifications	lysis conditions
cancer cell lines		
HEK 293T	human embryonic kidney cells	IP lysis buffer
HeLa	human cervical cancer cells	IP lysis buffer
LNT-229	human glioma cells	IP lysis buffer
Ntera2	human metastatic testis cells	IP lysis buffer
mouse cell lines		
MEF Ago2 -/-	mouse embryonic fibroblasts	IP lysis buffer
MEF Dicer -/-	mouse embryonic fibroblasts	IP lysis buffer
MEF ADicer +/+	mouse embryonic fibroblasts	IP lysis buffer
N2A mouse	neuroblastoma cells	IP lysis buffer
CMT93	colorectal cancer	IP lysis buffer
suspension cell lines		
Raji	T-cell lymphoma	Sonication, Pull-down buffer
Jijoye	T-cell lymphoma	Sonication, Pull-down buffer
Primary cells		
MRC5	primary lung fibroblasts	Sonication, Pull-down/IP lysis buffer
HEK293T Flp/In T-Rex	human embryonic kidney cells	IP lysis buffer

4.1.4 DNA oligonucleotides

DNA probes for northern blot listed in the appendix 5.1.5

DNA oligonucleotides for PCR listed in the appendix 5.1.6

DNA oligonucleotides for qRT-PCR listed in Hannus *et al*, 2014

4.1.5 Plasmids

Table 12 Plasmids

Plasmid	tag	application
pGEM T easy	no tag	template for PCRs
EBV		miRNAs BHRF1-1/1-3; BART1-22
CMV		miRNAs US4-1 to UL148D
HSV1		miRNAs H1-H8/H11-H17/H26-H27
MCV		miRNA M1
BKV		miRNA B1
HPV41		miRNA H1
psuperior	GFP	overexpression of miRNAs in mammalian cells
EBV		miRNAs BHRF1-1/1-3; BART1-22
CMV		miRNAs US4-1 to UL148D
HSV1		miRNAs H1-H8/H11-H17/H26-H27
MCV		miRNA M1
BKV		miRNA B1
HPV41		miRNA H1
PCDNA3 SK2L2	Flag	clones by Franziska Weichmann
VP5 (modified pIRES neo)	Flag-/HA	overexpression of mammalian Proteins in cells
NONO, ZCHC3, PTCD3, Rbfox2, UL97, UNG, UL77, PORTL, PP65, K0020, CPSF5, CPSF7		this work
C9orf114, NOL8, TRIM25, PUm1/2, Zincfinger346, SDOS, PTBP1,		cloned by Nora Treiber used in Treiber *et al,* 2017
PURA, PURB		clones by Hung-Xuan Ho
VP5 (modified pIRES neo)	Flag-/HA	overexpression of TNRC6A-phospho-mutants
TTS736/738/739AAA, TTS736/738/739EEE		
S991A, S991E		
S1582A, S1582E		
SSS1582/1585/1599AAA, SSS1582/1585/1599EEE		
S1548A, S1548E		
T1549A, T1549E		
T1844A, T1844E		
PCIneo	HA/NHA	TNRC6A-phospho-mutants for tethering assays
TTS736/738/739AAA, TTS736/738/739EEE		
S991A, S991E		
S1582A, S1582E		
SSS1582/1585/1599AAA, SSS1582/1585/1599EEE		
S1548A, S1548E		
T1549A, T1549E		
T1844A, T1844E		

4.1.6 Antibodies

Table 13 **Primary and secondary antibodies**

antibody	origin	application	dilution	supplier
antibodies against endogenous proteins				
Hs Ago1, clone 1BX rat		WB, IP	1:5	
Hs Ago1, clone 1C9 rat		WB, IP	1:5	Dr. E. Kremmer,Dr Regina Federle
Hs Ago2, clone 11A9 [187] rat		WB, IP	1:5	Helmholtz Zentrum München
Mm Ago2, clone 6F4 rat		WB, IP	1:5	
Hs TNRC6B, clone 6G3 rat		WB, IP	1:5	
Hs TNRC6A–C, clone 7A9 rat		WB, IP	1:5	
Hs TNRC6A–C, clone 11C12 rat		WB, IP	1:5	
Rmc (IgG control) rat		IP	1:5	
antibodies against tags				
HA, clone 16B12 mouse		WB	1:1000	Covance Research Products
FLAG M2 rabbit		WB	1:1000	Sigma-Aldrich
c-Myc polycl. C3956		WB	1:1000	Sigma-Aldrich
secondary antibodies				
rat IRDye® 800CW goat		WB	1:10.000	LI-COR Biosciences
mouse IRDye® 800CW goat		WB	1:15.000	LI-COR Biosciences
rabbit IRDye® 800CW goat		WB	1:10.000	LI-COR Biosciences
rat IRDye® 680CW goat		WB	1:10.000	LI-COR Biosciences
mouse IRDye® 680CW goat		WB	1:15.000	LI-COR Biosciences
rabbit IRDye® 680CW goat		WB	1:10.000	LI-COR Biosciences

Table 14 **peptides and proteins for monoclonal antibody production***

label	tag/protein/part
TNRC6B	His-TNRC6B full length
TNRC6C	His-TNRC6C full length
Bct	His-TNRC6B C-term (999-1723 aa)
BmI	His-GST-TNRC6B motif I (597-683 aa)
BmII	His-GST-TNRC6B motif II (861-911 aa)
A RRM	GST-TNRC6A RRM (1525-1609 aa)
B RRM	GST-TNRC6B RRM (1535-1619 aa)
C RRM	GST-TNRC6C RRM (1511-1595 aa)

*peptides and proteins were generated by former lab alumni's (Simone Harlander, Janina Pfaff, Sabine Rüdel)

4.1.7 Heavy peptides for SRM measurements

Peptides were obtained as SpikeTides™ TQL peptides that contain a quantifiable tag that is cleaved of during tryptic digest. Amino acid sequences of the proteotypic peptides used in selected reaction monitoring experiments are listed in Table 155.

Table 15 Peptides

Uniprot	Protein name	Position [aa]	Peptide
Q8NDV7	TNR6A	151-167	GQHFPVIAANLGSAVK
Q8NDV7	TNR6A	1196-1206	QEEAWINPFVK
Q8NDV7	TNR6A	1458-1467	QLDPNLLVK
Q8NDV7	TNR6A	883-892	SVSGWNELGK
Q9UPQ9	TNR6B	73-85	VAVPNGQPPSAAR
Q9UPQ9	TNR6B	1209-1225	GLHTPVQPLNSSPSLR
Q9UPQ9	TNR6B	747-757	NGWGEEVDQTK
Q9UPQ9	TNR6B	1470-1487	SSNASWPPEFQPGVPWK
Q9HCJ0	TNR6C	456-467	QNTAWEFEESPR
Q9HCJ0	TNR6C	1323-1337	HGAIPGGLSIGPPGK

4.2 Methods

4.2.1 Molecular biological methods

4.2.1.1 Polymerase chain reaction and site-directed mutagenesis

4.2.1.1.1 PCR with Phusion DNA polymerase for cloning

General PCR composition is listed below (Oligonucleotides are listed inappendix 5.1.6). Amplified PCR products were purified with an agarose gel (0,7-2 %), cut and extracted using the NucleoSpin Gel and PCR Clean-up kit (Macherey-Nagel GmbH). Phusion DNA Polymerase was used for cloning of Proteins (and mutants) and site-directed mutagenesis (described in 4.2.1.1.3).

Phusion PCR mix	50 µL	20µl
DNA template	10-100 ng	10 ng
5x HF/GC Buffer	10 µl	4 µl
dNTPs	0,2 mM	0,08 mM
forward Primer	0,5 µM	0,2 µM
reverse Primer	0,5 µM	0,2 µM
Phusion	0,5 µl (2U)	0,2 µl (0,8 U)
H_2O (bidest.)	ad 50 µl	ad 20 µl

PCR program, phusion		
Initial denaturation	98 °C	30 s
Denaturation	98 °C	10 s
Annealing	50-72 °C	30 s
Elongation	72 °C	30 s/kb
Terminal elongation	72 °C	7 min
30-35 cycles		

4.2.1.1.2 PCR with Taq DNA polymerase for cloning

General PCR composition is listed below. Amplified PCR products were purified with an agarose gel (0,7-2 %), cut and extracted using the NucleoSpin Gel and PCR Clean-up kit (Macherey-Nagel GmbH). Taq Polymerase was used for amplification of viral pri-miRNAs.

Taq PCR mix, 50 µL	
DNA template	10-100 ng
10x buffer	5 µl
$MgCl_2$	4 µl
dNTPs	0,2 mM
forward Primer	0,5 µM
reverse Primer	0,5 µM
Phusion DNA Polymerase	0,5 µl (2U)
H_2O (bidest.)	ad 50 µl

PCR program, taq		
Initial denaturation	95 °C	30 s
Denaturation	95 °C	10 s
Annealing	50-72 °C	30 s
Elongation	72 °C	30 s/kb
Terminal elongation	72 °C	7 min
30-35 cycles		

4.2.1.1.3 Site-directed mutagenesis

Changes of 1 to 7 basepaires of plasmid constructs or amino acid changes were inserted by site-directed mutagenesis. The whole plasmid was amplified with PCR through mutagenic primers forming bulges in case non-complementarity. Template DNA was removed by *DpnI* digestion. Reaction conditions are listed below

PCR mix, 50 µl	
DNA Template	50 ng
5x HF Buffer	10 µl
dNTPs	0,2 mM
forward Primer	0,5 µM
reverse Primer	0,5 µM
Phusion DNA Polymerase	0,5 µl (2U)
H_2O (bidest.)	ad 50 µl

PCR programm		
Initial denaturation	98 °C	30 s
Denaturation	98 °C	10 s
Annealing	50 °C	30 s
Elongation	72 °C	1 min/kb
Terminal elongation	72 °C	10 min
18 cycles		

4.2.1.1.4 Scale up PCRs

For amplification of large amounts of DNA templates for In-vitro-transcription a scale-up PCR was performed after following conditions. PCR product was gel-purified using the NucleoSpin Gel and PCR Clean-up kit (Macherey-Nagel GmbH).

PCR mix, 50 µl	
DNA Template	200 ng
5x HF/GC Buffer	10 µl
dNTPs	0,2 mM
forward Primer	0,5 µM
reverse Primer	0,5 µM
Phusion DNA Polymerase	0,5 µl (2U)
H_2O (bidest.)	ad 200 µl

PCR programm		
Initial denaturation	98 °C	2 min
Denaturation	98 °C	30 s
Annealing	50 °C	30 s
Elongation	72 °C	10 s
Terminal elongation	72 °C	7 min
35 cycles		

4.2.1.1.5 Annealing PCRs

Small DNA fragments were produced through a fill-up PCR reaction with the Phusion DNA polymerase after oligonucleotides were annealed in a separate heat gradient from 95 to 30 °C.

4.2.1.2 General restriction and ligation of DNA constructs

PCR fragments were purified from Agarose gels using the Nucleospin Gel and PCR Clean-up Kit (Macherey-Nagel GmbH) after manufacturer's protocol. 1-3 µg of PCR fragments were digested with restriction enzymes (FastDigest) after manufacturers protocol (Thermo Fischer Scientific) at 37 °C, purified by agarose gel and NucleoSpin Gel and PCR Clean-Up Kit. For ligation 50 ng of the vector and appropriate amounts of PCR fragments were taken. Ligations were done for 1-2 h at 22 °C or overnight at 16 °C.
Alternatively FastAP (Thermo Fisher Scientific) was added to vector restriction reactions for de-phosphorylation.

4.2.1.3 Transformation of competent *E.coli*

For (Re-) Transformations 50 µl of chemically competent XL Blue 1 *E.coli* cells were thawed on ice. Approximately 100 ng of Plasmid DNA, 5-10 µl ligation reaction mixtures or the whole *DpnI*-resctriction mixture of site-directed-mutagenesis were added and incubated on ice for 10 to 30

min, followed by a heat shock step at 42 °C for 1 min. Afterwards bacteria were chilled on ice for 2 min and alternatively incubated with 1 ml LB medium at 37 °C for 30 min while shaking.
Whole transformation mix was plated on LB plates containing appropriate antibiotics and incubated overnight at 37 °C.

4.2.1.4 Cloning with pGEM T easy Kit

For subcloning without restriction sites the pGEM T easy Kit (Promega) was used after the manufacturer's protocol. Therefore the PCR fragments were A-tailed by the Taq polymerase and afterwards ligated in the pGEM T easy multiple cloning site with T-overhangs at its 3'-and 5'-ends. After standard transformation bacteria were plated out on LB Amp plates containing 20µl 1 M IPTG and 35 µl X-Gal (50µg/ml). White colonies were picked for plasmid extraction.

4.2.1.5 Plasmid purification and sequencing

Plasmid DNA was extracted for all applications with the NucleoBond® Plasmid and Xtra Midi kits (Macherey-Nagel) according to the manufacturer's protocols. Plasmid sequence was verified by sequencing with convenient sequencing primers by GATC (Köln, Germany) or Macrogen (Amsterdam, Netherlands).

4.2.2 Cell biological methods

4.2.2.1 Cultivation of mammalian cells

Human and murine cells were in general cultured under standard atmosphere conditions of 5 % CO2 at 37 °C in a Cell culture incubator. Dulbecco's modified Eagle's medium (DMEM, Sigma-Aldrich) supplemented with 10% FBS (Sigma- Aldrich; Gibco, Thermo Fischer Scientific) and 1 % Penicillin/Streptomycin (Sigma-Aldrich)..

4.2.2.2 Cell transfections

4.2.2.2.1 Cell transfection by Lipofectamin 2000

6-wells with 60-80 % confluent cells were transfected with 1µg plasmid DNA using Lipofectamin 2000 according to the manufacturer's protocol. Medium was changed after 6-18 h and cells were harvested after 24-48 h.

4.2.2.2.2 Cell transfection by calcium phosphate

Per 15 cm^2 cell culture plate with 20-50 % confluent cells, 2-20 µg of Plasmid DNA mixed with 123 µl 2 M $CaCl_2$ and filled up to 1 ml with sterile H_2O. 1ml of 2x HEPES buffer was added while shaking to the DNA containing mix and incubated for 10-15 min at RT. Afterwards DNA mix was added to the adherent cells and incubated for 24-48 h, alternatively medium can be changed after 24 hours to remove precipitated DNA.

2x HEPES-buffered saline	274 mM NaCl, 1.5 mM Na_2HPO_4, 54.6 mM HEPES (pH 7.1)

4.2.2.3 Cultivation and induction of stable HEK T-REx 293 FLP/IN cell lines

Stable cell lines were used as described in Schraivogel et al. 2015. Briefly, cells were cultivated as described in 4.2.2.2.1 supplemented with Balstidcidin 15 µg/ml and Hygromycin 200 µg/ml. Expression was induced 24 h with 1 µg/ml Doxycycline and 48 h with Tetracycline 1µg/ml. Medium was changed 2-4 h before harvesting.

4.2.2.4 Tethering assay with Luciferase reporters

HeLa cells were grown to 60 % confluence on 48 well-plates. Per well, 300 ng of HA/NHA-constructs, 120 ng *Renilla*-5 boxB luciferase (RNL20) and 80 ng Firefly-Luciferase (FF) were transfected using Nanofectin (PAA Laboratories/GE Healthcare) according to the manufacturer's guidelines. Cells were lysed 48 h after transfection with 60-100 µl Passive Lysis Buffer (Promega) for 15 min at RT while shaking. Luciferase activity was measured on a Mithras LB 940 luminometer (Berthold Technologies). Coelenterazine and DTT were added freshly before use. Data was analyzed by calculating the ratio of FF/RNL20 and the normalization of the NHA-tagged plasmid sample to the appropriate HA-tagged plasmid sample and compared to empty vector. All samples were measured in 3 technical and 3 biological replicates.

4.2.2.5 Immunofluorescence of cells

Immunofluorescence was conducted as described previously in Schraivogel et al. 2015. After incubation with the first and secondary antibody, cells which were grown on a glass slide were washed once with blocking solution, three times with 1xPBS and mounted using Prolong Gold containing DAPI (Thermo Fisher Scientific–Life Technologies). Confocal microscopy was done on a TCSSP8 (Leica Microsystems) equipped with acousto-optical beam splitter, 405 nm laser (for DAPI), argon laser (488 nm for Alexa 488), and DPSS laser 561 nm.

4.2.2.6 Cultivation of Human Herpes Virus containing cells

The Cultivation of cells and viruses classified as risk group 2 as well as all other molecular biochemical work were performed in the S2 laboratory of PD Dr. Hans-Helmut Niller, PD Dr. Michael Nevels and Dr. Christina Paulus.

4.2.2.6.1 Generation of virus stocks

Virus stocks were generated through infection of the primary fibroblast cell line MRC5 and havesting of the medium supernatant containing the viruses through centrifugation. Afterwards the virus titer was estimated with plaque assays.

4.2.2.6.2 Infection of confluent cells

For infection of the cells, viruses stock was first gently sonicated, and diluted to a moi of 5. Afterwards virus was added to confluent MRC5 cells and incubated for 2 hours, cells were washed with DMEM medium and further cultivated until certain time points.

4.2.2.6.3 Cultivation of virus-latent suspension cells

Suspension cells were in general cultivated with RMPI 1640 mediumsupplemented with 10 % FBS (Gibco, thermos fischer scientific) and 1 % Pen/Strep (sigma-aldrich) under standard conditions of 37 °C and 5 % CO_2 in 25-, 75,-175 cm^2 cell culture flasks.

4.2.3 RNA based methods

4.2.3.1 *In vitro* Transcription, gel purification by UREA-Page and RNA purification

The T7 RNA Polymerase was purified by Dr. Nora Treiber and Dr. Thomas Treiber (both belong to the Meister lab, Biochemistry I, University of Regensburg) and used for large scale *in vitro* transcriptions. Reactions were incubated for 4 to 6 h at 37°C with Pyrophosphatase (Fermentas/ Thermo Fischer Scientific) and inactivated with DNA sample buffer. Reactions were gel-purified using a 15 % UREA-page, monitored under UV light shadowing and eluted with 300 mM NaCl followed by a precipitaiton with 0,8 volume Isopropanol and several washing steps with 75 % EtOH p.a.. RNA pellet was solved in 300 µl DEPC-H_2O. Reaction composition is listed below.

In-vitro-transcription mix, 1 ml		
DNA Template	2 µg	
NTPs (0.2M each)	50 µl	10 mM
1M Tris pH 8.0	30µl	30 mM
1M MgCl2 1M	25µl	25 mM
Triton X-100	10µl	1%
1M DTT	10 µl	10 mM
Spermidin	2µl	2mM
Pyrophosphatase	1µl	
T7 RNA Polymerase (5mg/ml)	20µl	
DEPC-H_2O	ad 1ml	

4.2.3.2 RNA extraction

RNA was extracted from cells, lysates (inputs) and IPs with TRIzol (Thermo Fisher Scientific) according to the manufacturer's guidelines. Additionally a second chloroform purification step was added for qRT-PCR experiments.

4.2.3.3 Quantitative real time-PCR

For quantitative real time-PCR (qRT-PCR) for quantitative detection of input RNA and immunoprecipitated RNA levels, 1µg of extracted RNA or complete RNA yield from IPs was digested with DNaseI (Thermo Fisher Scientific) for 30 min at 37 °C and inactivated by heating at 72 °C for 10 min and adding 1µl 100 mM EDTA.
cDNA was synthesized with First Strand cDNA synthesis kit (Thermo Fisher Scientific) using random hexamer primer and following the manufacturer's protocol. cDNA was diluted with 30µl H_2O. qRT-PCR was performed with Sso Fast Eva Green Mix (Bio-Rad Laboratories), 0,4µM forward and reverse primer. DNA was amplified using standard PCR programs from the Sso Fast Eva Green Mix manual with denaturation and annealing/ extension times of 5 s and 40 cycles. Reaction monitoring was performed on a C1000 thermal cycler with CFX96TM real time detection system (Bio-Rad Laboratories).
Data were evaluated using ΔΔCt method with GAPDH as reference mRNA and normalized to control sample. Error bars were calculated based on the standard deviations from three biological replicates..

4.2.3.4 Small RNA detection by UREA-page and northern blotting

Northern blots for small RNA detection were basically performed as described in Pall and Hamilton, 2008. RNA was separated on a 12 % UREA-polyacrylamide gel at 400 V with 1x TBE buffer after preheating the gel. Gel pockets were flushed and 5-20 µg of RNA mixed with RNA sample buffer was loaded. After disassembling of the UREA-gel, RNA quality was verified with etidiumbromide staining and blotting was performed onto an Amersham Hybond-N membrane (GE Healthcare) for 30 min at 20 V with a semi-dry blotting chamber (Bio-rad Laboratories).

10x TBE	890 mM Tris, 890 mM boric acid, 20 mM EDTA
2x RNA sample buffer	0,025 % (w/v) Xylencyanol, 0,025 % (w/v) Bromphenolblau in
Formamide Ethidiumbromide staining solution	1 µg/ml ethidiumbromide in 1x TBE

Afterwards the miRNA 5' ends were subsequently chemically crosslinked for 1 h at 50°C to the membrane with a freshly prepared EDC crosslinking solution. Therefore the membrane was placed on an EDC-soaked-whatman paper and wrapped with plastic. After gentle washing the membrane was prehybridized with Hybridization solution at 50 °C while rolling. Probe was labeled using 20 pmol DNA oligonucleotide with 20 µCi of ^{32}P-ATP (Hartmann Analytics) in a T4 PNK reaction according to the manufacturer's protocol (Thermo Fischer Scientific) for 1h at 37°C. Reaction was stopped by adding 30µl 30 mM EDTA and probes were purified by Illustra MicroSpin G-25 columns (GE Healthcare). Flowtrough was added to the prehybridized membrane after PNK reaction verification and incubated overnight while rolling at 50 °C. Membrane was washed on the turning wheel first twice with wash buffer I followed by a third time with wash buffer II at 50°C for 10 min. Liquid was discarded and plastic was wrapped around membrane and exposed to a imaging screen. RNA signals were detected with the Personal Molecular Imager system (Bio-Rad laboratories). Alternatively current probe can be stripped off the membrane for re-usage. Therefore H_2O was boiled, membrane was added and 10 % SDS was added to a final concentration of 0,1 %. After 10 min incubation at RT on a shaker this step was repeated followed by a third step with boiled water.

EDC crosslinking solution	184 mg EDC (1-ethyl-3-(3-dimethyl-aminopropyl)-carbodiimid), 61.25 µl 1-methylimidazol (12.5 M), 75 µl HCl (1M), adjust to 6 ml with H_2O
20x SSC	3 M NaCl, 0.3 M trisodium citrate (pH 7)
50x Denhardt's solution	1 % Bovine serum albumin fraction V, 1 % Polyvinylpyrrolidon K30, 1 % Ficoll 400
Hybridization solution	1x SSC, 20mM Na_2HPO_4 pH 7.2, 7 % SDS, 1x Denhardt's solution
Wash buffer I	5x SSC, 1 % SDS
Wash buffer II	1x SSC, 1 % SDS

4.2.4 Proteinbiochemical methods

4.2.4.1 Lysate preparation

Total protein concentration of lysates after preparation was determined by Bradford measurements with BSA as standard.

4.2.4.1.1 Lysate preparation from cultured cells

Cells were grown under standard conditions on 12-, 6-well, 10 cm^2 or 15 cm^2 cell culture dishes. Cells were harvested after medium was removed, washed with cold PBS and additionally cell pellet was weighted after centrifugation (300 g/ 5 min/ 4°C) and removal of PBS supernatant. Pellet was either divided into more samples, frozen in liquid nitrogen and stored at -80 °C or lysed directly with IP lysis buffer. For lysis 1ml/15cm^2 IP lysis buffer was added to the pellet, resolved and incubated for 10-30 min. Lysates were cleared by centrifugation (15.000 g/ 20 min/ 4°C). For mass spectrometric analyses cells were lysed with IP lysis buffer MS or RNAse/MS followed by immunoprecipitation.

IP lysis buffer	150 mM KCl, 25 mM Tris pH 7,5, 2 mM EDTA, 1 mM NaF, 0,5 % NP-40, 1 mM DTT, 1mM AEBSF
IP lysis buffer MS	150 mM KCl, 25 mM Tris pH 7,5, 2 mM EDTA, 5 mM NaF, 0,5 % NP-40, 1 mM DTT, 1mM AEBSF, 1x tablet/10ml buffer PhosSTOP phosphatase inhibitor (Roche)
IP lysis buffer RNase A/MS	150 mM KCl, 25 mM Tris pH 7,5, 2 mM EDTA, 5 mM NaF, 0,5 % NP-40, 1 mM DTT, 1mM AEBSF, 1x tablet/10ml buffer PhosSTOP phosphatase inhibitor (Roche), RNase A 1 µg/ml (Thermo Fischer Scientific)

4.2.4.1.2 Nuclear and cytoplasmic fractionation

Nuclear and Cytoplasmic fractionations were performed in general as described in Gagnon et al. 2014 with slight modifications. Hek 293 T cells were cultured up to 80 % confluency, washed with PBS, harvested and washed again with ice-cold PBS. After centrifugation (100 g/ 5 min/ 4°C), cell pellet was resuspended by gentle pipetting with ice-cold hypotonic lysis buffer (HLB) with 1ml/ 75 mg cell pellet or 10 mio. cells and incubated for 10 min and mixed by gentle inversion. Afterwards cells were centrifuged (800g/ 4 °C/ 8 min), supernatant (= cytoplasmic fraction) was transferred in a new tube and 140 mM NaCl was added to a final concentration of 150 mM for IPs. The nuclei pellet was washed gentle for three times with HLB through pipetting and centrifugation (200 g/ 4°C/ 2 min). Nuclei were resuspended in 0,5 ml/75mg or 10 mio. cells and sonicated on ice three

times with 10-20 % power for 15 s with cooling periods between sonication steps. For fraction clearance centrifuge (15.000 g/ 15 min/4 °C)

Hypotonic lysis buffer (HLB)	10 mM Tris (pH 7.5), 10 mM NaCl, 3 mM MgCl2, 0.3% (vol/vol) NP-40 and 10 % (vol/vol) glycerol1 mM DTT, 1mM AEBSF, 1x tablet/10ml buffer PhosSTOP phosphatase inhibitor (Roche)
Nuclear lysis buffer (NLB)	20 mM Tris (pH 7.5), 150 mM KCl, 3 mM MgCl2, 0.3% (vol/vol) NP-40 and 10 % (vol/vol) glycerol1 mM DTT, 1mM AEBSF, 1x tablet/10ml buffer PhosSTOP phosphatase inhibitor (Roche)

4.2.4.1.3 Lysate preparation from tissues

Mouse tissue lysates were prepared in 800 µl NET buffer and mechanically disrupted by FastPrep®-24 with lysing matrix D (45 s at 6.5 m/s) or with a 6 ml douncing homogenizer with a thight douncing spatel until suspension was homogeneous. Lysates were spinned down (13,000 g/ 1 min/ 4 °C) and transferred to a new reaction tube and centrifuged (15.000 g/ 20 min/ 4 °C).

NET buffer	50mM Tris/HCl pH 7.5, 150mM NaCl, 5mM EDTA, 0.5 % NP-40, 10 % Glycerol, 1mM NaF, 0.5mM DTT, 1mM AEBSF, 1x tablet/10ml buffer PhosSTOP phosphatase inhibitor (Roche), RNase A 1 µg/ml (Thermo Fischer Scientific)

4.2.4.1.4 Lysate preparation for protein-pull-down assays

Virus infected cells were harvested on ice and washed twice with ice-cold DMEM. Cell pellet was resuspended in pull-down buffer 1ml/ 50 mio. cells and two times sonicated (power: 10 %/ duty cycle: 50 %/ 20 pulses) for inactivation. Afterwards lysate was centrifuged (20000 g/ 10 min/4 °C) and diluted to 5-10 mg/ml total protein and frozen with liquid nitrogen and stored on -80 °C.

Pull-down buffer for lysate preparation	50mM Tris pH 8, 150mM NaCl, 5% Glycerin, 1 mM DTT, 1mM AEBSF

4.2.4.2 Immunoprecipitation

For immunoprecipitations (IP) of endogenous proteins from cell lysates, monoclonal or polyclonal antibodies were coupled after washing twice with PBS to Protein G Sepharose beads (GE Healthcare). Depending of the amount of protein material and experimental set up 30 to 200 µl of beads were used and coupled overnight at 4 °C while shaking. Afterwards beads were washed once with PBS through centrifugation (1000g/ 2 min/ 4 °C) to remove excess antibody.
For Flag-/HA-tagged overexpressed proteins, IPs were performed with anti-FLAG M2 agarose beads (Sigma-Aldrich) for mass spectrometry and RNA experiments and for western blots with the monoclonal antibody 6F7 coupled to Protein G Sepharose beads.

Covalent coupling of monoclonal antibodies to Protein G Sepharose (GE Healthcare) was performed after for selective elution of proteins without co-elution of ABs (Gersten and Marchalonis, 1978; Schneider et al. 1982 und Simanis and Lane, 1985). First beads were washed with PBS by centrifugation (1000 g/ 2 min/ 4 °C), AB was added and incubated for 1h at RT while shaking. Afterwards beads were washed with 10x bead-volume 0,2 M Sodiumborat (pH 9.0, RT) and resuspended with 0,2 M Sodiumborat containing 20 mM Dimethylpimelimidate and incubated for 30 min at RT while shaking. Coupling reaction was stopped by washing once with 10x bead-volume of 0,2 M Ethanolamine (pH 8.0) and repetition of this step and further incubation for 2 h at RT while shaking. Afterwards beads were washed again with PBS twice and stored in PBS supplemented with 0,025 % NaN_3 at 4 °C.

Antibody-coupled beads were added to prepared lysates (described in 4.2.4.1) for 1-3 h at 4 °C while rotating. After incubation supernatant was removed and alternatively mixed with SDS sample buffer. Beads were washed four times with IP wash buffer by centrifugation (1000g/ 2 min/ 4 °C) and transferred into a new tube. Beads were eluted with 1-,5-2,5 SDS sample buffer after a final wash step with PBS.
For extraction of co-immunoprecipitated RNA TRizol was used as described in 4.2.3.2.

Antibody hybridoma supernatants were partly purified by Robert Hett with a 3-step purification protocol. Briefly, an appropriate amount of Ammoniumsulfate was added to the hybridoma supernatants. After centrifugation the pellet was resolved in PBS and antibodies were bound by an IMAC column with Co-IDA-beads (Fastflow Sepharose). After elution fine polishing was performed by a gelfiltration.

IP wash buffer	300 mM NaCl, 50 mM Tris pH 7,5, 1 mM NaF, 0,01 % NP-40, 5 mM MgCl2, 0,1-1 mM DTT, 0,1-1 mM AEBSF
IP lysis buffer	150 mM KCl, 25 mM Tris pH 7,5, 2 mM EDTA, 1 mM NaF, 0,5 % NP-40, 1 mM DTT, 1mM AEBSF
5x SDS sample buffer	300 mMTris/HCl pH 6.8, 10 % SDS, 62.5 % glycerol, 0.05 % bromophenol blue, 10 % β –mercaptoethanol

4.2.4.3 SDS-Page, Western Blot and coomassie-stainings

For separation and visualization of proteins a 6-15 % SDS polyacrylamide gel was poured depending on the molecular weight of the protein of interest. Pockets were loaded with

appropriate amounts of denatured and preheated (95 °C/ 5 min) protein lysates mixed with SDS sample buffer form input (subsequently taken after lysate preparation) and IP samples for western blots and mass spectrometric analysis. Gels were run at 140 V for 30 min, followed by 220 V until dye front ran out.

Stacking gel 0.05 % APS	125 mM Tris/HCl pH 6.8, 0.1 % SDS, 0.15 % TEMED, 5 % Acrylamide/Bis solution (37.5:1),
Separating gel (37.5:1), 0.05 % APS,	380 mM Tris/HCl PH 8.8, 0.1 % SDS, 0.1 % TEMED, 6-10 % Acrylamide/Bis solution
SDS running buffer	25mM Tris, 192mM glycine, 1 % SDS
5x SDS sample buffer	300 mMTris/HCl pH 6.8, 10 % SDS, 62.5 % glycerol, 0.05 % bromophenol blue, 10 % β – mercaptoethanol

For Western Blotting, three Whatman papers soaked with towbin blotting buffer were placed under a Hybond ECL membrane (GE Healthcare) onto the positive electrode. SDS gel and another three Whatmann papers were exactly applied to the membrane and air bubbles were removed. Western blots were performed in a semi-dry blotting chamber (Bio-rad) either at 10 V with a blotting time of 3 h or 1 min/ kDa protein and 2 mA/ 1 cm^2. Alternatively proteins were blotted at 30 V by wet-blotting overnight for 16 h at 4°C with wet blot buffer. Afterwards membrane was blocked with 5 % milk in TBS-T for at least 1 h and primary antibodies (AB) were diluted in 5 % milk in TBS-T and incubated with the blocked membrane for 1 h. To remove unspecific bound AB membrane was washed three times with TBST-T for 10 min each and secondary antibody was applied for 30-60 min. Signals were detected after washing the membrane three times with TBS-T through scanning with the Odyssey Infrared Imaging System (Bio-rad). For antibody subtype identification specific secondary-HRP (supplied by Elisabeth Kremmer group) labeled antibodies were used and incubated with SuperSignal West Femto Maximum Sensitivity Substrate (Thermo Fisher Scientific) and detected by film.

For coomassie-staining, first the SDS gel was washed once with H_2O and then placed in coomassie-staining Solution for at least 1-2 h. Destaining was performed as long as protein bands were clearly visible.

Towbin blotting buffer	25mM Tris, 192mM glycine, 20 % methanol pH 8.6
TBS-T	10mM Tris, 150mM NaCl, 0.05 % Tween pH 8
Wet blot buffer	25mM Tris, 192mM glycine, 20 % methanol pH 8.6, 0,05 % SDS
Blocking milk	5 % milk powder in TBS-T, 0,025 NaN_3
Coomassie stain	10 % acetic acid, 30 % ethanol, 0.25 % Coomassie R250
Coomassie destain	10 % acetic acid, 20 % ethanol

4.2.4.4 RNA-pull-downs

For RNA generation large amounts of DNA template were amplified in scale-up PCR reactions. *In vitro* transcriptions were performed as described in 4.2.3.1 and UREA-gel-purified. Afterwards 80µl magnetic Dynabeads Streptavidin M270 (GE healthcare) were coupled with 2 µg biotinylated RNA "Hook"-oligo (Metabion) in 500 µl pull-down Puffer (PP) for 2h at 4 °C while shaking. Beads were washed and 10 µg of *in vitro* transcribed pre-miRNA was added and incubated overnight at 4 °C while shaking.

Meanwhile 1ml of lysate was thawed (described in 4.2.4.1.4) and precleared with 80 µl of magnetic Dynabeads Streptavidin M270 (GE healthcare) coupled with 2 µg biotinylated RNA "Hook"-oligo (Metabion) for 2-4 h at 4 °C while shaking. Afterwards precleared lysate was added to pre-miRNA coupled beads and incubated overnight at 4 °C. Lysate was removed and washed first with PPP supplemented with 0.1% Triton-X 100, second with PPP supplemented with additional 150 mM NaCl and third with PPP. Proteins were eluted with 25 µl of 1x LDS buffer (Invitrogen) and separated on a bis/tris bufferd 4-12 % gradient gel (Invitrogen) for mass spectrometric analysis. Alternatively pull-down was down scaled to 20-40 µl magnetic Dynabeads Streptavidin M270 per sample and eluted with 1,5x SDS sample buffer and separated by SDS-page for western blots.

Pull-down buffer (PP)	50mM Tris pH 8, 150mM NaCl, 5% Glycerin
Pull-down buffer for lysate preparation (PPP)	50mM Tris pH 8, 150mM NaCl, 5% Glycerin, 1 mM DTT, 1mM AEBSF
5x SDS sample buffer	300 mMTris/HCl pH 6.8, 10 % SDS, 62.5 % glycerol, 0.05 % bromophenol blue, 10 % β -mercaptoethanol

4.2.5 Mass spectrometry

All mass spectrometric measurements were performed at the MS facility of Biochemistry I, University of Regensburg under the guidance of Prof. Dr. Rainer Deutzmann and Dr. Astrid Bruckmann.

4.2.5.1 Sample preparation

After gradient-gels or SDS gels were destained, bands or gel parts were excised and transferred into 2ml micro tubes (Eppendorf), washed for 30 min with 500 µl 50 mM NH_4HCO_3, 50 mM NH_4HCO_3/ acetonitrile (3/1), 10 mM NH_4HCO_3/ acetonitrile (3/1), 10 mM NH_4HCO_3/ acetonitrile (1/1) and lyophilized. After reduction and alkylation of cysteines with 100 µl 1mg/ml DTT (57 °C/

35 min) and 200 µl 5 mg/ml Iodoacetamide (RT/ 35 min) solved in 50 mM NH_4HCO_3, gel slices were washed again and lyophilized. Proteins were subjected to *in gel* tryptic digest overnight at 37 °C with 0,8 µg Trypsin Gold mass spectrometry grade (Promega) per sample. Peptides were first extracted twice with 100 mM NH4HCO3, followed by 100 mM NH_4HCO_3/ acetonitrile (2/1) and eluates were combined and lyophilized.

Further processing was executed by Dr. Astrid Bruckmann or Eduard Hochmuth.

4.2.5.2 Selected Reaction Monitoring measurements with heavy labeled peptides

For quantification of TNRC6 proteins, IPs with different antibodies and input samples were applied to the QTRAP 4500 mass spectrometer combined with a SRM based method. SRM measurements were in general performed by Dr. Astrid Bruckmann.

Briefly, unique synthetic peptides with a $^{13}C^{15}N$-labeled C-terminal lysine or arginine for every human TNRC6 homolog were synthesized and used as standard (listed in Tab. 4.7). After samples were washed, 100 fmol of stable isotope-labeled peptide mix was spiked into tryptic digests and incubated over night at 37 °C. Afterwards peptides were extracted and applied to mass spectrometer

4.2.5.3 MS data analysis

Data obtained from samples analyzed on the MaXiS mass spectrometer were transferred to MASCOT 2.5.1 using the Protein-Scape software 3.1.3 (Bruker Daltonics). MASCOT aligned the obtained data to the annotated proteins of the NCBI protein data base or the SWISS-PROT database. Annotated proteins were exported as excel sheet and further analyzed depending on the experimental question. Therefore the expectation value, annotated peptides, protein size and Score served as analyses basement.

Data obtained from relative quantification of TNRC6 protein levels was first exported to MS Office Excel and ratios of spike-in peptides of 100 fmol compared to measured peptides were calculated. Afterwards the mean value and median was calculated assuming that measured results represent 100 % of TNRC6 proteins.

Data obtained in the viral biogenesis screening project were combined and compared in Excel sheets and the selection of potential candidates was performed through the distinct parameters. These ones were the Score, Protein size and annotated peptides in both replicates. For visualization, a heatmap was designed with the candidates on the y-axis and the miRNAs on the

x-axis. Data sets were then for every single protein normalized to the whole score value of all detected single hits. Duplicates were averaged and thresholds for the different data sets were fixed.

4.2.6 Computational methods and statistical analyses

GO Term. For Go term analyses the browser programme GO.princeton.edu was used. Therefore selected protein lists were transformed to Uniprot nomenclature and processed.

Sequence alignments. For Sequence and multiple Sequence alignments of annotated proteins and DNA/ RNA the browser programme Clustal W and TCoffee was used.

Networks analysis. For the analysis of protein networks the programme STRING 10.0 was used.

Kinase prediction. Kinases for selected TNRC6 phospho-sites were predicted with NETphos3.1 (Blom et al. 2004).

Browser based tools can be found under following www-links:

http://www.cbs.dtu.dk/services/NetPhos-3.1/output.php

http://www.uniprot.org

http://pantherdb.org/

http://go.princeton.edu/cgi-bin/GOTermFinder

http://www.ebi.ac.uk/Tools/services/web/toolresult.ebi?jobId=clustalo-I20170730-092917-0605-20657726-pg&analysis=alignments

http://string-db.org

http://www.biovenn.nl/index.php

5 APPENDIX

5.1 Supplementary information

5.1.1 Herpesviral miRNAs and their function

Table 16 Herpesviral miRNAs and their function
hg host gene, vg viral gene, modified from (Grundhoff and Sullivan 2011; Grundhoff and Sullivan 2012; R. L. S. and B. R. Cullen 2013; Stern-Ginossar et al. 2009; Kang, Skalsky, and Cullen 2015; Bruscella et al. 2017; Piedade and Azevedo-Pereira 2016; Fruci, Rota, and Gallo 2017).

mature miRNAs		target	function	publication
hcmv-mir-UL22A	5p/3p			
hcmv-mir-UL36	5p/3p	UL138 (vg), ANT3 (hg)	Latent infection, cell survival	(Y. Guo et al. 2015)
hcmv-mir-UL112	5p/3p	IE72 (vg), UL112/113 (vg), UL120/121 (vg) MICB (hg); IKKα and IKKβ (Iκβ kinase), IL32 (hg), type IIF sig. (hg), TLR3 (hg), VAMP3 (hg),RAB5C (hg), RAB11A (hg), SNAP23 (hg), CDC42 (hg)	Natural killer cell killing of virus-infected cells, Regulation of viral replication, latency Inhibition of proinflammatory cytokine response, tumor necrosis factor alpha, viral infection, immune evasion, vesicle pathway	(G J Seo et al. 2008; Stern-Ginossar et al. 2009; Jeang 2008) (Hook et al. 2014) (Hancock et al. 2017)
hcmv-mir-UL148D		CCL5 (hg), IEX-1 (hg), CDC25B (hg), ACVR1B (hg)	Immune evasion, cell survival, latent infection	(Pan et al. 2016; B. Lau et al. 2016)
hcmv-mir-US33	5p/3p	Syntaxin3	Inhibition of viral DNA synthesis	(X. Guo et al. 2015)
hcmv-mir-US5-1	5p/3p	IKKα and IKKβ (hg) (Iκβ kinase), US7 (vg), VAMP3 (hg),RAB5C (hg), RAB11A (hg), SNAP23 (hg), CDC42 (hg)	Inhibition of proinflammatory cytokine response, tumor necrosis factor alpha, viral infection, vesicle pathway	(Hancock et al. 2017) (Hook et al. 2014)
hcmv-mir-US5-2	5p/3p	US7 (vg), VAMP3 (hg),RAB5C (hg), RAB11A (hg), SNAP23 (hg), CDC42 (hg)	viral infection, vesicle pathway	(Hook et al. 2014)
hcmv-mir-US25-1	5p/3p	YWHAE (hg), UBB (hg), NPM1 (hg), and HSP90AA1 (hg),), VAMP3 (hg),RAB5C (hg), RAB11A (hg), SNAP23 (hg), CDC42 (hg), E2 (hg), BRCC3 (hg), MAPRE2 (hg), CD147 (hg)	Inhibition of viral DNA replication, vesicle pathway	(Jiang et al. 2015) (Hook et al. 2014)
hcmv-mir-US25-2	5p/3p	eIF4A1	Viral infection	(M. Qi et al. 2013)
hcmv-mir-US4	5p/3p	ERAP1 (hg), QARS (hg)	Immune evasion, cell survival	
hcmv-mir-UL70	5p/3p	unknown	Upregulation of Sox2 in CMV-mediated Glioblastoma multiforme cells	(Ulasov et al. 2016)
hcmv-mir-US22	5p/3p			
hcmv-mir-US29	5p/3p			
hcmv-mir-UL59				
hcmv-mir-UL69				

mature miRNAs		target	function	publication
ebv-mir-BHRF1-1				
ebv-mir-BHRF1-2	5p/3p	PRDM1/Blimp1	tumor suppressor gene in B- and T-cells	(Ma et al. 2016)
ebv-mir-BHRF1-3		CXCL11 (hg)	Immune evasion	
ebv-mir-BART1	5p/3p	LMP1 (vg)/Caspase-3 (hg), BIM (hg)	Inhibits apoptosis/ Immune evasion	(Lo et al. 2007) (Marquitz et al. 2011) (Vereide et al. 2014)
ebv-mir-BART2	5p/3p	MICB (hg)	Immune evasion	(Nachmani et al. 2009)
ebv-mir-BART3	5p/3p	BIM (hg), Dice1 (hg), FEM1B (hg), CASZ1a (hg)	Inhibits apoptosis	(Kang, Skalsky, and Cullen 2015), (Lei et al. 2013)
ebv-mir-BART4	5p/3p			
ebv-mir-BART5	5p/3p	PUMA (hg)	Inhibits apoptosis	(Choy et al. 2008)
ebv-mir-BART6		Dicer (hg), OCT1 (hg)	Regulation of miRNA biogenesis	(Kang, Skalsky, and Cullen 2015; Godshalk, Bhaduri-McIntosh, and Slack 2008)
ebv-mir-BART7	5p/3p	APC (hg)	Cell transformation and proliferation	(Wong et al. 2012)
ebv-mir-BART8	5p/3p	ARID2 (hg)		(Kang, Skalsky, and Cullen 2015)
ebv-mir-BART9	5p/3p	BIM (hg), E-cadherin (hg)	Inhibits apoptosis, Induction of mesenchymal-like phenotype, Migration of NPC cells	(Hsu et al. 2014) (Marquitz et al. 2011)
ebv-mir-BART10	5p/3p			
ebv-mir-BART11	5p/3p	EBF1/BCR/BIM (hg)	B-cell differentiation, Inhibits apoptosis	(Ross, Gandhi, and Nourse 2013), (Marquitz et al. 2011)
ebv-mir-BART12		BIM (hg)	Inhibits apoptosis	(Marquitz et al. 2011)
ebv-mir-BART13	5p/3p			
ebv-mir-BART14	5p/3p			
ebv-mir-BART15		BZLF1 (vg), BRLF1 (vg), NLRP3 (hg), LMP1 (hg)	Immune evasion	(Murphy et al. 2008),(Haneklaus et al. 2012)
ebv-mir-BART16		TOMM22 (hg), Caspase-3 (hg), CREBBP (hg), SH2B3 (hg)	Inhibits apoptosis, Immune evasion	(Kang, Skalsky, and Cullen 2015)
ebv-mir-BART17	5p/3p	LMP1 (vg), WIF1 (hg)	Inhibits apoptosis, Proliferation	(Lo et al. 2007), (Wong et al. 2012)
ebv-mir-BART18	5p/3p			
ebv-mir-BART19	5p/3p	APC (hg)	Proliferation	(Wong et al. 2012)
ebv-mir-BART20	5p/3p	BAD (hg)	Inhibits apoptosis	
ebv-mir-BART21	5p/3p			
ebv-mir-BART22		PPP3R1 (hg), PAK2 (hg), TP53INP1 (hg)	Inhibits apoptosis	(Kang, Skalsky, and Cullen 2015)

mature miRNAs		target	function	publication
hsv1-mir-H2	5p/3p	ICP0 (vg)		(S. Tang et al. 2008; S. Tang, Patel, and Krause 2009; S. Tang et al. 2013)
hsv1-mir-H3	5p/3p	ICP34,5 (vg)		(S. Tang et al. 2008; S. Tang, Patel, and Krause 2009; S. Tang et al. 2013)
hsv1-mir-H6	5p/3p	ICP4 (vg)		(S. Tang et al. 2008; S. Tang, Patel, and Krause 2009; S. Tang et al. 2013)

5.1.2 Virus hairpin pull-down - data sets and analysis

A

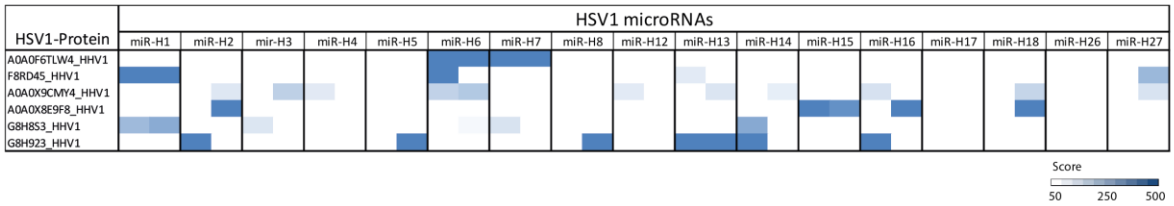

B

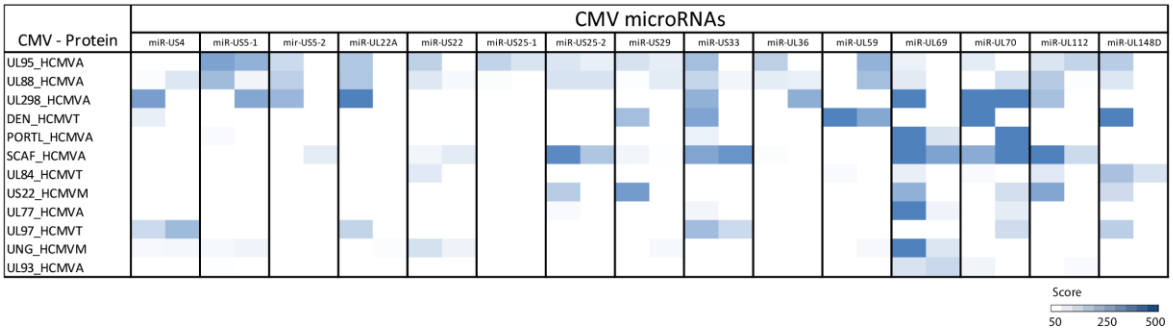

C

	Gene names	Domain	Subcellular location	Gene ontology (GO)
HSV1-Proteins	UL6		Host nucleus	DNA packaging; viral release from host cell
	UL25 CVC2		Host nucleus	viral capsid; viral entry into host cell; viral genome packaging ; viral penetration into host nucleus ; viral release from host cell
	UL52	CHC2-type	Host nucleus	host cell nucleus ; DNA primase activity ; metal ion binding ; bidirectional double-stranded viral DNA replication
	UL29 DBP	Zinc-finger	Host nucleus	host cell nucleus ; metal ion binding ; single-stranded DNA binding ; bidirectional double-stranded viral DNA replication
	UL10 gM		Virion membrane	host cell endosome membrane ; host cell Golgi membrane ; host cell nuclear inner membrane ; integral component of membrane ; viral envelope ; virion membrane
	UL38 TRX1		Virion, Host nucleus	viral capsid ; DNA binding ; viral capsid assembly
CMV-Proteins	UL95		Host nucleus	
	UL88		Virion	virion
	UL29		Host nucleus, cytoplasm	virion
	UL48	Peptidase C76	Virion tegument, Host cytoplasm	viral tegument ; thiol-dependent ubiquitinyl hydrolase activity ; modulation by virus of host protein ubiquitination
	UL104		Virion, Host nucleus	virion ; DNA packaging ; viral release from host cell
	UL80 APNG	ACD, CCD	Host cytoplasm, nucleus	serine-type endopeptidase activity ; viral release from host cell
	UL84		Host nucleus, cytoplasm	
	US22		Virion tegument	viral tegument
	CVC2 UL77		Virion, Host nucleus	viral capsid ; viral entry into host cell ; viral genome packaging ; viral penetration into host nucleus ; viral release from host cell
	UL97		Virion	virion ; ATP binding ; protein kinase activity ; modulation by virus of host cell cycle
	UL114		Host nucleus	uracil DNA N-glycosylase activity ; base-excision repair
	CVC1 UL93		Virion, Host nucleus	viral capsid ; DNA packaging ; viral release from host cell

Figure 39 Pull-down heat map and *in silico* analysis of all bound viral candidates from EBV, CMV and HSV1 and BKV, MCV, HPV41.
(A), (B) Heatmap of mass spectrometric identified viral proteins. Gene symbols on the y-axis and used pre-miRNAs on the x-axis. Annotated protein hits were defined by score (obtained with Mascot and proteinscape). (C) Classification of viral candidates by subcellular localization, RBDs and Gene Ontology

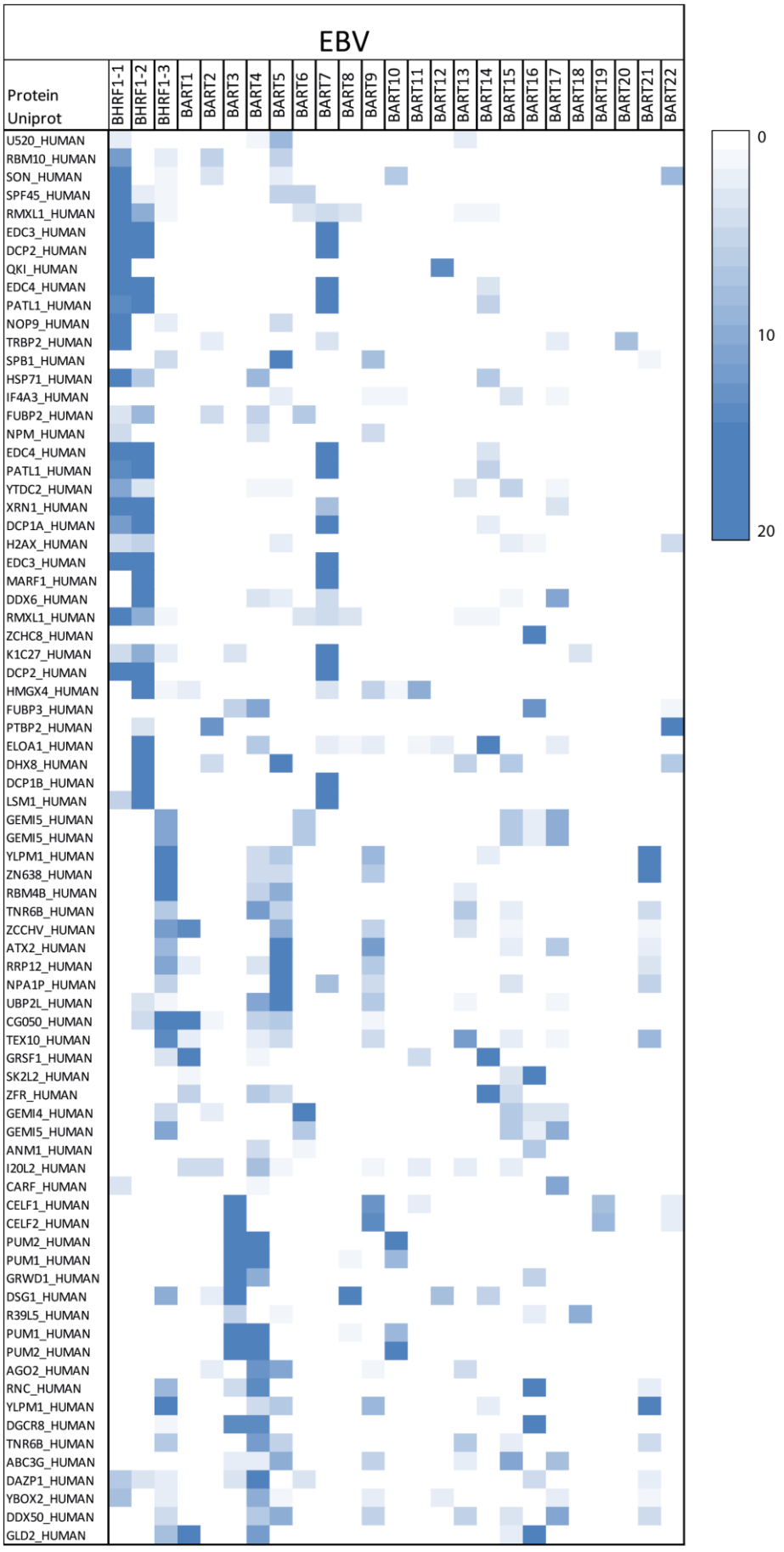

Figure 40 Pull-down heat map of all bound viral candidates from EBV.
Heatmap of mass spectrometric identified proteins. Gene symbols on the y-axis and used pre-miRNAs on the x-axis. Annotated protein hits were defined by score (obtained with Mascot and proteinscape) and normalized to the summarized counts of one protein. Pull-downs were performed in replicates and averaged afterwards. Specific binding is indicated in blue shades (from white = 0 to blue = 20).
Continued on next page

Continued on next page

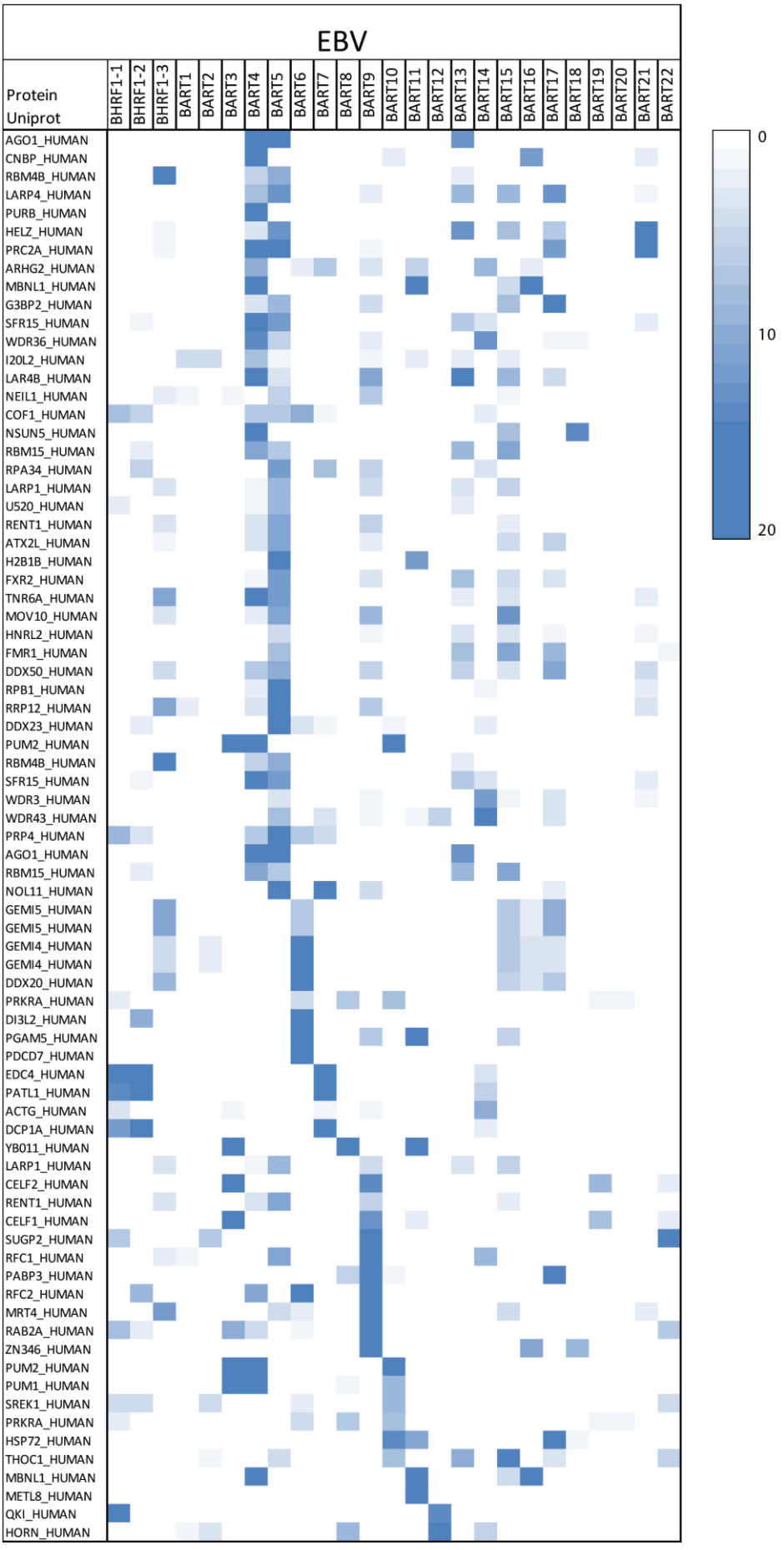
EBV
Protein
Uniprot
BHRF1-1
BHRF1-2
BHRF1-3
BART1
BART2
BART3
BART4
BART5
BART6
BART7
BART8
BART9
BART10
BART11
BART12
BART13
BART14
BART15
BART16
BART17
BART18
BART19
BART20
BART21
BART22
AGO1_HUMAN
CNBP_HUMAN
RBM4B_HUMAN
LARP4_HUMAN
PURB_HUMAN
HELZ_HUMAN
PRC2A_HUMAN
ARHG2_HUMAN
MBNL1_HUMAN
G3BP2_HUMAN
SFR15_HUMAN
WDR36_HUMAN
I20L2_HUMAN
LAR4B_HUMAN
NEIL1_HUMAN
COF1_HUMAN
NSUN5_HUMAN
RBM15_HUMAN
RPA34_HUMAN
LARP1_HUMAN
U520_HUMAN
RENT1_HUMAN
ATX2L_HUMAN
H2B1B_HUMAN
FXR2_HUMAN
TNR6A_HUMAN
MOV10_HUMAN
HNRL2_HUMAN
FMR1_HUMAN
DDX50_HUMAN
RPB1_HUMAN
RRP12_HUMAN
DDX23_HUMAN
PUM2_HUMAN
RBM4B_HUMAN
SFR15_HUMAN
WDR3_HUMAN
WDR43_HUMAN
PRP4_HUMAN
AGO1_HUMAN
RBM15_HUMAN
NOL11_HUMAN
GEMI5_HUMAN
GEMI5_HUMAN
GEMI4_HUMAN
GEMI4_HUMAN
DDX20_HUMAN
PRKRA_HUMAN
DI3L2_HUMAN
PGAM5_HUMAN
PDCD7_HUMAN
EDC4_HUMAN
PATL1_HUMAN
ACTG_HUMAN
DCP1A_HUMAN
YB011_HUMAN
LARP1_HUMAN
CELF2_HUMAN
RENT1_HUMAN
CELF1_HUMAN
SUGP2_HUMAN
RFC1_HUMAN
PABP3_HUMAN
RFC2_HUMAN
MRT4_HUMAN
RAB2A_HUMAN
ZN346_HUMAN
PUM2_HUMAN
PUM1_HUMAN
SREK1_HUMAN
PRKRA_HUMAN
HSP72_HUMAN
THOC1_HUMAN
MBNL1_HUMAN
METL8_HUMAN
QKI_HUMAN
HORN_HUMAN
0
10
20

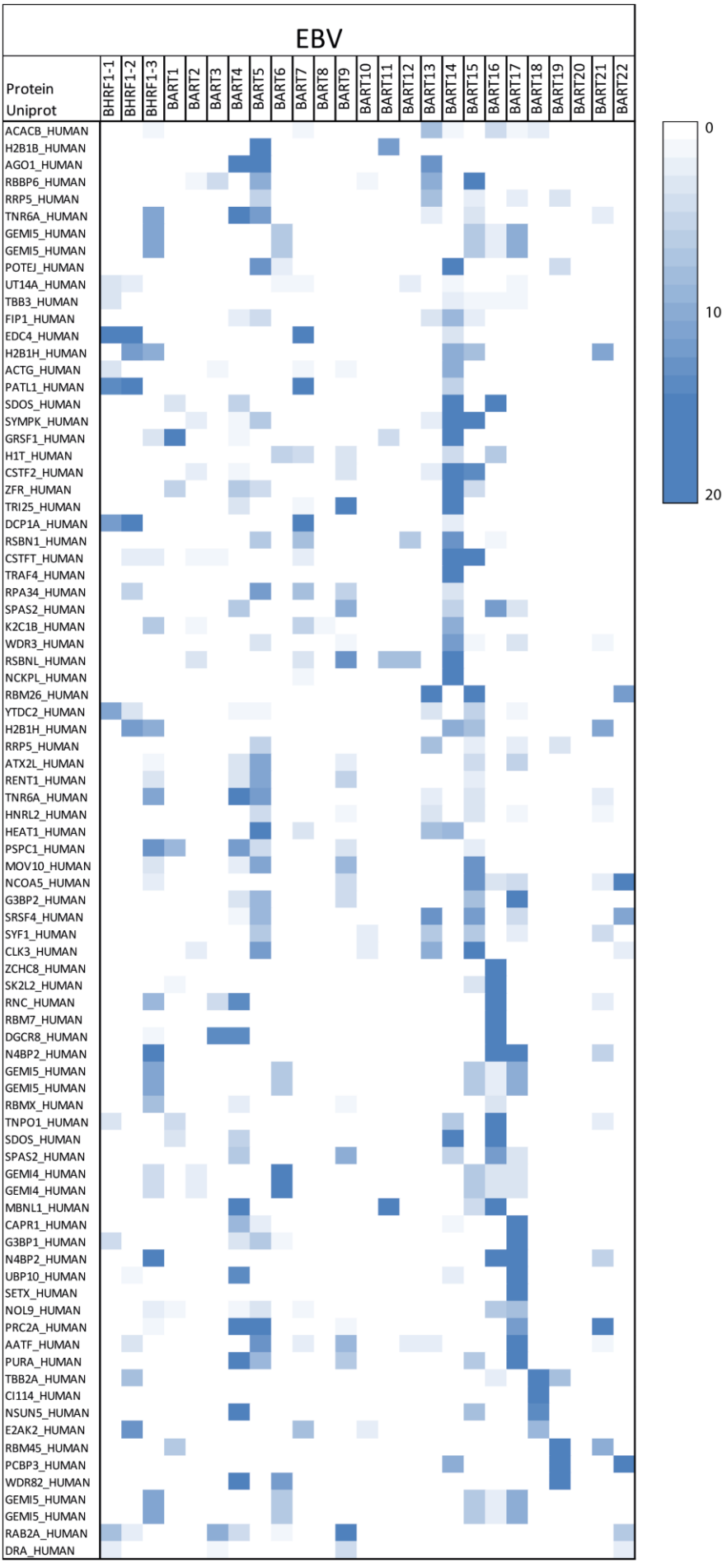
EBV
Protein
Uniprot
BHRF1-1
BHRF1-2
BHRF1-3
BART1
BART2
BART3
BART4
BART5
BART6
BART7
BART8
BART9
BART10
BART11
BART12
BART13
BART14
BART15
BART16
BART17
BART18
BART19
BART20
BART21
BART22
ACACB_HUMAN
H2B1B_HUMAN
AGO1_HUMAN
RBBP6_HUMAN
RRP5_HUMAN
TNR6A_HUMAN
GEMI5_HUMAN
GEMI5_HUMAN
POTEJ_HUMAN
UT14A_HUMAN
TBB3_HUMAN
FIP1_HUMAN
EDC4_HUMAN
H2B1H_HUMAN
ACTG_HUMAN
PATL1_HUMAN
SDOS_HUMAN
SYMPK_HUMAN
GRSF1_HUMAN
H1T_HUMAN
CSTF2_HUMAN
ZFR_HUMAN
TRI25_HUMAN
DCP1A_HUMAN
RSBN1_HUMAN
CSTFT_HUMAN
TRAF4_HUMAN
RPA34_HUMAN
SPAS2_HUMAN
K2C1B_HUMAN
WDR3_HUMAN
RSBNL_HUMAN
NCKPL_HUMAN
RBM26_HUMAN
YTDC2_HUMAN
H2B1H_HUMAN
RRP5_HUMAN
ATX2L_HUMAN
RENT1_HUMAN
TNR6A_HUMAN
HNRL2_HUMAN
HEAT1_HUMAN
PSPC1_HUMAN
MOV10_HUMAN
NCOA5_HUMAN
G3BP2_HUMAN
SRSF4_HUMAN
SYF1_HUMAN
CLK3_HUMAN
ZCHC8_HUMAN
SK2L2_HUMAN
RNC_HUMAN
RBM7_HUMAN
DGCR8_HUMAN
N4BP2_HUMAN
GEMI5_HUMAN
GEMI5_HUMAN
RBMX_HUMAN
TNPO1_HUMAN
SDOS_HUMAN
SPAS2_HUMAN
GEMI4_HUMAN
GEMI4_HUMAN
MBNL1_HUMAN
CAPR1_HUMAN
G3BP1_HUMAN
N4BP2_HUMAN
UBP10_HUMAN
SETX_HUMAN
NOL9_HUMAN
PRC2A_HUMAN
AATF_HUMAN
PURA_HUMAN
TBB2A_HUMAN
CI114_HUMAN
NSUN5_HUMAN
E2AK2_HUMAN
RBM45_HUMAN
PCBP3_HUMAN
WDR82_HUMAN
GEMI5_HUMAN
GEMI5_HUMAN
RAB2A_HUMAN
DRA_HUMAN
0
10
20

Figure 41 Pull-down heat map of all bound viral candidates from HSV1. Heatmap of mass spectrometric identified proteins. Gene symbols on the y-axis and used pre-miRNAs on the x-axis. Annotated protein hits were defined by score (obtained with Mascot and proteinscape) and normalized to the summarized counts of one protein. Pull-downs were performed in replicates and averaged afterwards. Specific binding is indicated in blue shades (from white = 0 to blue = 22,5).

Continued on next page

Continued on next page

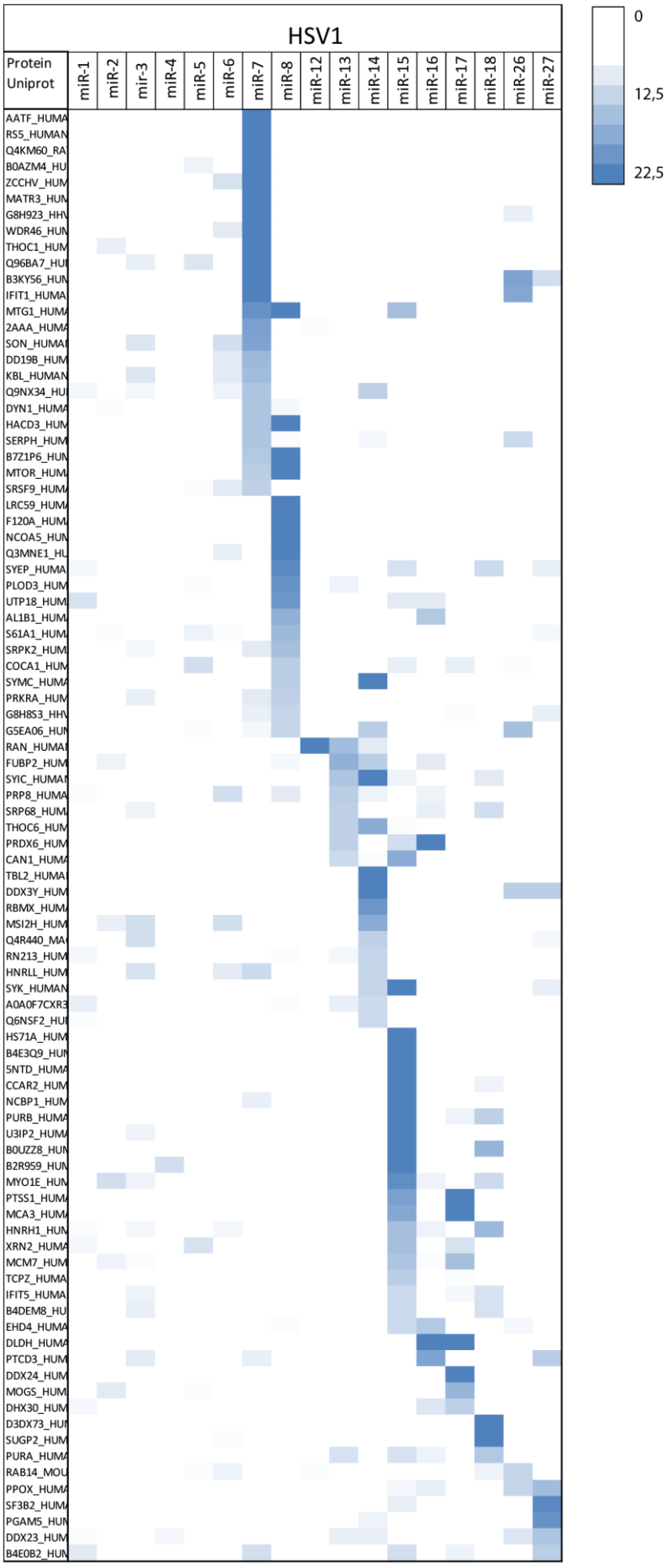
HSV1
Protein Uniprot
miR-1
miR-2
mir-3
miR-4
miR-5
miR-6
miR-7
miR-8
miR-12
miR-13
miR-14
miR-15
miR-16
miR-17
miR-18
miR-26
miR-27
0
12,5
22,5

A

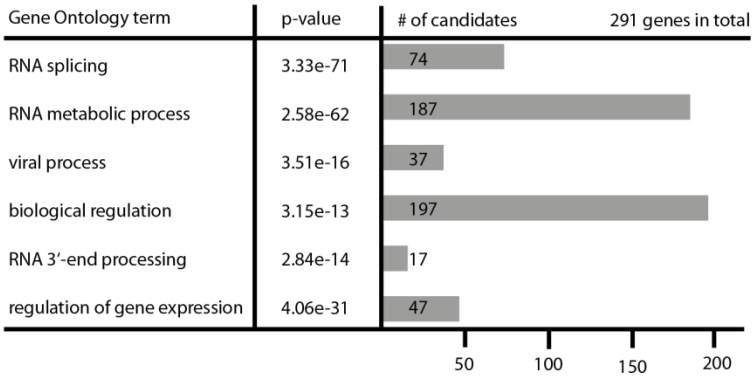

B

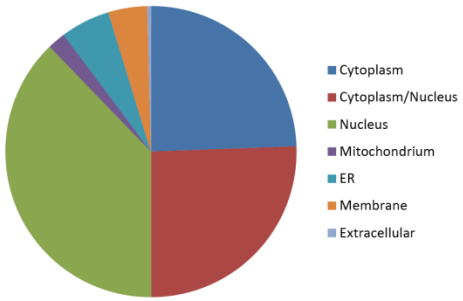

C

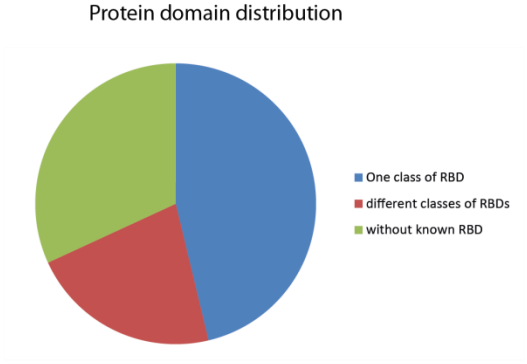

D

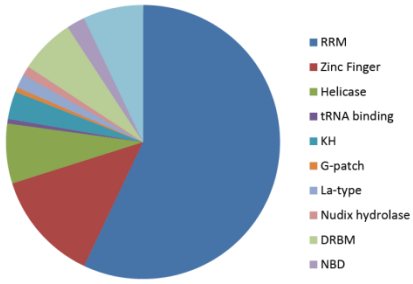

Figure 42 Combined *in silico* analysis of all bound candidates of the herpesviral, papilloma and polyoma virus pull-downs.

(A) GO term analysis classifications with high p-values and cluster frequency. (B) Subcellular localization of identified proteins (classified with uniprot database). (C) RNA binding domains distributed within the identified proteins. (D) Distribution of RNA binding domains within the identified proteins.

PLOD3

```
hsv1-miR-H6        ---------------------------CGGGGGGCCGGAG-----GGUGGAAGGCAG--GG        27
hsv1-miR-H3        -------CCGCGGGCGCGCUCCUGACCGCGGGUUCCGAGUUGGGCGUGGAGGUUACCUGG        53
hcmv-miR-UL70      GGUUGCGUCUCGGCCU-CGUCCAGACU--------------------GGCGAUGAGCGCC        39
                                                                  **     *

hsv1-miR-H6        GGGUGU-AGGAUGGGUAUCAGGACUUCCACUUCCCGUCCUUCCAUCCCCCGUUCCCCUCG        86
hsv1-miR-H3        GACUGUGCGGUUGGG-------ACGG----CGCCCGUGG---------------------        81
hcmv-miR-UL70      GAGAGG-GGGAUGGG-------CUGG----CGCGCGGCC---------------------        66
                   *   *   ** ****                 * **
```

B

```
hsv1-miR-H3
          gc   ug      -      g  u   g g
ccgcgggcgc  ucc  accgcg gguucc ag ugg c u
||||||||||  |||  |||||| |||||| || ||| | g
ggugcccgcg  agg  uggcgu ucaggg uc auu g g
          gc   gu      g      -  c   g a

hsv1-miR-H6
       -c   a          ca        u   --a  g
cgggggg  cgg ggguggaagg  ggggggug agg   ug g
|||||||  ||| ||||||||||  ||||||| |||   || u
gcucccc  gcc ccuaccuucc  cccuucac uuc   ac a
       uu   c          ug        c   agg  u
```

```
hcmv-miR-UL70
          c      u     -aga  -    a
gguugcgu ucggcc cgucc     cu ggcg u
||||||| |||||| |||||     || |||| g
ccggcgcg ggucgg guagg     ga ccgc a
          c      -     ggga  g    g
```

PTBP1

```
hsv1-miR-H8        -----------------GUCCCUGUAU-----AUAUAGGGUCAGGGGGUUCCGCACCCCCU        39
hcmv-miR-UL59      ---------------------CGACGGUUCUCUCGCUCGUCAUGCCGUUCUGAGC--UCC        37
hpv41-miR-H1       GGUAUUGUGGUGCGGUGUCCUCGACGGUCCAUG----UGUCAUCU---UAUAAUC-----        48
                                        *               ****      *     *
hsv1-miR-H8        AACAUG-GCGCCCCCGGUCCCUGUAUAUAU---AGUUGUC        75
hcmv-miR-UL59      GACAUG-GCGGACGAGA-----GAAAAUGGCGUCG-----        66
hpv41-miR-H1       -ACUUGGUCAGUCCAGG-----GUACACCACUCCAUUAUC        82
```

```
>hcmv-miR-UL59
    ----g        cu       c  uucu
cgacg     uucucucg  cgucaug cg    g
|||||     ||||||||  ||||||| ||
gcugc     aagagagc  gcgguac gc    a
     gguaa        ag       a  cucg
```

```
>hsv1-miR-H8
-gucc              u a      u   caccc
     cuguauauauaggg c gggggu ccg     c
     ||||||||||||||| | ||||||| |||
     gauauauauguccc g cccccg ggu     c
cuguu              u g      c   acaau
```

Figure 43 Multiple sequence alignments from pri-miRNAs interacting with one particular candidate.
MSA of pri-miRNA sequence of different specific RBP interacting pri-miRNAs performed with Clustal Omega from EMBL-ebi-tools. Location of consensus sequence within the pri-miRNA hairpins marked with yellow, mature miRNAs are shown in yellow. Complementary base pairing is illustrated with lines between the corresponding bases. Hairpin structures were taken from the miRBase.

PURA

```
hcmv-miR-UL148D      AGCAGGUGAGGU-------UGGGGCGGACAACGUGUUGCGGAUUGU----GGCGAGAACG     49
hsv1-miR-H3          ----------CCGCGGGCGCGCUCCUGACCGCGGGUUCCGAGUUGGGCGUGGAGGUUACC     50
hcmv-miR-UL70        ---GGUUGCGUCUCGGCCU-CGUCCAGACU--------------------GGCGAUGAGC     36
                                         * ***                      ** *   *


hcmv-miR-UL148D      UCGUCCUCCCCUUCUUC-A--CCGCC-----      72
hsv1-miR-H3          UGGGACUGUGCGGUUGGGACGGCGCCCGUGG      81
hcmv-miR-UL70        GCCGAGAGG-GGGAUGGGCUGGCGCGCGGCC      66
                              *       ***
```

B

```
  hsv1-miR-H3
          gc   ug      -      g  u   g g
ccgcgggcgc  ucc  accgcg gguucc ag ugg c u
||||||||||  |||  |||||| |||||| || ||| | g
ggugcccgcg  agg  uggcgu ucaggg uc auu g g
          gc   gu      g      -  c   g a

hcmv-miR-UL148D
a  a       uu    c    a    -g    gga
 gc ggugagg  gggg ggac acgu  uugc   u
 || |||||||  |||| |||| ||||  ||||
 cg ccacuuc  cccc ccug ugca  agcg   u
c  -       uu    u    c    ag    gug
```

```
hcmv-miR-UL70

       c      u     -aga  -    a
gguugcgu ucggcc cgucc    cu ggcg u
|||||||| |||||| |||||    || |||| g
ccggcgcg ggucgg guagg    ga ccgc a
         c      -     ggga  g    g
```

NOL11

```
bkv-miR-B1           GGGAAUCUUCAGCAGGGGCUGAAGUAUCUGAGACUUGGGAAGAGCAUUGUGAUUGGGAUU      60
hcmv-miR-UL112       -GAC--------------------------AGCCUCCGGA-UCACAUGGUUA------CU      26
                      *                           ** **  ***    *** ** *       *

bkv-miR-B1           CAGUGCUUG---------AUCC------AUGUCCAGAGUCUUCAGUUUCUGAAUCCU 102
hcmv-miR-UL112       CAGCGUCUGCCAGCCUAAGUGACGGUGAGAUCCAGGCUGUC--------------- 67
                     *** *  **         *          *  *****  * *
```

```
bkv-miR-B1
    aucuucag   gg       ua    a   u    aa        u   u
ggga        cag  gcugaag  ucug gac uggg  gagcauug gau g
||||        |||  |||||||  |||| ||| ||||  |||||||| |||
uccu        guc  ugacuuc  agac cug accu  uucgugac uua g
    ------aa   uu       ug    -   u    ag        -   g
```

```
hcmv-miR-UL112
        cc     a   g      c  c  cu
gacagccu  ggauc cau guuacu ag gu  g
||||||||  ||||| ||| |||||| || ||
cugucgga  ccuag gug caguga uc cg  c
        --     a   g      a  -  ac
```

Figure 44 Multiple sequence alignments from pri-miRNAs interacting with one particular candidate.
MSA of pri-miRNA sequence of different specific RBP interacting pri-miRNAs performed with Clustal Omega from EMBL-ebi-tools. Location of consensus sequence within the pri-miRNA hairpins marked with yellow, mature miRNAs are shown in yellow. Complementary base pairing is illustrated with lines between the corresponding bases. Hairpin structures were taken from the miRBase.

5.1.3 MS results

Table 17 human TNRC6 proteins

Isoform	Residue [phospho-site]	p-value RP1	p-value RP2	p-value RP3 [H1]
TNRC6A_Iso1	S[245]			1.80E-05
	T[287]	2.40E-02	3.20E-02	8.10E-03
	T[323]		1.30E-02	
	S[389]		4.00E-03	
	T[397]		9.20E-03	
	S[463]			6.60E-02
	S[497], T[502]			9.50E-03
	T[502], S[503], S[505]	7.50E-03		
	T[603], T[608]		4.30E-02	
	T[644]	1.10E-03		
	S[678]	7.20E-05		
	T[679]	6.00E-05		
	T[736]	2.00E-04		
	T[738]	2.70E-04	3.60E-04	
	S[739]	3.40E-07	2.30E-05	7.20E-08
	S[771]			1.60E-04
	S[781]			1.10E-03
	S[798]		6.00E-09	
	S[942]			5.90E-04
	S[943]	2.80E-03		1.20E-06
	S[991]	5.30E-05	5.80E-10	1.40E-08
	S[938]			3.40E-04
	S[1214]			1.40E-02
	S[1217]	1.10E-04		8.60E-05
	S[1333]	5.00E-03		
	S[1405]	1.30E-02		1.70E-02
	S[1448]		2.10E-02	
	S[1503]			4.10E-04
	S[1582], S[1585]			8.70E-03
	S[1585]	1.30E-11	1.20E-06	6.50E-14
	S[1599]	4.00E-06	3.40E-02	4.70E-05
	S[1605]			2.10E-02
	Y[1631]	3.50E-05		
	S[1636]	4.40E-02		
	S[1686]	4.50E-02		
	T[1702]	1.20E-04		
	S[1704]	3.30E-06		8.40E-07
	T[1845]	9.70E-06		
	S[1884]	2.50E-03	1.40E-06	

Isoform	Residue [phospho-site]	p-value RP1	p-value RP2	p-value RP3 [H1]
TNRC6B_Iso1	T[51]			2.00E-02
	S[54]	1.10E-03		8.70E-03
	S[58]			1.10E-02
	S[59]			1.00E-04
	S[61]	2.90E-03		1.20E-07
	T[168]		9.80E-09	
	S[195]		1.30E-03	
	S[212]			1.00E-04
	S[243]		6.60E-07	4.10E-02
	S[247]		2.70E-04	
	S[250]			1.60E-02
	S[273]		1.80E-03	
	S[309]		1.20E-03	
	S[332]			6.30E-06
	S[333]	7.30E-03		
	S[332], S[333]	1.40E-03		
	S[343], S[348]			5.10E-03
	S[384]	1.70E-03	2.90E-02	6.40E-04
	S[385]	5.00E-05	9.30E-07	7.10E-11
	T[419]	3.00E-04		
	S[421]	3.70E-06		
	T[480]			2.40E-08
	S[483]			9.20E-06
	S[534]	1.80E-02		
	T[535]	3.40E-02		
	T[596]	1.00E-05	7.00E-04	1.60E-04
	T[606]	5.80E-04		
	S[609]	2.60E-03		
	T[687]	3.00E-02		
	T[782]		7.90E-03	
	S[803]			3.20E-03
	S[879]	4.40E-09	2.50E-07	2.50E-10
	Y[904]			2.20E-04
	S[990], S[992]	1.30E-03		
	S[1011]			3.00E-03
	S[1057]			2.50E-05
	S[1067]			2.40E-05
	S[1080], S[1081]	1.40E-03		
	S[1197]	7.30E-03		
	T[1213], S[1220], S[1221]			2.20E-03
	S[1220], S[1221], S[1223]			2.60E-02
	S[1221]	3.00E-03		
	S[1223]	3.00E-03		5.00E-02
	S[1336]			1.10E-05
	S[1338]			1.10E-04

	S[1401]			2.20E-02
Isoform	**Residue [phospho-site]**	**p-value RP1**	**p-value RP2**	**p-value RP3 [H1]**
TNRC6B_Iso1	T[1411]			5.00E-03
	S[1432]	1.70E-08		7.20E-10
	S[1432], S[1461]			3.40E-02
	S[1461]	1.80E-03		3.30E-05
	S[1512]	8.20E-06		6.00E-11
	T[1517]	2.80E-05		3.40E-09
	S[1539]			3.30E-03
	S[1570]	2.50E-03		5.60E-04
	T[1596]			3.60E-02
	S[1647]			2.00E-02
	T[1701]	1.10E-03		5.70E-02
	T[1701], T[1711]			8.30E-03
	T[1712]	6.50E-07		
	S[1816]	7.60E-04		1.50E-06
	S[1830]			4.60E-02
	S[1832]	6.80E-06		1.90E-05
TNRC6C_Iso1	S[59]		2.90E-03	
	S[465]	9.70E-05	9.80E-04	6.90E-07
	S[568]	2.00E-11	8.20E-04	2.90E-04
	T[570]	1.60E-03		
	S[669]			4.30E-02
	S[705]			9.00E-03
	S[714]	3.90E-06	2.00E-07	1.60E-07
	S[717]			6.80E-03
	T[777]	1.90E-03	1.70E-06	7.90E-05
	S[865]		1.10E-03	
	S[1010]	3.30E-02		
	S[1011]	6.50E-06	2.60E-02	3.50E-03
	T[1016]	4.20E-05		
	S[1305]	6.90E-02		
	S[1358]	3.10E-03		
	T[1578]	1.80E-04		
	S[1628]		1.10E-03	
	T[1674]	2.90E-06		6.70E-04
	T[1678]			1.20E-02

5.1.4 MSA, *in silico* and MS phospho-analysis of TNRC6

Table 18 Immunoprecipitated interactors of TNRC6 (kinases and phosphatases are marked in red)

Accession	Protein	MW [kDa]	Scores
AGO2_HUMAN	Protein argonaute-2 OS=Homo sapiens	97.1	3216.5
AGO1_HUMAN	Protein argonaute-1 OS=Homo sapiens	97.2	2489.8
LMNB1_HUMAN	Lamin-B1 OS=Homo sapiens	66.4	2408.8
SHIP2_HUMAN	Phosphatidylinositol 3,4,5-trisphosphate 5-phosphatase 2 OS=Homo sapiens	138.5	2159.8
HNRPM_HUMAN	Heterogeneous nuclear ribonucleoprotein M OS=Homo sapiens	77.5	2066.2
TOP2B_HUMAN	DNA topoisomerase 2-beta OS=Homo sapiens	183.2	1670.6
AGO3_HUMAN	Protein argonaute-3 OS=Homo sapiens	97.3	1647.2
SMC1A_HUMAN	Structural maintenance of chromosomes protein 1A OS=Homo sapiens	143.1	1557.5
LMNA_HUMAN	Prelamin-A/C OS=Homo sapiens	74.1	1543.2
ENPL_HUMAN	Endoplasmin OS=Homo sapiens	92.4	1483
HSP71_HUMAN	Heat shock 70 kDa protein 1A/1B OS=Homo sapiens	70.0	1238.5
NOP56_HUMAN	Nucleolar protein 56 OS=Homo sapiens	66.0	1203
TR150_HUMAN	Thyroid hormone receptor-associated protein 3 OS=Homo sapiens	108.6	1202.1
HS90B_HUMAN	Heat shock protein HSP 90-beta OS=Homo sapiens	83.2	1035.9
SMCA5_HUMAN	SWI/SNF-related matrix-associated actin-dependent regulator of chromatin subfamily A member 5 OS=Homo sapiens	121.8	1003.6
AGO4_HUMAN	Protein argonaute-4 OS=Homo sapiens	97.0	946.8
TNR6B_HUMAN	Trinucleotide repeat-containing gene 6B protein OS=Homo sapiens	193.9	910.7
SSRP1_HUMAN	FACT complex subunit SSRP1 OS=Homo sapiens	81.0	896.5
HSP72_HUMAN	Heat shock-related 70 kDa protein 2 OS=Homo sapiens	70.0	885.8
TOP2A_HUMAN	DNA topoisomerase 2-alpha OS=Homo sapiens	174.3	871.5
BAZ1B_HUMAN	Tyrosine-protein kinase BAZ1B OS=Homo sapiens	170.8	810.5
DHX9_HUMAN	ATP-dependent RNA helicase A OS=Homo sapiens	140.9	805.8
DDX27_HUMAN	Probable ATP-dependent RNA helicase DDX27 OS=Homo sapiens	89.8	788.4
KLH22_HUMAN	Kelch-like protein 22 OS=Homo sapiens	71.6	777.8
WDR36_HUMAN	WD repeat-containing protein 36 OS=Homo sapiens	105.3	735.5
RFA1_HUMAN	Replication protein A 70 kDa DNA-binding subunit OS=Homo sapiens	68.1	704.8
DDX5_HUMAN	Probable ATP-dependent RNA helicase DDX5 OS=Homo sapiens	69.1	685.7
PESC_HUMAN	Pescadillo homolog OS=Homo sapiens	68.0	667
DDX21_HUMAN	Nucleolar RNA helicase 2 OS=Homo sapiens	87.3	643.8
ZY11B_HUMAN	Protein zyg-11 homolog B OS=Homo sapiens	83.9	621.4
HS90A_HUMAN	Heat shock protein HSP 90-alpha OS=Homo sapiens	84.6	607.7
DHX30_HUMAN	Putative ATP-dependent RNA helicase DHX30 OS=Homo sapiens	133.9	561.3

Accession	Protein	MW [kDa]	Scores
SP16H_HUMAN	FACT complex subunit SPT16 OS=Homo sapiens	119.8	545.3
LMNB2_HUMAN	Lamin-B2 OS=Homo sapiens	67.6	543.5
DHX15_HUMAN	Putative pre-mRNA-splicing factor ATP-dependent RNA helicase DHX15 OS=Homo sapiens	90.9	529.2
DDX18_HUMAN	ATP-dependent RNA helicase DDX18 OS=Homo sapiens	75.4	523.4
SAFB1_HUMAN	Scaffold attachment factor B1 OS=Homo sapiens	102.6	502.2
CUL5_HUMAN	Cullin-5 OS=Homo sapiens	90.9	499.6
ODP2_HUMAN	Dihydrolipoyllysine-residue acetyltransferase component of pyruvate dehydrogenase complex, mitochondrial OS=Homo sapiens	69.0	487.1
UTP18_HUMAN	U3 small nucleolar RNA-associated protein 18 homolog OS=Homo sapiens	62.0	485.5
GELS_HUMAN	Gelsolin OS=Homo sapiens	85.6	461.4
K1C14_HUMAN	Keratin, type I cytoskeletal 14 OS=Homo sapiens	51.5	447.9
GRP75_HUMAN	Stress-70 protein, mitochondrial OS=Homo sapiens	73.6	427.8
GTF2I_HUMAN	General transcription factor II-I OS=Homo sapiens	112.3	425.9
NOL11_HUMAN	Nucleolar protein 11 OS=Homo sapiens	81.1	407.6
PININ_HUMAN	Pinin OS=Homo sapiens	81.6	396.1
GRP78_HUMAN	78 kDa glucose-regulated protein OS=Homo sapiens	72.3	393.3
BCLF1_HUMAN	Bcl-2-associated transcription factor 1 OS=Homo sapiens	106.1	390.2
IMMT_HUMAN	Mitochondrial inner membrane protein OS=Homo sapiens	83.6	388.5
H90B2_HUMAN	Putative heat shock protein HSP 90-beta 2 OS=Homo sapiens	44.3	382.2
PELP1_HUMAN	Proline-, glutamic acid- and leucine-rich protein 1 OS=Homo sapiens	119.6	369
NOL10_HUMAN	Nucleolar protein 10 OS=Homo sapiens	80.3	366.3
NCOA5_HUMAN	Nuclear receptor coactivator 5 OS=Homo sapiens	65.5	365.7
CRNL1_HUMAN	Crooked neck-like protein 1 OS=Homo sapiens	100.4	364.1
RBM14_HUMAN	RNA-binding protein 14 OS=Homo sapiens	69.4	360
TBL3_HUMAN	Transducin beta-like protein 3 OS=Homo sapiens	89.0	355.9
DDX41_HUMAN	Probable ATP-dependent RNA helicase DDX41 OS=Homo sapiens	69.8	352.4
WDR43_HUMAN	WD repeat-containing protein 43 OS=Homo sapiens	74.8	344.4
TDIF2_HUMAN	Deoxynucleotidyltransferase terminal-interacting protein 2 OS=Homo sapiens	84.4	344.3
ATD3B_HUMAN	ATPase family AAA domain-containing protein 3B OS=Homo sapiens	72.5	332.1
SYRC_HUMAN	Arginine--tRNA ligase, cytoplasmic OS=Homo sapiens	75.3	324.6
RAD21_HUMAN	Double-strand-break repair protein rad21 homolog OS=Homo sapiens	71.6	324.1
DDX17_HUMAN	Probable ATP-dependent RNA helicase DDX17 OS=Homo sapiens	80.2	320.8
IMB1_HUMAN	Importin subunit beta-1 OS=Homo sapiens	97.1	314.1
NOC3L_HUMAN	Nucleolar complex protein 3 homolog OS=Homo sapiens	92.5	311.5
AIFM1_HUMAN	Apoptosis-inducing factor 1, mitochondrial OS=Homo sapiens	66.9	298.3
MBB1A_HUMAN	Myb-binding protein 1A OS=Homo sapiens	148.8	296.1
XRCC6_HUMAN	X-ray repair cross-complementing protein 6 OS=Homo sapiens	69.8	295.5
SAFB2_HUMAN	Scaffold attachment factor B2 OS=Homo sapiens	107.4	293.3
IRS4_HUMAN	Insulin receptor substrate 4 OS=Homo sapiens	133.7	292.2
TIF1A_HUMAN	Transcription intermediary factor 1-alpha OS=Homo sapiens	116.8	280.6
SAS10_HUMAN	Something about silencing protein 10 OS=Homo sapiens	54.5	276
LAS1L_HUMAN	Ribosomal biogenesis protein LAS1L OS=Homo sapiens	83.0	272.4
A2MG_HUMAN	Alpha-2-macroglobulin OS=Homo sapiens	163.2	264.6
NEK9_HUMAN	Serine/threonine-protein kinase Nek9 OS=Homo sapiens	107.1	263.7
TITIN_HUMAN	Titin OS=Homo sapiens	3813.7	256.5

HS71L_HUMAN	Heat shock 70 kDa protein 1-like OS=Homo sapiens	70.3	254.9
Accession	**Protein**	**MW [kDa]**	**Scores**
KHDR1_HUMAN	KH domain-containing, RNA-binding, signal transduction-associated protein 1 OS=Homo sapiens	48.2	249.4
HSP7C_HUMAN	Heat shock cognate 71 kDa protein OS=Homo sapiens	70.9	246
PABP1_HUMAN	Polyadenylate-binding protein 1 OS=Homo sapiens	70.6	245.4
DDX3X_HUMAN	ATP-dependent RNA helicase DDX3X OS=Homo sapiens	73.2	244.5
ZN326_HUMAN	DBIRD complex subunit ZNF326 OS=Homo sapiens	65.6	244.4
VSIG8_HUMAN	V-set and immunoglobulin domain-containing protein 8 OS=Homo sapiens	43.9	240.3
CO3_HUMAN	Complement C3 OS=Homo sapiens	187.0	239.3
MTA2_HUMAN	Metastasis-associated protein MTA2 OS=Homo sapiens	75.0	231.9
SYIC_HUMAN	Isoleucine--tRNA ligase, cytoplasmic OS=Homo sapiens	144.4	206.9
ALBU_HUMAN	Serum albumin OS=Homo sapiens	69.3	202
NU160_HUMAN	Nuclear pore complex protein Nup160 OS=Homo sapiens	162.0	190.6
ADNP_HUMAN	Activity-dependent neuroprotector homeobox protein OS=Homo sapiens	123.5	181
RB12B_HUMAN	RNA-binding protein 12B OS=Homo sapiens	118.0	167.8

Figure 45 Multiple sequence alignments from murine and human TNRC6 proteins
(A) Conservation of TNRC6 paralogs human vs. mouse. (B) MSA of murine and human TNRC6 proteins. Known domains are colored. Phospho-sites are indicated in red letters.

A

1:	TNR6B_HUMAN	100.00	96.44	40.63	40.40	40.40	40.29
2:	TNR6B_MOUSE	96.44	100.00	40.44	39.62	40.20	40.28
3:	TNR6C_HUMAN	40.63	40.44	100.00	91.38	46.77	46.23
4:	TNR6C_MOUSE	40.40	39.62	91.38	100.00	46.41	45.85
5:	TNR6A_HUMAN	40.40	40.20	46.77	46.41	100.00	94.73
6:	TNR6A_MOUSE	40.29	40.28	46.23	45.85	94.73	100.00

B

Paralog	Domain	Position [aa]	Length	Function
TNRC6A	ABD	1 – 932	932	Interaction with Argonaute family proteins
	RRM	1781 – 1853	73	Function unknown
	PAM2	1604 – 1622	19	PABPC1-interacting motif-2
	Gln – rich	93 – 127	35	
	Gln – rich	1330 – 1476	116	Function unknown, p-body localization?
	Ser – rich	192 – 365	174	Function unknown
	SD	1476 – 1962	486	Interaction with CNOT1 and PAN3
TNRC6B	ABD	1 – 994	994	Interaction with Argonaute family proteins
	RRM	1648 – 1720	73	Function unknown
	PAM2	1472 – 1490	19	PABPC1-interacting motif-2
	Gln – rich	1196 – 1373	77	Function unknown, p-body localization?
	Pro – rich	825 – 880	56	Function unknown
	SD	1218 – 1723	506	Interaction with CNOT1 and PAN3
TNRC6C	ABD	1 – 926	926	Interaction with Argonaute family proteins
	RRM	1565 – 1632	68	Function unknown
	PAM2	1381 – 1399	19	PABPC1-interacting motif-2
	Pro – rich	1215 – 1248	34	Function unknown, p-body localization?
	SD	1260 – 1690	431	Interaction with CNOT1 and PAN3
	n.n.	1596 – 1690	95	Interaction with the CCR4-NOT
	n.n.	1371 – 1690	320	Sufficient for translational repression when tethered to target
	UBA	933 – 978	46	Ubi interaction site
	Gly – rich	204 – 430	227	Function unknown
	Thr – rich	756 – 777	22	Function unknown

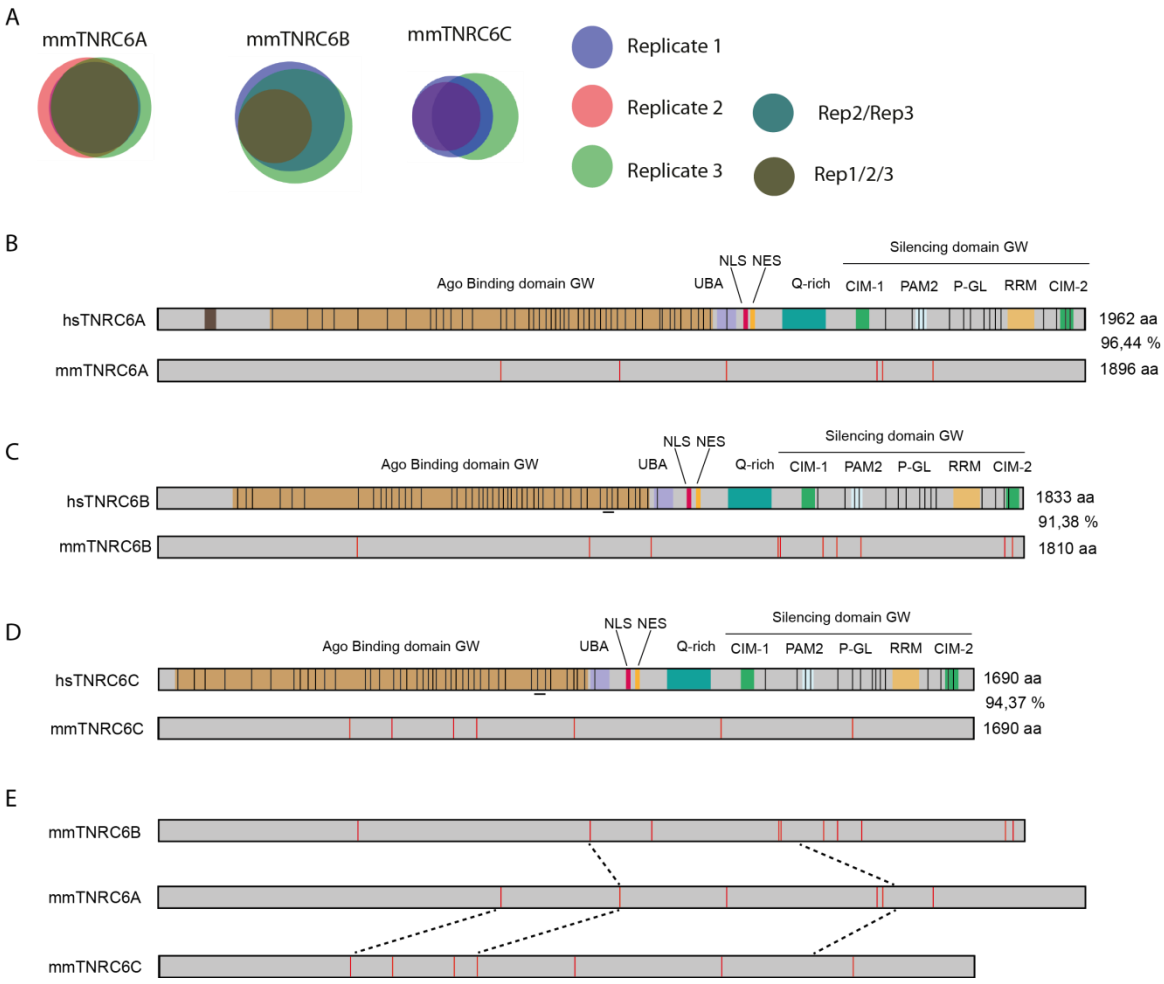

Figure 46 Mass spectrometric detection of potential phosphorylation sites in endogenous TNRC6A-C proteins.
(A) Venn diagrams depict overlapping phosphorylation sites of biological human replicates. Diagrams were conducted with the browser based software Biovenn. (B), (C), (D) Overview of potential phosphorylation sites according to their individual localization within the TNRC6 paralog. Grey bars represent TNRC6 proteins, red bars represent potential phosphorylation sites and black lines between the phosphor-sites indicate conservation. Hs: Homo sapiens, Mm: mus musculus. (E) Schematic representation of the location of phospho-sites conserved between the different paralogs. Unique and conserved phosphorylation sites are indicated in red. Black lines indicate conserved phospho-sites among the three human TNRC6 and three murine paralogues

A

Phosphosite	aa seq	Probability	Kinase
1585 S	TSPASPPGS	0.990	unsp
1585 S	TSPASPPGS	0.590	p38MAPK
1585 S	TSPASPPGS	0.581	cdk5
1585 S	TSPASPPGS	0.521	GSK3
739 S	DTETSPRGE	0.974	unsp
739 S	DTETSPRGE	0.552	CKI
739 S	DTETSPRGE	0.507	cdk5
739 S	DTETSPRGE	0.503	p38MAPK
943 S	KPVSSPDWN	0.992	unsp
771 S	IDKTSPNGN	0.903	unsp
771 S	IDKTSPNGN	0.536	CKI
771 S	IDKTSPNGN	0.504	p38MAPK
1217 S	FSRDSPEEN	0.998	unsp
1599 S	PRAKSPNGS	0.977	unsp
1599 S	PRAKSPNGS	0.620	cdk5
1599 S	PRAKSPNGS	0.603	RSK
1599 S	PRAKSPNGS	0.522	GSK3
991 S	WEEPSPESI	0.988	unsp
991 S	WEEPSPESI	0.506	GSK3
1704 S	KLTWSPGSV	0.562	cdk5
1704 S	KLTWSPGSV	0.544	p38MAPK

B

Phosphosite	aa seq	Probability	Kinase
1512 S	GTATSPIVD	0.840	unsp
1512 S	GTATSPIVD	0.541	cdc2
385 S	LNLSSPNPM	0.488	GSK3
385 S	LNLSSPNPM	0.462	p38MAPK
385 S	LNLSSPNPM	0.446	CaM-II
879 S	WEEPSPQSI	0.518	cdk5
879 S	WEEPSPQSI	0.501	GSK3
879 S	WEEPSPQSI	0.442	p38MAPK
1432 S	TRGGSPYNQ	0.997	unsp
1432 S	TRGGSPYNQ	0.770	PKA
1432 S	TRGGSPYNQ	0.502	GSK3
1432 S	TRGGSPYNQ	0.487	RSK
1816 S	HRMGSPAPL	0.790	unsp
1816 S	HRMGSPAPL	0.675	PKA
1816 S	HRMGSPAPL	0.511	GSK3
1816 S	HRMGSPAPL	0.507	PKG
1816 S	HRMGSPAPL	0.505	RSK
1816 S	HRMGSPAPL	0.484	cdk5
1336 S	GMKHSPSHP	0.906	unsp
1336 S	GMKHSPSHP	0.572	cdk5
1336 S	GMKHSPSHP	0.507	GSK3
1336 S	GMKHSPSHP	0.494	cdc2
1832 S	GGSDSI---	0.491	CKII
1832 S	GGSDSI---	0.476	cdc2
1832 S	GGSDSI---	0.451	GSK3
1517 T	PIVDTDHQL	0.434	CaM-II
1517 T	PIVDTDHQL	0.420	GSK3
1517 T	PIVDTDHQL	0.407	CKII
1517 T	PIVDTDHQL	0.363	CKI
480 T	NNRSTGGSW	0.457	PKC
480 T	NNRSTGGSW	0.442	GSK3
480 T	NNRSTGGSW	0.436	CaM-II
1461 S	LPAKSPPTN	0.550	cdk5
1461 S	LPAKSPPTN	0.506	GSK3
1461 S	LPAKSPPTN	0.448	CaM-II
1461 S	LPAKSPPTN	0.395	cdc2

C

Phosphosite	aa seq	Probability	Kinase
465 S	EFEESPRSE	0.955	unsp
465 S	EFEESPRSE	0.550	p38MAPK
465 S	EFEESPRSE	0.483	GSK3
714 S	WEEPSPPSI	0.628	unsp
714 S	WEEPSPPSI	0.568	cdk5
714 S	WEEPSPPSI	0.513	GSK3
714 S	WEEPSPPSI	0.495	p38MAPK
714 S	WEEPSPPSI	0.426	CKI
777 T	HRVETPPPH	0.959	unsp
777 T	HRVETPPPH	0.628	cdk5
777 T	HRVETPPPH	0.515	p38MAPK
777 T	HRVETPPPH	0.494	GSK3
1674 T	IGSPTPLTT	0.546	cdk5
1674 T	IGSPTPLTT	0.474	GSK3
1674 T	IGSPTPLTT	0.462	p38MAPK
1011 S	SKESSVDRP	0.990	unsp
1011 S	SKESSVDRP	0.589	PKC
1011 S	SKESSVDRP	0.526	cdc2
1011 S	SKESSVDRP	0.450	CaM-II
1016 T	VDRPTFLDK	0.449	GSK3
1016 T	VDRPTFLDK	0.433	PKC
1016 T	VDRPTFLDK	0.421	CKI
568 S	QEDKSPTWG	0.995	unsp
568 S	QEDKSPTWG	0.493	cdk5
568 S	QEDKSPTWG	0.489	p38MAPK
568 S	QEDKSPTWG	0.478	GSK3
1010 S	ISKESSVDR	0.989	unsp
1010 S	ISKESSVDR	0.514	PKG
1010 S	ISKESSVDR	0.448	GSK3
1010 S	ISKESSVDR	0.431	cdc2

Table 19 Kinase prediction of TNRC6A-C phosphor-sites

(A), (B), (C) Prediction of TNRC6 phospho-site specific kinases with NETphos3.1. Abbreviations: unsp = unknown;, ATM, CKI, CKII, CaM-II, DNAPK, EGFR, GSK3, INSR, PKA, PKB, PKC, PKG, RSK, SRC, cdc2, cdk5 and p38MAPK.

Table 20 De-phosphorylation of phosphorylated sites of TNRC6 proteins

Protein	FASTAP/ 37°C		PBS/37°C		PBS/4°C	
	p-value	position	p-value	position	p-value	position
TNRC6A	0,000000039	S[991]	0,000000089	S[1585]	0,000000000054	S[1585]
	0,0000011	S[739]	0,00000008	S[991]	0,000000021	S[991]
	0,000048	S[614]	0,00018	S[1589]	0,0000024	S[1884]
	0,0021	S[798]	0,0007	S[1333]	0,0000063	S[943]
	0,0097	T[1633]	0,0015	S[1503]	0,000041	S[1704]
	0,018	S[1405]	0,0017	T[1845]	0,00014	S[739]
	0,02	T[287]	0,0022	S[991]	0,00021	S[943]
	0,024	S[1603]	0,004	S[739]	0,00045	T[738]
	0,0019	S[1884]	0,0061	S[943]	0,0017	S[1333]
			0,0056	S[1704]	0,0017	S[622]
			0,0073	S[1224]	0,0016	T[1845]
			0,012	S[938]	0,0023	S[388]
			0,018	T[287]	0,0023	T[287]
			0,041	S[1599]	0,0041	S[1599]
					0,0047	S[1217]
					0,0053	T[1633]
					0,012	T[397]
					0,012	T[287]
					0,021	S[1869]
					0,029	Y[1382]
					0,041	S[938]
					0,055	S[396]
TNRC6B	0,000028	T[342]	0,0000000029	S[879]	0,0000000053	S[879]
	0,00025	S[879]	0,00000005	S[879]	0,00000015	S[271]
	0,0043	S[609]	0,000000085	S[1512]	0,0000013	T[1701]
	0,02	T[596]	0,000064	S[1816]	0,0000031	S[385]
	0,041	S[1401]	0,00022	S[385]	0,0000074	S[1816]
			0,00035	S[1401]	0,0000093	S[385]
			0,00045	S[1432]	0,000016	S[273]
			0,004	S[384]	0,000027	S[879]
			0,0037	S[1816]	0,00006	S[1432]
			0,0049	S[882]	0,00006	S[609]
			0,014	T[596]	0,000066	S[1512]
			0,021	S[1401]	0,00094	T[611]
			0,046	Y[593]	0,0021	S[882]
					0,0035	S[1401]
					0,0057	S[882]
					0,0088	S[1816]
					0,017	S[61]
					0,021	T[1517]
					0,028	S[1832]
					0,038	S[1432]
					0,046	T[1676]
TNRC6C	0,0014	T[777]	0,00013	S[714]	0,00001	T[777]
			0,00015	T[1674]	0,000011	S[714]
			0,00037	S[1011]	0,000017	S[465]
			0,00039	T[777]	0,00071	T[1674]
			0,042	S[714]	0,0018	S[1011]
			0,042	S[717]	0,023	S[1038]
					0,05	T[272]

5.1.5 DNA oligonucleotides for northern blot

Sequence name	Sequence 5' to 3'	hsv1-mir-H3 -NB	GTCCCAACCGCACAGTCCCAG
Ebv-mir-BART1-3p NB	GACATAGTGGATAGCGGTGCTA	hsv1-mir-H4 -NB	TGCTTGCCTGTCAAACTCTACC
Ebv-mir-BART17-3p NB	ACTAAGGGGACACCAGGCATACA	hsv1-miR-H5-5p -NB	GTAGAGATGCCCGAACCCCCCC
Ebv-mir-BART6-5p NB	CCTATGGATTGGACCAACCTTA	hsv1-miR-H5-3p -NB	CCGGAGGGTTTGGATCTCTGAC
Ebv-mir-BART6-3p NB	TCTAAGGCTAGTCCGATCCCCG	hsv1-miR-H6-5p -NB	TACACCCCCCTGCCTTCCACC
Ebv-mir-BART21-5p NB	GTTAGTTGCCTTCACTAGTGA	hsv1-miR-H6-3p -NB	GGGATGGAAGGACGGGAAGTG
Ebv-mir-BART21-3p NB	AAACACCAGTGGGCACAACTAG	hsv1-mir-H11 -NB	GCGTTCGCACTTTGTCCTAA
Ebv-mir-BART18-5p NB	TGTATAGGAAGTGCGAACTTGA	hsv1-mir-H12 -NB	AAGCGTTCGCACTTCGTCCCAA
Ebv-mir-BART18-3p NB	GACGAAGCCCAAACTTCCGATA	hsv1-mir-H13 -NB	CCAGTGCTCGCACTTCGCCCTAA
Ebv-mir-BART7 NB	CCCTGGACACTGGACTATGATG	hsv1-miR-H14-5p -NB	CCTGAGCCAGGGACGAGTGCGACT
Ebv-mir-BART8 NB	CTGTACAATCTAGGAAACCGTA	hsv1-mir-H15 NB	CGTGGCGGCCCGGCCCGGGGCC
Ebv-mir-BART9 NB	ACTACGGGACCCATGAAGTGTTA	hsv1-mir-H16 -NB	GCCTTCGATCCCAGCCTCCTGG
Ebv-mir-BART22 NB	ACTACTAGACCATGACTTTGTAA	hsv1-mir-H17 -NB	CCGCCTCGCGCCCCAGCGCCA
Ebv-mir-BART10 NB	ACAGCCAACTCCATGGTTATGTA	hsv1-mir-H18 -NB	GGTCCCGGCGTCCGGCGGGCGGG
Ebv-mir-BART11-5p NB	CAACTAGCGCACCAAACTGTCTGA	hsv1-mir-H26 -NB	GACCGTCGCTCACCGAGCCA
Ebv-mir-BART11-3p NB	GGCAGTCAGCCTGGTGTGCGT	hsv1-miR-H27 -NB	AAGAGGGGGGAGAAAGGGGTCTG
Ebv-mir-BART12 NB	AACCACACCAAACACCACAGGA	hcmv-mir-UL22A-1-5p NB	TCTCACGGGAAGGCTAGTTA
Ebv-mir-BART19-5p NB	CATGTCATGTTTGCGGGGAATGT	hcmv-mir-UL22A-1-3p NB	CTACAAACTAGCATTCTGGTGA
Ebv-mir-BART19-3p NB	AGCATTCCCAAGCAAACAAAA	hcmv-mir- UL36-1 NB	TCTTTCCAGGTGTCTTCAACGA
Ebv-mir-BART20-5p NB	GGAATGAAGACATGCCTGCTA	hcmv-mir-UL112-5p NB	TGAGTAACCATGTGATCCGGAGG
Ebv-mir-BART20-3p NB	GGTAACAGGCTGTGCCTTCATG	hcmv-mir-UL112-3p NB	AGCCTGGATCTCACCGTCACTT
Ebv-mir-BART13 NB	TCAGCCGTCCCTGGCAAGTTACA	hcmv-mir- UL148D NB	CGGTGAAGAAGGGGAGGACGA
Ebv-mir-BART14 NB	ATCCCTACTACTGCAGCATTTA	hcmv-mir- US33-5p NB	CGCCCACGGTCCGGGCACAATC
Ebv-mir-BART2-5p NB	GCAAGGGCGAATGCAGAAAATA	hcmv-mir- US33-3p NB	TTGGATGTGCTCGGACCGTGA
Ebv-mir-BART2-3p NB	TTTATTTTCTCCAAATCGCTCCTT	hcmv-mir-UL5-1 NB	ACGCTCTCGTCAGGCTTGTCA
BHRF 1-1 NB loop rev	TAATACGACTCACTATAGGGTAACCTGATCAGCCCCG GAGTTGCCTGTTTCAT	hcmv-mir- US25-1 NB	GGTCCGAGCCACTGAGCGGTT
BHRF 1-3 NB loop rev	TAATACGACTCACTATAGGGTAACGGGAAGTGTGTA AGCACACACGTAATTTGCA	hcmv-mir- US25-2-5p NB	TCATCCACCTGAACAGACCGCT
BART 3 NB loop rev	TAATACGACTCACTATAGGGTAAATAAGTGTCCAGC GCACCACTAGTCACCAGGTGT	hcmv-mir- US25-2-3p NB	ACCGCGGGAGCTCTCCAAGTGGAT
BART 6 5p NB loop rev	TAATACGACTCACTATAGGG TAAGGTTGGTCCAATCCATAGGCTTTTTTTGT	hcmv-mir- US4-5p NB	CAGACATCCCCCTGCACGTCCA
BART 6 3p NB loop rev	TAATACGACTCACTATAGGGTTGTGAAAACCCGGGG ATCGGACTAGCCTTAGAGT	hcmv-mir- US4-3p NB	AGAGGTGTAGCGGGCTGTCA
BART 22 NB loop rev	TAATACGACTCACTATAGGGTACCACTCGGTTACAAA GTCATGGTCTAGTAGT	hcmv-mir- UL70-5p NB	TCTGGACGAGGCCGAGACGCA
BHRF1-3 trans for	TAATACGACTCACTATAGGGAGATCTTATCTTTTGCG GCAGAAATTG	hcmv-mir- UL70-3p NB	CCGCGCGCCAGCCCATCCCC
BHRF1-3 trans rev	GAGCTCAGTATTCCCATCTTCCCACACTCACC	hcmv-mir-UL59 NB	ACGGCATGACGAGCGAGAGAAC
BART16 trans for	TAATACGACTCACTATAGGGAGATCTGAAACCGGTG GGCCGCTGTTC	hcmv-mir-UL69 NB	CGGTTTCGGCTTAGCCTCTGG
BART16 trans rev	GAGCTCCTTGTATGCCTGCGTCCTCTTAG	hcmv-mir-US5-2-5p NB	CTTTCAGGATAGGTGTGGCGAAAG
BART22 trans for	TAATACGACTCACTATAGGGAGATCTTGACAACTATG CTGAATATCTTG	hcmv-mir-US5-2-3p NB	AGACATCGTCACACCTATCATA
BART22 trans rev	GAGCTCCCCCGGGACACTCCTCTGGGGTTCC	hcmv-mir-US22-5p NB	CCCGCGGACACACGCTGAAACA
BHRF1-3 trans rev 1	CTCGAGAGTATTCCCATCTTCCCACACTCACC	hcmv-mir-US22-3p NB	CCTGGTTACAGCGCGGCCGGCGA
BART16 trans rev 1	CTCGAGCTTGTATGCCTGCGTCCTCTTAG	hcmv-mir-US29-5p NB	CGTCACGGTCCGAGCACATCCA

BART22 trans rev 1	CTCGAGCCCCGGGACACTCCTCTGGGGTTCC
BHRF 1-1 RNA loop	TAATACGACTCACTATAGGGATGAAACAGGCAACTC CGGGGCTGATCAGGTTA
BHRF 1-1 RNA loop g	TAACCTGATCAGCCCCGGAGTTGCCTGTTTCATCCCT ATAGTGAGTCGTATTA
BHRF 1-3 RNA loop	TAATACGACTCACTATAGGGTTGCAAATTACGTGTGT GCTTACACACTTCCCGTTA
BHRF 1-3 RNA loop g	TAACGGGAAGTGTGTAAGCACACACGTAATTTGCAA CCCTATAGTGAGTCGTATTA
BART 3 RNA loop	TAATACGACTCACTATAGGGACACCTGGTGACTAGT GGTGCGCTGGACACTTATTTA
BART 3 RNA loop g	TAAATAAGTGTCCAGCGCACCACTAGTCACCAGGTG TCCCTATAGTGAGTCGTATTA

hcmv-mir-US29-3p NB	TGATTGTGCCCGGACCGTGGG
BART 6 5p RNA loop	TAATACGACTCACTATAGGGACAAAAAAAGCCTATGGATTGGACCAACCTT A
BART 6 5p RNA loop g	TAAGGTTGGTCCAATCCATAGGCTTTTTTTGTCCCTATAGTGAGTCGTATTA
BART 6 3p	TAATACGACTCACTATAGGGACTCTAAGGCTAGTCCGATCCCCGGGTTTTCA CAA
BART 22 RNA loop	TAATACGACTCACTATAGGGACTACTAGACCATGACTTTGTAACCGAGTGG TA
BART 22 RNA loop g	TACCACTCGGTTACAAAGTCATGGTCTAGTAGTCCCTATAGTGAGTCGTATT A
hsv1-mir-H7 -NB	CCTTTGGTTGCAGACCCCTTT
hsv1-mir-H8 -NB	GAACCCCCTGACCCTATATA
hsv1-mir-H1 -NB	TCCACTTCCCGTCCTTCCATC
hsv1-miR-H2-NB	AGTCGCACTCGTCCCTGGCTCAGG

5.1.6 DNA Oligonucleotides

Sequence name	Sequence 5' to 3'
BHRF1-1-for	TAATACGACTCACTATAGGGAGACCTAGCCTTATTAACCTGATCAGCCCCGG
BHRF1-1-rev	TTGTCAACCTCTTCAGGCC
BHRF1-2-for	TAATACGACTCACTATAGGGAGACCTAGCCTCTTTTAAATTCTGTTGCAGC
BHRF1-2-rev	CTTTCAATTTCTGCCGC
BHRF1-3-for	TAATACGACTCACTATAGGGAGACCTAGCCTTCTAACGGGAAGTGTGTAAGC
BHRF1-3-rev	ATTTTAACGAAGAGCGTGAAGC
BART3-for	TAATACGACTCACTATAGGGAGACCTAGCCTCCTTTGGTGGAACCTAGTGTTAG
BART3-rev	CCTCCGGTGACACCTGGTGAC
BART4-for	TAATACGACTCACTATAGGGAGACCTAGCCTTTTGGTGGGACCTGATGC
BART4-rev	CCTGGTGACACCTGGTGCC
BART1-for	TAATACGACTCACTATAGGGAGACCTAGCCTGGGGGTCTTAGTGGAAGTGACG
BART1-rev	CGGGCGAGACATAGTGGATAGC
BART15-for	TAATACGACTCACTATAGGGAGACCTAGCCTTGTGCCGCTTGGAGGGAAAC
BART15-rev	TGTGTCTCTATCAAGGAAACAAAACC
BART5-for	TAATACGACTCACTATAGGGAGACCTAGCCTGCTCTGTGGCACCTCAAGG
BART5-rev	ACCTTGCGTCACTTTAGG
BART16-for	TAATACGACTCACTATAGGGAGACCTAGCCTAGGCTTTCAGGTGTGGAATTTAG
BART16-rev	AGGTTTATCAATTGTGGGATATGG
BART17-for	TAATACGACTCACTATAGGGAGACCTAGCCTGTTGAACAGGATGTGGCACCC
BART17-rev	GCTACCTAGGCCTGCGTC
BART6-for	TAATACGACTCACTATAGGGAGACCTAGCCTTGACCTTGTTGGTACTTTAAGG
BART6-rev	TGGCCTTGAGTTACTCTAAGGC
BART21-for	TAATACGACTCACTATAGGGAGACCTAGCCTGGGCTGGGTATTCACTAGTG
BART21-rev	GGACCGGATAAACACCAGTGG
BART18-for	TAATACGACTCACTATAGGGAGACCTAGCCTGGGCTGGGTATTCACTAGTG
BART18-rev	GGACCGGATAAACACCAGTGG
BART7-for	TAATACGACTCACTATAGGGAGACCTAGCCTTCCAGTGTCCTGATCCTGG
BART7-rev	TCCGAGTGCACTGTCCCTGG
BART8-for	TAATACGACTCACTATAGGGAGACCTAGCCTTGGGTTCACTGATTACGGTTTCC
BART8-rev	TAAGCACACTGTCTACGACC
BART9-for	TAATACGACTCACTATAGGGAGACCTAGCCTCAGCTGTTGTTTGTACTGGACC
BART9-rev	CAGCATAGTTGTCACTACGGG
BART22-for	TAATACGACTCACTATAGGGAGACCTAGCCTGTCACAGGTGCTAGACCCTGG
BART22-rev	GTCACAACTACTAGACCATGAC
BART10-for	TAATACGACTCACTATAGGGAGACCTAGCCTCAGAGGAGTGTCCCGGGG
BART10-rev	CAGATGGAGTGCACCACAGC
BART11-for	TAATACGACTCACTATAGGGAGACCTAGCCTGGCTTCTGTTGGGTCAGACAG
BART11-rev	GGCCACACTGCTAAGGCAG
BART12-for	TAATACGACTCACTATAGGGAGACCTAGCCTCTGGTGACCTAACACCCGC
BART12-rev	CTGCGTACCCCAAAACCAC
BART19-for	TAATACGACTCACTATAGGGAGACCTAGCCTGTATCCGTGTCCTGACAACATTCC
BART19-rev	GCTTCCAGGCCCTAAGAGC
BART20-for	TAATACGACTCACTATAGGGAGACCTAGCCTGTATCCGTGTCCTGACAACATTCC
BART20-rev	GCTTCCAGGCCCTAAGAGC

Sequence name	Sequence 5' to 3'
hcmv-mir-UL5-1for	TAATACGACTCACTATAGGGAGACCTAGCCTTGAACGCTTTCGTCGTG
hcmv-mir-UL5-1-rev	TGAACGCTCTCGTCAGG
hcmv-mir- US25-1 for	TAATACGACTCACTATAGGGAGACCTAGCCTTGTGAACCGCTCAGTGG
hcmv-mir- US25-1-rev	TGAGAACCGACCTAGCG
hcmv-mir- US25-2-for	TAATACGACTCACTATAGGGAGACCTAGCCTCGGTTAGCGGTCTGTTCAGG
hcmv-mir- US25-2-rev	CGGACCGCGGGAGCTCTC
hcmv-mir- US4-for	TAATACGACTCACTATAGGGAGACCTAGCCTCGTGTCGCGACATGGACG
hcmv-mir- US41-rev	CATGTCGCGACAGAGAGG
hcmv-mir- UL70-for	TAATACGACTCACTATAGGGAGACCTAGCCTGGTTGCGTCTCGGCCTC
hcmv-mir- UL70-rev	GGCCGCGCGCCAGCCCATC
hcmv-mir-UL59-for	TAATACGACTCACTATAGGGAGACCTAGCCTCGACGGTTCTCTCGCTC
hcmv-mir-UL59-rev	CGACGCCATTTTCTCTCGTCC
hcmv-mir-UL69-for	TAATACGACTCACTATAGGGAGACCTAGCCTAGGCCAGAGGCTAAGCC
hcmv-mir-UL69-rev	GCACCAAAGGCTAAGTCG
hcmv-mir- US5-2-for	TAATACGACTCACTATAGGGAGACCTAGCCTGGAGGCTTTCGCCACACC
hcmv-mir- US5-2-rev	AAAGACATCGTCACACC
hcmv-mir-US22 for	TAATACGACTCACTATAGGGAGACCTAGCCTGGGGACCTGTTTCAGC
hcmv-mir-US22-rev	GAGGCCTGGTTACAGC
hcmv-mir-US29-for	TAATACGACTCACTATAGGGAGACCTAGCCTTCACGTTTGGATGTGCTCG
hcmv-mir-US29-rev	CCACGGTTGATTGTGC
hcmv-148d-g-f	AGCAGGUGAGGUUGGGGCGGACAACGUGUUGCGGAUUGUGGCGAGA
hcmv-148d-g-r	GGCGGTGAAGAAGGGGAGGACGACGTTCTCGCCACAATCCGCAAC
GST BglII fwd	GATAGATCTatgtcccctatactaggttattgg
Lin28a-NotI-fwd	Gat gcggccgc ATGGGCTCCGTGTCCAACC
Lin28a-BamHI-rev	Atc ggatcc TCAATTCTGTGCCTCCGGGAG
ebv-long-BH1-1-f	gtt agatct CCTTTAGGAAGCACCACGT
ebv-long-BH1-1-r	aac ctcgag CACCCCGGTTCGAAATGG
ebv-long-BH1-2-f	gtt agatct CCAGTAGGATATTAGGC
ebv-long-BH1-2-r	gtt ctcgag CACTTCCCGTTAGAACAC
ebv-long-BH1-3-f	gtt agatct GTGTTCTAACGGGAAGTG
ebv-long-BH1-3-r	gtt ctcgag GCAGTATAGGCTCTCACC
ebv-long-BART5-f	gtt agatct CTGTTAACCAGGTCAGTGG
ebv-long-BART5-r	gtt ctcgag CAAGAGCACACACCCACTC
ebv-long-BART6-f	gtt agatct CCTTAGTGGGACGCAG
ebv-long-BART6-r	gtt ctcgag GATCTGTGGTTACATGGtgc
ebv-long-BART9-f	gtt agatct ccaGACTTCCATGGAAGATG
ebv-long-BART9-r	gtt ctcgag CTATAACACTAGGACCCTC
ebv-long-BART11-f	gtt agatct GTTTACCTGCCTTGGGTTAC
ebv-long-BART11-r	gtt ctcgag GTACGTCTCAGGGCATG
ebv-long-BART14-f	gtt agatct GACTAATGGGGGGTGTGG
ebv-long-BART14-r	gtt ctcgag CAAGGGCTCACCAGGGAG
ebv-long-BART17-f	gtt agatct cacCCTCTATCCATATCCCAc
ebv-long-BART17-r	gtt ctcgag GGATTGGACCAACCTTAAAG
ebv-long-BART18-f	gtt agatct GCTCAACAGCCCCACCTGG
ebv-long-BART18-r	gtt ctcgag GTCTGGCTTAAGGGTCCCTC

BART13-for	TAATACGACTCACTATAGGGAGACCTAGCCTTTGGGCACCTCGATAACCGG	ebv-long-BART19-f	gtt agatct GACCCTGGTGCTAGGGTC
BART13-rev	CTAAACACATCGTCAGCCG	ebv-long-BART19-r	gtt ctcgag CTGCTACAATAGGCCCTACg
BART14-for	TAATACGACTCACTATAGGGAGACCTAGCCTCAGGGGTGGCCGGTACCC	ebv-long-BART16-f	gtt agatct gtatGCTGGAAACCGGTGG
BART14-rev	CAGGTCGCGCGTCCAGATC	ebv-long-BART16-r	gtt ctcgag cCTGCGTCCCACTAAGG
BART2-for	TAATACGACTCACTATAGGGAGACCTAGCCTACTATTTTCTGCATTCGCCCTTGC	CMV-miR4-long-f	gtt agatct GTCAAGAGTCACGTCAGTC
BART2-rev	TTTATTTTCTCCAAATCGCTCC	CMV-miR4-long-r	aac ctcgag CTGTCGCGATAGTCGAC
BART18-for 1	TAATACGACTCACTATAGGGAGACCTAGCCTTTGTTGCCGTTGAAAGACGGGTG	CMV-miR5-1-long-f	gtt agatct gaGATCCATAGTGAAGGAGTG
BART18-rev 1	TCGCAGCAGTCGACATTATCG	CMV-miR5-1-long-r	aac ctcgag GTGTGGCGAAAGCCTCC
BART20-for 1	TAATACGACTCACTATAGGGAGACCTAGCCTTACAGGCGTAGGGCCTATTG	CMV-miR5-2-long-f	gtt agatct CTGACGAGAGCGTTCATC
BART20-rev 1	TACATGGAAAAAAGGTGCCAATGG	CMV-miR5-2-long-r	aac ctcgag GGTTTACCGGAAAACCtac
BHRF1-3 trans for	TAATACGACTCACTATAGGGAGATCTTATCTTTTGCGGCAGAAATTG	CMV-miR22a-long-f	gtt agatct GCAGACCCCAAGGGTTAACG
BHRF1-3 trans rev	GAGCTCAGTATTCCCATCTTCCCACACTCACC	CMV-miR22a-long-r	aac ctcgag CGAGTCGCGTGTGTTTTGAC
BART16 trans for	TAATACGACTCACTATAGGGAGATCTGAAACCGGTGGGCCGCTGTTC	CMV-miR22-long-f	gtt agatct CGCACACACGTGATTTGC
BART16 trans rev	GAGCTCCTTGTATGCCTGCGTCCTCTTAG	CMV-miR22-long-r	aac ctcgag CTCCAGAAACCCCGTG
BART22 trans for	TAATACGACTCACTATAGGGAGATCTTGACAACTATGCTGAATATCTTG	CMV-miR33-long-f	gtt agatct cCACGACCATTTCCGTGC
BART22 trans rev	GAGCTCCCCCGGGACACTCCTCTGGGGTTCC	CMV-miR33-long-r	aac ctcgag CTGAGGTGGCAGGGGAC
BHRF1-3 trans rev 1	CTCGAGAGTATTCCCATCTTCCCACACTCACC	CMV-miR59-long-f	gtt agatct CATCCGACAAAACCGTGTC
BART16 trans rev 1	CTCGAGCTTGTATGCCTGCGTCCTCTTAG	CMV-miR59-long-r	aac ctcgag GTACCGAGGCGGTGC
BART22 trans rev 1	CTCGAGCCCCGGGACACTCCTCTGGGGTTCC	CMV-miR69-long-f	gtt agatct CGTGTACCGACCAAAGC
GST XbaI fwd	GAT TCTAGA TCT ATG TCC CCT ATA CTA GGT TAT TGG	CMV-miR69-long-r	aac ctcgag CGATCGTTGTGCATCATAC
GST-Stopp-NotI rev	TAC GCGGCCGC TTA ATCCGATTTTGGAGGATGGTCGCC	CMV-miR70-long-f	gtt agatct cCTGGTTGAGATGACGTAG
QuikChange EcoRI pGex fwd	gggagctcgaat tc ggcgcacgtggtctcaattc	CMV-miR70-long-r	aac ctcgag CCTACAGACGCAAAAGTGc
QuikChange EcoRI pGex rev	gaattgagaccacgtgcgcc ga attcgagctccc	CMV-miR112-long-f	gtt agatct GGTCGTTGCCCACGAAG
BHRF1-1 trans for	TAATACGACTCACTATAGGGAGATCTGTGCCCATGCATTATAATTTAACC	CMV-miR112-long-r	aac ctcgag GGTGGACGGGTTTCAGC
BHRF1-1 trans rev	gta CTCGAGGTATCAGCTATCTGCTGCAACAG	CMV-miR148-long-f	gtt agatct CGTTAATGCAGCCGTTGatg
BHRF1-2 trans for	TAATACGACTCACTATAGGGAGATCTGGCCCCCACTTTTAAATTCTG	CMV-miR148-long-r	aac ctcgag cttGCACACCGGTGATTATG
BHRF1-2 trans rev	gta CTCGAGGCAAATTACGTGTGTGCTTAC	UL97-HCMVT-f	Agt gctagc ATGTCCTCCGCACTTCGGTC
BART3 trans for	TAATACGACTCACTATAGGGAGATCTCCTATAGGTCCTACCGGAGCTCC	UL97-HCMVT-r	Agt gaattc TTACTCGGGGAACAGTTGGc
BART3 trans rev	gtaCTCGAG CCCACCAAATGTTACAGAGC	RFOX2_HUMAN-f	Agt gcggccgc ATGGAGAAAAAGAAAATGGTAACTC
BART4 trans for	TAATACGACTCACTATAGGGAGATCTTCACCGGAGGCTACTTGCC	RFOX2_HUMAN-r	Agt ggatcc TCAGTAGGGGGCAAATCGG
BART4 trans rev	gtaCTCGAGAGCACGTCACTTCCACTAAG	UNG_HCMVM-f	Agt gctagc ATGGCCCTCAAGCAGTGGATG
BART1 trans for	TAATACGACTCACTATAGGGAGATCTTCACCAGGGCTACTTGCC	UNG_HCMVM-r	Agt gaattc TCACCCACAGAGTCGCCAG
BART1 trans rev	gtaCTCGAGCCTGGTTAACAGACTTCAGGTGG	UL77_HCMVA-f	Agt gctagc ATGAGTCTGTTGCACACCTTTTGG
BART15 trans for	TAATACGACTCACTATAGGGAGATCTATATGTCGCCTTACCTCCC	UL77_HCMVA-r	Agt gaattc TTACAACACCGCCACGCTCG
BART15 trans rev	gtaCTCGAGGAGGTGCCACAGAGCATCAG	PORTL_HCMVA-f	Agt gctagc ATGGAGCGAAACCACTGGaac
BART5 trans for	TAATACGACTCACTATAGGGAGATCTATAGAGACACAAGGACTGCC	PORTL_HCMVA-r	Agt gaattc CTAGTGAAATCCGTATGGACCTC
BART5 trans rev	gtaCTCGAGTTAAACAAGAGCACACACCC	K0020_HUMAN-f	Agt gctagc ATGGAAGTTAAAGGGAAAAAGCAATTC
BART17 trans for	TAATACGACTCACTATAGGGAGATCTTTACACCAAGATCACCACC	K0020_HUMAN-r	Agt gaattc CTATGTGCTCAGTTTTTCAAGTAG
BART17 trans rev	gtaCTCGAGCCTATGGATTGGACCAACC	PP65_HCMVM-f	Agt gctagc ATGGAGTCGCGCGGTCGC
BART6 trans for	TAATACGACTCACTATAGGGAGATCTTGTATGCCTGGTGTCCCCTTAG	PP65_HCMVM-r	Agt gaattc TCAACCTCGGTGCTTTTTGGg
BART6 trans rev	gtaCTCGAGTGAAACCCAAGTTTCCTTGCC	PURB_HUMAN-f	Agt gctagc ATGGCGGACGGCGACAG
BART21 trans for	TAATACGACTCACTATAGGGAGATCTTGTTAGCTTTTTTGGTGGG	PURB_HUMAN-r	Agt ggatcc TCAATCCTCATCCACCTCCTC
BART21 trans rev	gtaCTCGAGAGCATCCCCCACTCTGATAC	PURA_HUMAN-f	Agt gctagc ATGGCGGACCGAGACAGC
BART18 trans for	TAATACGACTCACTATAGGGAGATCTGTTGTAGGGTAACGAAGACC	PURA_HUMAN-r	Agt ggatcc TCAATCTTCTTCCCCTTCTTCC
BART18 trans rev	gtaCTCGAGAGCCAAGTGCACCTGCCTAAC	CPSF6_HUMAN-f	Agt gctagc ATGGCGGACGGCGTGG
BART7 trans for	TAATACGACTCACTATAGGGAGATCTGCCAAACCTCCAGAATATC	CPSF6_HUMAN-r	Agt ggatcc CTAACGATGACGATATTCGCG

BART7 trans rev	gtaCTCGAGCAGATGTCAGCAGCATGCCAG	CPSF5_HUMAN-f	Agt gctagc ATGTCTGTGGTACCGCCC
BART8 trans for	TAATACGACTCACTATAGGGAGATCTACCTGACTGGC CGGTGCAATTAG	CPSF5_HUMAN-r	Agt ggatcc TCAGTTGTAAATAAAATTGAACCTGCTC
BART8 trans rev	gtaCTCGAGTCACAAAGCCCCACTACATG	CPSF7_HUMAN-f	Agt gctagc ATGTCAGAAGGAGTGGACTTG
BART9 trans for	TAATACGACTCACTATAGGGAGATCTTGTGAATTTGC TGCTAGCTATATGG	CPSF7_HUMAN-r	Agt ggatcc TCAGTGGTGCCGGTCCc
BART9 trans rev 1	gtaCTCGAGCGCCCTATAACACTAGGACCCTC	A-TSS736/8/9AAA-QC-f	CAGAATACTGCCTGGGATgctGAAGCTGCTCCTAGAGGGGAACGAAAGACT GAC
BART10 trans for	TAATACGACTCACTATAGGGAGATCTGTAGTTGTGAC CCTGCAAAG	A-TSS736/8/9AAA-QC-r	GTCAGTCTTTCGTTCCCCTCTAGGAGCAGCTTCagcATCCCAGGCAGTATTCT G
BART10 trans rev	gtaCTCGAGAAAGGTGTGGTCGTTTGGAATAG	A-T1844A-QC-fwd	GTGTGTACTGGGGAACGCTACTATTCTTGCTGAG
BART11 trans for	TAATACGACTCACTATAGGGAGATCTGTTTACCTGCC TTGGGTTAC	A-T1844A-QC-rev	CTCAGCAAGAATAGTAGCGTTCCCCAGTACACAC
BART11 trans rev	gtaCTCGAGCGATTAAGTCCTAACTCGAG	A-T1844E-QC-fwd	CACATGTGTGTACTGGGGAACGAGACTATTCTTGCTGAGTTTGC
BART12 trans for	TAATACGACTCACTATAGGGAGATCTATGTAAGAGA GGTTGCCTAG	A-T1844E-QC-rev	GCAAACTCAGCAAGAATAGTCTCGTTCCCCAGTACACACATGTG
BART12 trans rev	gtaCTCGAG GTTATTGGCACCGTGTAAC	A-Y1631A-QC-fwd	CAAACATTGACCCTGAAACTGACCCTGCCGTCACTCCTGGCAGTGTCATAAA C
BART9 trans rev	gtaCTCGAGACATGCCTGCTACAATAGG	A-Y1631A-QC-rev	GTTTATGACACTGCCAGGAGTGACGGCAGGGTCAGTTTCAGGGTCAATGTT TG
BART20 trans for	TAATACGACTCACTATAGGGAGATCTAAACATGTTTT GTTTGCTTGGG	A-Y1631E-QC-fwd	GACCCTGAAACTGACCCTGAGGTCACTCCTGGCAGTGTC
BART20 trans rev	gtaCTCGAGAACGTCGAGATACCCTGGC	A-Y1631E-QC-rev	GACACTGCCAGGAGTGACCTCAGGGTCAGTTTCAGGGTC
BART13 trans for	TAATACGACTCACTATAGGGAGATCTTGATCCTGGGT CCTTTGG	A-SSS1582/5/9AAA-Qf	GACTTTATGAACAGCAGTACGTCACCAGCCgcTCCTCCAGGTGCAATAGGA GATGGCTGG
BART13 trans rev	gtaCTCGAGGACATCCCCAGACTCACC	A-SSS1582/5/9AAA-Qr	CCAGCCATCTCCTATTGCACCTGGAGGAgcGGCTGGTGACGTACTGCTGTTC ATAAAGTC
BART14 trans for	TAATACGACTCACTATAGGGAGATCTGTGTGGTATG GCACAGG	A-SSS1582/5/9EEE-Qf	CTATGACTTTATGAACAGCAGTACTGAACCAGCCgaaCCTCCAGGTgaAATA GGAGATGGCTGGCC
BART14 trans rev	gtaCTCGAG CGAGCAGTCGCATGGCG	A-SSS1582/5/9EEE-Qr	GGCCAGCCATCTCCTATTtcACCTGGAGGttcGGCTGGTTCAGTACTGCTGTT CATAAAGTCATAG
BART2 trans for	TAATACGACTCACTATAGGGAGATCTTGGTCAGAGC CAGACTG	T6A S1884A f	AGCCGGCTGGGCGCCCTCGACTGTT
BART2 trans rev	gtaCTCGAG TTCAGACAGCCGCGGTTGTC	T6A S1884A r	AACAGTCGAGGGCGCCCAGCCGGCT
hsv1-mir-H7 -for	TAATACGACTCACTATAGGGAGACCTAGCCTGAAGA GGGGGGAGAAAGG	T6A S1884E f	AGAGCCGGCTGGGCGAACTCGACTGTTCCCACTCATTCT
hsv1-mir-H7 -rev	GAGAAGAGGGAAGAAGAG	T6A S1884E r	AGAATGAGTGGGAACAGTCGAGTTCGCCCAGCCGGCTCT
hsv1-mir-H8 -for	TAATACGACTCACTATAGGGAGACCTAGCCTGTCCCT GTATATATAGG	PCIneo-FseIAscI-in-f	atctctagactgaggcgcgccatatggccggccatagcggccgcttat
hsv1-mir-H8 -rev	GACAACTATATATACAGG	PCIneo-FseIAscI-in-r	ataagcggccgctatggccggccatatggcgcgcctcagtctagagat
hsv1-mir-H1 -for	TAATACGACTCACTATAGGGAGACCTAGCCTCGAGG GGAACGGGGGATG	TC6A-3-EcoRI-rev1	cgact gaattc ttacatggactctccacc
hsv1-mir-H1 -rev	CGGGGGGCCGGAGGGTG	pGEM-QC-XbaI-fwd	GTGAATTGTAATACGACTCTAGATAGGGCGAATTGGGCCCG
hsv1-miR-H2-for	TAATACGACTCACTATAGGGAGACCTAGCCTGCCACC GTCGCACGCG	pGEM-QC-XbaI-rev	CGGGCCCAATTCGCCCTATCTAGAGTCGTATTACAATTCAC
hsv1-miR-H2-rev	GCCCCAGTCGCACTCGTC	TC6A-1-XbaI-fwd	atg tctaga atggatgctgattctgcc
hsv1-mir-H3 -for	TAATACGACTCACTATAGGGAGACCTAGCCTCCGCG GGCGCGCTCCTGAC	TC6A-1-SacII-rev	ggt ccgcgg atctaagtcagttctgtttac
hsv1-mir-H3 -rev	CCACGGGCGCCGTCCCAAC	TC6A-2-SacII-fwd	tac ccgcgg gtcctgtccaactctggttg
hsv1-mir-H4 -for	TAATACGACTCACTATAGGGAGACCTAGCCTGCCGG GGTGGTAGAGTTTG	TC6A-3-NotI-rev	cgact gcggccgc ttacatggactctccacc
hsv1-mir-H4 -rev	GCCGAGACTAGCGAGTTAG	TC6A_T736A_QC-f	CAGAATACTGCCTGGGATGCAGAAACATCACCTAGAG
hsv1-mir-H5 -for	TAATACGACTCACTATAGGGAGACCTAGCCTGCGCTC CCTCGGGGGGGTTC	TC6A_T736A_QC-r	CTCTAGGTGATGTTTCTGCATCCCAGGCAGTATTCTG
hsv1-mir-H5 -rev	GCGCCCCCGGAGGGTTTG	TC6A_T736E_QC-f	GAATACTGCCTGGGATGAAGAAACATCACCTAGAG
hsv1-mir-H6 -for	TAATACGACTCACTATAGGGAGACCTAGCCTCGGGG GGCCGGAGGGTGGAAG	TC6A_T736E_QC-r	CTCTAGGTGATGTTTCTTCATCCCAGGCAGTATTC
hsv1-mir-H6 -rev	CGAGGGGAACGGGGGATG	TC6A_T738A_QC-f	GCCTGGGATACAGAAGCATCACCTAGAGGGG
hsv1-mir-H11 -for	TAATACGACTCACTATAGGGAGACCTAGCCTGGGCG TGGCCGCTATTATAAAAAAAG	TC6A_T738A_QC-r	CCCCTCTAGGTGATGCTTCTGTATCCCAGGC
hsv1-mir-H11 -rev	GGGCGTGGCCGCTATTATAAAAAAAG	TC6A_T738E_QC-f	CTGCCTGGGATACAGAAGAATCACCTAGAGGGGAAC
hsv1-mir-H12 -for	TAATACGACTCACTATAGGGAGACCTAGCCTGGAGT CGGGCACGGCGCC	TC6A_T738E_QC-r	GTTCCCCTCTAGGTGATTCTTCTGTATCCCAGGCAG
hsv1-mir-H12 -rev	GAAGTGAGAACGCGAAGCG	TC6A_T739A_QC-f	GGGATACAGAAACAGCACCTAGAGGGGAAC
hsv1-mir-H13 -for	TAATACGACTCACTATAGGGAGACCTAGCCTGCGAA GCGTTCGCACTTCG	TC6A_T739A_QC-r	GTTCCCCTCTAGGTGCTGTTTCTGTATCCC
hsv1-mir-H13 -rev	GCGCCAGTGCTCGCACTTC	TC6A_T739E_QC-f	GGGATACAGAAACAGAACCTAGAGGGGAACG
hsv1-mir-H14 -for	TAATACGACTCACTATAGGGAGACCTAGCCTGCCGT GTGCCCCAGTCGCAC	TC6A_T739E_QC-r	CGTTCCCCTCTAGGTTCTGTTTCTGTATCCC
hsv1-mir-H14 -rev	GCCGCGCGCCACCGTCGC	TC6B-part1-XbaI-f	gat tctaga atgagagagaaggagcaagaaagg
hsv1-mir-H15 -for	TAATACGACTCACTATAGGGAGACCTAGCCTACCACA GCGCATGCG	TC6B-part2-NotI-r	GATGCGGCCGCtcagattgaatccgaccctc
hsv1-mir-H15 -rev	ACCGCCAACGGCCGGCCCCCGTG	TC6B-part2-SacII-f	ctaccgcgggaaccaaacctgcccacc

hsv1-mir-H16 -for	TAATACGACTCACTATAGGGAGACCTAGCCTGCGCA GAGAGCCTCGTTAAG
hsv1-mir-H16 -rev	GCGAAGAGTCCCCCGGCAG
hsv1-mir-H17 -for	TAATACGACTCACTATAGGGAGACCTAGCCTGGCCC ACTCGCACGCCGCCTG
hsv1-mir-H17 -rev	GGCCGGCGCGCACCGCCTC
hsv1-mir-H18 -for	TAATACGACTCACTATAGGGAGACCTAGCCTCGGTCC CGCCCGCCGGAC
hsv1-mir-H18 -rev	CGGTCCCGCCCGCCGGCCAATG
hsv1-mir-H26 -for	TAATACGACTCACTATAGGGAGACCTAGCCTTCAGG CTAGCGCGGCGGGCCTG
hsv1-mir-H26 -rev	CCAAGCAACCGGACCGTC
hsv1-miR-H27 -for	TAATACGACTCACTATAGGGAGACCTAGCCTAGAAG AGGGAAGAAGAGG
hsv1-miR-H27 -rev	GGAAGAGGGGGGAGAAAG
hsv1-mir-H15-g-for	ACCACAGCGCATGCGCCGGGCCGTTGTGGGGCCCCG GGCCGGGGCCCCTTGGGTCCG
hsv1-mir-H15-g-rev	TTGGGTCCGCCGGGGCCCCGGGCCGGGCCGCCACG GGGGCCGGCCGTTGGCGGT
hsv1-mir-H17-g-for	GGCCCACTCGCACGCCGCCTGCGCGCGCTGGGGCCT GGGCGCGCCGCTGCG
hsv1-mir-H17-g-rev	CGCCGCTGCGGCCCGTGTACGTGGCGCTGGGGCGC GAGGCGGTGCGCGCCGGCC
hsv1-mir-H18-g-for	CGGTCCCGCCCGCCGGACGCCGGGACCAACGGGAC GGCGGGCGGCCCAAGGGC
hsv1-mir-H18-g-rev	GCCCAAGGGCCGCCCGCCTTGCCGCCCCCCCATTGG CCGGCGGGCGGGACCG
hsv1-mir-H8-g-for	GTCCCTGTATATATAGGGTCAGGGGGTTCCGCACCC CCTA
hsv1-mir-H8-g-rev	GACAACTATATATACAGGGACCGGGGGCGCCATGTT AGGGGGTG
hsv1-mir-H11-g-for	GGGCGTGGCCGCTATTATAAAAAAAGTGAGAACGC GAAGCGTTCGCACTTTGTCCTAATAATATATATA
hsv1-mir-H11-g-rev	GGGCGTGGCCGCTATTATAAAAAAAGTGAGAACGC GAAGCGTTCGCACTTTGTCCTAATAATATATAT
hsv1-mir-H12-g-for	GGAGTCGGGCACGGCGCCAGTGCTCGCACTTCGCCC TAATAATATATATAT
hsv1-mir-H12-g-rev	GAAGTGAGAACGCGAAGCGTTCGCACTTCGTCCCAA TATATATAT
hsv1-mir-H15-g-r1	ACCGCCAACGGCCGGCCCCCGTGGCGGCCCGGCCCG GGGCCCCGGCGGACCCAA
hsv1-mir-H17-g-r1	GGCCGGCGCGCACCGCCTCGCGCCCCAGCGCCACGT ACACGGGCCGCAGCGGCG
hsv1-mir-H18-g-r1	CGGTCCCGCCCGCCGGCCAATGGGGGGGCGGCAAG GCGGGCGGCCCTTGGGC
QC-THSV1miR3C-for	AACTCGGAACCCGCGGTCAGGAGCG
QC-THSV1miR3C-rev	CGCTCCTGACCGCGGGTTCCGAGTT
HSV1-miR18mid-rev	GCAAGGCGGGCGGCCCTTGGGCCGCCCGCCGTCCCG TTGGTCCCGGCGTCCGGCGGGCGGGACCG
HSV1-miR11mid-for	TATTATAAAAAAAGTGAGAACGCGAAGCGTTCGCAC TTTGTCCTAATAATATATATTATTAGG
HSV1-miR11t7-l-rev	CGCGTTCTCACTTTTTTTATAATAGCGGCCACGCCCA GGCTAGGTCTCCCTATAGTGAGTCGTATTA
HSV1-miR12mid-for	CACGGCGCCAGTGCTCGCACTTCGCCCTAATAATATA TATATATTGGGACGAAGTGCG
HSV1-miR12t7-l-rev	GAGCACTGGCGCCGTGCCCGACTCCAGGCTAGGTCT CCCTATAGTGAGTCGTATTA
hcmv-mir-UL22A-1for	TAATACGACTCACTATAGGGAGACCTAGCCTCCTGTC TAACTAGCCTTCC
hcmv-mir-UL22A-1-rev	CCTCTACAAACTAGCATTC
hcmv-mir- UL36-1 for	TAATACGACTCACTATAGGGAGACCTAGCCTCCACGT CGTTGAAGACACC
hcmv-mir- UL36-1-rev	CCACGCACGTTGAAAACACC
hcmv-mir-UL112 for	TAATACGACTCACTATAGGGAGACCTAGCCTGACAG CCTCCGGATCACATG
hcmv-mir-UL112 rev	GACAGCCTGGATCTCAC
hcmv-mir- UL148D -for	TAATACGACTCACTATAGGGAGACCTAGCCTAGCAG GTGAGGTTGGG
hcmv-mir- UL148D -rev	GGCGGTGAAGAAGGGGAG
hcmv-mir- US33-1for	TAATACGACTCACTATAGGGAGACCTAGCCTCACGG TTGATTGTGCCCGGAC
hcmv-mir- US33-1-rev	CACGTTTGGATGTGCTCG
TNRC6B-seq-1f -new	ccaattcacatctgggacaagg
TNRC6B-seq-4f -new	ggtaatggtggcaatgcaagc
TNRC6C-seq-1f -new	gcacaacctcagaaccttaac
TNRC6C-seq-2f -new	GAA CGG GAG AAG GCC GAA G
TC6B-part1-SacII-r	gttccgcggtgctgggccccttgggaattc
VP5-SacIIexit-QC-f	GATATTCACCTGGCCCACGGTGATGCCTTTGAG
VP5-SacIIexit-QC-r	CTCAAAGGCATCACCGTGGGCCAGGTGAATATC
pGEMTe-NotIexit-Q-f	CGGCCGCCATGATGGCCGCGGGAATTCGATTATCACTAG
pGEMTe-NotIexit-Q-r	CTAGTGATAATCGAATTCCCGCGGCCATCATGGCGGCCG
TC6B-S879A-QC-f	GTGGTTGGGAAGAGCCAGCCCCACAGTCAATTAGTC
TC6B-S879A-QC-r	GACTAATTGACTGTGGGGCTGGCTCTTCCCAACCAC
TC6B-S879E-QC-f	GAACCCAGTGGTTGGGAAGAGCCAGAGCCACAGTCAATTAGTCGGAAAAT G
TC6B-S879E-QC-r	CATTTTCCGACTAATTGACTGTGGCTCTGGCTCTTCCCAACCACTGGGTTC
TC6B-S1711E-QC-f	CACATGTGTGTGTTGGGAAACGAGACCATCCTTGCTGAGTTTGCC
TC6B-S1711E-QC-r	GGCAAACTCAGCAAGGATGGTCTCGTTTCCCAACACACACATGTG
TC6B-S1711A-QC-f	GTGTGTGTTGGGAAACGCTACCATCCTTGCTGAG
TC6B-S1711A-QC-r	CTCAGCAAGGATGGTAGCGTTTCCCAACACACAC
TC6B-S1400E-QC-f	GTCTCGCTTTAAACAGTGGGAGTCCATGATGGAGGGGCTGC
TC6B-S1400E-QC-r	GCAGCCCCTCCATCATGGACTCCCACTGTTTAAAGCGAGAC
TC6B-S1400A-QC-f	CGCTTTAAACAGTGGGCCTCCATGATGGAGGG
TC6B-S1400A-QC-r	CCCTCCATCATGGAGGCCCACTGTTTAAAGCG
TC6A-S991E-QC-f	CACAGGCTGGGAGGAACCAGAGCCAGAATCTATACGTCGC
TC6A-S991E-QC-r	GCGACGTATAGATTCTGGCTCTGGTTCCTCCCAGCCTGTG
TC6A-S991A-QC-f	GGCTGGGAGGAACCAGCCCCAGAATCTATACG
TC6A-S991A-QC-r	CGTATAGATTCTGGGGCTGGTTCCTCCCAGCC
TC6A-T1844E-QC-f	GCACATGTGTGTACTGGGGAACGAGACTATTCTTGCTGAGTTTGCC
TC6A-T1844E-QC-r	GGCAAACTCAGCAAGAATAGTCTCGTTCCCCAGTACACACATGTGC
TC6A-T1844A-QC-f	CATGTGTGTACTGGGGAACGCTACTATTCTTGCTGAG
TC6A-T1844A-QC-r	CTCAGCAAGAATAGTAGCGTTCCCCAGTACACACATG
TC6A-T1548E-QC-f	CAAGACTAAGGAAGTGGGAGACAGTGGACAGCATTTC
TC6A-T1548E-QC-r	GAAATGCTGTCCACTGTCTCCCACTTCCTTAGTCTTG
TC6A-T1548A-QC-f	GTCAAGACTAAGGAAGTGGGCGACAGTGGACAGCATTTC
TC6A-T1548A-QC-r	GAAATGCTGTCCACTGTCGCCCACTTCCTTAGTCTTGAC
TC6A-T1549E-QC-f	CAAGACTAAGGAAGTGGACGGAGGTGGACAGCATTTCTGTGAAC
TC6A-T1549E-QC-r	GTTCACAGAAATGCTGTCCACCTCCGTCCACTTCCTTAGTCTTG
TC6A-T1549A-QC-f	GACTAAGGAAGTGGACGGCAGTGGACAGCATTTC
TC6A-T1549A-QC-r	GAAATGCTGTCCACTGCCGTCCACTTCCTTAGTC
TC6C-part1-FseI-f	gatggccggccatggctacagggag
TC6C-part2-AscI-r	gatggcgcgggctacagggactccc
TC6C-part1-XbaI-r	gtatctagaagaattcaagttttgcatgccc
TC6C-part2-XbaI-f	gtatctagacagataccgagtggcaatctg
TC6C-S714E-QC-f	CTGGGAAGAACCCGAGCCACCGTCCATTCGCCGCAAAATG
TC6C-S714E-QC-r	CATTTTGCGGCGAATGGACGGTGGCTCGGGTTCTTCCCAG
TC6C-S714A-QC-f	CTGGGAAGAACCCGCTCCACCGTCCATTCGCCGCAAAATG
TC6C-S714A-QC-r	CATTTTGCGGCGAATGGACGGTGGAGCGGGTTCTTCCCAG
TC6C-T1301E-QC-f	CTCCCCCAGTGGGAGCACCCCAACTCCATGGATAACTTG
TC6C-T1301E-QC-r	CAAGTTATCCATGGAGTTGGGGTGCTCCCACTGGGGGAG
TC6C-T1301A-QC-f	CTCCCCCAGTGGGCGCACCCCAACTCCATG
TC6C-T1301A-QC-r	CATGGAGTTGGGGTGCGCCCACTGGGGGAG
TC6C-T1577E-QC-f	CATGTGCGTCCTGGGAAACGAGACCATCCTGGCCGAGTTC

TNRC6C-seq-3f -new	CCA ACA GAA CTG GGC TAG C	TC6C-T1577E-QC-r	GAACTCGGCCAGGATGGTCTCGTTTCCCAGGACGCACATG
TNRC6C-seq-4f -new	CCA GTG GGA GGA TGA AGA AGG	TC6C-T1577A-QC-f	CATGTGCGTCCTGGGAAACGCTACCATCCTGG
TNRC6C-seq-5f -new	GGT CTC AAC CCT GCA CTA TTA ACC	TC6C-T1577A-QC-r	CCAGGATGGTAGCGTTTCCCAGGACGCACATG
VP5-NheI_XbaI-NotI-f	acggctagccgtaactctagaatgctcgcggccgcacg	pGEMtE-FseIAscI+-f	gacgtcgcatgcggccggccgccatggcgcgcccgggaattcg
VP5-NheI_XbaI-NotI-r	cgtgcggccgcgagcattctagagttacggctagccgt	pGEMtE-FseIAscI+-r	cgaattcccgggcgcgccatggcggccggccgcatgcgacgtc
VP5-QC-XbaI-exit-f	GGGATCAATTCTCTCAAGCTCGCTGATCAGC	PAN3-ISO4-f	Gat gctagc ATGGATGGAGGTGCTTTAACTGATAC
VP5-QC-XbaI-exit-r	GCTGATCAGCGAGCTTGAGAGAATTGATCCC	PAN3-ISO4-r	Gat ggccggcc CTACAACTGACCATTTGCAGCTGC
VP5-NheIXbaIEcoRI-f	acggctagctagatctagaacttcggcggccgcactggaattctag	NOT9-ISO1-F	Gat gctagc ATGCACAGCCTGGCGACGGCTG
VP5-NheIXbaIEcoRIr	ctagaattccagtgcggccgccgaagttctagatctagctagccgt	NOT9-ISO1-R	Gat ggccggcc TCACTGAGGGGGCAGGGGGATAC
VP5-TNRC6A-REs-for	acggctagctaggactctagaactgagagctcgttcggcggccgcac tggaattctag	A-TSS736/8/9EEE-QC-r	GTCAGTCTTTCGTTCCCCTCTAGGttcctcTTCctcATCCCAGGCAGTATTCTG
VP5-TC6A-REs-rev	ctagaattccagtgcggccgccgaacgagctctcagttctagagtcct agctagccgt	TC6B-S1432-A-fwd	GTAAAACCCGGGGAGGGgcACCGTACAAC
PAN3-hs-f	Gat gctagc ATGAACAGTGGCGGCGGC	TC6B-S1432-A-rev	GTTGTACGGTgcCCCTCCCCGGGTTTTAC
PAN3-hs-r	Gat ggccggcc CTACAACTGACCATTTGCAGC	TC6B-S385-A-fwd	CTTGAACTTAAGTgCACCAAACC
VP5-TC6A-Res-r-f	acggctagcaaggactctagaactgaccgcgggttcggcggccgca ctggaattctag	TC6B-S385-A-rev	GGTTTGGTGcACTTAAGTTCAAG
VP5-TC6A-Res-r-r	ctagaattccagtgcggccgccgaacccgcggtcagttctagagtcct tgctagccgt	TC6B-S609-A-fwd	CAGACTCTTTTGgcCCGAACTGATTTG
A-TSS736/8/9EEE-QC-f	CAGAATACTGCCTGGGATgagGAAgaggaaCCTAGAG GGGAACGAAAGACTGAC	TC6B-S609-A-rev	CAAATCAGTTCGGgcCAAAAGAGTCTG
ebv-long-BART4-f	gtt agatct GGAGCTCCTTGTCTTGATAATC	TC6B-S744-A-fwd	CAAGGATGGTCTgCTGGAAAGAATG
ebv-long-BART4-r	gtt ctcgag CAGCACACCAGCAGCATCAG	TC6B-S744-A-rev	CATTCTTTCCAGcAGACCATCCTTG
HCMV-miR148-l-pgem-f	gtt agatct GAATTGTAATACGACTCACTATAG	TC6B-T596-A-fwd	CGTACAGGCCCgCACATCCTGATTG
HCMV-miR148-l-pgem-r	gtt ctcgag CGCCAAGCTATTTAGGTGAC	TC6B-T596-A-rev	CAATCAGGATGTGcGGGCCTGTACG
pGem NotI exit 2 f	GCCGCCATGCAGGCCGCGGGAATTCGAT	TC6B-T626-A-fwd	GCTGGGGCCAAgCTCAAATTAAGC
pGem NotI exit 2 r	ATCGAATTCCCGCGGCCTGCATGGCGGCC	TC6B-T626-A-rev	GCTTAATTTGAGcTTGGCCCCAGC
BKV-long-M1sup-f	gtt agatctGCTTTTGTATAAGCCACTTTTAAGC	TC6B-S1432-E-fwd	GTAAAACCCGGGGAGGGgaACCGTACAAC
BKV-long-M1sup-r	aac ctcgagCAAAGTGGAATGACCTTGTTGC	TC6B-S1432-E-rev	GTTGTACGGTtcCCCTCCCCGGGTTTTAC
MCV-long-M1sup-f	gtt agatctCTCCTCGGCAGAGGAAGAC	TC6B-S385-E-fwd	CTTGAACTTAAGTgaACCAAACC
MCV-long-M1sup-r	aac ctcgagGTATGGGTCCTTCTCAGCGTC	TC6B-S385-E-rev	GGTTTGGTtcACTTAAGTTCAAG
HPV41-long-M1sup-f	gtt agatct CTGGTATCACTCAGTCATCATC	TC6B-S609-E-fwd	CAGACTCTTTTGgagCGAACTGATTTG
HPV41-long-M1sup-r	aac ctcgag GTGCCAAATCATGAGACATGAAC	TC6B-S609-E-rev	CAAATCAGTTCGctcCAAAAGAGTCTG
Bkv-miR-B1-f	TAATACGACTCACTATAGGGAGACCTAGCCTGGGAA TCTTCAGCAGGGGCTG	TC6B-S744-E-fwd	CAAGGATGGTCTgaaGGAAAGAATG
Bkv-miR-B1-r	AGGATTCAGAAACTGAAGACTCTGGAC	TC6B-S744-E-rev	CATTCTTTCCttcAGACCATCCTTG
mcv-miR-M1-f	TTAATACGACTCACTATAGGGAGACCTAGCCTAGGT GCCATACGTTCTGGAAG	TC6B-T596-E-fwd	CGTACAGGCCCgaACATCCTGATTG
mcv-miR-M1-r	AGGAGACCACCAATTCAGGAAG	TC6B-T596-E-rev	CTTGAACTTAAGTgaACCAAACC
hpv41-miR-f	TAATACGACTCACTATAGGGAGACCTAGCCTGGTATT GTGGTGCGGTGTCC	TC6B-T626-E-fwd	GCTGGGGCCAAgagCAAATTAAGC
hpv41-miR-r	GATAATGGAGTGGTGTACCCTGG	TC6B-T626-E-rev	GCTTAATTTGctcTTGGCCCCAGC
CRRM1-NotI-for	cat gcggccgc agcagctggctcgttcttcg	TC6C-T777-A-fwd	CACCACACACAGGGTCGAGgCGCCGCCCCCGCAC
CRRM1-BamHI-rev	cat ggatcc tca aggcccatgttgcaaacacaatg	TC6C-T777-A-rev	GTGCGGGGGCGGCGcCTCGACCCTGTGTGTGGTG
CRRM2-NotI-for	cat gcggccgc catgggcctcttatcacattcc	TC6C-S1628-A-fwd	CATGGCCTGGTACGCgcCGACGCTGGCCAC
CRRM2-BamHI-rev	gcccagaagtctctgcacatg tga ggatcc atg	TC6C-S1628-A-rev	GTGGCCAGCGTCGgcGCGTACCAGGCCATG
CRRM3-NotI-for	cat gcggccgc cacatgtgcgtcctgggaaac	TC6C-S1011-A-fwd	CTCCAAAGAGTCTgCCGTGGACC
CRRM3-BamHI-rev	cat ggatcc tcattgggctaagaagcgattcacttc	TC6C-S1011-A-rev	GGTCCACGGcAGACTCTTTGGAG
pGEX-QC-NotI-F	GGATCTGGAAGTTCTGTTCCAGCGGCCGCTGTGATC CCCGGAATTCGATTGTC	TC6C-T1016-A-fwd	GTGGACCGCCCCgcCTTTCTTGACAAG
pGEX-QC-NotI-R	GACAATCGAATTCCGGGGATCACAGCGGCCGCTGGA ACAGAACTTCCAGATCC	TC6C-T1016-A-rev	CTTGTCAAGAAAGgcGGGGCGGTCCAC
pGEX-QC-BamHI-F	GATGGGGGGAGCTCTGAGCGGATCCATCGTGACTG ACTGACGATC	TC6C-S714-A-fwd	GGAAGAACCCgCTCCACCGTCC
pGEX-QC-BamHI-R	GATCGTCAGTCAGTCACGATGGATCCGCTCAGAGCT CCCCCCATC	TC6C-S714-A-rev	GGACGGTGGAGcGGGTTCTTCC
CRRM2r-BamHI-rev	cat ggatcc tca catgtgcagagacttctgggc	TC6C-S465-A-fwd	GAATTTGAAGAAgCCCCTAGGTCTG
RFOX2-g1-f	cacc GCGTACTTCCGTAGAGTGTCAGG	TC6C-S465-A-rev	CAGACCTAGGGGcTTCTTCAAATTC

RFOX2-g1-r	caaa CCTGACACTCTACGGAAGTACGC
RFOX2-g2-f	cacc CGGAAGTACGCAAGCCCACGGGG
RFOX2-g2-r	caaa CCCCGTGGGCTTGCGTACTTCCG
CRIPPCR_FOX_for	CGCAGAATGGAATTCCCACAGAG
CRIPPCR_FOX_rev	cCGTAAGAGATCCATTTTGTGTGC
SYNC_hs_nhei-f	Agt gctagcATGGTGCTAGCAGAGCTGTAC
NONO_hs_fsei-f	Agt ggccggccatgcagagtaataaaacttttaacttg
NCOA5_hs_noti-f	Agt gcggccgc atgaatacggctccatcaagac
TIAR_hs_nhei-f	Agt gctagc atgatggaagacgacgggcag
PTCD3_hs_nhei-f	Agt gctagc atggcggttgtatctgctgttc
KRI1_hs_nhei-f	Agt gctagc atgggccacagaaccgccatg
ZCHC3_hs_fsei-f	Agt ggccggcc atggccaccggcggcggc
SYNC_hs_bamhi-r	Agt ggatcc TTATGGCGTGCAACGCTGGAC
NONO_hs_asci-r	Agt ggcgcgcc ttagtatcggcgacgtttgtttg
NCOA5_hs_ecori-r	Agt gaattc tcagtaatgcctctggtaagatc
TIAR_hs_bamhi-r	Agt ggatcc tcactgtgtttggtaacttgccatac
PTCD3_hs_bamhi-r	Agt ggatcc tcatttgccttcactggtgtcac
KRI1_hs_bamhi-r	Agt ggatcc tcaggagctgttcttgggcccctg
ZCHC3_hs_asci-r	Agt ggcgcgcc ttagtgcccggccacgccgg
pGEM-QC-NheI-fwd	GAATTGGGCCCGACGTCGCtaGCTCCCGGCCGCCATG
pGEM-QC-NheI-rev	CATGGCGGCCGGGAGCtaGCGACGTCGGGCCCAATT C
TC6A-1-NheI-fwd	atg gctagc atggatgctgattctgcc
TC6A-1-SpeI-rev	gtg actagt atcattaccattagggctag
TC6A-2-SpeI-fwd	cac actagt tctgtatcagggtggggcgatc
TC6A-2-SacI-rev	gtg gagctc aggtgtagtgtggggcatg
TC6A-3-SacI-fwd	aag gagctc caaaaagggccatcacc
TC6A-3-EcoRI-rev	ggtggagagtccatgtaa gaattc agtcg
A-TSS736/8/9AAA-fwd	gctgct cctagaggggaacgaaagac
A-TSS736/8/9AAA-rev	ttccgc atcccaggcagtattctgc
A-TSS736/8/9EEE-fwd	gaggaa cctagaggggaacgaaagac
A-TSS736/8/9EEE-rev	ttcttc atcccaggcagtattctgc
TC6C-S1358-A-fwd	GAGTCACCAGCCgcTCCTCCCGTAGC
TC6C-S1358-A-rev	GCTACGGGAGGAgcGGCTGGTGACTC
TC6C-S568-A-fwd	CAGGAGGACAAGgCACCCACCTGG
TC6C-S568-A-rev	CCAGGTGGGTGcCTTGTCCTCCTG
TC6C-T484-A-fwd	GGTTGTGCAGCTgCTCAGGCTTC
TC6C-T484-A-rev	GAAGCCTGAGcAGCTGCACAACC
TC6C-T777-E-fwd	CACCACACACAGGGTCGAGgaaCCGCCCCCGCAC
TC6C-T777-E-rev	GTGCGGGGGCGGttcCTCGACCCTGTGTGTGGTG
TC6C-S1628-E-fwd	CATGGCCTGGTACGCgaaGACGCTGGCCAC
TC6C-S1628-E-rev	GTGGCCAGCGTCttcGCGTACCAGGCCATG
TC6C-S1011-E-fwd	CTCCAAAGAGTCTgaaGTGGACC
TC6C-S1011-E-rev	GGTCCACttcAGACTCTTTGGAG
TC6C-T1016-E-fwd	GTGGACCGCCCCgaaTTTCTTGACAAG
TC6C-T1016-E-rev	CTTGTCAAGAAAttcGGGGCGGTCCAC
TC6C-S714-E-fwd	GGAAGAACCCgaaCCACCGTCC
TC6C-S714-E-rev	GGACGGTGGttcGGGTTCTTCC
TC6C-S465-E-fwd	GAATTTGAAGAAgaaCCTAGGTCTG
TC6C-S465-E-rev	CAGACCTAGGttcTTCTTCAAATTC
TC6C-S1358-E-fwd	GAGTCACCAGCCgaaCCTCCCGTAGC
TC6C-S1358-E-rev	GCTACGGGAGGttcGGCTGGTGACTC
TC6C-S568-E-fwd	CAGGAGGACAAGgaaCCCACCTGG
TC6C-S568-E-rev	CCAGGTGGGttcCTTGTCCTCCTG
TC6C-T484-E-fwd	GGTTGTGCAGCTgaaCAGGCTTC
TC6C-T484-E-rev	GAAGCCTGttcAGCTGCACAACC

5.2 List of figures

5.3 List of tables

5.4 List of abbreviations

_	Deletion	min	minute
aa	amino acid	Mio	million, 106
AEBSF	4-(2-aminoethyl) benzenesulfonyl .uoride hydrochloride	miRISC	miRNA induced silencing complex
Ago	Argonaute	miRNA	microRNA
Ago-APP	Ago a nity puri€cation by peptides	miRNP	micro-ribonucleoprotein
Amp	ampicillin	MKK	MAPK kinase
APS	ammonium persulphate	mRNA	messenger RNA
ATP	adenosine triphosphate	MS	mass spectrometry, mass spectrometric
bp	base pair(s)	Neo	neomycine
BSA	bovine serum albumin	NES	nuclear localization signal
C. elegans	Caenorhabditis elegans	NLS	nuclear export signal
cDNA	complementary DNA	NMR	nuclear magnetic resonance
CDS	coding sequence	NSC	neural stem cell
Ci	Curie	nt	nucleotides(s)
CoIP	co-immunoprecipitation	o/n	over night
CSC	cancer stem cell	OD	optical density
CTD	C-Terminal domain	ORF	open reading frame
cv	column volume	PABP	poly(A)-binding protein
D. melanogaster	Drosophila melanogaster	PACT	protein activator of the interferon-induced protein kinase
Da	Dalton	PAGE	polyacrylamide gel electrophoresis
DCL	-3 Dicer-like 3	PAM2	PABP interacting motif 2
DMEM	Dulbecco's Modi€ed Eagle's Medium	PAN2/3	PAB-dependent poly(A)-speci€c ribonuclease subunit 2/3
DNA	deoxyribonucleic acid	PAR-CLIP	Photoactivatable-Ribonucleoside-Enhanced Crosslinking and IP
dNTP	deoxynucleoside triphosphate	PAZ	PIWI-Argonaute-Zwille
ds	double-stranded	P-bodies	processing bodies
dsRBD	double-stranded RNA binding domain	PBS	Phosphate buffered saline
dT	desoxythymidine	PBS(-T)	phosphate-buffered saline (containing Tween 20)
DTT	dithiothreitol	PCR	polymerase chain reaction
DUF	domain of unknown function	piRNA	Piwi-interacting RNA
EDC	1-ethyl-3-(3-dimethyl-aminopropyl)-carbodiimid		
EDTA	ethylenediaminetetraacetic acid		
EGFR	epithelial growth factor receptor	piRNA	PIWI-interacting RNA
eIF	eukaryotic initiation factor	PIWI	P-element-induced wimpy testes
ERK	extracellular signal–regulated protein kinases	PNK	polynucleotide kinase
EtBr	ethidium bromide	pre-miRNA	precursor miRNA
Exp	Exportin	pri-miRNA	primary miRNA
FBS	fetal bovie serum	PTGS	post-transcriptional gene silencing
FDR	false discovery rate	PTM	post-translational modification
g	gram	PTP1B	protein tyrosine phosphatase 1B
GAPDH	glyceraldehyde 3-phosphate dehydrogenase	qRT-PCR	quantitative real-time polymerase chain reaction
GDP	guanosine diphosphate	RAS	rat sarcoma
GFP	green fluorescent protein	RdDM	RNA-dependent DNA methylation
GSH	glutathione	RdRP	RNA-dependent RNA polymerase
GSK3	glycogen synthase kinase 3_	RIPA	radioimmunoprecipitation assay
GST	glutahione-S-transferase	RISC	RNA-induced silencing complex
GTP	guanosine triphosphate	RNA	ribonucleic acid
h	hour	RNAi	RNA interference
H. sapiens	Homo sapiens	RNP	ribonucleoprotein
HA	hemagglutinin	ROS	reactive oxygen species

HEK 293T	human embryonic kidney 293T
HEPES	4-(2-hydroxyethyl)-1-piperazineethanesulfonic acid
HMGA2	high mobility group AT hook 2
HSP90	heat shock protein 90
IDA	iminodiacetate
Imp	Importin
IP	immunoprecipitation
IPTG	isopropyl _-D-1-thiogalactopyranoside
IRES	internal ribosome entry site
k	kilo
Kana	kanamycin
kb	kilobase
l	liter
LB	lysogeny broth
M	molar
MAPK	MAP (mitogen-activated protein) kinase
MAPKAPK2	MAP-activated protein kinase 2
MCS	multiple cloning site
mHESM	miRNAs regulated by hypoxia-dependent EGFR-suppressed maturation
rpm	revolutions per minute
RRM	RNA recognition motif
RT	room temperature
S. cerevisiae	Saccharomyces cerevisiae
sDMA	symmetric dimethyl arginine
SDS	sodium dodecyl sulfate
sec	second
shRNA	short hairpin RNA
siRNA	small interfering RNA
snoRNA	small nucleolar RNA
SRM	selected reaction monitoring
ss	single-stranded
SSC	saline-sodium citrate bu.er
TBE T	Tris/Borate/EDTA buffer
TBS	Tris buffered saline
TBS(-T)	Tris-bu.ered saline (containing Tween 20)
TEMED	tetramethylethylenediamine
TRBP	transactivating response RNA binding protein
TRIM71	tripartite motif-containing protein 71
tRNA	transfer RNA
UBA	ubiquitin-associated
UTP	uridine triphosphate
UTR	untranslated region
W	tryptophan
w/v	weight per volume
wt	wild type
YAP	Yes-associated protein

6 REFERENCES

Adam, S A, T Nakagawa, M S Swanson, T K Woodruff, and G Dreyfuss. 1986. “mRNA Polyadenylate-Binding Protein: Gene Isolation and Sequencing and Identification of a Ribonucleoprotein Consensus Sequence.” *Molecular and Cellular Biology* 6 (8): 2932–43. doi:10.1128/MCB.6.8.2932.

Ajiro, Masahiko, Rong Jia, Yanqin Yang, Jun Zhu, and Zhi Ming Zheng. 2015. “A Genome Landscape of SRSF3-Regulated Splicing Events and Gene Expression in Human Osteosarcoma U2OS Cells.” *Nucleic Acids Research* 44 (4): 1854–70. doi:10.1093/nar/gkv1500.

Alessi, Amelia F., Vishal Khivansara, Ting Han, Mallory A. Freeberg, James J. Moresco, Patricia G. Tu, Eric Montoye, John R. Yates, Xantha Karp, and John K. Kim. 2015. “Casein Kinase II Promotes Target Silencing by miRISC through Direct Phosphorylation of the DEAD-Box RNA Helicase CGH-1.” *Proceedings of the National Academy of Sciences*, 201509499. doi:10.1073/pnas.1509499112.

Amen, Alexandra M., Claudia R. Ruiz-Garzon, Jay Shi, Megha Subramanian, Daniel L. Pham, and Mollie K. Meffert. 2017. “A Rapid Induction Mechanism for Lin28a in Trophic Responses.” *Molecular Cell* 65 (3). Elsevier: 490–503.e7. doi:10.1016/j.molcel.2016.12.025.

Ameyar-Zazoua, Maya, Christophe Rachez, Mouloud Souidi, Philippe Robin, Lauriane Fritsch, Robert Young, Nadya Morozova, et al. 2012. “Argonaute Proteins Couple Chromatin Silencing to Alternative Splicing.” *Nature Structural & Molecular Biology* 19 (10). Nature Publishing Group: 998–1004. doi:10.1038/nsmb.2373.

Anantharaman, Vivek. 2002. “Comparative Genomics and Evolution of Proteins Involved in RNA Metabolism.” *Nucleic Acids Research* 30 (7): 1427–64. doi:10.1093/nar/30.7.1427.

Anderson, Paul, and Nancy Kedersha. 2008. “Stress Granules: The Tao of RNA Triage.” *Trends in Biochemical Sciences* 33 (3): 141–50. doi:10.1016/j.tibs.2007.12.003.

Androsavich, John R., and B. Nelson Chau. 2014. “Non-Inhibited miRNAs Shape the Cellular Response to Anti-miR.” *Nucleic Acids Research* 42 (11): 6945–55. doi:10.1093/nar/gku344.

Antonicka, Hana, Florin Sasarman, Tamiko Nishimura, Vincent Paupe, and Eric A. Shoubridge. 2013. “The Mitochondrial RNA-Binding Protein GRSF1 Localizes to RNA Granules and Is Required for Posttranscriptional Mitochondrial Gene Expression.” *Cell Metabolism* 17 (3). Elsevier Inc.: 386–98. doi:10.1016/j.cmet.2013.02.006.

Arcangeletti, Maria-Cristina, Rosita Vasile Simone, Isabella Rodighiero, Flora De Conto, Maria-Cristina Medici, Clara Maccari, Carlo Chezzi, and Adriana Calderaro. 2016. “Human Cytomegalovirus Reactivation from Latency: Validation of A ‘switch’ model in Vitro.” *Virology Journal* 13 (1). Virology Journal: 179. doi:10.1186/s12985-016-0634-z.

Aukrust, Ingvild, Linn Andersen Rosenberg, Mia Madeleine Ankerud, Vibeke Bertelsen, Hanne Hollås, Jaakko Saraste, Ann Kari Grindheim, and Anni Vedeler. 2017. “Post-Translational Modifications of Annexin A2 Are Linked to Its Association with Perinuclear Nonpolysomal mRNP Complexes.” *FEBS Open Bio* 7 (2): 160–73. doi:10.1002/2211-5463.12173.

Auyeung, Vincent C., Igor Ulitsky, Sean E. McGeary, and David P. Bartel. 2013. “Beyond Secondary Structure: Primary-Sequence Determinants License Pri-miRNA Hairpins for Processing.” *Cell* 152 (4). Elsevier Inc.: 844–58. doi:10.1016/j.cell.2013.01.031.

Avis, J M, F H Allain, P W Howe, G Varani, K Nagai, and D Neuhaus. 1996. “Solution Structure of the N-Terminal RNP Domain of U1A Protein: The Role of C-Terminal Residues in Structure Stability and RNA Binding.” *Journal of Molecular Biology* 257 (2): 398–411. doi:10.1006/jmbi.1996.0171.

Avraham, Roi, and Yosef Yarden. 2012. “Regulation of Signalling by microRNAs.” *Biochemical Society Transactions* 40 (1): 26–30.

doi:10.1042/BST20110623.

Ayache, Jessica, Marianne Bénard, Michèle Ernoult-Lange, Nicola Minshall, Nancy Standart, Michel Kress, and Dominique Weil. 2015. "P-Body Assembly Requires DDX6 Repression Complexes rather than Decay or Ataxin2/2L Complexes." *Molecular Biology of the Cell* 26: 1–30. doi:10.1091/mbc.E15-03-0136.

Baber, James L., Daniel Libutti, David Levens, and Nico Tjandra. 1999. "High Precision Solution Structure of the C-Terminal KH Domain of Heterogeneous Nuclear Ribonucleoprotein K, a c-Myc Transcription Factor." *Journal of Molecular Biology* 289 (4): 949–62. doi:10.1006/jmbi.1999.2818.

Baillat, David, and Ramin Shiekhattar. 2009. "Functional Dissection of the Human TNRC6 (GW182-Related) Family of Proteins." *Molecular and Cellular Biology* 29 (15): 4144–55. doi:10.1128/MCB.00380-09.

Baltz, Alexander G., Mathias Munschauer, Bj??rn Schwanh??usser, Alexandra Vasile, Yasuhiro Murakawa, Markus Schueler, Noah Youngs, et al. 2012. "The mRNA-Bound Proteome and Its Global Occupancy Profile on Protein-Coding Transcripts." *Molecular Cell* 46 (5): 674–90. doi:10.1016/j.molcel.2012.05.021.

Barman, Bahnisikha, and Suvendra N. Bhattacharyya. 2015. "mRNA Targeting to Endoplasmic Reticulum Precedes Ago Protein Interaction and MicroRNA (miRNA)-Mediated Translation Repression in Mammalian Cells." *Journal of Biological Chemistry* 290 (41): 24650–56. doi:10.1074/jbc.C115.661868.

Behm-Ansmant, Isabelle, Jan Rehwinkel, Tobias Doerks, Alexander Stark, Peer Bork, and Elisa Izaurralde. 2006. "MRNA Degradation by miRNAs and GW182 Requires Both CCR4 : NOT Deadenylase and DCP1 : DCP2 Decapping Complexes." *Genes & Development* 20: 1885–1898 ST–MRNA degradation by miRNAs and GW1. doi:10.1101/gad.1424106.

Beltran, Pierre M Jean, and Ileana M Cristea. 2015. "The Lifecycle and Pathogenesis of Human Cytomegalovirus Infection: Lessons from Proteomics." *Expert Rev Proteomics* 11 (6): 697–711. doi:10.1586/14789450.2014.971116.The.

Béthune, Julien, Caroline G Artus-Revel, and Witold Filipowicz. 2012. "Kinetic Analysis Reveals Successive Steps Leading to miRNA-Mediated Silencing in Mammalian Cells." *EMBO Reports* 13 (8): 716–23. doi:10.1038/embor.2012.82.

Blom, Nikolaj, Thomas Sicheritz-Pontén, Ramneek Gupta, Steen Gammeltoft, and Søren Brunak. 2004. "Prediction of Post-Translational Glycosylation and Phosphorylation of Proteins from the Amino Acid Sequence." *Proteomics* 4 (6): 1633–49. doi:10.1002/pmic.200300771.

Boersema, Paul J., Shabaz Mohammed, and Albert J.R. Heck. 2009. "Phosphopeptide Fragmentation and Analysis by Mass Spectrometry." *Journal of Mass Spectrometry* 44 (6): 861–78. doi:10.1002/jms.1599.

Bohnsack, Markus T, Kevin Czaplinski, and Dirk Gorlich. 2004. "Exportin 5 Is a RanGTP-Dependent dsRNA-Binding Protein That Mediates Nuclear Export of Pre-miRNAs." *RNA (New York, N.Y.)* 10 (2): 185–91. doi:10.1261/rna.5167604.

Braun, Joerg E., Eric Huntzinger, Maria Fauser, and Elisa Izaurralde. 2011. "GW182 Proteins Directly Recruit Cytoplasmic Deadenylase Complexes to miRNA Targets." *Molecular Cell* 44 (1). Elsevier Inc.: 120–33. doi:10.1016/j.molcel.2011.09.007.

Briata, P, W-J Lin, M Giovarelli, M Pasero, C-F Chou, M Trabucchi, M G Rosenfeld, C-Y Chen, and R Gherzi. 2012. "PI3K/AKT Signaling Determines a Dynamic Switch between Distinct KSRP Functions Favoring Skeletal Myogenesis." *Cell Death and Differentiation* 19 (3): 478–87. doi:10.1038/cdd.2011.117.

Bridge, Katherine S., Kunal M. Shah, Yigen Li, Daniel E. Foxler, Sybil C.K. Wong, Duncan C. Miller, Kathryn M. Davidson, et al. 2017. "Argonaute Utilization for miRNA Silencing Is Determined by Phosphorylation-Dependent Recruitment of LIM-Domain-Containing Proteins." *Cell Reports* 20 (1). ElsevierCompany.: 173–87. doi:10.1016/j.celrep.2017.06.027.

Brook, Matthew, and Nicola K Gray. 2012. "The Role of Mammalian poly(A)-Binding Proteins in Co-Ordinating mRNA Turnover." *Biochemical Society Transactions* 40 (4): 856–64. doi:10.1042/BST20120100.

Brook, Matthew, Lora McCracken, James P. Reddington, Zhi‐Liang Lu, Nicholas A. Morrice, and Nicola K. Gray. 2012. "The Multifunctional poly(A)-Binding Protein (PABP) 1 Is Subject to Extensive Dynamic Post-Translational Modification, Which Molecular Modelling Suggests Plays an Important Role in Co-Ordinating Its Activities." *Biochemical Journal* 441 (3): 803–12. doi:10.1042/BJ20111474.

Bruscella, Patrice, Silvia Bottini, Camille Baudesson, Jean Michel Pawlotsky, Cyrille Feray, and Michele Trabucchi. 2017. "Viruses and miRNAs: More Friends than Foes." *Frontiers in Microbiology* 8 (MAY): 1–11. doi:10.3389/fmicb.2017.00824.

Buchan, J. Ross, and Roy Parker. 2009. "Eukaryotic Stress Granules: The Ins and Outs of Translation." *Molecular Cell* 36 (6). Elsevier Ltd: 932–41. doi:10.1016/j.molcel.2009.11.020.

Buchberger, Alexander. 2002. "From UBA to UBX: New Words in the Ubiquitin Vocabulary." *Trends in Cell Biology* 12 (5): 216–21. doi:10.1016/S0962-8924(02)02269-9.

Burger, Kaspar, Margarita Schlackow, Martin Potts, Svenja Hester, Shabaz Mohammed, and Monika Gullerova. 2017. "Nuclear Phosphorylated Dicer Processes Double-Stranded RNA in Response to DNA Damage." *The Journal of Cell Biology*,

jcb.201612131. doi:10.1083/jcb.201612131.

Cai, Xuezhong, Curt H Hagedorn, and Bryan R Cullen. 2004. "Human microRNAs Are Processed from Capped, Polyadenylated Transcripts That Can Also Function as mRNAs." *RNA (New York, N.Y.)* 10 (12): 1957–66. doi:10.1261/rna.7135204.

Carl, Joseph W, Joanne Trgovcich, and Sridhar Hannenhalli. 2013. "Widespread Evidence of Viral miRNAs Targeting Host Pathways." *BMC Bioinformatics* 14 Suppl 2 (Suppl 2). BioMed Central Ltd: S3. doi:10.1186/1471-2105-14-S2-S3.

Casseb, S. M M, D. B. Simith, K. F L Melo, M. H. Mendon??a, A. C M Santos, V. L. Carvalho, A. C R Cruz, and P. F C Vasconcelos. 2016. "Drosha, DGCR8, and Dicer mRNAs Are down-Regulated in Human Cells Infected with Dengue Virus 4, and Play a Role in Viral Pathogenesis." *Genetics and Molecular Research* 15 (2): 3–4. doi:10.4238/gmr.15027891.

Castello, Alfredo, Bernd Fischer, Katrin Eichelbaum, Rastislav Horos, Benedikt M. Beckmann, Claudia Strein, Norman E. Davey, et al. 2012. "Insights into RNA Biology from an Atlas of Mammalian mRNA-Binding Proteins." *Cell* 149 (6). Elsevier Inc.: 1393–1406. doi:10.1016/j.cell.2012.04.031.

Chang, Hao-ming, Robinson Triboulet, James E Thornton, and Richard I Gregory. 2013. "A Role for the Perlman Syndrome Exonuclease Dis3l2 in the Lin28-Let-7 Pathway." *Nature* 497 (7448). Nature Publishing Group: 244–48. doi:10.1038/nature12119.

Chang, Hyeshik, Jaechul Lim, Minju Ha, and V. Narry Kim. 2014. "TAIL-Seq: Genome-Wide Determination of poly(A) Tail Length and 3' End Modifications." *Molecular Cell* 53 (6). Elsevier Inc.: 1044–52. doi:10.1016/j.molcel.2014.02.007.

Chaston, Jessica J., Alastair Gordon Stewart, Mary Christie, EJ Dodson, P Emsley, and PR Evans. 2017. "Structural Characterisation of TNRC6A Nuclear Localisation Signal in Complex with Importin-Alpha." *Plos One* 12 (8): e0183587. doi:10.1371/journal.pone.0183587.

Chaulk, Steven G, Gina L. Thede, Oliver a. Kent, Zhizhong Xu, Emily Gesner, Richard a. Veldhoen, Suneil K. Khanna, et al. 2011. "Role of Pri-miRNA Tertiary Structure in miR-17~92 miRNA Biogenesis." *RNA Biology* 8 (6): 1105–14. doi:10.4161/rna.8.6.17410.

Chekulaeva, Marina, Witold Filipowicz, and Roy Parker. 2009. "Multiple Independent Domains of dGW182 Function in miRNA-Mediated Repression in Drosophila." *RNA (New York, N.Y.)* 15 (5): 794–803. doi:10.1261/rna.1364909.

Chekulaeva, Marina, Hansruedi Mathys, Jakob T Zipprich, Jan Attig, Marija Colic, Roy Parker, and Witold Filipowicz. 2011a. "miRNA Repression Involves GW182-Mediated Recruitment of CCR4–NOT through Conserved W-Containing Motifs." *Nature Structural & Molecular Biology* 18 (11). Nature Publishing Group: 1218–26. doi:10.1038/nsmb.2166.

———. 2011b. "miRNA Repression Involves GW182-Mediated Recruitment of CCR4–NOT through Conserved W-Containing Motifs." *Nature Structural & Molecular Biology* 18 (11): 1218–26. doi:10.1038/nsmb.2166.

Chen, Cheng, Changhong Zhu, Jian Huang, Xian Zhao, Rong Deng, Hailong Zhang, Jinzhuo Dou, et al. 2015. "SUMOylation of TARBP2 Regulates miRNA/siRNA Efficiency." *Nature Communications* 6. Nature Publishing Group: 8899. doi:10.1038/ncomms9899.

Chen, Chun Jung, Jennifer E Cox, Kristopher Azarm, Karen N Wylie, D Kevin, Patricia A Pesavento, and Christopher S Sullivan. 2016. "NIH Public Access," 43–53. doi:10.1016/j.virol.2014.11.021.Identification.

Chen, Jianfu, Fan Lai, and Lee Niswander. 2012. "The Ubiquitin Ligase mLin41 Temporally Promotes Neural Progenitor Cell Maintenance through FGF Signaling." *Genes and Development* 26 (8): 803–15. doi:10.1101/gad.187641.112.

Chen, Ying, Andreas Boland, Duygu Kuzuoğlu-Öztürk, Praveen Bawankar, Belinda Loh, Chung Te Chang, Oliver Weichenrieder, and Elisa Izaurralde. 2014. "A DDX6-CNOT1 Complex and W-Binding Pockets in CNOT9 Reveal Direct Links between miRNA Target Recognition and Silencing." *Molecular Cell* 54 (5): 737–50. doi:10.1016/j.molcel.2014.03.034.

Chen, Yu, Lorena Zubovic, Fan Yang, Katherine Godin, Tom Pavelitz, Javier Castellanos, Paolo MacChi, and Gabriele Varani. 2016. "Rbfox Proteins Regulate microRNA Biogenesis by Sequence-Specific Binding to Their Precursors and Target Downstream Dicer." *Nucleic Acids Research* 44 (9): 4381–95. doi:10.1093/nar/gkw177.

Chendrimada, Thimmaiah P, Richard I Gregory, Easwari Kumaraswamy, Neil Cooch, Kazuko Nishikura, and Ramin Shiekhattar. 2010. "TRBP Recruits the Dicer Complex to Ago2 for microRNA Processing and Gene Silencing" 436 (7051): 740–44. doi:10.1038/nature03868.TRBP.

Cho, Charles J., Seung Jae Myung, and Suhwan Chang. 2017. "ADAR1 and MicroRNA; a Hidden Crosstalk in Cancer." *International Journal of Molecular Sciences* 18 (4). doi:10.3390/ijms18040799.

Choy, Elizabeth Yee-Wai, Kam-Leung Siu, Kin-Hang Kok, Raymond Wai-Ming Lung, Chi Man Tsang, Ka-Fai To, Dora Lai-Wan Kwong, Sai Wah Tsao, and Dong-Yan Jin. 2008. "An Epstein-Barr Virus-Encoded microRNA Targets PUMA to Promote Host Cell Survival." *The Journal of Experimental Medicine* 205 (11): 2551–60. doi:10.1084/jem.20072581.

Christie, Mary, Andreas Boland, Eric Huntzinger, Oliver Weichenrieder, and Elisa Izaurralde. 2013. "Structure of the PAN3 Pseudokinase Reveals the Basis for Interactions with the PAN2 Deadenylase and the GW182 Proteins." *Molecular Cell* 51 (3). Elsevier Inc.: 360–73. doi:10.1016/j.molcel.2013.07.011.

Cobbs, Charles S, Lualhati Harkins, Minu Samanta, G Yancey Gillespie, Suman Bharara, Peter H King, L Burt Nabors, C Glenn Cobbs, and

William J Britt. 2002. “Human Cytomegalovirus Infection and Expression in Human Malignant Glioma 1,” 3347–50.

Collart, Martine A. 2016. “The Ccr4-Not Complex Is a Key Regulator of Eukaryotic Gene Expression.” *Wiley Interdisciplinary Reviews: RNA* 7 (4): 438–54. doi:10.1002/wrna.1332.

Collart, Martine A., Olesya O. Panasenko, and Sergey I. Nikolaev. 2013. “The Not3/5 Subunit of the Ccr4-Not Complex: A Central Regulator of Gene Expression That Integrates Signals between the Cytoplasm and the Nucleus in Eukaryotic Cells.” *Cellular Signalling* 25 (4). Elsevier Inc.: 743–51. doi:10.1016/j.cellsig.2012.12.018.

Connerty, Patrick, Alireza Ahadi, and Gyorgy Hutvagner. 2015. “RNA Binding Proteins in the miRNA Pathway.” *International Journal of Molecular Sciences* 17 (1). doi:10.3390/ijms17010031.

Cullen, Bryan R. 2004. “Transcription and Processing of Human microRNA Precursors.” *Molecular Cell* 16 (6): 861–65. doi:10.1016/j.molcel.2004.12.002.

Cullen, Rebecca L. Skalsky and Bryan R. 2013. “Viruses, microRNAs, and Host Interactions,” no. Pol II: 123–41. doi:10.1146/annurev.micro.112408.134243.Viruses.

Davis, B N, A C Hilyard, G Lagna, and A Hata. 2008. “SMAD Proteins Control DROSHA-Mediated microRNA Maturation.” *Nature* 454 (7200): 56–61. doi:10.1038/nature07086.

Danner J.; Pai B., Wankerl L. and Gunter Meister. 2017. "Peptide-based inhibition of miRNA-guided gene silencing."Methods Mol. Biol.:199-210.doi: 10.1007/978-1-4939-6563-2_14.

Denli, Ahmet M, Bastiaan B J Tops, Ronald H a Plasterk, René F Ketting, and Gregory J Hannon. 2004. “Processing of Primary microRNAs by the Microprocessor Complex.” *Nature* 432 (7014): 231–35. doi:10.1038/nature03049.

Denzler, R??my, Sean E. McGeary, Alexandra C. Title, Vikram Agarwal, David P. Bartel, and Markus Stoffel. 2016. “Impact of MicroRNA Levels, Target-Site Complementarity, and Cooperativity on Competing Endogenous RNA-Regulated Gene Expression.” *Molecular Cell* 64 (3): 565–79. doi:10.1016/j.molcel.2016.09.027.

Deo, Rahul C., Jeffrey B. Bonanno, Nahum Sonenberg, and Stephen K. Burley. 1999. “Recognition of Polyadenylate RNA by the poly(A)-Binding Protein.” *Cell* 98 (6): 835–45. doi:10.1016/S0092-8674(00)81517-2.

Detzer, Anke, Christina Engel, Winfried Wünsche, and Georg Sczakiel. 2011. “Cell Stress Is Related to Re-Localization of Argonaute 2 and to Decreased RNA Interference in Human Cells.” *Nucleic Acids Research* 39 (7): 2727–41. doi:10.1093/nar/gkq1216.

Dhuruvasan, Kavitha, Geetha Sivasubramanian, and Philip E. Pellett. 2011. “Roles of Host and Viral microRNAs in Human Cytomegalovirus Biology.” *Virus Research* 157 (2): 180–92. doi:10.1016/j.virusres.2010.10.011.

Diebel, Kevin W, Anna L Smith, and Linda F van Dyk. 2010. “Mature and Functional Viral miRNAs Transcribed from Novel RNA Polymerase III Promoters.” *RNA (New York, N.Y.)* 16 (1): 170–85. doi:10.1261/rna.1873910.

Ding, Jianzhong, Mariko K. Hayashi, Ying Zhang, Lisa Manche, Adrian R. Krainer, and Rui Ming Xu. 1999. “Crystal Structure of the Two-RRM Domain of hnRNP A1 (UP1) Complexed with Single-Stranded Telomeric DNA.” *Genes and Development* 13 (9): 1102–15. doi:10.1101/gad.13.9.1102.

Djuranovic, Sergej, Ali Nahvi, and Rachel Green. 2012. “miRNA-Mediated Gene Silencing” 336 (April): 237–41.

Dölken, Lars, Astrid Krmpotic, Sheila Kothe, Lee Tuddenham, Mélanie Tanguy, Lisa Marcinowski, Zsolt Ruzsics, et al. 2010. “Cytomegalovirus microRNAs Facilitate Persistent Virus Infection in Salivary Glands.” *PLoS Pathogens* 6 (10): 2–9. doi:10.1371/journal.ppat.1001150.

Dölken, Lars, Georg Malterer, Florian Erhard, Sheila Kothe, Caroline C. Friedel, Guillaume Suffert, Lisa Marcinowski, et al. 2010. “Systematic Analysis of Viral and Cellular microRNA Targets in Cells Latently Infected with Human γ-Herpesviruses by RISC Immunoprecipitation Assay.” *Cell Host and Microbe*. doi:10.1016/j.chom.2010.03.008.

Drake, Melanie, Tokiko Furuta, Kin Man Suen, Gabriel Gonzalez, Bin Liu, Awdhesh Kalia, John E. Ladbury, Andrew Z. Fire, James B. Skeath, and Swathi Arur. 2014. “A Requirement for ERK-Dependent Dicer Phosphorylation in Coordinating Oocyte-to-Embryo Transition in C.elegans.” *Developmental Cell* 31 (5). Elsevier Inc.: 614–28. doi:10.1016/j.devcel.2014.11.004.

Du, Peng, Longfei Wang, Piotr Sliz, and Richard I. Gregory. 2015. “A Biogenesis Step Upstream of Microprocessor Controls miR-17∼92 Expression.” *Cell* 162 (4). Elsevier Inc.: 885–99. doi:10.1016/j.cell.2015.07.008.

Dudek, Steven M, Eddie T Chiang, Sara M Camp, Yurong Guo, Jing Zhao, Mary E Brown, Patrick a Singleton, et al. 2010. “Abl Tyrosine Kinase Phosphorylates Nonmuscle Myosin Light Chain Kinase to Regulate Endothelial Barrier Function.” *Molecular Biology of the Cell* 21 (22): 4042–56. doi:10.1091/mbc.E09.

Dueck, Anne, and Gunter Meister. 2014. “Assembly and Function of Small RNA-Argonaute Protein Complexes.” *Biological Chemistry* 395 (6): 611–29. doi:10.1515/hsz-2014-0116.

Dueck, Anne, Christian Ziegler, Alexander Eichner, Eugene Berezikov, and Gunter Meister. 2012. “MicroRNAs Associated with the

Different Human Argonaute Proteins." *Nucleic Acids Research* 40 (19): 9850–62. doi:10.1093/nar/gks705.

Elkayam, Elad, Christopher R. Faehnle, Marjorie Morales, Jingchuan Sun, Huilin Li, and Leemor Joshua-Tor. 2017. "Multivalent Recruitment of Human Argonaute by GW182." *Molecular Cell*. Elsevier Inc., 1–13. doi:10.1016/j.molcel.2017.07.007.

Eulalio, Ana, Isabelle Behm-Ansmant, and Elisa Izaurralde. 2007. "P Bodies: At the Crossroads of Post-Transcriptional Pathways." *Nature Reviews Molecular Cell Biology* 8 (1): 9–22. doi:10.1038/nrm2080.

Eulalio, Ana, Isabelle Behm-Ansmant, Daniel Schweizer, and Elisa Izaurralde. 2007. "P-Body Formation Is a Consequence, Not the Cause, of RNA-Mediated Gene Silencing." *Molecular and Cellular Biology* 27 (11): 3970–81. doi:10.1128/MCB.00128-07.

Eulalio, Ana, Eric Huntzinger, Tadashi Nishihara, Jan Rehwinkel, Maria Fauser, and Elisa Izaurralde. 2009. "Deadenylation Is a Widespread Effect of miRNA Regulation." *RNA (New York, N.Y.)* 15 (1): 21–32. doi:10.1261/rna.1399509.

Eulalio, Ana, Felix Tritschler, Regina Budie;ttner, Oliver Weichenrieder, Elisa Izaurralde, and Vincent Truffault. 2009. "The RRM Domain in GW182 Proteins Contributes to miRNA-Mediated Gene Silencing." *Nucleic Acids Research* 37 (9): 2974–83. doi:10.1093/nar/gkp173.

Eulalio, Ana, Felix Tritschler, and Elisa Izaurralde. 2009. "The GW182 Protein Family in Animal Cells: New Insights into Domains Required for miRNA-Mediated Gene Silencing." *RNA (New York, N.Y.)* 15 (8): 1433–42. doi:10.1261/rna.1703809.

Eystathioy T, Chan EK, Tenenbaum SA, Keene JD, Griffith K, Fritzler MJ. 2002. "A Phosphorylated Cytoplasmic Autoantigen, GW182, Associates with a Unique Population of Human mRNAs within Novel Cytoplasmic Speckles." *Molecular Biology of the Cell* 13 (6): 2170–79. doi:10.1091/mbc.01.

Fabian, Marc R., Géraldine Mathonnet, Thomas Sundermeier, Hansruedi Mathys, Jakob T. Zipprich, Yuri V. Svitkin, Fabiola Rivas, et al. 2009. "Mammalian miRNA RISC Recruits CAF1 and PABP to Affect PABP-Dependent Deadenylation." *Molecular Cell* 35 (6): 868–80. doi:10.1016/j.molcel.2009.08.004.

Fabian, Marc R, Filipp Frank, Christopher Rouya, Nadeem Siddiqui, Wi S Lai, Alexey Karetnikov, Perry J Blackshear, Bhushan Nagar, and Nahum Sonenberg. 2013a. "Structural Basis for the Recruitment of the Human CCR4-NOT Deadenylase Complex by Tristetraprolin." *Nature Structural & Molecular Biology* 20 (6): 735–39. doi:10.1038/nsmb.2572.

———. 2013b. "Structural Basis for the Recruitment of the Human CCR4-NOT Deadenylase Complex by Tristetraprolin." *Nature Structural & Molecular Biology* 20 (6): 735–39. doi:10.1038/nsmb.2572.

Fabian, Marc R, and Nahum Sonenberg. 2012. "The Mechanics of miRNA-Mediated Gene Silencing: A Look under the Hood of miRISC." *Nature Structural & Molecular Biology* 19 (6). Nature Publishing Group: 586–93. doi:10.1038/nsmb.2296.

Fareh, Mohamed, Kyu-Hyeon Yeom, Anna C. Haagsma, Sweeny Chauhan, Inha Heo, and Chirlmin Joo. 2016. "TRBP Ensures Efficient Dicer Processing of Precursor microRNA in RNA-Crowded Environments." *Nature Communications* 7. Nature Publishing Group: 13694. doi:10.1038/ncomms13694.

Flamand, Mathieu N., Hin Hark Gan, Vinay K. Mayya, Kristin C. Gunsalus, and Thomas F. Duchaine. 2017. "A Non-Canonical Site Reveals the Cooperative Mechanisms of microRNA-Mediated Silencing." *Nucleic Acids Research* 45 (12): 1–14. doi:10.1093/nar/gkx340.

Flamand, Mathieu N., Edlyn Wu, Ajay Vashisht, Guillaume Jannot, Brett D. Keiper, Martin J. Simard, James Wohlschlegel, and Thomas F. Duchaine. 2016. "Poly(A)-Binding Proteins Are Required for microRNA-Mediated Silencing and to Promote Target Deadenylation in C. Elegans." *Nucleic Acids Research* 44 (12): 5924–35. doi:10.1093/nar/gkw276.

Fletcher, Claire E., Jack D. Godfrey, Akifumi Shibakawa, Martin Bushell, and Charlotte L. Bevan. 2017. "A Novel Role for GSK3β as a Modulator of Drosha Microprocessor Activity and MicroRNA Biogenesis." *Nucleic Acids Research* 45 (5): 2809–28. doi:10.1093/nar/gkw938.

Flores, Omar, Sanae Nakayama, Adam W Whisnant, Hassan Javanbakht, Bryan R Cullen, and David C Bloom. 2013. "Mutational Inactivation of Herpes Simplex Virus 1 microRNAs Identifies Viral mRNA Targets and Reveals Phenotypic Effects in Culture." *Journal of Virology* 87 (12): 6589–6603. doi:10.1128/JVI.00504-13.

Forte, Eleonora, and Micah a. Luftig. 2011. "The Role of microRNAs in Epstein-Barr Virus Latency and Lytic Reactivation." *Microbes and Infection* 13 (14–15). Elsevier Masson SAS: 1156–67. doi:10.1016/j.micinf.2011.07.007.

Frappier, Lori. 2012. "EBNA1 and Host Factors in Epstein-Barr Virus Latent DNA Replication." *Current Opinion in Virology* 2 (6). Elsevier B.V.: 727–33. doi:10.1016/j.coviro.2012.09.005.

Frohn, A, H C Eberl, J Stohr, E Glasmacher, S Rudel, V Heissmeyer, M Mann, and G Meister. 2012. "Dicer-Dependent and -Independent Argonaute2 Protein Interaction Networks in Mammalian Cells." *Mol Cell Proteomics* 11 (11): 1442–56. doi:10.1074/mcp.M112.017756.

Fruci, Doriana, Rossella Rota, and Angela Gallo. 2017. "The Role of HCMV and HIV-1 MicroRNAs: Processing, and Mechanisms of Action during Viral Infection." *Frontiers in Microbiology* 8 (APR): 1–7. doi:10.3389/fmicb.2017.00689.

Fukuda, Toru, Kaoru Yamagata, Sally Fujiyama, Takahiro Matsumoto, Iori Koshida, Kimihiro Yoshimura, Masatomo Mihara, et al. 2007.

"DEAD-Box RNA Helicase Subunits of the Drosha Complex Are Required for Processing of rRNA and a Subset of microRNAs." *Nature Cell Biology* 9 (5): 604–11. doi:10.1038/ncb1577.

Fukunaga, Ryuya. 2005. "Dicer Partner Proteins Tune the Length of Mature miRNAs in Flies and Mammals." *Biophysical Chemistry* 257 (5): 2432–37. doi:10.1016/j.immuni.2010.12.017.Two-stage.

Gagnon, KeithT, Liande Li, Yongjun Chu, BethanyA Janowski, and DavidR Corey. 2014. "RNAi Factors Are Present and Active in Human Cell Nuclei." *Cell Reports* 6 (1). The Authors: 211–21. doi:10.1016/j.celrep.2013.12.013.

Garc??a-Mayoral, Mar??a Flor, David Hollingworth, Laura Masino, Irene D??az-Moreno, Geoff Kelly, Roberto Gherzi, Chu Fang Chou, Ching Yi Chen, and Andres Ramos. 2007. "The Structure of the C-Terminal KH Domains of KSRP Reveals a Noncanonical Motif Important for mRNA Degradation." *Structure* 15 (4): 485–98. doi:10.1016/j.str.2007.03.006.

Gerstberger, Stefanie, Markus Hafner, and Thomas Tuschl. 2014. "A Census of Human RNA-Binding Proteins." *Nature Reviews Genetics* 15 (12). Nature Publishing Group: 829–45. doi:10.1038/nrg3813.

Gibbings, D, S Mostowy, F Jay, Y Schwab, P Cossart, and O Voinnet. 2012. "Selective Autophagy Degrades DICER and AGO2 and Regulates miRNA Activity." *Nat Cell Biol* 14 (12). Nature Publishing Group: 1314–21. doi:10.1038/ncb2611.

Gibbings, Derrick, Serge Mostowy, Florence Jay, and Yannick Schwab. 2013. "Europe PMC Funders Group Selective Autophagy Degrades DICER and AGO2 and Regulates miRNA Activity" 14 (12): 1314–21. doi:10.1038/ncb2611.Selective.

Giraldez, A J, R M Cinalli, M E Glasner, A J Enright, J M Thomson, S Baskerville, S M Hammond, D P Bartel, and A F Schier. 2005. "MicroRNAs Regulate Brain Morphogenesis in Zebrafish." *Science* 308 (5723): 833–38. doi:10.1126/science.1109020.

Glisovic, Tina, Jennifer L. Bachorik, Jeongsik Yong, and Gideon Dreyfuss. 2008. "RNA-Binding Proteins and Post-Transcriptional Gene Regulation." *FEBS Letters* 582 (14): 1977–86. doi:10.1016/j.febslet.2008.03.004.

Godshalk, Sirie E., Sumita Bhaduri-McIntosh, and Frank J. Slack. 2008. "Epstein-Barr Virus-Mediated Dysregulation of Human microRNA Expression." *Cell Cycle* 7 (22): 3595–3600. doi:10.4161/cc.7.22.7120.

Golden, Ryan J., Beibei Chen, Tuo Li, Juliane Braun, Hema Manjunath, Xiang Chen, Jiaxi Wu, et al. 2017. "An Argonaute Phosphorylation Cycle Promotes microRNA-Mediated Silencing." *Nature*. Nature Publishing Group, 1–6. doi:10.1038/nature21025.

Gregory, Richard I., Thimmaiah P. Chendrimada, Neil Cooch, and Ramin Shiekhattar. 2005. "Human RISC Couples microRNA Biogenesis and Posttranscriptional Gene Silencing." *Cell* 123 (4): 631–40. doi:10.1016/j.cell.2005.10.022.

Gregory, Richard I, Kai-Ping Yan, Govindasamy Amuthan, Thimmaiah Chendrimada, Behzad Doratotaj, Neil Cooch, and Ramin Shiekhattar. 2004. "The Microprocessor Complex Mediates the Genesis of microRNAs." *Nature* 432 (7014): 235–40. doi:10.1038/nature03120.

Grey, Finn, and Jay Nelson. 2008. "Identification and Function of Human Cytomegalovirus microRNAs." *Journal of Clinical Virology* 41 (3): 186–91. doi:10.1016/j.jcv.2007.11.024.

Grimm, D, K L Streetz, C L Jopling, T A Storm, K Pandey, C R Davis, P Marion, F Salazar, and M A Kay. 2006. "Fatality in Mice due to Oversaturation of Cellular microRNA/short Hairpin RNA Pathways." *Nature* 441 (7092): 537–41. doi:nature04791 [pii]10.1038/nature04791 [doi].

Grishin, N. V. 2001. "KH Domain: One Motif, Two Folds." *Nucleic Acids Research* 29 (3): 638–43. doi:10.1093/nar/29.3.638.

Grundhoff, Adam, and Christopher S Sullivan. 2012. "NIH Public Access" 411 (2): 325–43. doi:10.1016/j.virol.2011.01.002.Virus-encoded.

Grundhoff, Adam, and Christopher S. Sullivan. 2011. "Virus-Encoded microRNAs." *Virology* 411 (2). Elsevier Inc.: 325–43. doi:10.1016/j.virol.2011.01.002.

Grundhoff, Adam, Christopher S Sullivan, and Don Ganem. 2006. "A Combined Computational and Microarray-Based Approach Identifies Novel microRNAs Encoded by Human Gamma-Herpesviruses." *RNA (New York, N.Y.)* 12 (5): 733–50. doi:10.1261/rna.2326106.

Gu, Shuo, Lan Jin, Feijie Zhang, Yong Huang, Dirk Grimm, John J Rossi, and Mark a Kay. 2011. "Thermodynamic Stability of Small Hairpin RNAs Highly Influences the Loading Process of Different Mammalian Argonautes." *Proceedings of the National Academy of Sciences of the United States of America* 108 (22): 9208–13. doi:10.1073/pnas.1018023108.

Guil, Sonia, and Javier F Cáceres. 2007. "The Multifunctional RNA-Binding Protein hnRNP A1 Is Required for Processing of miR-18a." *Nature Structural & Molecular Biology* 14 (7): 591–96. doi:10.1038/nsmb1250.

Guo, Xin, Ying Qi, Yujing Huang, Zhongyang Liu, Yanping Ma, Yaozhong Shao, Shujuan Jiang, Zhengrong Sun, and Qiang Ruan. 2015. "Human Cytomegalovirus miR-US33-5p Inhibits Viral DNA Synthesis and Viral Replication by down-Regulating Expression of the Host Syntaxin3." *FEBS Letters* 589 (4). Federation of European Biochemical Societies: 440–46. doi:10.1016/j.febslet.2014.12.030.

Guo, Yanwen, Jun Liu, Sarah J. Elfenbein, Yinghong Ma, Mei Zhong, Caihong Qiu, Ye Ding, and Jun Lu. 2015. "Characterization of the Mammalian miRNA Turnover Landscape." *Nucleic Acids Research* 43 (4): 2326–41. doi:10.1093/nar/gkv057.

Gupta, Ishaan, Zoltan Villanyi, Sari Kassem, Christopher Hughes, Olesya O. Panasenko, Lars M. Steinmetz, and Martine A. Collart. 2016. "Translational Capacity of a Cell Is Determined during Transcription Elongation via the Ccr4-Not Complex." *Cell Reports* 15 (8). The Author(s): 1782–94. doi:10.1016/j.celrep.2016.04.055.

Ha, Minju, and V Narry Kim. 2014. "Regulation of microRNA Biogenesis." *Nat Rev Mol Cell Biol* 15 (8). Nature Publishing Group: 509–24. doi:10.1038/nrm3838.

Haar, Janina, Maud Contrant, Katharina Bernhardt, Regina Feederle, Sven Diederichs, Sébastien Pfeffer, and Henri-Jacques Delecluse. 2015. "The Expression of a Viral microRNA Is Regulated by Clustering to Allow Optimal B Cell Transformation." *Nucleic Acids Research* 44 (3): gkv1330. doi:10.1093/nar/gkv1330.

Haas, Gabrielle, Semih Cetin, M??rossed Messmer, B??rossed Chane-Woon-Ming, Olivier Terenzi, Johana Chicher, Lauriane Kuhn, Philippe Hammann, and S??rossed Pfeffer. 2016. "Identification of Factors Involved in Target RNA-Directed microRNA Degradation." *Nucleic Acids Research* 44 (6): 2873–87. doi:10.1093/nar/gkw040.

Hafner, Markus, Markus Landthaler, Lukas Burger, Mohsen Khorshid, Jean Hausser, Philipp Berninger, Andrea Rothballer, et al. 2010. "Transcriptome-Wide Identification of RNA-Binding Protein and MicroRNA Target Sites by PAR-CLIP." *Cell* 141 (1): 129–41. doi:10.1016/j.cell.2010.03.009.

Hammell, Christopher M., Isabella Lubin, Peter R. Boag, T. Keith Blackwell, and Victor Ambros. 2009. "Nhl-2 Modulates MicroRNA Activity in Caenorhabditis Elegans." *Cell* 136 (5). Elsevier Ltd: 926–38. doi:10.1016/j.cell.2009.01.053.

Han, Jinju, Yoontae Lee, Kyu-hyun Yeom, Young-kook Kim, Hua Jin, and V Narry Kim. 2004. "The Drosha – DGCR8 Complex in Primary microRNA Processing." *Genes & Development*, 3016–27. doi:10.1101/gad.1262504.mic.

Han, Jinju, Yoontae Lee, Kyu Hyeon Yeom, Jin Wu Nam, Inha Heo, Je Keun Rhee, Sun Young Sohn, Yunje Cho, Byoung Tak Zhang, and V. Narry Kim. 2006. "Molecular Basis for the Recognition of Primary microRNAs by the Drosha-DGCR8 Complex." *Cell* 125 (5): 887–901. doi:10.1016/j.cell.2006.03.043.

Hancock, Meaghan H., Lauren M. Hook, Jennifer Mitchell, and Jay A. Nelson. 2017. "Human Cytomegalovirus microRNAs miR-US5-1 and miR-UL112-3p Block Proinflammatory Cytokine Production in Response to NF-κB-Activating Factors through Direct Downregulation of IKKα and IKKβ." *mBio* 8 (2): 1–19. doi:10.1128/mBio.00109-17.

Handa, N, O Nureki, K Kurimoto, I Kim, H Sakamoto, Y Shimura, Y Muto, and S Yokoyama. 1999. "Structural Basis for Recognition of the Tra mRNA Precursor by the Sex-Lethal Protein." *Nature* 398 (6728): 579–85. doi:10.1038/19242.

Handke, Wiebke, Eva Krause, and Wolfram Brune. 2012. "Live or Let Die: Manipulation of Cellular Suicide Programs by Murine Cytomegalovirus." *Medical Microbiology and Immunology* 201 (4): 475–86. doi:10.1007/s00430-012-0264-z.

Haneklaus, Moritz, Motti Gerlic, Mariola Kurowska-Stolarska, Ashleigh-Ann Rainey, Dagmar Pich, Iain B. McInnes, Wolfgang Hammerschmidt, Luke A. J. O'Neill, and Seth L. Masters. 2012. "Cutting Edge: miR-223 and EBV miR-BART15 Regulate the NLRP3 Inflammasome and IL-1β Production." *Journal of Immunology (Baltimore, Md.: 1950)* 189 (8): 3795–99. doi:10.4049/jimmunol.1200312.

Hasler, Daniele, Gerhard Lehmann, Yasuhiro Murakawa, Filippos Klironomos, Leonhard Jakob, Friedrich A. Gr??sser, Nikolaus Rajewsky, Markus Landthaler, and Gunter Meister. 2016. "The Lupus Autoantigen La Prevents Mis-Channeling of tRNA Fragments into the Human MicroRNA Pathway." *Molecular Cell* 63 (1): 110–24. doi:10.1016/j.molcel.2016.05.026.

Hauptmann, Judith, Daniel Schraivogel, Astrid Bruckmann, Sudhir Manickavel, Leonhard Jakob, Norbert Eichner, Janina Pfaff, et al. 2015a. "Biochemical Isolation of Argonaute Protein Complexes by Ago-APP." *Proceedings of the National Academy of Sciences* 112 (38): 201506116. doi:10.1073/pnas.1506116112.

———. 2015b. "Biochemical Isolation of Argonaute Protein Complexes by Ago-APP." *Proceedings of the National Academy of Sciences* 112 (38): 11841–45. doi:10.1073/pnas.1506116112.

Hausser, Jean, Afzal Pasha Syed, Biter Bilen, and Mihaela Zavolan. 2013. "Analysis of CDS-Located miRNA Target Sites Suggests That They Can Effectively Inhibit Translation." *Genome Research* 23 (4): 604–15. doi:10.1101/gr.139758.112.

He, Lin, Xingyue He, Lee P Lim, Elisa de Stanchina, Zhenyu Xuan, Yu Liang, Wen Xue, et al. 2007. "A microRNA Component of the p53 Tumour Suppressor Network." *Nature* 447 (7148): 1130–34. doi:10.1038/nature05939.

Heo, Inha, Minju Ha, Jaechul Lim, Mi Jeong Yoon, Jong Eun Park, S. Chul Kwon, Hyeshik Chang, and V. Narry Kim. 2012. "Mono-Uridylation of Pre-microRNA as a Key Step in the Biogenesis of Group II Let-7 microRNAs." *Cell* 151 (3). Elsevier Inc.: 521–32. doi:10.1016/j.cell.2012.09.022.

Heo, Inha, Chirlmin Joo, Jun Cho, Minju Ha, Jinju Han, and V. Narry Kim. 2008. "Lin28 Mediates the Terminal Uridylation of Let-7 Precursor MicroRNA." *Molecular Cell* 32 (2). Elsevier Inc.: 276–84. doi:10.1016/j.molcel.2008.09.014.

Heo, Inha, Chirlmin Joo, Young Kook Kim, Minju Ha, Mi Jeong Yoon, Jun Cho, Kyu Hyeon Yeom, Jinju Han, and V. Narry Kim. 2009. "TUT4 in Concert with Lin28 Suppresses MicroRNA Biogenesis through Pre-MicroRNA Uridylation." *Cell* 138 (4). Elsevier Ltd: 696–708. doi:10.1016/j.cell.2009.08.002.

Herbert, Kristina M., and Anita Nag. 2016. "A Tale of Two RNAs during Viral Infection: How Viruses Antagonize mRNAs and Small Non-Coding RNAs in the Host Cell." *Viruses* 8 (6): 1–19. doi:10.3390/v8060154.

Hock, J, L Weinmann, C Ender, S Rudel, E Kremmer, M Raabe, H Urlaub, and G Meister. 2007. "Proteomic and Functional Analysis of Argonaute-Containing mRNA-Protein Complexes in Human Cells." *EMBO Rep* 8 (11): 1052–60. doi:10.1038/sj.embor.7401088.

Hook, Lauren M., Finn Grey, Robert Grabski, Rebecca Tirabassi, Tracy Doyle, Meaghan Hancock, Igor Landais, et al. 2014. "Cytomegalovirus miRNAs Target Secretory Pathway Genes to Facilitate Formation of the Virion Assembly Compartment and Reduce Cytokine Secretion." *Cell Host and Microbe* 15 (3). Elsevier Inc.: 363–73. doi:10.1016/j.chom.2014.02.004.

Hooykaas, Marjolein J G, Elisabeth Kruse, Emmanuel J H J Wiertz, and Robert Jan Lebbink. 2016. "Comprehensive Profiling of Functional Epstein-Barr Virus miRNA Expression in Human Cell Lines." *BMC Genomics* 17: 644. doi:10.1186/s12864-016-2978-6.

Horman, Shane R., Maja M. Janas, Claudia Litterst, Bingbing Wang, Ian J. MacRae, Mary J. Sever, David V. Morrissey, et al. 2013. "Akt-Mediated Phosphorylation of Argonaute 2 Downregulates Cleavage and Upregulates Translational Repression of MicroRNA Targets." *Molecular Cell* 50 (3). Elsevier Inc.: 356–67. doi:10.1016/j.molcel.2013.03.015.

Hsu, Chung Yuan, Yung Hsiang Yi, Kai Ping Chang, Yu Sun Chang, Shu Jen Chen, and Hua Chien Chen. 2014. "The Epstein-Barr Virus-Encoded MicroRNA MiR-BART9 Promotes Tumor Metastasis by Targeting E-Cadherin in Nasopharyngeal Carcinoma." *PLoS Pathogens* 10 (2). doi:10.1371/journal.ppat.1003974.

Huang, Kai-Lieh, Amanda B Chadee, Chyi-Ying a Chen, Yueqiang Zhang, and Ann-Bin Shyu. 2013. "Phosphorylation at Intrinsically Disordered Regions of PAM2 Motif-Containing Proteins Modulates Their Interactions with PABPC1 and Influences mRNA Fate." *RNA (New York, N.Y.)* 19 (3): 295–305. doi:10.1261/rna.037317.112.

Huntzinger, Eric, and Elisa Izaurralde. 2011. "Gene Silencing by microRNAs: Contributions of Translational Repression and mRNA Decay." *Nature Reviews. Genetics* 12 (2). Nature Publishing Group: 99–110. doi:10.1038/nrg2936.

Huntzinger, Eric, Duygu Kuzuoğlu-Öztürk, Joerg E. Braun, Ana Eulalio, Lara Wohlbold, and Elisa Izaurralde. 2013. "The Interactions of GW182 Proteins with PABP and Deadenylases Are Required for Both Translational Repression and Degradation of miRNA Targets." *Nucleic Acids Research* 41 (2): 978–94. doi:10.1093/nar/gks1078.

Ishihama, Yasushi, Yoshiya Oda, Tsuyoshi Tabata, Toshitaka Sato, Takeshi Nagasu, Juri Rappsilber, and Matthias Mann. 2005. "Exponentially Modified Protein Abundance Index (emPAI) for Estimation of Absolute Protein Amount in Proteomics by the Number of Sequenced Peptides per Protein." *Molecular & Cellular Proteomics* 4 (9): 1265–72. doi:10.1074/mcp.M500061-MCP200.

Iwasaki, Shintaro, Maki Kobayashi, Mayuko Yoda, Yuriko Sakaguchi, Susumu Katsuma, Tsutomu Suzuki, and Yukihide Tomari. 2010. "Hsc70/Hsp90 Chaperone Machinery Mediates ATP-Dependent RISC Loading of Small RNA Duplexes." *Molecular Cell* 39 (2). Elsevier Ltd: 292–99. doi:10.1016/j.molcel.2010.05.015.

Jackson, Richard J, Christopher U T Hellen, and Tatyana V Pestova. 2010. "The Mechanism of Eukaryotic Translation Initiation and Principles of Its Regulation." *Nature Reviews. Molecular Cell Biology* 11 (2). Nature Publishing Group: 113–27. doi:10.1038/nrm2838.

Jacobsen, Anders, Joachim Silber, Girish Harinath, Jason T Huse, Nikolaus Schultz, and Chris Sander. 2013. "Analysis of microRNA-Target Interactions across Diverse Cancer Types." *Nature Structural & Molecular Biology* 20 (11). Nature Publishing Group: 1325–32. doi:10.1038/nsmb.2678.

Jain, Niyati, Hsuan-Chun Lin, Christopher E. Morgan, Michael E. Harris, and Blanton S. Tolbert. 2017. "Rules of RNA Specificity of hnRNP A1 Revealed by Global and Quantitative Analysis of Its Affinity Distribution." *Proceedings of the National Academy of Sciences* 114 (9): 201616371. doi:10.1073/PNAS.1616371114.

James, Victoria, Yining Zhang, Daniel E Foxler, Cornelia H de Moor, Yi Wen Kong, Thomas M Webb, Tim J Self, et al. 2010. "LIM-Domain Proteins, LIMD1, Ajuba, and WTIP Are Required for microRNA-Mediated Gene Silencing." *Proceedings of the National Academy of Sciences of the United States of America* 107 (28): 12499–504. doi:10.1073/pnas.0914987107.

Jeang, Ralph Grassmann and Kuan-Teh. 2008. "The Roles of microRNAs in Mammalian Virus Infection Ralph" 76 (October 2009): 211–20. doi:10.1007/s11103-011-9767-z.Plastid.

Jiang, Shujuan, Ying Qi, Rong He, Yujing Huang, Zhongyang Liu, Yanping Ma, Xin Guo, Yaozhong Shao, Zhengrong Sun, and Qiang Ruan. 2015. "Human Cytomegalovirus microRNA miR-US25-1-5p Inhibits Viral Replication by Targeting Multiple Cellular Genes during Infection." *Gene* 570 (1). Elsevier B.V.: 108–14. doi:10.1016/j.gene.2015.06.009.

Jin, Peng, Daniela C Zarnescu, Stephanie Ceman, Mika Nakamoto, Julie Mowrey, Thomas a Jongens, David L Nelson, Kevin Moses, and Stephen T Warren. 2004. "Biochemical and Genetic Interaction between the Fragile X Mental Retardation Protein and the

microRNA Pathway." *Nature Neuroscience* 7 (2): 113–17. doi:10.1038/nn1174.

Jinek, Martin, Scott M. Coyle, and Jennifer A. Doudna. 2011. "Coupled 5' Nucleotide Recognition and Processivity in Xrn1-Mediated mRNA Decay." *Molecular Cell* 41 (5). Elsevier Inc.: 600–608. doi:10.1016/j.molcel.2011.02.004.

Jing, Qing, Shuang Huang, Sabine Guth, Tyler Zarubin, Andrea Motoyama, Jianming Chen, Franco Di Padova, Sheng Cai Lin, Hermann Gram, and Jiahuai Han. 2005. "Involvement of MicroRNA in AU-Rich Element-Mediated mRNA Instability." *Cell* 120 (5): 623–34. doi:10.1016/j.cell.2004.12.038.

Jonas, Stefanie, Mary Christie, Daniel Peter, Dipankar Bhandari, Belinda Loh, Eric Huntzinger, Oliver Weichenrieder, and Elisa Izaurralde. 2014. "An Asymmetric PAN3 Dimer Recruits a Single PAN2 Exonuclease to Mediate mRNA Deadenylation and Decay." *Nature Structural & Molecular Biology* 21 (7): 599–608. doi:10.1038/nsmb.2837.

Jonas, Stefanie, and Elisa Izaurralde. 2015. "Towards a Molecular Understanding of microRNA-Mediated Gene Silencing." *Nature Reviews. Genetics* 16 (7). Nature Publishing Group: 421–33. doi:10.1038/nrg3965.

Josa-Prado, Fernando, Jeremy M. Henley, and Kevin A. Wilkinson. 2015. "SUMOylation of Argonaute-2 Regulates RNA Interference Activity." *Biochemical and Biophysical Research Communications* 464 (4). Elsevier Ltd: 1066–71. doi:10.1016/j.bbrc.2015.07.073.

Jourdain, Alexis A., Mirko Koppen, Mateusz Wydro, Chris D. Rodley, Robert N. Lightowlers, Zofia M. Chrzanowska-Lightowlers, and Jean Claude Martinou. 2013. "GRSF1 Regulates RNA Processing in Mitochondrial RNA Granules." *Cell Metabolism* 17 (3). Elsevier Inc.: 399–410. doi:10.1016/j.cmet.2013.02.005.

Jurak, I, M F Kramer, J C Mellor, A L van Lint, F P Roth, D M Knipe, and D M Coen. 2010. "Numerous Conserved and Divergent microRNAs Expressed by Herpes Simplex Viruses 1 and 2." *Journal of Virology* 84 (9): 4659–72. doi:10.1128/JVI.02725-09.

Kadlec, Jan, Elisa Izaurralde, and Stephen Cusack. 2004. "The Structural Basis for the Interaction between Nonsense-Mediated mRNA Decay Factors UPF2 and UPF3." *Nature Structural & Molecular Biology* 11 (4): 330–37. doi:10.1038/nsmb741.

Kalantari, Roya, Cheng-Ming Chiang, and David R Corey. 2016. "Regulation of Mammalian Transcription and Splicing by Nuclear RNAi." *Nucleic Acids Research* 44 (2): 524–37. doi:10.1093/nar/gkv1305.

Kalantari, Roya, Jessica A Hicks, Liande Li, Keith T Gagnon, Viswanadham Sridhara, Andrew Lemoff, Hamid Mirzaei, and David R Corey. 2016. "Stable Association of RNAi Machinery Is Conserved between the Cytoplasm and Nucleus of Human Cells." *RNA (New York, N.Y.)* 22 (7): 1085–98. doi:10.1261/rna.056499.116.

Kamenska, Anastasiia, Clare Simpson, Caroline Vindry, Helen Broomhead, Marianne Bénard, Michèle Ernoult-Lange, Benjamin P. Lee, Lorna W. Harries, Dominique Weil, and Nancy Standart. 2016. "The DDX6-4E-T Interaction Mediates Translational Repression and P-Body Assembly." *Nucleic Acids Research* 44 (13): 6318–34. doi:10.1093/nar/gkw565.

Kang, Dong, Rebecca L. Skalsky, and Bryan R. Cullen. 2015. "EBV BART MicroRNAs Target Multiple Pro-Apoptotic Cellular Genes to Promote Epithelial Cell Survival." *PLOS Pathogens* 11 (6): e1004979. doi:10.1371/journal.ppat.1004979.

Kataoka, Naoyuki, Megumi Fujita, and Mutsuhito Ohno. 2009. "Functional Association of the Microprocessor Complex with the Spliceosome." *Molecular and Cellular Biology* 29 (12): 3243–54. doi:10.1128/MCB.00360-09.

Kawahara, Yukio, and Ai Mieda-Sato. 2012. "TDP-43 Promotes microRNA Biogenesis as a Component of the Drosha and Dicer Complexes." *Pnas* 109 (9): 3347–52. doi:10.1073/pnas.1112427109.

Kawai, Shinji, and Atsuo Amano. 2012. "BRCA1 Regulates microRNA Biogenesis via the DROSHA Microprocessor Complex." *Journal of Cell Biology* 197 (2): 201–8. doi:10.1083/jcb.201110008.

Kawamata, Tomoko, and Yukihide Tomari. 2010. "Making RISC." *Trends in Biochemical Sciences* 35 (7). Elsevier Ltd: 368–76. doi:10.1016/j.tibs.2010.03.009.

Keith T. Gagnon, Liande Li, Bethany A. Janowski, and David R. Corey. 2012. "Analysis of Nuclear RNA Interference (RNAi) in Human Cells by Subcellular Fractionation and Argonaute Loading." *Changes* 29 (6): 997–1003. doi:10.1016/j.biotechadv.2011.08.021.Secreted.

Kenney, Shannon C., and Janet E. Mertz. 2014. "Regulation of the Latent-Lytic Switch in Epstein-Barr Virus." *Seminars in Cancer Biology* 26. Elsevier Ltd: 60–68. doi:10.1016/j.semcancer.2014.01.002.

Kenny, Phillip J., Hongjun Zhou, Miri Kim, Geena Skariah, Radhika S. Khetani, Jenny Drnevich, Mary Luz Arcila, Kenneth S. Kosik, and Stephanie Ceman. 2014. "MOV10 and FMRP Regulate AGO2 Association with MicroRNA Recognition Elements." *Cell Reports* 9 (5). The Authors: 1729–42. doi:10.1016/j.celrep.2014.10.054.

Kielkopf, Clara L., Natalia A. Rodionova, Michael R. Green, and Stephen K. Burley. 2001. "A Novel Peptide Recognition Mode Revealed by the X-Ray Structure of a Core U2AF35/U2AF65 Heterodimer." *Cell* 106 (5): 595–605. doi:10.1016/S0092-8674(01)00480-9.

Kim, Kee K, Yanqin Yang, Jun Zhu, Robert S Adelstein, and Sachiyo Kawamoto. 2014. "Rbfox3 Controls the Biogenesis of a Subset of microRNAs." *Nature Structural & Molecular Biology* 21 (10). Nature Publishing Group: 901–10. doi:10.1038/nsmb.2892.

Kim, V N, J Han, and M C Siomi. 2009. “Biogenesis of Small RNAs in Animals.” *Nat Rev Mol Cell Biol* 10 (2): 126–39. doi:10.1038/nrm2632.

Kim, Yoosik, Jinah Yeo, Jung Hyun Lee, Jun Cho, Daekwan Seo, Jong Seo Kim, and V. Narry Kim. 2014. “Deletion of Human tarbp2 Reveals Cellular microRNA Targets and Cell-Cycle Function of TRBP.” *Cell Reports* 9 (3). The Authors: 1061–74. doi:10.1016/j.celrep.2014.09.039.

Kim, Young-Kook, Boseon Kim, and V Narry Kim. 2016. “Re-Evaluation of the Roles of DROSHA, Exportin 5, and DICER in microRNA Biogenesis.” *Proceedings of the National Academy of Sciences of the United States of America* 113 (13): E1881-1889. doi:10.1073/pnas.1602532113.

Kim, Young-Kook, and V Narry Kim. 2007. “Processing of Intronic microRNAs.” *The EMBO Journal* 26 (3): 775–83. doi:10.1038/sj.emboj.7601512.

Kim, Young Kook, Inha Heo, and V. Narry Kim. 2010. “Modifications of Small RNAs and Their Associated Proteins.” *Cell* 143 (5). Elsevier Inc.: 703–9. doi:10.1016/j.cell.2010.11.018.

Kim, Yun Ju, Alexis Maizel, and Xuemei Chen. 2014. “Traffic into Silence: Endomembranes and Post-Transcriptional RNA Silencing.” *EMBO Journal* 33 (9): 968–80. doi:10.1002/embj.201387262.

Kramer, Martha F., Igor Jurak, Jean M. Pesola, Sandrine Boissel, David M. Knipe, and Donald M. Coen. 2011. “Herpes Simplex Virus 1 microRNAs Expressed Abundantly during Latent Infection Are Not Essential for Latency in Mouse Trigeminal Ganglia.” *Virology* 417 (2): 239–47. doi:10.1016/j.virol.2011.06.027.

Krol, Jacek, Inga Loedige, and Witold Filipowicz. 2010. “The Widespread Regulation of microRNA Biogenesis, Function and Decay.” *Nature Reviews. Genetics* 11 (9). Nature Publishing Group: 597–610. doi:10.1038/nrg2843.

Kulkarni, Meeta, Sevim Ozgur, and Georg Stoecklin. 2010. “On Track with P-Bodies” 38: 242–51. doi:10.1042/BST0380242.

Kwak, Pieter Bas, and Yukihide Tomari. 2012. “The N Domain of Argonaute Drives Duplex Unwinding during RISC Assembly.” *Nature Structural & Molecular Biology* 19 (2): 145–51. doi:10.1038/nsmb.2232.

Kwon, S. Chul, Tuan Anh Nguyen, Yeon Gil Choi, Myung Hyun Jo, Sungchul Hohng, V. Narry Kim, and Jae Sung Woo. 2016. “Structure of Human DROSHA.” *Cell* 164 (1–2). Elsevier Inc.: 81–90. doi:10.1016/j.cell.2015.12.019.

La Rocca, Gaspare, Scott H. Olejniczak, Alvaro J. González, Daniel Briskin, Joana a. Vidigal, Lee Spraggon, Raymond G. DeMatteo, et al. 2015. “In Vivo, Argonaute-Bound microRNAs Exist Predominantly in a Reservoir of Low Molecular Weight Complexes Not Associated with mRNA.” *Proceedings of the National Academy of Sciences* 112 (3): 767–72. doi:10.1073/pnas.1424217112.

Landthaler, Markus, Abdullah Yalcin, and and Thomas Tuschl1. 2004. “The Human DiGeorge Syndrome Critical Region Gene 8 and Its D. Melanogaster Homolog Are Required for miRNA Biogenesis.” doi:10.1016/j.

Lau, Betty, Emma Poole, Benjamin Krishna, Immaculada Montanuy, Mark R. Wills, Eain Murphy, and John Sinclair. 2016. “The Expression of Human Cytomegalovirus MicroRNA MiR-UL148D during Latent Infection in Primary Myeloid Cells Inhibits Activin A-Triggered Secretion of IL-6.” *Scientific Reports* 6 (1): 31205. doi:10.1038/srep31205.

Lau, Nga Chi, Klaas W. Mulder, Arjan B. Brenkman, Shabaz Mohammed, Niels J.F. van den Broek, Albert J.R. Heck, and H. Th Marc Timmers. 2010. “Phosphorylation of Not4p Functions Parallel to BUR2 to Regulate Resistance to Cellular Stresses in Saccharomyces Cerevisiae.” *PLoS ONE* 5 (4): 1–9. doi:10.1371/journal.pone.0009864.

Lau, Vivian Su and Alan F. 2009. “Ubiquitin-like and Ubiquitin-Associated Domain Proteins: Significance in Proteasomal Degradation” 66 (17): 2819–33. doi:10.1007/s00018-009-0048-9.Ubiquitin-like.

Lazzaretti, Daniela, Isabelle Tournier, and Elisa Izaurralde. 2009. “The C-Terminal Domains of Human TNRC6A, TNRC6B, and TNRC6C Silence Bound Transcripts Independently of Argonaute Proteins.” *RNA (New York, N.Y.)* 15 (6): 1059–66. doi:10.1261/rna.1606309.

Lee, Ho Young, Kaihong Zhou, Alison Marie Smith, Cameron L. Noland, and Jennifer A. Doudna. 2013. “Differential Roles of Human Dicer-Binding Proteins TRBP and PACT in Small RNA Processing.” *Nucleic Acids Research* 41 (13): 6568–76. doi:10.1093/nar/gkt361.

Lee, Sooncheol, and Shobha Vasudevan. 2013. “Ten Years of Progress in GW/P Body Research.” *Advances in Experimental Medicine and Biology* 768 (Bartel 2009): 97–126. doi:10.1007/978-1-4614-5107-5.

Lee, Y, M Kim, J Han, KH Yeom, S Lee, SH Baek, and VN Kim. 2004. “MicroRNA Genes Are Transcribed by RNA Polymerase II.” *Embo J* 23 (20): 4051–60. doi:10.1038/sj.emboj.7600385.

Lee, Yoontae, Inha Hur, Seong-Yeon Park, Young-Kook Kim, Mi Ra Suh, and V Narry Kim. 2006. “The Role of PACT in the RNA Silencing Pathway.” *The EMBO Journal* 25 (3): 522–32. doi:10.1038/sj.emboj.7600942.

Lei, Ting, Kit San Yuen, Rui Xu, Sai Wah Tsao, Honglin Chen, Mengfeng Li, Kin Hang Kok, and Dong Yan Jin. 2013. “Targeting of DICE1 Tumor Suppressor by Epstein-Barr Virus-Encoded miR-BART3* microRNA in Nasopharyngeal Carcinoma.” *International Journal*

of Cancer 133 (1): 79–87. doi:10.1002/ijc.28007.

Leung, Anthony K L, J Mauro Calabrese, and Phillip a Sharp. 2006. "Quantitative Analysis of Argonaute Protein Reveals microRNA-Dependent Localization to Stress Granules." *Proceedings of the National Academy of Sciences of the United States of America* 103 (48): 18125–30. doi:10.1073/pnas.0608845103.

Leung, Anthony K L, Sejal Vyas, Jennifer E. Rood, Arjun Bhutkar, Phillip A. Sharp, and Paul Chang. 2011. "Poly(ADP-Ribose) Regulates Stress Responses and MicroRNA Activity in the Cytoplasm." *Molecular Cell* 42 (4). Elsevier Inc.: 489–99. doi:10.1016/j.molcel.2011.04.015.

Li, Gaopeng, Xiaoli Wu, Wenchang Qian, Huayong Cai, Xinbao Sun, Weijie Zhang, Sheng Tan, et al. 2016. "CCAR1 5' UTR as a Natural miRancer of miR-1254 Overrides Tamoxifen Resistance." *Cell Research* 26 (6). Nature Publishing Group: 655–73. doi:10.1038/cr.2016.32.

Li, Shitao, Lingyan Wang, Bishi Fu, Michael a Berman, Alos Diallo, and Martin E Dorf. 2014. "TRIM65 Regulates microRNA Activity by Ubiquitination of TNRC6." *Proceedings of the National Academy of Sciences of the United States of America* 111 (19): 6970–75. doi:10.1073/pnas.1322545111.

Li, Shitao, Lingyan Wang, Bishi Fu, and Martin E Dorf. 2014. "Trim65: A Cofactor for Regulation of the microRNA Pathway." *RNA Biology* 11 (9): 1113–21. doi:10.4161/rna.36179.

Libri, Valentina, Pascal Miesen, Ronald P. Van Rij, and Amy H. Buck. 2013. "Regulation of microRNA Biogenesis and Turnover by Animals and Their Viruses." *Cellular and Molecular Life Sciences* 70 (19): 3525–44. doi:10.1007/s00018-012-1257-1.

Liu, Jidong, Fabiola V Rivas, James Wohlschlegel, John R Yates, Roy Parker, and Gregory J Hannon. 2005. "A Role for the P-Body Component GW182 in microRNA Function." *Nature Cell Biology* 7 (12): 1261–66. doi:10.1038/ncb1333.

Liu, Xi, Jennifer Hein, Simon C W Richardson, Per H. Basse, Tuna Toptan, Patrick S. Moore, Ole V. Gjoerup, and Yuan Chang. 2011. "Merkel Cell Polyomavirus Large T Antigen Disrupts Lysosome Clustering by Translocating Human Vam6p from the Cytoplasm to the Nucleus." *Journal of Biological Chemistry* 286 (19): 17079–90. doi:10.1074/jbc.M110.192856.

Liu, Xiangyuan, Min Chen, Long Li, Liyan Gong, Hu Zhou, and Daming Gao. 2017. "ERK Kinases Phosphorylate Lin28a to Modulate P19 Cell Proliferation and Differentiation." *Journal of Biological Chemistry* 292 (10): jbc.C117.775122. doi:10.1074/jbc.C117.775122.

Lo, Angela Kwok Fung, Ka Fai To, Kwok Wai Lo, Raymond Wai Ming Lung, Jan Wai Ying Hui, Gangling Liao, and S Diane Hayward. 2007. "Modulation of LMP1 Protein Expression by EBV-Encoded microRNAs." *Proceedings of the National Academy of Sciences of the United States of America* 104 (41): 16164–69. doi:10.1073/pnas.0702896104.

Loedige, Inga, Dimos Gaidatzis, Ragna Sack, Gunter Meister, and Witold Filipowicz. 2013. "The Mammalian TRIM-NHL Protein TRIM71/LIN-41 Is a Repressor of mRNA Function." *Nucleic Acids Research* 41 (1): 518–32. doi:10.1093/nar/gks1032.

Loedige, Inga, Leonhard Jakob, Thomas Treiber, Debashish Ray, Mathias Stotz, Nora Treiber, Janosch Hennig, et al. 2015. "The Crystal Structure of the NHL Domain in Complex with RNA Reveals the Molecular Basis of Drosophila Brain-Tumor-Mediated Gene Regulation." *Cell Reports* 13 (6). The Authors: 1206–20. doi:10.1016/j.celrep.2015.09.068.

Loedige, Inga, Mathias Stotz, Saadia Qamar, Katharina Kramer, Janosch Hennig, Thomas Schubert, Patrick Löffler, et al. 2014. "The NHL Domain of BRAT Is an RNA-Binding Domain That Directly Contacts the Hunchback mRNA for Regulation." *Genes and Development* 28 (7): 749–64. doi:10.1101/gad.236513.113.

Louloupi, Annita, Evgenia Ntini, Julia Liz, and Ulf Andersson Ørom. 2017. "Microprocessor Dynamics Shows Co- and Post-Transcriptional Processing of Pri-miRNAs." *Rna*, rna.060715.117. doi:10.1261/rna.060715.117.

Lu, Shihua, and Bryan R Cullen. 2004. "Adenovirus VA1 Noncoding RNA Can Inhibit Small Interfering RNA and MicroRNA Biogenesis Adenovirus VA1 Noncoding RNA Can Inhibit Small Interfering RNA and MicroRNA Biogenesis." *Journal of Virology* 78 (23): 12868–76. doi:10.1128/JVI.78.23.12868.

Luftig, Eleonora Forte and Micah A. 2016. "The Role of microRNAs in Epstein-Barr Virus Latency and Lytic Reactivation" 527 (7576): 59–63. doi:10.1038/nature15709.Ion.

Lunde, Bradley M, Claire Moore, and Gabriele Varani. 2007. "{RNA}-Binding Proteins: Modular Design for Efficient Function." *Nat Rev Mol Cell Biol* 8 (6): 479–90. doi:10.1038/nrm2178.

Ma, J, K Nie, D Redmond, Y Liu, O Elemento, D M Knowles, and W Tam. 2016. "EBV-miR-BHRF1-2 Targets PRDM1/Blimp1: Potential Role in EBV Lymphomagenesis." *Leukemia* 30 (3): 594–604. doi:10.1038/leu.2015.285.

MacRae, I. J., F. Li, K. Zhou, W. Z. Cande, and J. A. Doudna. 2006. "Structure of Dicer and Mechanistic Implications for RNAi." *Cold Spring Harbor Symposia on Quantitative Biology* 71: 73–80. doi:10.1101/sqb.2006.71.042.

Makino, Shiho, Yuichiro Mishima, Kunio Inoue, and Toshifumi Inada. 2015. "Roles of mRNA Fate Modulators Dhh1 and Pat1 in TNRC6-Dependent Gene Silencing Recapitulated in Yeast." *Journal of Biological Chemistry* 290 (13): 8331–47. doi:10.1074/jbc.M114.615088.

Maris, Christophe, Cyril Dominguez, and Frédéric H.T. Allain. 2005. “The RNA Recognition Motif, a Plastic RNA-Binding Platform to Regulate Post-Transcriptional Gene Expression.” *FEBS Journal* 272 (9): 2118–31. doi:10.1111/j.1742-4658.2005.04653.x.

Marquitz, Aron R., Anuja Mathur, Cyd Stacy Nam, and Nancy Raab-Traub. 2011. “The Epstein-Barr Virus BART microRNAs Target the pro-Apoptotic Protein Bim.” *Virology* 412 (2). Elsevier Inc.: 392–400. doi:10.1016/j.virol.2011.01.028.

Martinez, N J, and R I Gregory. 2013. “Argonaute2 Expression Is Post-Transcriptionally Coupled to microRNA Abundance.” *Rna* 19 (5): 605–12. doi:10.1261/rna.036434.112.

Martinez, Natalia J, Hao-ming Chang, Jacob De E Riba Borrajo, Jacob De E Riba Borrajo, and Richard I Gregory. 2013. “The Co-Chaperones Fkbp4/5 Control Argonaute2 Expression and Facilitate RISC Assembly.” *Rna* 19 (11): 1583–93. doi:10.1261/rna.040790.113.

Mathys, Hansruedi, JérÔme Basquin, Sevim Ozgur, Mariusz Czarnocki-Cieciura, Fabien Bonneau, Aafke Aartse, Andrzej Dziembowski, Marcin Nowotny, Elena Conti, and Witold Filipowicz. 2014. “Structural and Biochemical Insights to the Role of the CCR4-NOT Complex and DDX6 ATPase in MicroRNA Repression.” *Molecular Cell* 54 (5): 751–65. doi:10.1016/j.molcel.2014.03.036.

Mauri, Marta, Marieluise Kirchner, Reuven Aharoni, Camilla Ciolli Mattioli, David Van Den Bruck, Nadya Gutkovitch, Vengamanaidu Modepalli, Matthias Selbach, Yehu Moran, and Marina Chekulaeva. 2017. “Conservation of miRNA-Mediated Silencing Mechanisms across 600 Million Years of Animal Evolution.” *Nucleic Acids Research* 45 (2): 938–50. doi:10.1093/nar/gkw792.

McKee, Adrienne E, Emmanuel Minet, Charlene Stern, Shervin Riahi, Charles D Stiles, and Pamela A Silver. 2005. “A Genome-Wide in Situ Hybridization Map of RNA-Binding Proteins Reveals Anatomically Restricted Expression in the Developing Mouse Brain.” *BMC Developmental Biology* 5 (1): 14. doi:10.1186/1471-213X-5-14.

McKenzie, Andrew J., and and Alissa M. Weaver , Daisuke Hoshino, Nan Hyung Hong1, Diana J. Cha, Jeffrey L. Franklin, Robert J. Coffey, James G. Patton. 2016. “KRAS-MEK Signaling Controls Ago2 Sorting into Exosomes” 527 (7576): 59–63. doi:10.1038/nature15709.Ion.

Meister, Gunter, Markus Landthaler, Lasse Peters, Po Yu Chen, Henning Urlaub, Reinhard Lührmann, and Thomas Tuschl. 2005. “Identification of Novel Argonaute-Associated Proteins.” *Current Biology* 15 (23): 2149–55. doi:10.1016/j.cub.2005.10.048.

Mertins, Philipp, D. R. Mani, Kelly V. Ruggles, Michael A. Gillette, Karl R. Clauser, Pei Wang, Xianlong Wang, et al. 2016. “Proteogenomics Connects Somatic Mutations to Signalling in Breast Cancer.” *Nature* 534 (7605). Nature Publishing Group: 55–62. doi:10.1038/nature18003\rhttp://www.nature.com/nature/journal/v534/n7605/abs/nature18003.html#supplementary-information.

Michlewski, Gracjan, and Javier F Cáceres. 2010. “Antagonistic Role of hnRNP A1 and KSRP in the Regulation of Let-7a Biogenesis.” *Nature Structural & Molecular Biology* 17 (8): 1011–18. doi:10.1038/nsmb.1874.

Michlewski, Gracjan, Sonia Guil, Colin A. Semple, and Javier F. Cáceres. 2008. “Posttranscriptional Regulation of miRNAs Harboring Conserved Terminal Loops.” *Molecular Cell* 32 (3): 383–93. doi:10.1016/j.molcel.2008.10.013.

Miller, C L, J H Lee, E Kieff, and R Longnecker. 1994. “An Integral Membrane Protein (LMP2) Blocks Reactivation of Epstein-Barr Virus from Latency Following Surface Immunoglobulin Crosslinking.” *Proceedings of the National Academy of Sciences of the United States of America* 91 (2): 772–76. doi:10.1073/pnas.91.2.772.

Mishima, Yuichiro, and Yukihide Tomari. 2016. “Codon Usage and 3’ UTR Length Determine Maternal mRNA Stability in Zebrafish.” *Molecular Cell* 61 (6). Elsevier Inc.: 874–85. doi:10.1016/j.molcel.2016.02.027.

Miyoshi, Keita, Tomoko N Okada, Haruhiko Siomi, and Mikiko C Siomi. 2009. “Characterization of the miRNA-RISC Loading Complex and miRNA-RISC Formed in the Drosophila miRNA Pathway.” *Rna* 15 (7): 1282–91. doi:10.1261/rna.1541209.

Miyoshi, Tomohiro, Akiko Takeuchi, Haruhiko Siomi, and Mikiko C Siomi. 2010. “A Direct Role for Hsp90 in Pre-RISC Formation in Drosophila.” *Nature Structural & Molecular Biology* 17 (8): 1024–26. doi:10.1038/nsmb0411-516a.

Monteys, Alex Mas, Ryan M Spengler, Ji Wan, Luis Tecedor, Kimberly A Lennox, Yi Xing, and Beverly L Davidson. 2010. “Structure and Activity of Putative Intronic miRNA Promoters.” *Rna* 16 (3): 495–505. doi:10.1261/rna.1731910.

Morlando, Mariangela, Monica Ballarino, Natalia Gromak, Francesca Pagano, Irene Bozzoni, and Nick J Proudfoot. 2008. “Primary microRNA Transcripts Are Processed Co-Transcriptionally.” *Nature Structural & Molecular Biology* 15 (9): 902–9. doi:10.1038/nsmb.1475.

Motsch, Natalie, Julia Alles, Jochen Imig, Jiayun Zhu, Stephanie Barth, Tanja Reineke, Marianne Tinguely, et al. 2012. “MicroRNA Profiling of Epstein-Barr Virus-Associated NK/T-Cell Lymphomas by Deep Sequencing.” *PLoS ONE* 7 (8). doi:10.1371/journal.pone.0042193.

Murphy, Eain, Jirí Vanícek, Harlan Robins, Thomas Shenk, and Arnold J Levine. 2008. “Suppression of Immediate-Early Viral Gene Expression by Herpesvirus-Coded microRNAs: Implications for Latency.” *Proceedings of the National Academy of Sciences of the United States of America* 105 (14): 5453–58. doi:10.1073/pnas.0711910105.

Musco, Giovanna, Gunter Stier, Catherine Joseph, Maria Antonietta Castiglione Morelli, Michael Nilges, Toby J Gibson, and Annalisa Pastore. 1996. "Three-Dimensional Structure and Stability of the KH Domain: Molecular Insights into the Fragile X Syndrome." *Cell* 85 (2): 237–45. doi:10.1016/S0092-8674(00)81100-9.

Nachmani, Daphna, Noam Stern-Ginossar, Ronit Sarid, and Ofer Mandelboim. 2009. "Diverse Herpesvirus MicroRNAs Target the Stress-Induced Immune Ligand MICB to Escape Recognition by Natural Killer Cells." *Cell Host and Microbe* 5 (4). Elsevier Ltd: 376–85. doi:10.1016/j.chom.2009.03.003.

Nakanishi, Kotaro. 2016. "Anatomy of RISC: How Do Small RNAs and Chaperones Activate Argonaute Proteins?" *Wiley Interdisciplinary Reviews: RNA* 7 (5): 637–60. doi:10.1002/wrna.1356.

Newman, Martin a, J Michael Thomson, and Scott M Hammond. 2008. "Lin-28 Interaction with the Let-7 Precursor Loop Mediates Regulated microRNA Processing." *RNA (New York, N.Y.)* 14 (8): 1539–49. doi:10.1261/rna.1155108.

Nguyen, Tuan Anh, Myung Hyun Jo, Yeon-Gil Choi, Joha Park, S Chul Kwon, Sungchul Hohng, V Narry Kim, and Jae-Sung Woo. 2015. "Functional Anatomy of the Human Microprocessor." *Cell* 161 (6). Elsevier Inc.: 1374–87. doi:10.1016/j.cell.2015.05.010.

Nicastro, Giuseppe, Ian A. Taylor, and Andres Ramos. 2015. "KH-RNA Interactions: Back in the Groove." *Current Opinion in Structural Biology* 30. Elsevier Ltd: 63–70. doi:10.1016/j.sbi.2015.01.002.

Nishi, Kenji, Ai Nishi, Tatsuya Nagasawa, and Kumiko Ui-Tei. 2013. "Human TNRC6A Is an Argonaute-Navigator Protein for microRNA-Mediated Gene Silencing in the Nucleus. (Supplemental Materials)." *Rna* 19 (1): 17–35. doi:10.1261/rna.034769.112.

Nishihara, Tadashi, Latifa Zekri, Joerg E. Braun, and Elisa Izaurralde. 2013. "MiRISC Recruits Decapping Factors to miRNA Targets to Enhance Their Degradation." *Nucleic Acids Research* 41 (18): 8692–8705. doi:10.1093/nar/gkt619.

Nishimura, Tamiko, Zoya Padamsi, Hana Fakim, Simon Milette, Wade H. Dunham, Anne Claude Gingras, and Marc R. Fabian. 2015. "The eIF4E-Binding Protein 4E-T Is a Component of the mRNA Decay Machinery That Bridges the 5′ and 3′ Termini of Target mRNAs." *Cell Reports* 11 (9). The Authors: 1425–36. doi:10.1016/j.celrep.2015.04.065.

Noh, Ji Heon, Kyoung Mi Kim, Kotb Abdelmohsen, Je Hyun Yoon, Amaresh C. Panda, Rachel Munk, Jiyoung Kim, et al. 2016. "HuR and GRSF1 Modulate the Nuclear Export and Mitochondrial Localization of the lncRNA RMRP." *Genes and Development* 30 (10): 1224–39. doi:10.1101/gad.276022.115.

Okada, Chimari, Eiki Yamashita, Soo Jae Lee, Satoshi Shibata, Jun Katahira, Atsushi Nakagawa, Yoshihiro Yoneda, and Tomitake Tsukihara. 2009. "A High-Resolution Structure of the Pre-microRNA Nuclear Export Machinery." *Science (New York, N.Y.)* 326 (5957): 1275–79. doi:10.1126/science.1178705.

Olejniczak, Scott H, Gaspare La Rocca, Joshua J Gruber, and Craig B Thompson. 2013. "Long-Lived microRNA-Argonaute Complexes in Quiescent Cells Can Be Activated to Regulate Mitogenic Responses." *Proceedings of the National Academy of Sciences of the United States of America* 110 (1): 157–62. doi:10.1073/pnas.1219958110.

Olejniczak, Scott H, Gaspare La Rocca, Megan R Radler, Shawn M Egan, Qing Xiang, Ralph Garippa, and Craig B Thompson. 2016. "Coordinated Regulation of Cap-Dependent Translation and microRNA Function by Convergent Signaling Pathways." *Molecular and Cellular Biology* 36 (18): 2360–73. doi:10.1128/MCB.01011-15.

Ørom, Ulf Andersson, Finn Cilius Nielsen, and Anders H. Lund. 2008. "MicroRNA-10a Binds the 5′UTR of Ribosomal Protein mRNAs and Enhances Their Translation." *Molecular Cell* 30 (4): 460–71. doi:10.1016/j.molcel.2008.05.001.

Ostareck-Lederer, Antje, Dirk H. Ostareck, and Matthias W. Hentze. 1998. "Cytoplasmic Regulatory Functions of the KH-Domain Proteins hnRNPs K and E1/E2." *Trends in Biochemical Sciences* 23 (11): 409–11. doi:10.1016/S0968-0004(98)01301-2.

Ozgur, Sevim, Jérôme Basquin, Anastasiia Kamenska, Witold Filipowicz, Nancy Standart, and Elena Conti. 2015. "Structure of a Human 4E-T/DDX6/CNOT1 Complex Reveals the Different Interplay of DDX6-Binding Proteins with the CCR4-NOT Complex." *Cell Reports* 13 (4): 703–11. doi:10.1016/j.celrep.2015.09.033.

Palumbo, Amanda M, and Gavin E Reid. 2008. "Evaluation of Gas-Phase Rearrangement and Competing Fragmentation Reactions on Protein Phosphorylation Site Assignment Using Collision Induced Dissociation-MS / MS and MS Evaluation of Gas-Phase Rearrangement and Competing Fragmentation Reactions on Prote" 80 (24): 9735–47. doi:10.1016/j.jasms.2008.06.025.9736.

Pan, Chaoyun, Dihan Zhu, Yan Wang, Limin Li, Donghai Li, Fenyong Liu, Chen Yu Zhang, and Ke Zen. 2016. "Human Cytomegalovirus miR-UL148D Facilitates Latent Viral Infection by Targeting Host Cell Immediate Early Response Gene 5." *PLoS Pathogens* 12 (11): 1–26. doi:10.1371/journal.ppat.1006007.

Park, Jong-Eun, Inha Heo, Yuan Tian, Dhirendra K Simanshu, Hyeshik Chang, David Jee, Dinshaw J Patel, and V Narry Kim. 2011. "Dicer Recognizes the 5′ End of RNA for Efficient and Accurate Processing." *Nature* 475 (7355). Nature Publishing Group: 201–5. doi:10.1038/nature10198.

Paroo, Zain, Xuecheng Ye, She Chen, and Qinghua Liu. 2009. "Phosphorylation of the Human MicroRNA-Generating Complex Mediates MAPK/Erk Signaling." *Cell* 139 (1). Elsevier Ltd: 112–22. doi:10.1016/j.cell.2009.06.044.

Patel, Prajal H., Scott A. Barbee, and J. Todd Blankenship. 2016. “GW-Bodies and P-Bodies Constitute Two Separate Pools of Sequestered Non-Translating RNAs.” *PLoS ONE* 11 (3): 1–23. doi:10.1371/journal.pone.0150291.

Pérez Cañadillas, José Manuel, and Gabriele Varani. 2003. “Recognition of GU-Rich Polyadenylation Regulatory Elements by Human CstF-64 Protein.” *EMBO Journal* 22 (11): 2821–30. doi:10.1093/emboj/cdg259.

Peter, Daniel, Cátia Igreja, Ramona Weber, Lara Wohlbold, Catrin Weiler, Linda Ebertsch, Oliver Weichenrieder, and Elisa Izaurralde. 2015. “Molecular Architecture of 4E-BP Translational Inhibitors Bound to eIF4E.” *Molecular Cell* 57 (6): 1074–87. doi:10.1016/j.molcel.2015.01.017.

Pfaff, Janina, Janosch Hennig, Franz Herzog, Ruedi Aebersold, Michael Sattler, Dierk Niessing, and Gunter Meister. 2013. “Structural Features of Argonaute – GW182 Protein Interactions.” *Proceedings of the National Academy of Sciences of the United States of America* 110 (40): E3770–79. doi:10.1073/pnas.1308510110/-/DCSupplemental.www.pnas.org/cgi/doi/10.1073/pnas.1308510110.

Pfeffer, Sébastien, Alain Sewer, Mariana Lagos-Quintana, Robert Sheridan, Chris Sander, Friedrich a Grässer, Linda F van Dyk, et al. 2005. “Identification of microRNAs of the Herpesvirus Family.” *Nature Methods* 2 (4): 269–76. doi:10.1038/nmeth746.

Piao, Xianghua, Xue Zhang, Ligang Wu, and Joel G Belasco. 2010. “CCR4-NOT Deadenylates mRNA Associated with RNA-Induced Silencing Complexes in Human Cells.” *Molecular and Cellular Biology* 30 (6): 1486–94. doi:10.1128/MCB.01481-09.

Piedade, Diogo, and José Miguel Azevedo-Pereira. 2016. “The Role of microRNAs in the Pathogenesis of Herpesvirus Infection.” *Viruses* 8 (6). doi:10.3390/v8060156.

Pillai, Ramesh S, Suvendra N Bhattacharyya, Caroline G Artus, Tabea Zoller, Nicolas Cougot, Eugenia Basyuk, Edouard Bertrand, and Witold Filipowicz. 2005. “Inhibition of Translational Initiation by Let-7 MicroRNA in Human Cells.” *Science* 309 (5740): 1573–76. doi:10.1126/science.1115079.

Pitchiaya, Sethuramasundaram, Laurie A. Heinicke, Jun I. Park, Elizabeth L. Cameron, and Nils G. Walter. 2017. “Resolving Subcellular miRNA Trafficking and Turnover at Single-Molecule Resolution.” *Cell Reports* 19 (3). ElsevierCompany.: 630–42. doi:10.1016/j.celrep.2017.03.075.

Piwecka, Monika, Luis R Hernandez-miranda, Sebastian Memczak, Susanne A Wolf, Agnieszka Rybak-wolf, Andrei Filipchyk, Filippos Klironomos, et al. 2017. “Loss of a Mammalian Circular RNA Locus Causes miRNA Deregulation and Affects Brain Function” 8526: 1–14. doi:10.1126/science.aam8526.

Qi, Hank H, Pat P Ongusaha, Johanna Myllyharju, Dongmei Cheng, Outi Pakkanen, Yujiang Shi, Sam W Lee, Junmin Peng, and Yang Shi. 2008. “Prolyl 4-Hydroxylation Regulates Argonaute 2 Stability.” *Nature* 455 (7211): 421–24. doi:10.1038/nature07186.

Qi, Manlong, Ying Qi, Yanping Ma, Rong He, Yaohua Ji, Zhengrong Sun, and Qiang Ruan. 2013. “Over-Expression of Human Cytomegalovirus miR-US25-2-3p Downregulates eIF4A1 and Inhibits HCMV Replication.” *FEBS Letters* 587 (14). Federation of European Biochemical Societies: 2266–71. doi:10.1016/j.febslet.2013.05.057.

Quevillon Huberdeau, Miguel, Daniela M Zeitler, Judith Hauptmann, Astrid Bruckmann, Lucile Fressign?, Johannes Danner, Sandra Piquet, et al. 2017. “Phosphorylation of Argonaute Proteins Affects mRNA Binding and Is Essential for microRNA?guided Gene Silencing *In?vivo*.” *The EMBO Journal* 36 (14): e201696386. doi:10.15252/embj.201696386.

Quick-cleveland, Jen, Jose P Jacob, Sara H Weitz, Grant Shoffner, and Rachel Senturia. 2015. “microRNAs by Clamping the Hairpin” 7 (6): 1994–2005. doi:10.1016/j.celrep.2014.05.013.The.

Rajgor, Dipen, Jason A. Mellad, Daniel Soong, Jerome B. Rattner, Marvin J. Fritzler, and Catherine M. Shanahan. 2014. “Mammalian Microtubule P-Body Dynamics Are Mediated by Nesprin-1.” *Journal of Cell Biology* 205 (4): 457–75. doi:10.1083/jcb.201306076.

Ramalingam, Dhivya, and Joseph M. Ziegelbauer. 2017. “Viral microRNAs Target a Gene Network, Inhibit STAT Activation, and Suppress Interferon Responses.” *Scientific Reports* 7 (January). Nature Publishing Group: 40813. doi:10.1038/srep40813.

Ramalingam, Pradeep, Jayanth Kumar Palanichamy, Anand Singh, Prerna Das, Mohita Bhagat, Muzaffer Ahmad Kassab, Subrata Sinha, and Parthaprasad Chattopadhyay. 2014. “Biogenesis of Intronic miRNAs Located in Clusters by Independent Transcription and Alternative Splicing.” *RNA (New York, N.Y.)* 20 (1): 76–87. doi:10.1261/rna.041814.113.

Rammelt, Christiane, Biter Bilen, Mihaela Zavolan, and Walter Keller. 2011. “PAPD5, a Noncanonical poly(A) Polymerase with an Unusual RNA-Binding Motif.” *RNA (New York, N.Y.)* 17 (9): 1737–46. doi:10.1261/rna.2787011.

Rau, Frédérique, Fernande Freyermuth, Charlotte Fugier, Jean-Philippe Villemin, Marie-Christine Fischer, Bernard Jost, Doulaye Dembele, et al. 2011. “Misregulation of miR-1 Processing Is Associated with Heart Defects in Myotonic Dystrophy.” *Nature Structural & Molecular Biology* 18 (7). Nature Publishing Group: 840–45. doi:10.1038/nsmb.2067.

Raver-Shapira, Nina, Efi Marciano, Eti Meiri, Yael Spector, Nitzan Rosenfeld, Neta Moskovits, Zvi Bentwich, and Moshe Oren. 2007. “Transcriptional Activation of miR-34a Contributes to p53-Mediated Apoptosis.” *Molecular Cell* 26 (5): 731–43. doi:10.1016/j.molcel.2007.05.017.

Richards, Kathleen F., Anna Guastafierro, Masahiro Shuda, Tuna Toptan, Patrick S. Moore, and Yuan Chang. 2015. "Merkel Cell Polyomavirus T Antigens Promote Cell Proliferation and Inflammatory Cytokine Gene Expression." *Journal of General Virology* 96 (12): 3532–44. doi:10.1099/jgv.0.000287.

Rieckher, Matthias, and Nektarios Tavernarakis. 2017. "P-Body and Stress Granule Quantification in Caenorhabditis Elegans." *Bio-Protocol* 7 (2). doi:10.21769/BioProtoc.2108.

Rnas, Dicer-dependent, Joshua E Babiarz, J Graham Ruby, Yangming Wang, David P Bartel, and Robert Blelloch. 2008. "Mouse ES Cells Express Endogenous shRNAs , siRNAs , and Other," 2773–85. doi:10.1101/gad.1705308.).

Robles, Maria S., Sean J. Humphrey, and Matthias Mann. 2017. "Phosphorylation Is a Central Mechanism for Circadian Control of Metabolism and Physiology." *Cell Metabolism* 25 (1). Elsevier Inc.: 118–27. doi:10.1016/j.cmet.2016.10.004.

Roden, Christine, Jonathan Gaillard, Shaveta Kanoria, William Rennie, Syndi Barish, Jijun Cheng, Wen Pan, et al. 2017. "Novel Determinants of Mammalian Primary microRNA Processing Revealed by Systematic Evaluation of Hairpin-Containing Transcripts and Human Genetic Variation." *Genome Research* 27 (3): 374–84. doi:10.1101/gr.208900.116.

Ross, Nathan, Maher K Gandhi, and Jamie P Nourse. 2013. "The Epstein-Barr Virus microRNA BART11-5p Targets the Early B-Cell Transcription Factor EBF1." *American Journal of Blood Research* 3 (3): 210–24. http://www.pubmedcentral.nih.gov/articlerender.fcgi?artid=3755520&tool=pmcentrez&rendertype=abstract.

Roth, Braden M., Daniella Ishimaru, and Mirko Hennig. 2013. "The Core Microprocessor Component DiGeorge Syndrome Critical Region 8 (DGCR8) Is a Nonspecific RNA-Binding Protein." *Journal of Biological Chemistry* 288 (37): 26785–99. doi:10.1074/jbc.M112.446880.

Röther, Susanne, and Gunter Meister. 2011. "Small RNAs Derived from Longer Non-Coding RNAs." *Biochimie* 93 (11). Elsevier Masson SAS: 1905–15. doi:10.1016/j.biochi.2011.07.032.

Rüdel, Sabine, Andrew Flatley, Lasse Weinmann, Elisabeth Kremmer, and Gunter Meister. 2008. "A Multifunctional Human Argonaute2-Specific Monoclonal Antibody." *RNA (New York, N.Y.)* 14 (6): 1244–53. doi:10.1261/rna.973808.

Rüdel, Sabine, Yanli Wang, René Lenobel, Roman Körner, He Hsuan Hsiao, Henning Urlaub, Dinshaw Patel, and Gunter Meister. 2011. "Phosphorylation of Human Argonaute Proteins Affects Small RNA Binding." *Nucleic Acids Research* 39 (6): 2330–43. doi:10.1093/nar/gkq1032.

Rüegger, Stefan, and Helge Großhans. 2012. "MicroRNA Turnover: When, How, and Why." *Trends in Biochemical Sciences* 37 (10): 436–46. doi:10.1016/j.tibs.2012.07.002.

Rybak, Agnieszka, Heiko Fuchs, Kamyar Hadian, Lena Smirnova, Ellery A. Wulczyn, Geert Michel, Robert Nitsch, Daniel Krappmann, and F Gregory Wulczyn. 2009. "The Let-7 Target Gene Mouse Lin-41 Is a Stem Cell Specific E3 Ubiquitin Ligase for the miRNA Pathway Protein Ago2." *Nature Cell Biology* 11 (12). Nature Publishing Group: 1411–20. doi:10.1038/ncb1987.

Rybak, Agnieszka, Heiko Fuchs, Lena Smirnova, Christine Brandt, Elena E Pohl, Robert Nitsch, and F Gregory Wulczyn. 2008. "A Feedback Loop Comprising Lin-28 and Let-7 Controls Pre-Let-7 Maturation during Neural Stem-Cell Commitment." *Nature Cell Biology* 10 (8): 987–93. doi:10.1038/ncb1759.

Sabin, Leah R., Rui Zhou, Joshua J. Gruber, Nina Lukinova, Shelly Bambina, Allison Berman, Chi Kong Lau, Craig B. Thompson, and Sara Cherry. 2009. "Ars2 Regulates Both miRNA- and siRNA- Dependent Silencing and Suppresses RNA Virus Infection in Drosophila." *Cell* 138 (2). Elsevier Ltd: 340–51. doi:10.1016/j.cell.2009.04.045.

Sahin, Umut, Pierre Lapaquette, Alexandra Andrieux, Guilhem Faure, and Anne Dejean. 2014. "Sumoylation of Human Argonaute 2 at Lysine-402 Regulates Its Stability." *PLoS ONE* 9 (7): 1–11. doi:10.1371/journal.pone.0102957.

Sakamoto, Shuji, Kazuma Aoki, Takuma Higuchi, Hiroshi Todaka, Keiko Morisawa, Nobuyuki Tamaki, Etsuro Hatano, Atsuki Fukushima, Taketoshi Taniguchi, and Yasutoshi Agata. 2009. "The NF90-NF45 Complex Functions as a Negative Regulator in the microRNA Processing Pathway." *Molecular and Cellular Biology* 29 (13): 3754–69. doi:10.1128/MCB.01836-08.

Schraivogel, Daniel, Susann G. Schindler, Johannes Danner, Elisabeth Kremmer, Janina Pfaff, Stefan Hannus, Reinhard Depping, and Gunter Meister. 2015. "Importin-?? Facilitates Nuclear Import of Human GW Proteins and Balances Cytoplasmic Gene Silencing Protein Levels." *Nucleic Acids Research* 43 (15): 7447–61. doi:10.1093/nar/gkv705.

Schraivogel, Daniel, Susann G Schindler, Johannes Danner, Elisabeth Kremmer, Janina Pfaff, Stefan Hannus, Reinhard Depping, and Gunter Meister. n.d. "Importin- β Facilitates Nuclear Import of Human GW Proteins and Balances Cytoplasmic Gene Silencing Protein Levels Daniel Schraivogel, Susann G. Schindler, Johannes Danner, Elisabeth Kremmer, Janina Pfaff, Stefan Hannus, Reinhard Depping & Gunter Meister."

Schratt, Gerhard M, Fabian Tuebing, Elizabeth a Nigh, Christina G Kane, Mary E Sabatini, Michael Kiebler, and Michael E Greenberg. 2006. "A Brain-Specific microRNA Regulates Dendritic Spine Development." *Nature* 439 (7074): 283–89. doi:10.1038/nature04909.

Seo, G J, L H L Fink, B O'Hara, W J Atwood, and C S Sullivan. 2008. "Evolutionarily Conserved Function of a Viral microRNA." *Journal of Virology* 82 (20): 9823–28. doi:10.1128/JVI.01144-08.

Seo, Gil Ju, Chun Jung Chen, and Christopher S. Sullivan. 2009. "Merkel Cell Polyomavirus Encodes a microRNA with the Ability to Autoregulate Viral Gene Expression." *Virology* 383 (2). Elsevier Inc.: 183–87. doi:10.1016/j.virol.2008.11.001.

Sewer, Alain, Nicola Iovino, Alexei Aravin, Sébastien Pfeffer, and Amanda Rice. 2007. "A Mammalian microRNA Expression Atlas Based on Small RNA Library Sequencing." *Cell* 129 (7): 1401–14. doi:10.1016/j.cell.2007.04.040.A.

Sharif, Humayun, and Elena Conti. 2013. "Architecture of the Lsm1-7-Pat1 Complex: A Conserved Assembly in Eukaryotic mRNA Turnover." *Cell Reports* 5 (2). The Authors: 283–91. doi:10.1016/j.celrep.2013.10.004.

Sharma, Kirti, Rochelle C J D'Souza, Stefka Tyanova, Christoph Schaab, JacekR Wiśniewski, Jürgen Cox, and Matthias Mann. 2014. "Ultradeep Human Phosphoproteome Reveals a Distinct Regulatory Nature of Tyr and Ser/Thr-Based Signaling." *Cell Reports* 8 (5): 1583–94. doi:10.1016/j.celrep.2014.07.036.

Sharma, Nishi R., Xiaohong Wang, Vladimir Majerciak, Masahiko Ajiro, Michael Kruhlak, Craig Meyers, and Zhi Ming Zheng. 2016. "Cell Type- and Tissue Contextdependent Nuclear Distribution of Human Ago2." *Journal of Biological Chemistry* 291 (5): 2302–9. doi:10.1074/jbc.C115.695049.

Shen, J, W Xia, Y B Khotskaya, L Huo, K Nakanishi, S O Lim, Y Du, et al. 2013. "EGFR Modulates microRNA Maturation in Response to Hypoxia through Phosphorylation of AGO2." *Nature* 497 (7449): 383–87. doi:10.1038/nature12080.

Shyh-Chang, Ng, and George Q. Daley. 2013. "Lin28: Primal Regulator of Growth and Metabolism in Stem Cells." *Cell Stem Cell* 12 (4). Elsevier Inc.: 395–406. doi:10.1016/j.stem.2013.03.005.

Sinclair, John H., and Matthew B. Reeves. 2013. "Human Cytomegalovirus Manipulation of Latently Infected Cells." *Viruses* 5 (11): 2803–24. doi:10.3390/v5112803.

Sinclair, John, and Matthew Reeves. 2014. "The Intimate Relationship between Human Cytomegalovirus and the Dendritic Cell Lineage." *Frontiers in Microbiology* 5 (AUG): 1–14. doi:10.3389/fmicb.2014.00389.

Sissons, J. G.P., A. J. Carmichael, N. McKinney, J. H. Sinclair, and M. R. Wills. 2002. "Human Cytomegalovirus and Immunopathology." *Springer Seminars in Immunopathology* 24 (2): 169–85. doi:10.1007/s00281-002-0104-0.

Song, Min-Sun, and John J Rossi. 2017. "Molecular Mechanisms of Dicer: Endonuclease and Enzymatic Activity." *The Biochemical Journal* 474 (10): 1603–18. doi:10.1042/BCJ20160759.

Speck, Samuel H., and Don Ganem. 2010. "Viral Latency and Its Regulation: Lessons from the γ-Herpesviruses." *Cell Host and Microbe* 8 (1). Elsevier Inc.: 100–115. doi:10.1016/j.chom.2010.06.014.

Stakaityte, Gabriele, Jennifer J. Wood, Laura M. Knight, Hussein Abdul-Sada, Noor Suhana Adzahar, Nnenna Nwogu, Andrew Macdonald, and Adrian Whitehouse. 2014. "Merkel Cell Polyomavirus: Molecular Insights into the Most Recently Discovered Human Tumour Virus." *Cancers* 6 (3): 1267–97. doi:10.3390/cancers6031267.

Stamatiou, Dimitris P., Stavros P. Derdas, Odysseas L. Zoras, and Demetrios A. Spandidos. 2016. "Herpes and Polyoma Family Viruses in Thyroid Cancer." *Oncology Letters* 11 (3): 1635–44. doi:10.3892/ol.2016.4144.

Steen, Hanno, Judith A. Jebanathirajah, John Rush, Nicolas Morrice, and Marc W. Kirschner. 2006. "Phosphorylation Analysis by Mass Spectrometry." *Molecular & Cellular Proteomics* 5 (1): 172–81. doi:10.1074/mcp.M500135-MCP200.

Stern-Ginossar, Noam, Niveen Saleh, Miri D Goldberg, Mark Prichard, Dana G Wolf, and Ofer Mandelboim. 2009. "Analysis of Human Cytomegalovirus-Encoded microRNA Activity during Infection." *Journal of Virology* 83 (20): 10684–93. doi:10.1128/JVI.01292-09.

Stowell, James A W, Michael W. Webster, Alexander K??gel, Jana Wolf, Kathryn L. Shelley, and Lori A. Passmore. 2016. "Reconstitution of Targeted Deadenylation by the Ccr4-Not Complex and the YTH Domain Protein Mmi1." *Cell Reports* 17 (8): 1978–89. doi:10.1016/j.celrep.2016.10.066.

Subtelny, Alexander O, Stephen W Eichhorn, Grace R Chen, Hazel Sive, and David P Bartel. 2014. "Poly(A)-Tail Profiling Reveals an Embryonic Switch in Translational Control." *Nature* 508 (7494). Nature Publishing Group: 66–71. doi:10.1038/nature13007\rhttp://www.nature.com/nature/journal/v508/n7494/abs/nature13007.html#supplementary-information.

Sullivan, Christopher S, Adam T Grundhoff, Satvir Tevethia, James M Pipas, and Don Ganem. 2005. "SV40-Encoded microRNAs Regulate Viral Gene Expression and Reduce Susceptibility to Cytotoxic T Cells." *Nature* 435 (7042): 682–86. doi:10.1038/nature03576.

Sun, Mai, Björn Schwalb, Nicole Pirkl, Kerstin C. Maier, Arne Schenk, Henrik Failmezger, Achim Tresch, and Patrick Cramer. 2013. "Global Analysis of Eukaryotic mRNA Degradation Reveals Xrn1-Dependent Buffering of Transcript Levels." *Molecular Cell* 52 (1): 52–62. doi:10.1016/j.molcel.2013.09.010.

Suzuki, Hiroshi I, Kaoru Yamagata, Koichi Sugimoto, Takashi Iwamoto, Shigeaki Kato, and Kohei Miyazono. 2009. "Modulation of

microRNA Processing by p53." *Nature* 460 (7254). Nature Publishing Group: 529–33. doi:10.1038/nature08199.

Swanson, M S, T Y Nakagawa, K LeVan, and G Dreyfuss. 1987. "Primary Structure of Human Nuclear Ribonucleoprotein Particle C Proteins: Conservation of Sequence and Domain Structures in Heterogeneous Nuclear RNA, mRNA, and Pre-rRNA-Binding Proteins." *Molecular and Cellular Biology* 7 (5): 1731–39. doi:10.1128/MCB.7.5.1731.

Tabach, Yuval, Allison C Billi, Gabriel D Hayes, Martin a Newman, Or Zuk, Harrison Gabel, Ravi Kamath, et al. 2013. "Identification of Small RNA Pathway Genes Using Patterns of Phylogenetic Conservation and Divergence." *Nature* 493 (7434). Nature Publishing Group: 694–98. doi:10.1038/nature11779.

Takimoto, Koji, Motoaki Wakiyama, and Shigeyuki Yokoyama. 2009. "Mammalian GW182 Contains Multiple Argonaute-Binding Sites and Functions in microRNA-Mediated Translational Repression." *RNA (New York, N.Y.)* 15 (6): 1078–89. doi:10.1261/rna.1363109.

Tang, Rui, Limin Li, Dihan Zhu, Dongxia Hou, Ting Cao, Hongwei Gu, Jing Zhang, Junyuan Chen, Chen-Yu Zhang, and Ke Zen. 2012. "Mouse miRNA-709 Directly Regulates miRNA-15a/16-1 Biogenesis at the Posttranscriptional Level in the Nucleus: Evidence for a microRNA Hierarchy System." *Cell Research* 22 (3). Nature Publishing Group: 504–15. doi:10.1038/cr.2011.137.

Tang, Shuang, Andrea S Bertke, Amita Patel, Kening Wang, Jeffrey I Cohen, and Philip R Krause. 2008. "An Acutely and Latently Expressed Herpes Simplex Virus 2 Viral microRNA Inhibits Expression of ICP34.5, a Viral Neurovirulence Factor." *Proceedings of the National Academy of Sciences of the United States of America* 105 (31): 10931–36. doi:10.1073/pnas.0801845105.

Tang, Shuang, Nini Guo, Amita Patel, and Philip R Krause. 2013. "Herpes Simplex Virus 2 Expresses a Novel Form of ICP34.5, a Major Viral Neurovirulence Factor, through Regulated Alternative Splicing." *Journal of Virology* 87 (10): 5820–30. doi:10.1128/JVI.03500-12.

Tang, Shuang, Amita Patel, and Philip R Krause. 2009. "Novel Less-Abundant Viral microRNAs Encoded by Herpes Simplex Virus 2 Latency-Associated Transcript and Their Roles in Regulating ICP34.5 and ICP0 mRNAs." *Journal of Virology* 83 (3): 1433–42. doi:10.1128/JVI.01723-08.

Tang, Xiaoli, Ming Li, Lynne Tucker, and Bharat Ramratnam. 2011. "Glycogen Synthase Kinase 3 Beta (GSK3β) Phosphorylates the RNAase III Enzyme Drosha at S300 and S302." *PLoS ONE* 6 (6): 1–6. doi:10.1371/journal.pone.0020391.

Tang, Xiaoli, Sicheng Wen, Dong Zheng, Lynne Tucker, Lulu Cao, Dennis Pantazatos, Steven F. Moss, and Bharat Ramratnam. 2013. "Acetylation of Drosha on the N-Terminus Inhibits Its Degradation by Ubiquitination." *PLoS ONE* 8 (8). doi:10.1371/journal.pone.0072503.

Tang, Xiaoli, Yingjie Zhang, Lynne Tucker, and Bharat Ramratnam. 2010. "Phosphorylation of the RNase III Enzyme Drosha at Serine300 or Serine302 Is Required for Its Nuclear Localization." *Nucleic Acids Research* 38 (19): 6610–19. doi:10.1093/nar/gkq547.

Tarasov, Valery, Peter Jung, Berlinda Verdoodt, Dmitri Lodygin, Alexey Epanchintsev, Antje Menssen, Gunter Meister, and Heiko Hermeking. 2007. "Differential Regulation of microRNAs by p53 Revealed by Massively Parallel Sequencing: miR-34a Is a p53 Target That Induces Apoptosis and G 1-Arrest." *Cell Cycle* 6 (13): 1586–93. doi:10.4161/cc.6.13.4436.

Taylor, David W, Enbo Ma, Hideki Shigematsu, Michael A Cianfrocco, Cameron L Noland, Kuniaki Nagayama, Eva Nogales, Jennifer A Doudna, and Hong-Wei Wang. 2013. "Substrate-Specific Structural Rearrangements of Human Dicer." *Nature Structural & Molecular Biology* 20 (6): 662–70. doi:10.1038/nsmb.2564.

Thillainadesan, Gobi, Jennifer Mary Chitilian, Majdina Isovic, Jailal Nicholas George Ablack, Joe Stephen Mymryk, Marc Tini, and Joseph Torchia. 2012. "TGF-β-Dependent Active Demethylation and Expression of the p15 ink4b Tumor Suppressor Are Impaired by the ZNF217/CoREST Complex." *Molecular Cell* 46 (5). Elsevier Inc.: 636–49. doi:10.1016/j.molcel.2012.03.027.

Thornton, James E., Peng Du, Lili Jing, Ljiljana Sjekloca, Shuibin Lin, Elena Grossi, Piotr Sliz, Leonard I. Zon, and Richard I. Gregory. 2014. "Selective microRNA Uridylation by Zcchc6 (TUT7) and Zcchc11 (TUT4)." *Nucleic Acids Research* 42 (18): 11777–91. doi:10.1093/nar/gku805.

Trabucchi, Michele, Paola Briata, Mariaflor Garcia-Mayoral, Astrid D Haase, Witold Filipowicz, Andres Ramos, Roberto Gherzi, and Michael G Rosenfeld. 2009. "The RNA-Binding Protein KSRP Promotes the Biogenesis of a Subset of microRNAs." *Nature* 459 (7249). Nature Publishing Group: 1010–14. doi:10.1038/nature08025\rnature08025 [pii].

Treiber, Thomas, Nora Treiber, Uwe Plessmann, Simone Harlander, Julia Lisa Daiß, Norbert Eichner, Gerhard Lehmann, Kevin Schall, Henning Urlaub, and Gunter Meister. 2017. "A Compendium of RNA-Binding Proteins That Regulate MicroRNA Biogenesis." *Molecular Cell* 66 (2). Elsevier Inc.: 270–284.e13. doi:10.1016/j.molcel.2017.03.014.

Triboulet, Robinson, Mehdi Pirouz, and Richard I. Gregory. 2015. "A Single Let-7 MicroRNA Bypasses LIN28-Mediated Repression." *Cell Reports* 13 (2). The Authors: 260–66. doi:10.1016/j.celrep.2015.08.086.

Tritschler, Felix, Joerg E. Braun, Ana Eulalio, Vincent Truffault, Elisa Izaurralde, and Oliver Weichenrieder. 2009. "Structural Basis for the Mutually Exclusive Anchoring of P Body Components EDC3 and Tral to the DEAD Box Protein DDX6/Me31B." *Molecular Cell* 33 (5). Elsevier Ltd: 661–68. doi:10.1016/j.molcel.2009.02.014.

Tsanov, K M, D S Pearson, Z Wu, A Han, R Triboulet, M T Seligson, J T Powers, et al. 2017. “LIN28 Phosphorylation by MAPK/ERK Couples Signalling to the Post-Transcriptional Control of Pluripotency.” *Nat Cell Biol* 19 (1): 60–67. doi:10.1038/ncb3453.

Uchida, J. 1999. “Mimicry of CD40 Signals by Epstein-Barr Virus LMP1 in B Lymphocyte Responses.” *Science* 286 (5438): 300–303. doi:10.1126/science.286.5438.300.

Ufer, Christoph, Chi Chiu Wang, Michael Fähling, Heike Schiebel, Bernd J Thiele, E Ellen Billett, Hartmut Kuhn, and Astrid Borchert. 2008. “Translational Regulation of Glutathione Peroxidase 4 Expression through Guanine- Rich Sequence-Binding Factor 1 Is Essential for Embryonic Brain Development.” *Genes & Development* 22: 1838–50. doi:10.1101/gad.466308.7.

Ulasov, Ilya V., Natalya V. Kaverina, Dhimankrishna Ghosh, Marya A. Baryshnikova, Zaira G. Kadagidze, Apollon I. Karseladze, Anatoly Y. Baryshnikov, and Charles S. Cobbs. 2016. “CMV70-3P miRNA Contributes to the CMV Mediated Glioma Stemness and Represents a Target for Glioma Experimental Therapy.” *Oncotarget* 8 (16): 25989–99. doi:10.18632/oncotarget.11175.

Umbach, Jennifer L, Kening Wang, Shuang Tang, Philip R Krause, Erik K Mont, Jeffrey I Cohen, and Bryan R Cullen. 2010. “Identification of Viral microRNAs Expressed in Human Sacral Ganglia Latently Infected with Herpes Simplex Virus 2.” *Journal of Virology* 84 (2): 1189–92. doi:10.1128/JVI.01712-09.

Umbach, Jennifer Lin, Martha F Kramer, Igor Jurak, Heather W Karnowski, Donald M, and Bryan R Cullen. 2009. “NIH Public Access.” *Biological Chemistry* 454 (7205): 780–83. doi:10.1038/nature07103.MicroRNAs.

Valverde, Roberto, Laura Edwards, and Lynne Regan. 2008. “Structure and Function of KH Domains.” *FEBS Journal* 275 (11): 2712–26. doi:10.1111/j.1742-4658.2008.06411.x.

van Rooij, Eva, Lillian B Sutherland, Xiaoxia Qi, James a Richardson, Joseph Hill, and Eric N Olson. 2007. “Control of Stress-Dependent Cardiac Growth and Gene Expression by a microRNA.” *Science* 316 (5824): 575–79. doi:10.1126/science.1139089.

Vereide, D T, E Seto, Y-F Chiu, M Hayes, T Tagawa, A Grundhoff, W Hammerschmidt, and B Sugden. 2014. “Epstein-Barr Virus Maintains Lymphomas via Its miRNAs.” *Oncogene* 33 (10). Nature Publishing Group: 1258–64. doi:10.1038/onc.2013.71.

Viswanathan, S. R., G. Q. Daley, and R. I. Gregory. 2008. “Selective Blockade of microRNA Processing by Lin-28.” *Science (New York, N.Y.)* 320 (5872): 97–100. doi:10.1126/science.1154040.

Vos, Shoko, Farhad Vesuna, Venu Raman, Paul J van Diest, and Petra van der Groep. 2015. “miRNA Expression Patterns in Normal Breast Tissue and Invasive Breast Cancers of BRCA1 and BRCA2 Germ-Line Mutation Carriers.” *Oncotarget* 6 (31): 32115–37. doi:10.18632/oncotarget.5617.

Wahle, Elmar, and G. Sebastiaan Winkler. 2013. “RNA Decay Machines: Deadenylation by the Ccr4-Not and Pan2-Pan3 Complexes.” *Biochimica et Biophysica Acta - Gene Regulatory Mechanisms* 1829 (6–7). Elsevier B.V.: 561–70. doi:10.1016/j.bbagrm.2013.01.003.

Wang, Chris, Pratyush Gupta, Lucile Fressigne, Gabriel D. Bossé, Xin Wang, Martin J. Simard, and Dave Hansen. 2016. “TEG-1 CD2BP2 Controls miRNA Levels by Regulating miRISC Stability in *C. Elegans* and Human Cells.” *Nucleic Acids Research* 45 (3): gkw836. doi:10.1093/nar/gkw836.

Wang, Longfei, Yunsun Nam, Anna K. Lee, Chunxiao Yu, Kira Roth, Casandra Chen, Elizabeth M. Ransey, and Piotr Sliz. 2017. “LIN28 Zinc Knuckle Domain Is Required and Sufficient to Induce Let-7 Oligouridylation.” *Cell Reports* 18 (11). ElsevierCompany.: 2664–75. doi:10.1016/j.celrep.2017.02.044.

Wilczynska, A, and M Bushell. 2015. “The Complexity of miRNA-Mediated Repression.” *Cell Death and Differentiation* 22 (1). Nature Publishing Group: 22–33. doi:10.1038/cdd.2014.112.

Wilson, Ross C., Akshay Tambe, Mary Anne Kidwell, Cameron L. Noland, Catherine P. Schneider, and Jennifer A. Doudna. 2015. “Dicer-TRBP Complex Formation Ensures Accurate Mammalian MicroRNA Biogenesis.” *Molecular Cell* 57 (3). Elsevier Inc.: 397–408. doi:10.1016/j.molcel.2014.11.030.

Wolf, Jana, Eugene Valkov, Mark D Allen, Birthe Meineke, Yuliya Gordiyenko, Stephen H Mclaughlin, Tayla M Olsen, et al. 2014. “Structural Basis for Pan3 Binding to Pan2 and Its Function in mRNA Recruitment and Deadenylation.” *The EMBO Journal* 33 (14): 1514–26. doi:10.15252/embj.

Wong, Alissa Michelle Go, Kar Lok Kong, Janice Wing Hang Tsang, Dora Lai Wan Kwong, and Xin Yuan Guan. 2012. “Profiling of Epstein-Barr Virus-Encoded microRNAs in Nasopharyngeal Carcinoma Reveals Potential Biomarkers and Oncomirs.” *Cancer* 118 (3): 698–710. doi:10.1002/cncr.26309.

Wu, Edlyn, Ajay A Vashisht, Clément Chapat, Mathieu N Flamand, Emiliano Cohen, Mihail Sarov, Yuval Tabach, Nahum Sonenberg, James Wohlschlegel, and Thomas F Duchaine. 2016. “A Continuum of mRNP Complexes in Embryonic microRNA-Mediated Silencing.” *Nucleic Acids Research* 45 (4): gkw872. doi:10.1093/nar/gkw872.

Wu, Han, Shuying Sun, Kang Tu, Yuan Gao, Bin Xie, Adrian R. Krainer, and Jun Zhu. 2010. “A Splicing-Independent Function of SF2/ASF in MicroRNA Processing.” *Molecular Cell* 38 (1). Elsevier Ltd: 67–77. doi:10.1016/j.molcel.2010.02.021.

Wu, Hong, Priya Kapoor, and Lori Frappier. 2002. “Separation of the DNA Replication , Segregation , and Transcriptional Activation Functions of Epstein-Barr Nuclear Antigen 1 Separation of the DNA Replication , Segregation , and Transcriptional Activation Functions of Epstein-Barr Nuclear Antigen 1.” *Journal of Virology* 76 (5): 2480–90. doi:10.1128/JVI.76.5.2480.

Wu, S, S Huang, J Ding, Y Zhao, L Liang, T Liu, R Zhan, and X He. 2010. “Multiple microRNAs Modulate p21Cip1/Waf1 Expression by Directly Targeting Its 3’ Untranslated Region.” *Oncogene* 29 (15): 2302–8. doi:10.1038/onc.2010.34.

Xhemalce, Blerta, Samuel C. Robson, and Tony Kouzarides. 2012. “Human RNA Methyltransferase BCDIN3D Regulates MicroRNA Processing.” *Cell* 151 (2). Elsevier: 278–88. doi:10.1016/j.cell.2012.08.041.

Xing, Li, and Elliott Kieff. 2007. “Epstein-Barr Virus BHRF1 Micro- and Stable RNAs during Latency III and after Induction of Replication.” *Journal of Virology* 81 (18): 9967–75. doi:10.1128/JVI.02244-06.

Xu, Chi, Hui Zheng, Horace H Loh, Ping-yee Law, and Cancer Biology Group. 2016. “Activation and TRBP Phosphorylation” 33 (9): 2762–72. doi:10.1002/stem.2055.Morphine.

Xu, Rui-Ming, Lana Jokhan, Xiaodong Cheng, Akila Mayeda, and Adrian R Krainer. 1997. “Crystal Structure of Human UP1, the Domain of hnRNP A1 That Contains Two RNA-Recognition Motifs.” *Structure* 5 (4): 559–70. doi:10.1016/S0969-2126(97)00211-6.

Yamashita, Akio, Tsung-Cheng Chang, Yukiko Yamashita, Wenmiao Zhu, Zhenping Zhong, Chyi-Ying a Chen, and Ann-Bin Shyu. 2005. “Concerted Action of poly(A) Nucleases and Decapping Enzyme in Mammalian mRNA Turnover.” *Nature Structural & Molecular Biology* 12 (12): 1054–63. doi:10.1038/nsmb1016.

Yates, J L, N Warren, and B Sugden. 1985. “Stable Replication of Plasmids Derived from Epstein-Barr Virus in Various Mammalian Cells.” *Nature* 313 (6005): 812–15. doi:10.1038/314731a0.

Yi, Rui, Yi Qin, Ian G Macara, and Bryan R Cullen. 2003. “Exportin-5 Mediates the Nuclear Export of Pre-microRNAs and Short Hairpin RNAs Exportin-5 Mediates the Nuclear Export of Pre-microRNAs and Short Hairpin RNAs,” 3011–16. doi:10.1101/gad.1158803.

Zekri, Latifa, Eric Huntzinger, Susanne Heimstädt, and Elisa Izaurralde. 2009. “The Silencing Domain of GW182 Interacts with PABPC1 to Promote Translational Repression and Degradation of microRNA Targets and Is Required for Target Release.” *Molecular and Cellular Biology* 29 (23): 6220–31. doi:10.1128/MCB.01081-09.

Zekri, Latifa, Duygu Kuzuoğlu-Öztürk, and Elisa Izaurralde. 2013. “GW182 Proteins Cause PABP Dissociation from Silenced miRNA Targets in the Absence of Deadenylation.” *The EMBO Journal* 32 (7): 1052–65. doi:10.1038/emboj.2013.44.

Zeng, Yan, Heidi Sankala, Xiaoxiao Zhang, and Paul R Graves. 2008. “Phosphorylation of Argonaute 2 at Serine-387 Facilitates Its Localization to Processing Bodies.” *The Biochemical Journal* 413 (3): 429–36. doi:10.1042/BJ20080599.

Zhang, Bo, Qian Shi, Sapna N. Varia, Siyuan Xing, Bethany M. Klett, Laura A. Cook, and Paul K. Herman. 2016. “The Activity-Dependent Regulation of Protein Kinase Stability by the Localization to P-Bodies.” *Genetics* 203 (3): 1191–1202. doi:10.1534/genetics.116.187419.

Zhang, Haidi, Fabrice A. Kolb, Lukasz Jaskiewicz, Eric Westhof, and Witold Filipowicz. 2004. “Single Processing Center Models for Human Dicer and Bacterial RNase III.” *Cell* 118 (1): 57–68. doi:10.1016/j.cell.2004.06.017.

Zhang, Xinna, Guohui Wan, Franklin G. Berger, Xiaoming He, and Xiongbin Lu. 2011. “The ATM Kinase Induces MicroRNA Biogenesis in the DNA Damage Response.” *Molecular Cell* 41 (4). Elsevier Inc.: 371–83. doi:10.1016/j.molcel.2011.01.020.

Zhu, Changhong, Cheng Chen, Jian Huang, Hailong Zhang, Xian Zhao, Rong Deng, Jinzhuo Dou, et al. 2015. “SUMOylation at K ^{707} of DGCR8 Controls Direct Function of Primary microRNA.” *Nucleic Acids Research* 43 (16): 7945–60. doi:10.1093/nar/gkv741.

Zhu, Jia Yun, Thorsten Pfuhl, Natalie Motsch, Stephanie Barth, John Nicholls, Friedrich Grässer, and Gunter Meister. 2009. “Identification of Novel Epstein-Barr Virus microRNA Genes from Nasopharyngeal Carcinomas.” *Journal of Virology* 83 (7): 3333–41. doi:10.1128/JVI.01689-08.

Zielezinski, Andrzej, and Wojciech M Karlowski. 2015. “Early Origin and Adaptive Evolution of the GW182 Protein Family, the Key Component of RNA Silencing in Animals.” *RNA Biology* 12 (7): 761–70. doi:10.1080/15476286.2015.1051302.

Zipprich, Jakob T, Sankar Bhattacharyya, Hansruedi Mathys, and Witold Filipowicz. 2009. “Importance of the C-Terminal Domain of the Human GW182 Protein TNRC6C for Translational Repression.” *RNA (New York, N.Y.)* 15 (5): 781–93. doi:10.1261/rna.1448009.

Zisoulis, Dimitrios G., Zoya S. Kai, Roger K. Chang, and Amy E. Pasquinelli. 2012. “Autoregulation of microRNA Biogenesis by Let-7 and Argonaute.” *Nature* 486 (7404). Nature Publishing Group: 541–44. doi:10.1038/nature11134.

Toker, C. Trabecular Carcinoma of the Skin. Arch. Dermatol. 1972, 105, 107–110.

Meyer KD, Saletore Y, Zumbo P, Elemento O, Mason CE, Jaffrey SR. Comprehensive analysis of mRNA methylation reveals enrichment in 30 UTRs and near stop codons. Cell 2012; 149: 1635–1646

Semotok, J.L., Cooperstock, R.L., Pinder, B.D., Vari, H.K., Lipshitz, H.D., and Smibert, C.A. (2005). Smaug recruits the CCR4/POP2/NOT deadenylase complex to trigger maternal transcript localization in the early Drosophila embryo.Curr. Biol.

Eidesstattliche Erklärung

Ich erkläre hiermit an Eides statt, dass ich die vorliegende Arbeit ohne unzulässige Hilfe Dritter und ohne Benutzung anderer als der angegebenen Hilfsmittel angefertigt habe; die aus anderen Quellen direkt oder indirekt übernommenen Daten und Konzepte sind unter Angabe des Literaturzitats gekennzeichnet.
Weitere Personen waren an der inhaltlich-materiellen Herstellung der vorliegenden Arbeit nicht beteiligt. Insbesondere habe ich hierfür nicht die entgeltliche Hilfe eines Promotionsberaters oder anderer Personen in Anspruch genommen. Niemand hat von mir weder unmittelbar noch mittelbar geldwerte Leistungen für Arbeiten erhalten, die im Zusammenhang mit dem Inhalt der vorgelegten Dissertation stehen.
Die Arbeit wurde bisher weder im In- noch im Ausland in gleicher oder ähnlicher Form einer anderen Prüfungsbehörde vorgelegt.

Ort, Datum

Unterschrift